

b5a3k9771



STUDIES OF PROSTHETIC LOADING
BY MEANS OF PYLON TRANSDUCERS
Volume 1

Thesis presented for
The Degree of Doctor of Philosophy

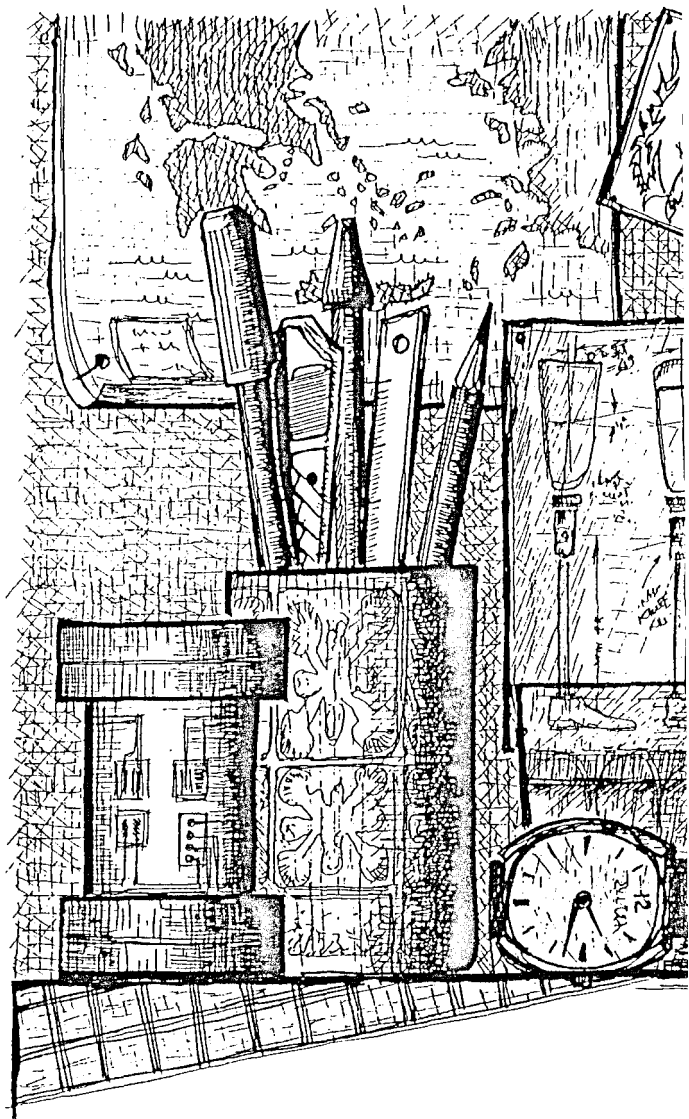
Bioengineering Unit
University of Strathclyde

Evangelos A. Magnissalis

1992

Glasgow

' The copyright of this thesis belongs to the author under the terms of the United Kingdom Copyright Acts as qualified by the University of Strathclyde Regulation 3.49 . Due acknowledgement must always be made of the use of any material contained in , or derived from , this thesis.'





ABSTRACT

The multi-component pylon transducer has been used for several years for prosthetic loading measurements for the assessment of many tasks during various amputee activities with a corresponding number of important results.

The project work presented in this thesis was undertaken in order to improve the existing calibration equipment and techniques as well as the methods of analysis relating to the use of the transducer in various prosthetic research applications.

The use of an Instron materials testing machine for the calibration of the transducer is reported . The problems encountered during these tests showed that standard dead-weights methods are more appropriate for this purpose, because they rely on fewer components and the introduced unwanted friction can be more readily quantified. Moreover , dead-weights methods followed by former researchers were shown to provide sensitivity coefficients which compared closely to theoretically derived values.

Experimental work conducted on the transducer and reported in this thesis showed that the transducer is practically free of second-order effects which may generally affect transducers due to the presence of elastic deformations during actual loading.

The alignment of a prosthesis , ie the relative position and orientation of its constituent parts in space is important for the function of the artificial leg and the comfort of the amputee. The knowledge established by former researchers on the subject of prosthetic alignment was used in the current project to develop a method for the determination of alignment, based on 3-D modelling of the alignment adaptors adjustability. The new method is reported in this thesis

as well as its implementation by a computer program, which calculates the geometrical configuration during fitting and following each adjustment on the limb. This method was used during amputee level walking tests in association with the pylon transducer for measurement of the prosthetic loading.

This thesis also reports the development and use of a method for the determination of prosthetic loading during amputee kneeling. This "highly-loaded" position was studied and the first ever amputee tests were conducted involving the simultaneous use of the pylon transducer and two Kistler force platforms. The reported results were subsequently used for reviewing the values in the standards for the structural testing of lower limb prostheses.

ACKNOWLEDGEMENTS

The work presented in this thesis was carried out in the Bioengineering Unit of the University of Strathclyde and the tuition fees for the three years of this work were provided by the Science and Engineering Research Council.

I would like to express my gratitude to Professor J.P.Paul for all his support throughout the work and to my supervisor Mr S.E.Solomonidis for his substantial scientific assistance and personal encouragement.

I would also like to thank Mr W.D.Spence for his constructive prosthetic advice and Mr D.J.A.Smith for his assistance with the use of the Instron machine as well as Mr S.A.Floyd and A.J.Tullis for their advice and help in electronics and Mr W.D.Lyle of the Engineering Application Centre for his assistance with the use of the coordinate measuring machine. In addition to the above, I would like to thank Mr H.E.Fleming for the provision of the program Hameco.Pas and Mr Lazaros Karagiannopoulos and Mr Duncan Ainscough for their contribution during the amputee tests.

Thanks are given to all the technicians of the Mechanical Workshop of the Bioengineering Unit for their skillful contribution to the realization of the componentry and to the amputee-subjects involved in the tests for their friendly cooperation.

I would also like to say how lucky I feel for having met my dear friend Pedro Oliveira, whom I thank for all his support and priceless friendship.

Above all I want to express my deep gratitude to my family for their invaluable encouragement, patience and support throughout all these years.

CONTENTS

VOLUME 1

	page
ABSTRACT	i
ACKNOWLEDGEMENTS	iii
CONTENTS	iv
CHAPTER 1 INTRODUCTION	1
CHAPTER 2 LITERATURE REVIEW	
2.1 Introduction	7
2.2 Normal Gait	8
2.3 Pathological Gait	12
2.4 Force Measuring Systems	13
2.5 Standards for Structural Testing of Prostheses and Design Criteria	25
2.6 Prosthetic Alignment	30
2.7 Definitions and Conventions used in this Thesis	38
2.8 The Calibration of the Pylon Transducer	44
2.9 Summary	55
CHAPTER 3 THEORETICAL ANALYSIS FOR A FIRST APPROXIMATION OF THE STRAIN GAUGE RESPONSE OF THE SHORT PYLON TRANSDUCER	
3.1 Introduction	59
3.2 Initial Considerations and Assumptions	59
3.3 Study of transducer for applied Shear forces	63
3.4 Study of transducer for applied Axial force	65
3.5 Study of transducer for applied Bending moments	66
3.6 Study of transducer for applied Torque	71
3.7 Quantitative Results of the Analysis	72

	page
3.8 Discussion	73
3.9 Conclusions	76
CHAPTER 4 THE CALIBRATION OF THE SHORT PYLON TRANSDUCER	
4.1 Introduction	78
4.2 Followed Approach	79
4.3 The Calibration using the Instron machine	80
4.4 Results and Discussion	91
4.6 Conclusions	96
CHAPTER 5 VALIDATION OF THE CALIBRATION MATRIX	
5.1 Introduction	99
5.2 Development of the required Device	99
5.3 Preparation of the Device and Set-up	105
5.4 Testing Procedure and Program for Analysis of Data	108
5.5 Tests and Results	109
5.6 Discussion and Conclusions	110
CHAPTER 6 INVESTIGATION FOR A SECOND-ORDER MODEL FOR THE CALIBRATION OF THE PYLON TRANSDUCER	
6.1 Introduction	114
6.2 Description of the Set-up and Tests	115
6.3 Processing of the Data	118
6.4 Results	119
6.5 Discussion	123
6.6 Conclusions	125
CHAPTER 7 MODELLING OF THE ADAPTORS AND OF THE STRUCTURE OF A LOWER LIMB PROSTHESIS	
7.1 Introduction	128
7.2 Technical and Prosthetic Considerations	129

7.3	Initial Steps in the Study of the Adaptors	130
7.4	First Attempt to Model an Adaptor Analytically	131
7.5	First Attempt to Calibrate an Adaptor	138
7.6	Further Considerations of the Adaptors	139
7.7	Mathematical Modelling of a Prosthesis	143
7.8	Discussion	149
7.9	Conclusions	150
CHAPTER 8	A NEW METHOD FOR THE ASSESSMENT OF ALIGNMENT OF LOWER LIMB PROSTHESES	
8.1	Introduction	153
8.2	Adaptor screws and Measuring Device	153
8.3	Measurement of the adaptors	155
8.4	Measurements on the Prosthesis	160
8.5	Simulation of the Alignment Procedure	168
8.6	Simulated Alignment Sessions for Evaluation of the New Method	171
8.7	Discussion	174
8.8	Conclusions	176
CHAPTER 9	PROSTHETIC LOADING DURING LEVEL WALKING	
9.1	Introduction	179
9.2	Equipment Used	179
9.3	Preparation of the Prosthesis	181
9.4	Description of the Tests	182
9.5	Manipulation of the Files	183
9.6	Results	184
9.7	Discussion and Conclusions	187
CHAPTER 10	PROSTHETIC LOADING DURING KNEELING	
10.1	Introduction	191
10.2	Equipment Used	191
10.3	Preparation of the Prosthesis	193
10.4	Method for the Analysis	193

	page
10.5 Planning and Execution of the Test Procedure	208
10.6 Manipulation of the Files	210
10.7 Results	211
10.8 Discussion and Conclusions	215
CHAPTER 11 DISCUSSION , CONCLUSIONS AND FUTURE RECOMMENDATIONS	
11.1 Discussion	219
11.2 Conclusions	221
11.3 Future Recommendations	223
BIBLIOGRAPHY	224

VOLUME 2

APPENDIX I	Resistance strain gauges and their experimental use	238
APPENDIX II	Data and graphs obtained from calibration of the pylon transducer	247
APPENDIX III	Design of components for chapter 5 and data acquired from the related tests	272
APPENDIX IV	Print-outs obtained from the kneeling tests	277
APPENDIX V	Spatial descriptions and transforms	319
APPENDIX VI	Print-outs obtained from the new alignment method	326
APPENDIX VII	Results obtained from the level walking tests	333
APPENDIX VIII	Derivation of the shear stress equations for a pure shear load configuration	338

APPENDIX IX	Information regarding Wiring connections and Settings of the system used in this study	341
APPENDIX X	Presentation of the inverse alignment problem mentioned in chapter 7	345
APPENDIX XI	The data for the investigation of the second-order calibration model and the statistical results	352
APPENDIX XII	A new suggested method for combined study of prosthetic alignment and loading	360
APPENDIX XIII	Listings of the developed programs	369

CHAPTER 1

INTRODUCTION

Studies involving pylon transducers have been the subject of a considerable number of projects in the Bioengineering Unit since the late 1960s (eg Lowe , 1969 ; Berme et al., 1976).

These projects were related to lower limb prosthetics and their objectives were oriented towards the development of new pylon transducer designs and related recording equipment as well as towards the expansion of the transducers' experimental use for various prosthetic purposes. Thus, not only pylon transducers have become shorter and the related equipment more versatile, but they have also been used through the years for the formulation of testing standards for prostheses , investigations into the kinetics of amputee locomotion, the evaluation of various types of modular prostheses and in other projects.

The short pylon transducer in particular (Berme et al., 1976) is the transducer which has offered the most of the contribution described above. The reason for this was its short length, which allowed many more amputees to be fitted with such a measuring device for the first time. This pylon transducer was the basis of the newly developed portable recording systems which have been used in the Unit to test amputees during outdoor activities (Lovely, 1981 and Tilford, 1985).

For several years, prosthetic research covered the field of prosthetic alignment. The term "alignment" signifies the relative position and orientation of the prosthetic parts in space. Since very early (Thomas, 1944) , alignment was recognised as a major determinant in the quality of the amputee's walking pattern and many projects were carried out in order to investigate its effect on gait, its mathematical description, the existence of optimum configurations and other considerations (eg Arcan et al., 1981; Seliktar et al., 1982; Mizrahi et al., 1985).

Various studies on prosthetic alignment resulted

in a series of important conclusions which highlighted many aspects of the subject. Among other significant contributions, these thorough studies proved for the first time (Zahedi et al., 1986) that no single alignment configuration exists for a certain patient and that optimum ranges of alignment should be considered instead.

The progress achieved in the above fields resulted not only in a substantial contribution in the study of lower limb prosthetics, but also in the identification of new research tasks.

When the current project was initiated, it was considered that further investigations were needed in order to determine the behaviour of the short pylon transducer and develop additional equipment and methods for its calibration and evaluation and its use in the determination of prosthetic loading in various prosthetic applications. It must be pointed out that the presentation of the project work in this thesis follows a sequence that the author considered as the most appropriate and does not necessarily reflect the actual succession of the various stages. The important references from the force measurement literature for example (eg Dubois,1974 ; Bray,1981 ; Bray et al.1990), were discovered by the author of this thesis after the work on the Instron machine was carried out and had proved to have disadvantages . Having recognised the technical problems encountered during these tests , the author initiated an investigation in the force measurement literature and eventually cross-checked the conclusion that dead-weight methods provide more reliable means for calibration and evaluation of force transducers.

Initially however, the objectives of the current project work were set-out as follows :

- 1) To provide further information on the pylon transducer's behaviour in static loading.
- 2) To develop a new series of set-ups for the pylon transducer's calibration.
- 3) To develop a system for the evaluation of the calibration matrix of the pylon transducer.
- 4) To investigate the possibility of using a second-order model for the calibration of the pylon transducer.
- 5) To develop a method, which would allow a quicker assessment of prosthetic alignment and which could be used in association with the pylon transducer in studies combining prosthetic loading and alignment.
- 6) To develop a method for the evaluation of prosthetic loading during the kneeling position of the amputee, which had been estimated to be a highly loaded configuration.

The presentation of the work carried out during this project follows the same order as the objectives described above :

Chapter 2 presents a literature review on prosthetic loading and alignment studies as well as a detailed reference to the development of criteria for the structural testing of lower limb prostheses and pylon transducer calibration techniques.

Chapter 3 presents the theoretical work carried out on the stress analysis and for predicting the strain gauge response of the pylon transducer for all six load components monitored by the device.

Chapter 4 presents the work carried out on the calibration of the pylon transducer. It describes a new attempt to calibrate the transducer using a materials testing machine (Instron).

Chapter 5 presents a newly developed method for the evaluation of the calibration matrix, using again a materials testing machine.

Chapter 6 presents the investigation on the possibility of calibrating the pylon transducer using a different approach, viz modelling the device's behaviour using second-order polynomials techniques, used in other scientific fields.

Chapter 7 presents the work carried out on the mathematical modelling of the alignment adjustability of lower limb prostheses. The main subject of this chapter is the development of 3-D modelling of the adaptors and the structure of an Otto Bock modular prosthesis.

Chapter 8 presents an alignment assessment method based on the work presented in chapter 7 and demonstrates its use in detail.

Chapter 9 presents the results of the patient tests carried out using the pylon transducer and the new method for the assessment of the alignment. These tests involved level walking and the results were also used, as a first approach to the testing standards of lower limb prostheses.

Chapter 10 highlights another aspect of prosthetic loading. Using the pylon transducer and two force platforms, tests were carried out for the first time, in order to monitor the prosthetic loading during kneeling, for above-knee patients wearing Blatchford Endolite prostheses.

Chapter 11 presents the general discussion and the conclusions drawn from the project work. This chapter also presents a series of relevant future recommendations.

CHAPTER 2

LITERATURE REVIEW

2.1 Introduction

2.2 Normal Gait

2.3 Pathological Gait

2.4 Force Measuring Systems

2.4.1 Introduction

2.4.2 Force Platforms

2.4.3 Pylon Transducers

2.4.3 Methods of Data Acquisition and Processing

2.4.5 The short Pylon Transducer designed by Berme et al. (1976)

2.5 Standards for Structural Testing of Prostheses and Design Criteria

2.6 Prosthetic Alignment

2.6.1 Introduction

2.6.2 Terminology

2.6.3 Studies on Optimum Alignment

2.6.4 The Alignment Rig

2.7 Definitions and Conventions used in this Thesis

2.7.1 Introduction

2.7.2 Frames of Reference

2.7.3 Forces and Moments

2.7.4 Alignment Parameters

2.8 The Calibration of the Pylon Transducer

2.8.1 Introduction

2.8.2 Linear Approach

2.8.3 Non-linear Approach

2.9 Summary

2.1 Introduction

One of the major issues in rehabilitation engineering, is the study of amputees' locomotion from the kinematic and kinetic points of view.

Kinematics and kinetics are complementary fields and , as far as human locomotion is concerned , are defined as follows :

kinematics : the study of displacement, velocity, and acceleration of the various landmarks of the body segments and,

kinetics : the study of the forces acting upon the various segments, as a result of gravity and inertia effects (external causes) or muscles and ligaments (internal causes) and their effect on the motion of the body.

The thorough studies on human locomotion carried out in California (University of California, Berkeley, 1947) highlighted the major aspects in the field and emphasised the importance of kinematic and kinetic analysis in the understanding of normal and amputee locomotion.

In the field of amputee rehabilitation and of prosthetics , the understanding of the mechanics of amputee locomotion is of major importance. Conducting research on the kinematics and kinetics of amputee activities, particularly gait, allows comparisons with normals to be made and eventually leads to improvements in amputee management and rehabilitation.

The study of loading of the prosthetic side in particular is of major interest , for it provides the information for the formulation of criteria for the design of the prostheses themselves . Since an artificial leg has to satisfy both weight and strength requirements, the data acquired from such studies, are very useful in establishing the optimum compromise

between these two requirements. Special equipment has been designed and built , through the years , for the measurement of prosthetic loading for this purpose.

Satisfactory amputee rehabilitation also relies upon the function of the artificial leg , which depends considerably on the relative position and orientation of the various components to each other. As will be explained later , these geometrical relations are referred to by the term "alignment" .

It current prosthetic practice, the alignment of a prosthesis is based on the prosthetist's subjective judgement and feedback from the comments made by the patient. Researchers in recent years have tried to establish more objective criteria which could be used by the prosthetist in the achievement of the best possible alignment configuration.

The literature review focused on the following : the development of loading measurement equipment , the development of loading standards and design criteria , the various studies carried out for the determination of the optimum alignment and the methods for measurement of alignment . The most recently developed devices for the assessment of prosthetic loading are the pylon transducers and therefore the review also focuses on the various approaches and techniques adopted for the calibration of such devices . The presentation of the review starts with a general discussion on normal and pathological gait.

2.2 Normal Gait

Since gait is a very personal and unique feature of all subjects, the term `n o r m a l` describes that population which exhibits a commonly acceptable gait pattern.

In order to establish the definitions needed for the gait cycle, the feet of a walking subject are considered , by referring to figure 2.1 .

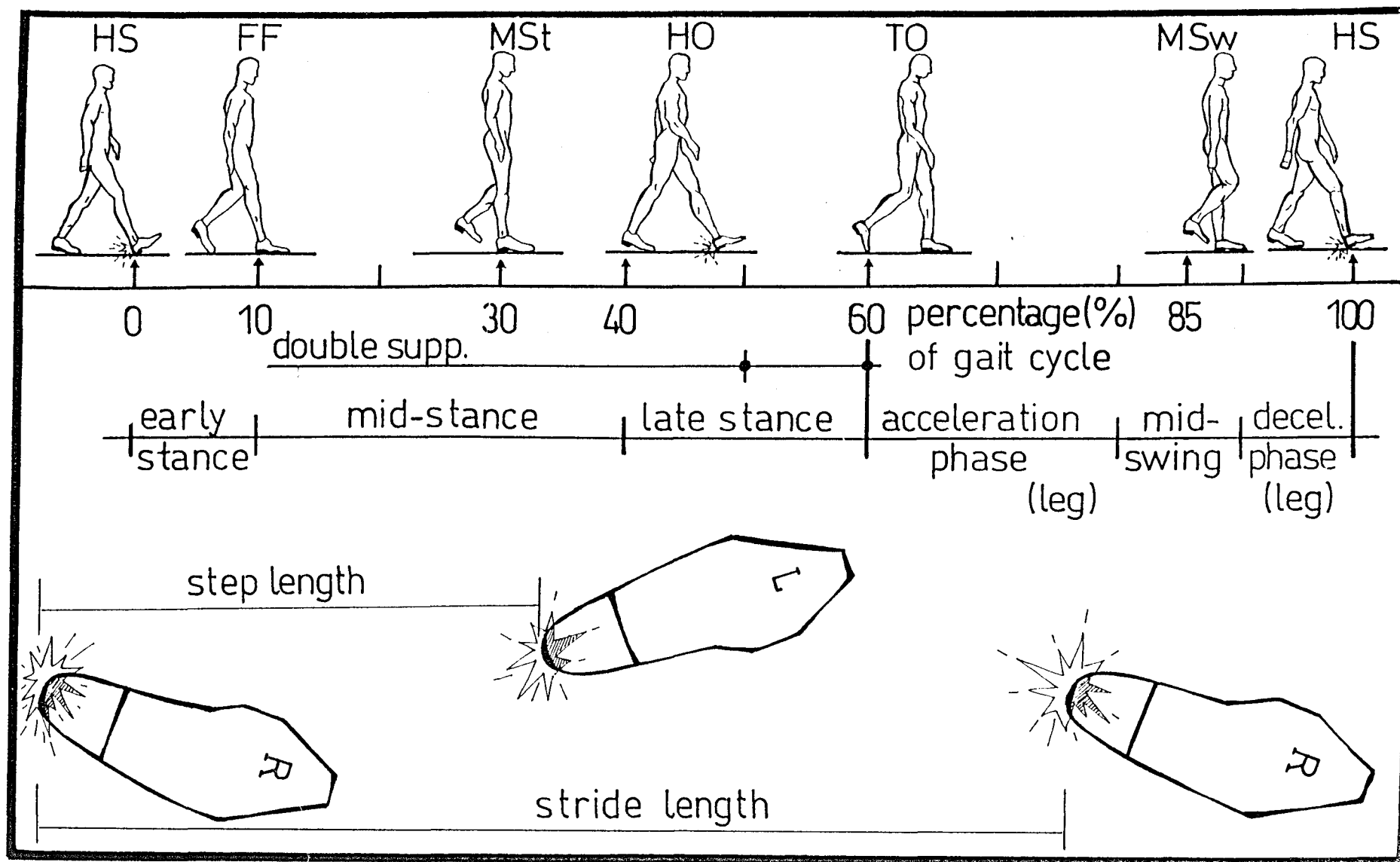


Fig 2.1 The gait cycle for normal walking

There is, however, a particular phase of the gait cycle, where there is an overlap between the stance phases of both feet. This phase, as shown, is called the double support and is defined between the heel strike and foot-flat on the leading side and heel-off and toe-off on the contralateral one.

Two lengths can be defined within a gait cycle :

the stride length , which is the distance between the point of heel strike and the corresponding point of the ipsilateral heel strike , representing the distance covered by the corresponding foot within a gait cycle and,

the step length , which is the distance between the point of heel strike and the corresponding point of the contralateral heel strike.

Both these lengths are measured along the direction of walking. The stride length is equal to the sum of the two contralateral step lengths.

The gait of a subject can be described by the cadence of the gait . The cadence is the total number of steps taken by both legs per unit time (70 to 130 steps/min depending on the walking speed). In the ideal case of equal step lengths the following formulae can be written :

$$(\text{stride length}) = 2 \cdot (\text{step length})$$

$$(\text{walking speed}) = (\text{cadence}) \cdot (\text{step length})$$

The time distribution within a gait cycle, for normal walking speeds , is : approximately 60 % of the time is spent in stance and 40 % of the time is spent in swing, with an overlap time during double support approximately equal to 10 % of the gait cycle.

Increase in the cadence causes a relative (ie. expressed as a percentage) increase of the time spent in swing and a decrease in the cadence causes a relative decrease of the time spent in swing , with opposite results on the stance respectively. Increase in the cadence, though, causes relative decrease of the time spent on double support and decrease in the cadence causes a relative increase of the time spent in double support. A consideration of the latter relationship to the limits, would result in no double support at all, when cadence is very high (running), and to double support only, when cadence is zero (standing).

In terms of kinematics and kinetics the gait cycle could be divided into several phases considering the accelerations occurring and the ground reaction forces. Considering the leading limb again, one can distinguish the following phases :

E a r l y s t a n c e , during which the ground force develops its action on the leading foot and the trunk is decelerating. This phase is defined from heel strike to foot-flat.

M i d s t a n c e , during which the body progresses over the stationary foot. The single limb support is established and the foot is flat on the ground. This phase is defined between foot-flat and heel-off.

L a t e s t a n c e , during which the body is accelerated forward and finally falls to the contralateral limb. This phase is defined between heel-off and toe-off.

L e g a c c e l e r a t i o n p h a s e, during which the leg must be accelerated to lead the body to the next heel strike. This phase is initiated after toe-off.

M i d s w i n g , during which the leg gradually crosses through the midcoronal plane of the body , with the knee flexed to allow the foot to clear the ground. This phase ends with a vertical tibial position.

L e g d e c e l e r a t i o n p h a s e , during which the leg decelerates forward in order to control the correct landing of the foot at heel strike. This phase ends with full knee extension, creating step length. In this phase the deceleration of the foot has its maximum value during the gait cycle (approximately 4g at the ankle joint).

2.3 Pathological Gait

The type of pathological gait with which prosthetics are related is that of the amputees. Amputee locomotion has important differences, in comparison to the normal, resulting from the following:

- a) the presence of their artificial leg, which is a passive limb , with no musculature and reduced proprioceptive capability,
- b) the imbalance caused by mass and mass moment of inertia differences , between the sound and artificial sides,
- c) problems regarding comfort, fitting or alignment,
- d) clinical condition of the stump mainly in terms of the residual musculature.

Therefore, the amputee's walking performance depends largely on the condition of the body, the quality of the limb substitute and of course on the man-machine matching at the stump-socket interface.

The next sections cover a literature review on the relevant subjects involved in the work presented in this thesis.

2.4 Force Measuring Systems

2.4.1 Introduction

For the acquisition of kinetic data, concerning the loads applied during locomotion, several devices have been used since the last century. The first approaches mainly concentrated on the vertical component of the force applied on the body by the ground during a particular step and in the beginning of this century the first force platforms were designed. These devices provided, for the first time, the possibility of simultaneous measurement of more than one component of the ground reaction force . Later, pylon transducers were introduced, which expanded the multi-component measurements to a larger number of steps. A detailed review of the evolution in this field follows.

2.4.2 Force Platforms

Cunningham and Brown (1952) , presenting a review of force measurement on human locomotion, mention some of the earliest contributions in this field. Those first approaches involved mainly the measurement of the vertical component of the ground reaction force. Carlet in 1872 and Marey in 1873 used a pneumatic cell in the sole of the shoe and monitored the variations of the vertical load. Beeley (1882) investigated the pressure distribution on the plantar surface of the foot, by studying the indentations caused during gait on plaster of Paris.

These first approaches, although significant, provided poor kinetic data because neither other components nor the position of the resultant ground reaction force could be derived.

As Cunningham and Brown (1952) report, the first use of force platform was reported by Amar in 1916. The design of Amar was mainly based on a platform supported by springs in three directions : vertical, lateral and fore-and-aft. The deflections on the springs were meant

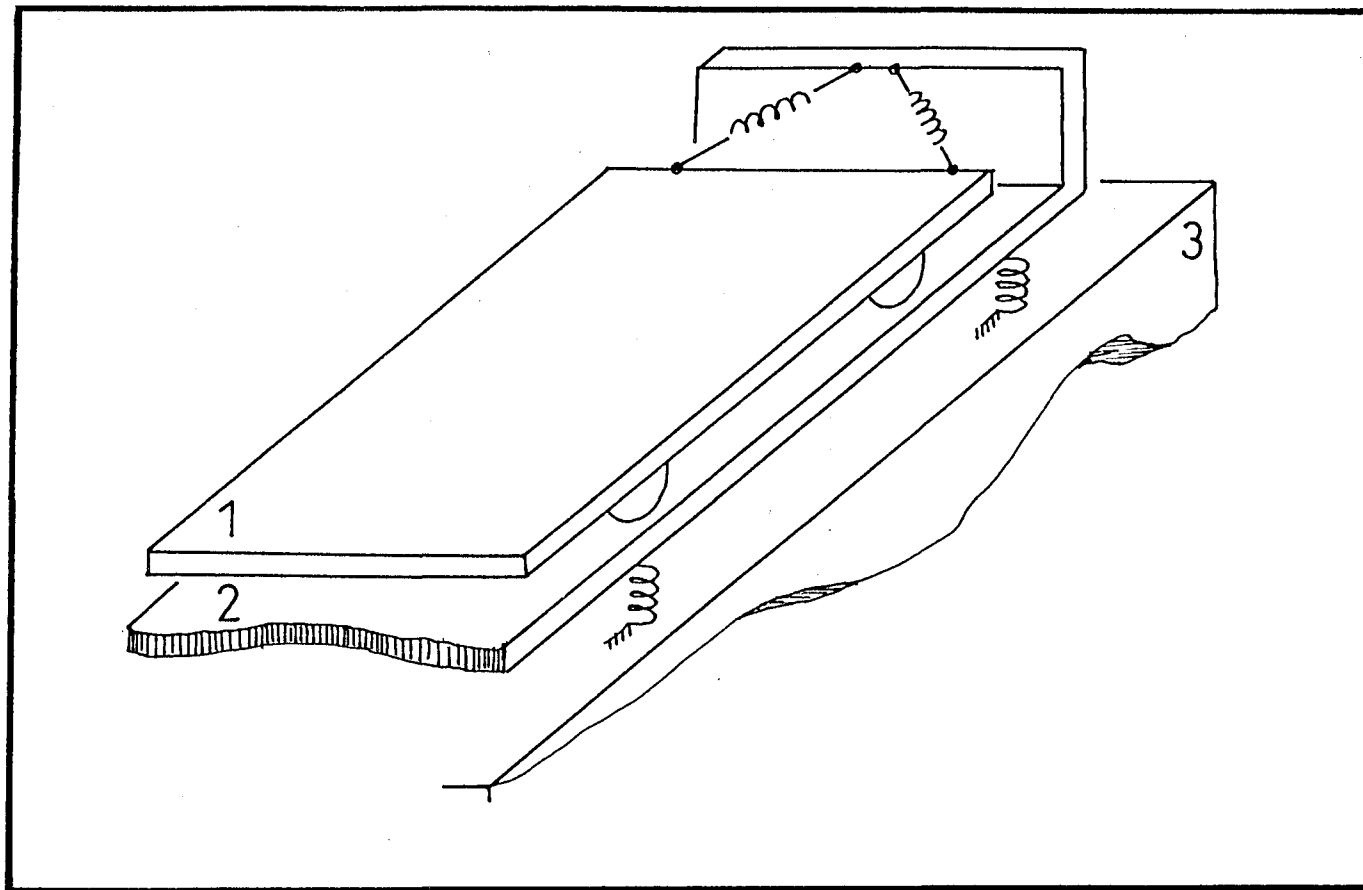


Fig 2.2 The force platform designed by Elftman
(adapted from Elftman, 1938)

to reflect the loads applied on them. Amar was, thus, able to monitor the three independent components of the ground reaction force (Pashalides, 1989).

The same principle was also used by Elftman (1938). As shown in figure 2.2 , the upper platform (1) was supported by means of ball bearings and horizontal springs on the lower platform (2). Everything was mounted on the base shown (3) . Displacements in the vertical springs reflected the vertical component and displacements in the horizontal springs reflected the antero-posterior and medio-lateral shear components of the reaction force. The position of the reaction force could be derived by calculations involving the individual displacements of the vertical springs. The three components and the position were then used to derive the applied torque . For better monitoring of the displacements, properly designed linkages were used (not shown).

This type of design that Elftman reported was an improved version of an earlier design they had developed together with Manter (cited in Elftman, 1938). It was a very important contribution to the study of kinetics of human locomotion but as Amar's design was considered not very reliable, mainly because of the large amount of deflection on the springs, the inertia effect on the platforms themselves and the high level of friction at the linkage systems used for recording.

The first version of the modern force platforms was reported by Cunningham and Brown (1952) and referred to the platform designed and used for the studies on human locomotion carried out in the University of California, Berkeley (1947). The new force platform provided the possibility of measuring the three components of the reaction force as well as the torque applied by the ground to the foot. The new device could also provide the user with the location of the centre of pressure. As shown in figure 2.3 , the

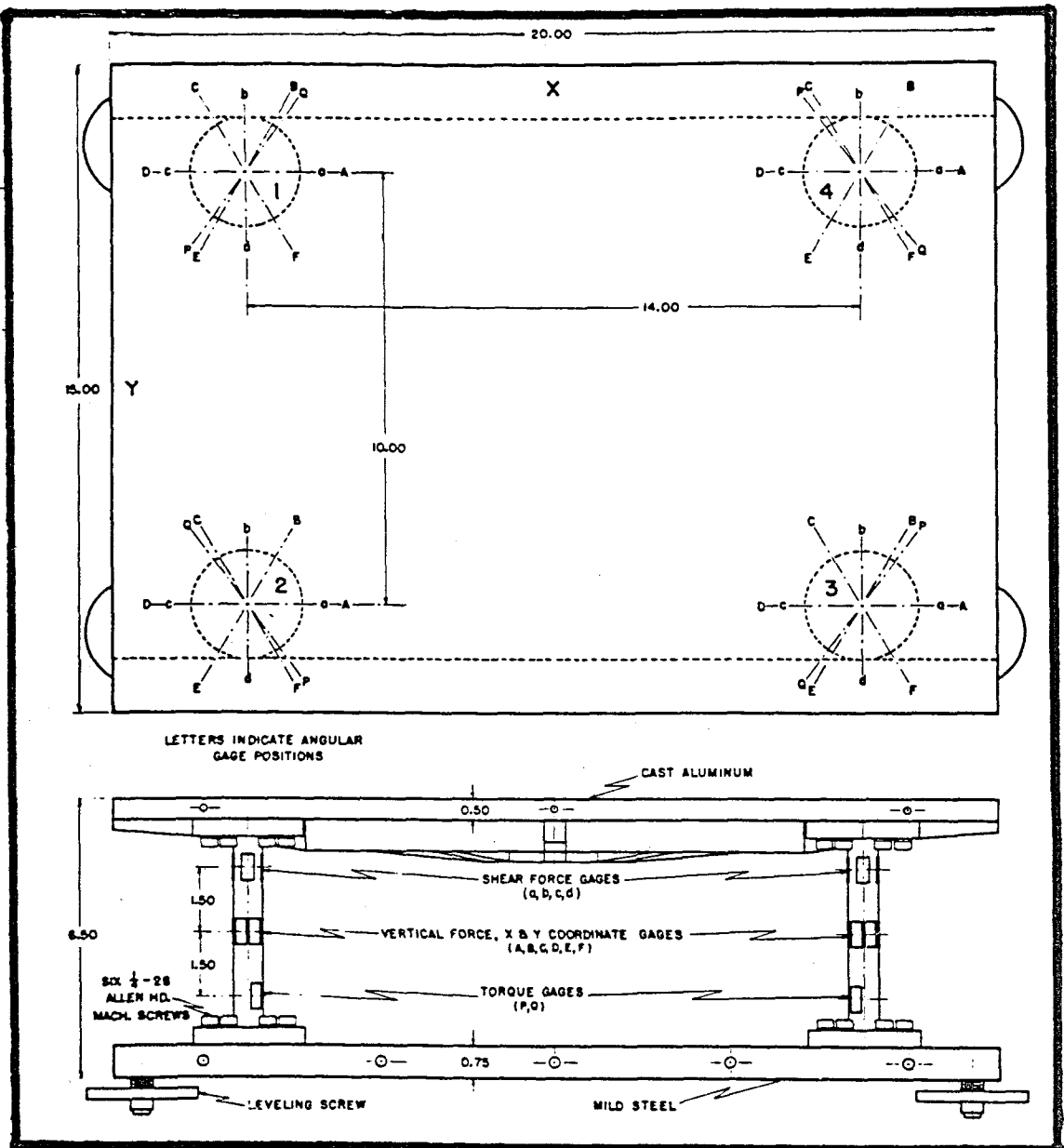


Fig 2.3 The force platform developed by Cunningham and Brown (extracted : Cunningham and Brown, 1952)

principle used consisted of the use of four electrical resistance strain gauged tubular columns. These columns were bolted to the top platform and to the steel base. Any load applied onto the platform resulted in the generation of corresponding electrical signals from the gauges. These signals were monitored and recorded. Calibration of the device allowed the derivation of the forces and torque from the output signals.

With this design Cunningham and Brown (1952) eliminated the problems which existed in the previous designs induced by friction and large displacements. However, having solved the previous problems, a new concern arose during those years for the first time: the frequency response of the measuring and recording system.

A force measuring device, meant to work under dynamic conditions (eg. human locomotion), must have a response rapid enough to follow the monitored phenomenon. In other words, if the output signals of a force platform, for example, are meant to reflect the strains which generate them, then both the electrical network and the mechanical system must have oscillatory characteristics which allow them to follow the rates of change of these strains.

Cunningham and Brown (1952) reported that the electrical circuitry had a very high natural frequency and could accurately follow rates of change of strain much higher than those encountered. However, the force platform did not respond as well to high frequencies, due to the mass of the top plate. Unwanted oscillations were thus affecting the quality of the output signals mainly in the shear and torque directions. This problem was solved with viscous damping and the response of the force platform was thus considerably improved.

The force platform that Cunningham and Brown designed had a natural frequency of 105 Hz for shear and 140 Hz for torque.

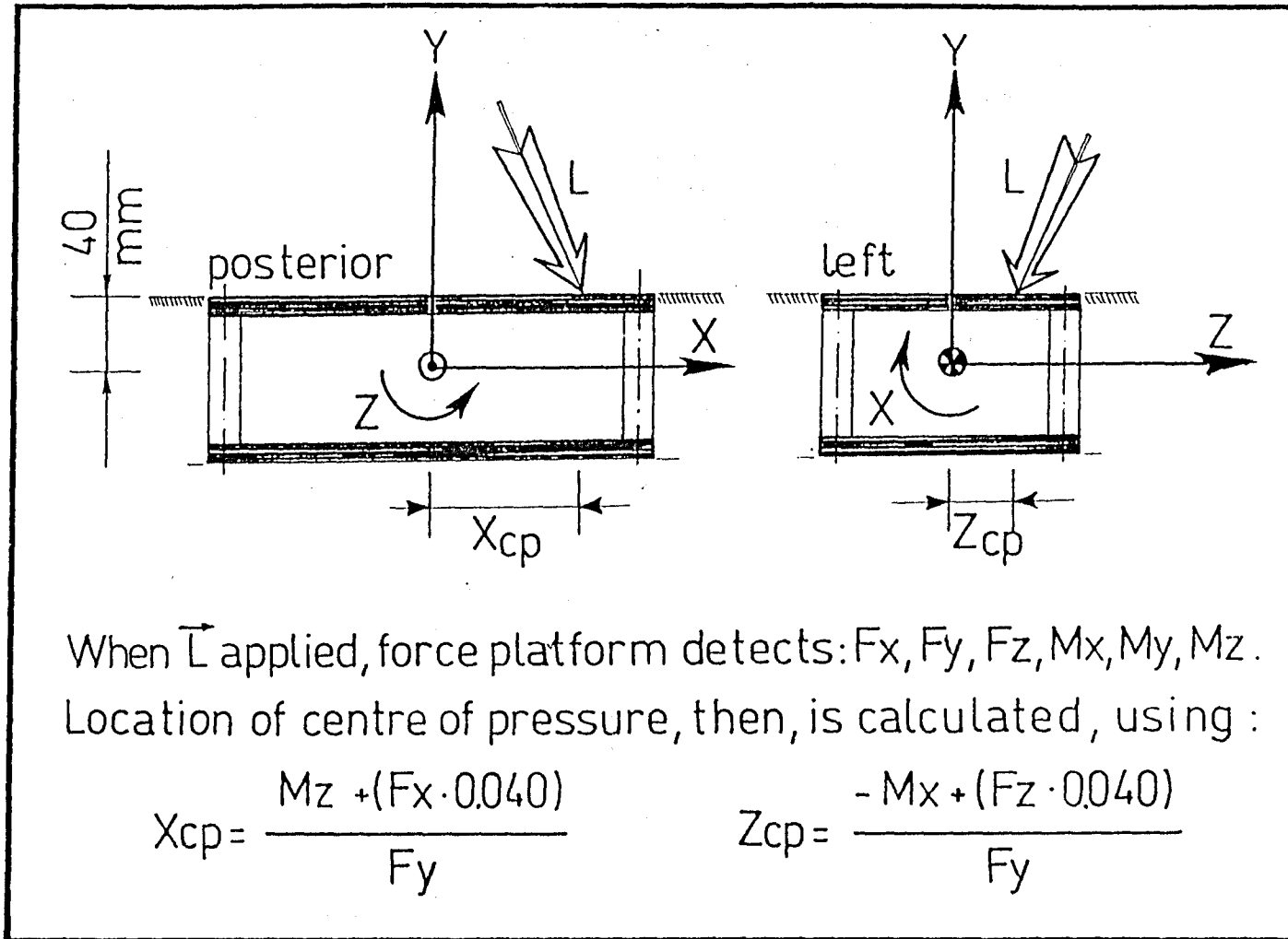


Fig 2.4 Diagram of the Kistler force platform

Later it was discovered that piezoelectric crystals would be better, if used instead of the strain gauged pillars. The advantages were considered to be the higher rigidity, natural frequency and sensitivity of this system, together with a lower cross sensitivity between different channels. Thus, in 1975 Kistler Instrument AG of Switzerland introduced a force platform using the piezoelectric principle for its transducers.

As shown in figure 2.4 ,two cast aluminium plates were separated by four 3-force component quartz transducers. The system allowed the measurement of all loads, as well as the calculation of the position of the centre of pressure , providing a natural frequency greater than 200 Hz and a maximum cross effect between channels of less than 3% .This type of force platform is used in the Bioengineering Unit. Figure 2.4 also shows the reference frames and the conventions used in the Unit.

The disadvantages of this type of force measuring device in human locomotion studies are that they allow data acquisition for one step only and also, because the subject must hit the platform, it is difficult, due to psychological reasons, to obtain unbiased readings.

Force platforms have been used for several years in load data acquisition and are still used, but the two problems mentioned above were understood since very early on.

2.4.3 Pylon Transducers

One of the main tasks of the studies carried out in the University of California, Berkeley (UCB, 1947) was the understanding and measurement of the differences in walking patterns adopted by amputees when carrying loads , using different sockets , walking on different surfaces and slopes etc.

Since the platforms could not provide such a broad range of data, pylon transducers were developed, which

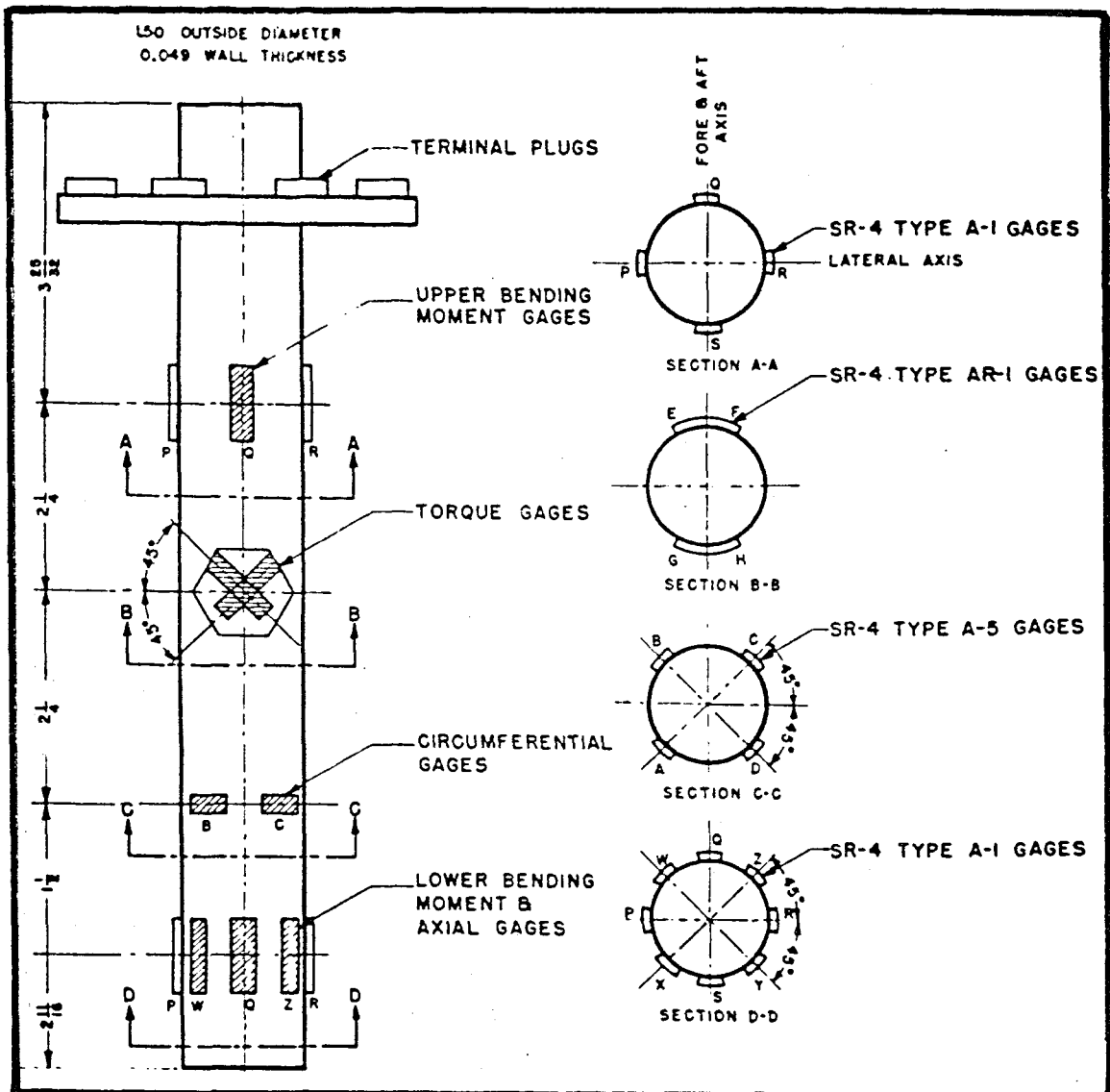


Fig 2.5 The pylon transducer developed by Cunningham and Brown
(extracted from Cunningham and Brown, 1952)

although not usable for normals, were considered very satisfactory for amputees.

Cunningham and Brown (1952) reported their own design (fig 2.5) . It was a 12 inch (≈ 305 mm) long strain gauged aluminium alloy column with an external diameter of 1.5 inches (≈ 37 mm) and a wall thickness of 0.049 inch (1.2 mm).

The pylon transducer of Cunningham and Brown was meant to replace the shank of the artificial limbs and record loads applied on it. The gauges were placed at two levels along the tubular surface and monitored the axial load, the torque and the bending moments at the anteroposterior and mediolateral directions at both levels. Those moments allowed the calculation of the shear forces in both directions.

Cunningham and Brown reported that the response of the new device in dynamic loads was acceptable. The only limitations to such a response were considered to be the length of time required for a shock wave to travel along the pylon and the damping capacity of the material.

Besides, the frequency response, which was always considered an important quality of the measuring system, the development of the pylon transducer introduced another concern for the researchers, namely the overall length of the device. It was obvious since the beginning that, if a large population of amputees was to be tested, the pylon length should be decreased. This was necessary so that the transducer could be fitted to a large number of amputees, regardless of whether they were above the knee amputees (AKs) or below the knee amputees (BKs) and whether, in the case of BKs, the stump was long or short. Nevertheless, the pylon length was also critical in the AK case where swing phase control mechanisms were mounted in the knee units.

An effort was therefore initiated in the 60s, for designing shorter pylon transducers. The development of

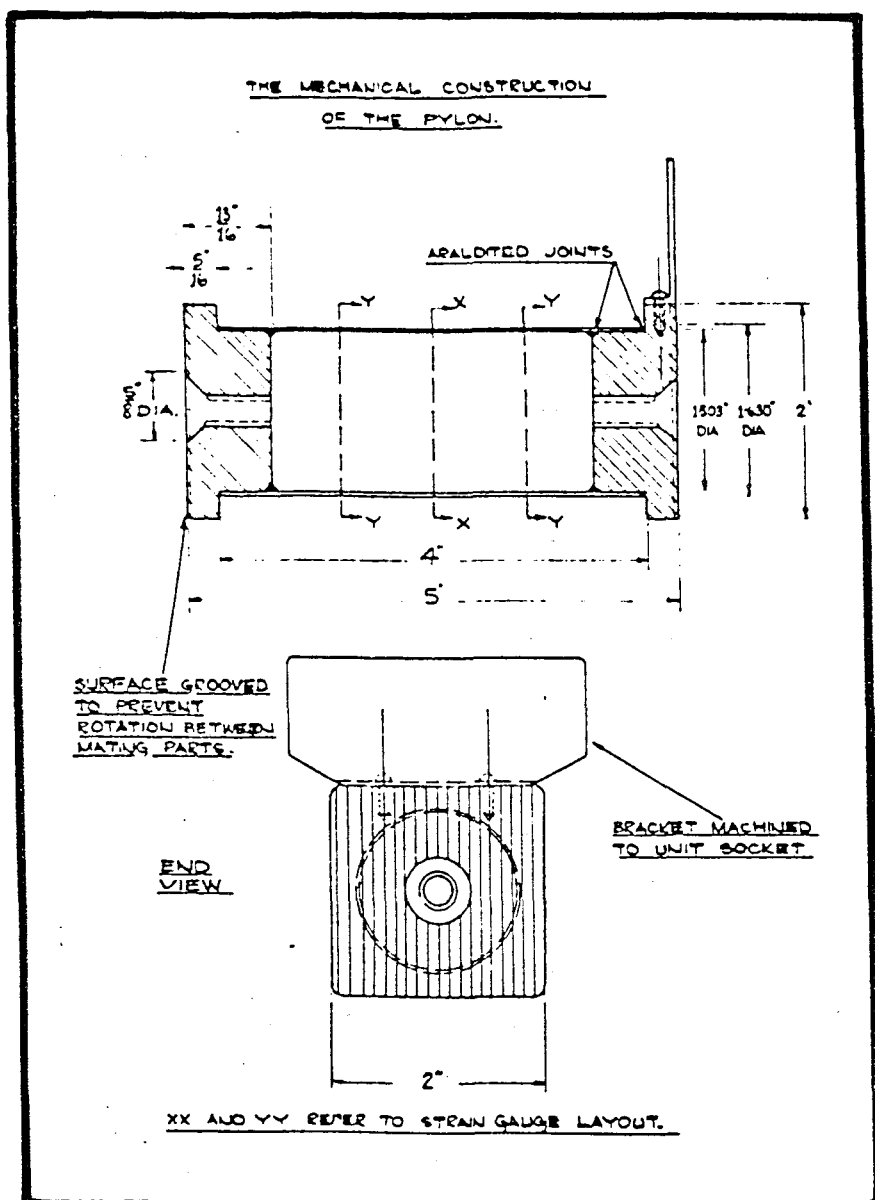


Fig 2.6 The pylon transducer designed by Lowe
(extracted from Lowe, 1969)

modular prostheses facilitated the use of pylon transducers in the biomechanics studies of locomotion and new designs started appearing.

Lowe (1969) reported the development of a pylon transducer with a length shorter than Cunningham and Brown's design. Lowe developed the pylon transducer in order to study the performance of various knee mechanisms. Similarly to Cunningham and Brown, Lowe used the principle of two-level gauging (fig 2.6).

Obviously the problem in reducing the length further, had two aspects related to the following: the allowed overall length of the pylon, the accuracy in calculating shear forces and the elimination of end-effects. The individual importance of each one of these three factors is highlighted below.

The overall length of the pylon, as explained earlier, had to be kept to a minimum, in order to fit more amputees (1st factor). Within this overall length, the two series of gauges should be accommodated, achieving a balance between the other two factors. This means that the two series of gauges should be not too close to each other so that the shear forces could accurately be calculated as the ratio of the moment difference to the distance between the two gauging levels (2nd factor), but also not too far apart, so that the two series of gauges would not be close to the end flanges, thus introducing undesired end-effects (3rd factor). A compromise led Lowe to adopt a total length of 5 inches (≈ 122 mm) and a separation distance between gauging levels of 1.75 inches (≈ 43 mm).

The design adopted by Lowe was later considered not very reliable, mainly because the performance of the transducer involved many unwanted cross-effects between the various channels. The strain gauge bridges of the transducer did not only respond to the load components meant to be monitored but also to other load components. Researchers, who used this pylon transducer to investigate hip disarticulation

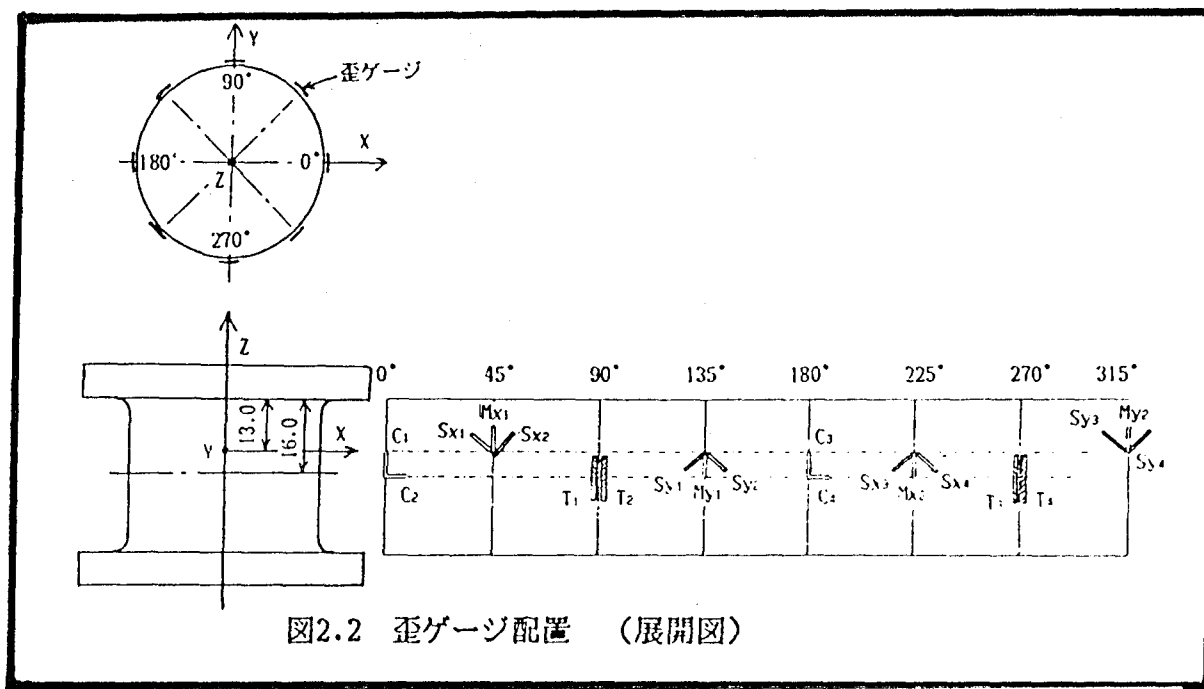


Fig 2.7 The pylon transducer designed by Nishihara et al
(extracted from the Japanese manual)

prosthetic loading and to produce data for the formulation of loading standards, found that the method used for mounting the two flanges (they were glued) on the main cylinder as well as the bonding of the gauges were the source of those cross - effects (Solomonidis, 1989). Thus, the design of a new pylon transducer was decided (Berme et al., 1976).

Overcoming the problem of two-level gauging, Berme et al. (1976) reported the development of a pylon transducer which was shorter , because it had been gauged in a single area , introducing direct shear measurement , in prosthetics , for the first time. This device measured all six components directly by means of six full bridges bonded on an aluminium alloy tube , which had a total length of 70 mm , just over half of Lowe's design. This pylon transducer is described in detail in section 2.4.5 .

An even more recent design is the one reported by Nishihara et al. (1989) (see fig 2.7). According to these authors , this pylon transducer ".....can be described as a 30 mm long pylon load cell". Although experimental results have not been published to date, the authors suggested that the new design would be of major importance in the acquisition of prosthetic loading data, since it allows for an even broader amputee population to be tested. In the same publication, the authors reported having designed an effectively zero-length pylon transducer, which does not disrupt the mechanical continuity of the prosthetic shank.

Research workers having successively solved the problem introduced by the restrictive nature of force platforms and then the problem regarding the pylon transducer length, turned their attention to signal transmission and recording. In the late 70s researchers considered the possibility of solving the problem of the umbilical cable needed for transmission of the power supply and output signals. If the subject was to

be tested in conditions of daily life , outdoors tests should also be considered and the acquisition system had to be portable.

2.4.4 Methods of Data Acquisition and Processing

After the introduction of pylon transducers in the study of prosthetic loading, a major concern of the scientists was the development of techniques which would allow the acquisition of data for various prosthetic applications both indoors and outdoors. A critical parameter in this field was again the frequency response of the system.

The output signals of the pylon transducer reported by Cunningham and Brown (1952) were amplified and recorded on an oscillograph.

Another development was performed by Lowe (1969), who recorded the output signals of the pylon transducer in a hard copy form on an oscillograph U/V recorder and then sampled the continuous traces by means of a trace analyser, providing a sampling frequency of 100 Hz. Thus, Lowe obtained digitized signals with time intervals of 10 ms, achieving (theoretically) a maximum resolvable signal frequency of 50 Hz.

Judge and Murray (1973) used a pylon transducer similar to that of Lowe (1969) in order to record signals of prosthetic loading during various walking activities. They recorded the data on an analogue magnetic tape, together with synchronized foot - ground contact signals from foot switches and cine - synchronization pulses. Analogue processing was further performed and resulted to the desirable loads. The system' s frequency bandwidth was 0-200 Hz. One major drawback of this system was the limited possible testing area, due to the umbilical cable connecting the transducer to the rest of the equipment.

Mason (Department of Health and Social Security , 1974) tried to clarify some aspects of the problem of the frequency response by investigating results

obtained by the testing of an amputee. Thus, the conclusion was drawn that for level walking a 0-100Hz bandwidth is sufficient to accurately record the data. However, Mason suggested that for other activities wider bandwidths would be required (0-250 Hz).

Jones (1976) used the pylon transducer developed by Berme et al. (1976) and worked on the data handling of the amputee performance. After amplifying the signals, Jones recorded the data on a magnetic tape and then sampled them using a PDP-12 computer. No significant components were reported to exist above 15 Hz (spectral components above 15 Hz were all at least 50 dB down on the fundamental) and it was therefore suggested that an analogue signal processor with a bandwidth of 20 Hz would be adequate for normal level walking. As with previous methods the method used by Jones had the drawback of the umbilical cable.

Similarly, Solomonidis (1980) conducted studies for the evaluation of modular above the knee prosthetic systems. A sampling frequency of 200 Hz was used. The considerable amount of prosthetic loading data produced by these studies were later used for the development of structural testing of prostheses.

Mc Court (1977) who also used a pylon transducer system, tested amputees for various walking speeds and for various walking conditions (level and up/down ramp). This researcher conducted the data handling by an analogue computer, a U/V recorder and a tape-recorder. This system's bandwidth was determined by the pre-amplifiers used and was 0-120 Hz.

Dewar (1977) developed a single channel monitor device using solid state techniques to monitor the antero-posterior bending moment in terms of the number of times that this single load reached several preset levels, during an amputee's daily activity. The set-up consisted of a strain gauge bonded on the shin of the prosthesis and a set of counters recording the number of times the load on the shank

reached the preset thresholds. For these studies Dewar enrolled two BK amputees . The author of this thesis believes that despite the fact that this system was the first published portable equipment, the results did not allow for valid conclusions, but only for indications; the reason being that the system reported by Dewar (1977) did not have the facility to record results at regular intervals, but only when it was convenient for the amputee.

A new recording approach was attempted by Boenick et al. (1978) who used an 8-channel telemetry system to transmit the six pylon transducer signals and the signals of foot switches. An 8-channel recorder stored the analogue signals after demodulation. It was the first attempt at building a system, providing a solution to the problem of the restrictions imposed by the umbilical cable in the laboratory. Several walking terrains were tried in normal outdoor environment but only two subjects were tested (one AK and one BK) and therefore it was suggested that the confidence level in the reported figures needed to be increased with further work.

Another technique was developed by Lovely (1981) in order to record prosthetic loading from amputee outdoor activities. An 8-channel portable cassette recorder was used for recording the loads developed on the pylon transducer, which was of the design that Berme et al.(1976) had introduced. The recording system had its own battery power supply and was fitted into a back pack suspended on the waist of the subject by a belt. The pylon transducer signals were amplified, filtered with a cut-off frequency of 40 Hz, then multiplexed with a signal from a goniometer and an eighth signal, which was a pulse intended to indicate the type of terrain. The two resulting multiplexed outputs were then modulated using frequency modulation to obtain a 0-40 Hz bandwidth for each channel.

For the playback procedure , Lovely used a tape

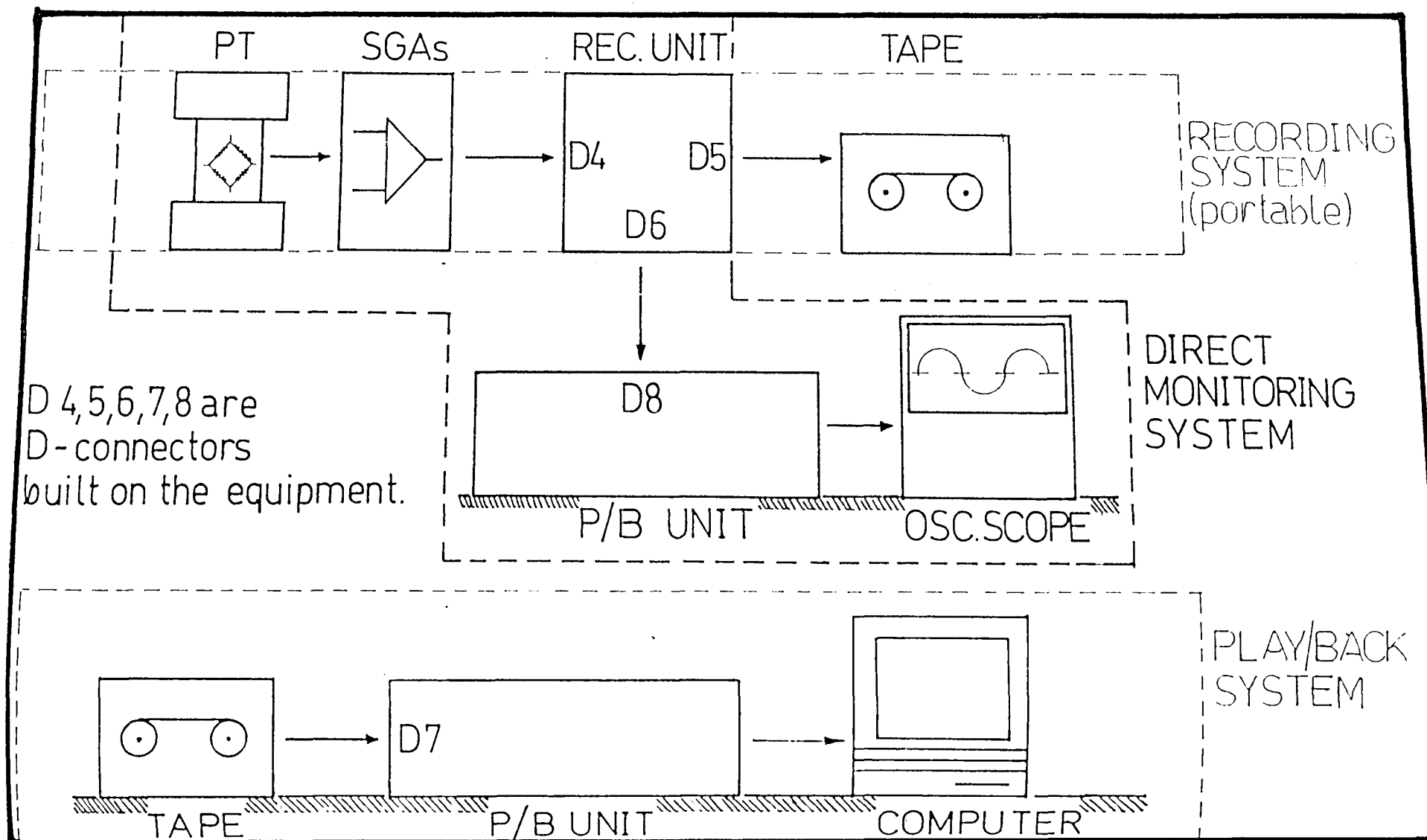


Fig 2.8 Data acquisition system developed by Paschalides, 1989

player. The analogue output signals, already in a demultiplexed form from the playback unit , were recorded on an U/V sensitive paper, using an oscillograph recorder and then fed into a microcomputer and processed. However, Lovely suggested later, that direct connection to PDP-12 computer would be preferable avoiding the errors and the delay caused by the U/V recorder (Solomonidis, 1989). This system was used for several outdoor tests (Tilford, 1985).

Pashalides (1989) developed a new system for recording and playback of the data (fig 2.8). As shown, the portable system consisted of the pylon transducer (shown as PT) mounted on the prosthesis , the strain gauge amplifiers (shown as SGAs) also mounted on the prosthesis , the recording unit (with its installed batteries), suspended on the subject's waist belt and the tape recorder/player carried on the same belt.

The recorded data could be played back, using the playback unit, resulting in analogue signals, which could then be fed into a computer (PDP-11) for further processing. Pashalides' design incorporated a direct monitoring facility which enabled the monitoring of the system's performance on an oscilloscope, before leaving the laboratory for outdoor tests. The succession of signal processing stages that the design of Pashalides adopted was as follows :

the output signals from the pylon transducer were first amplified in the strain gauge amplifiers, then fed into the recording unit where they were filtered, normalised, joined by another two signals (foot - switch , goniometer or others) and multiplexed resulting in four analogue multiplexed signals, which were digitized by an A/D Converter and then recorded onto the tape in a digital form. For the playback procedure the inverse steps were followed resulting , after demultiplexing , in eight analogue outputs.

Some improvements of the system, regarding the

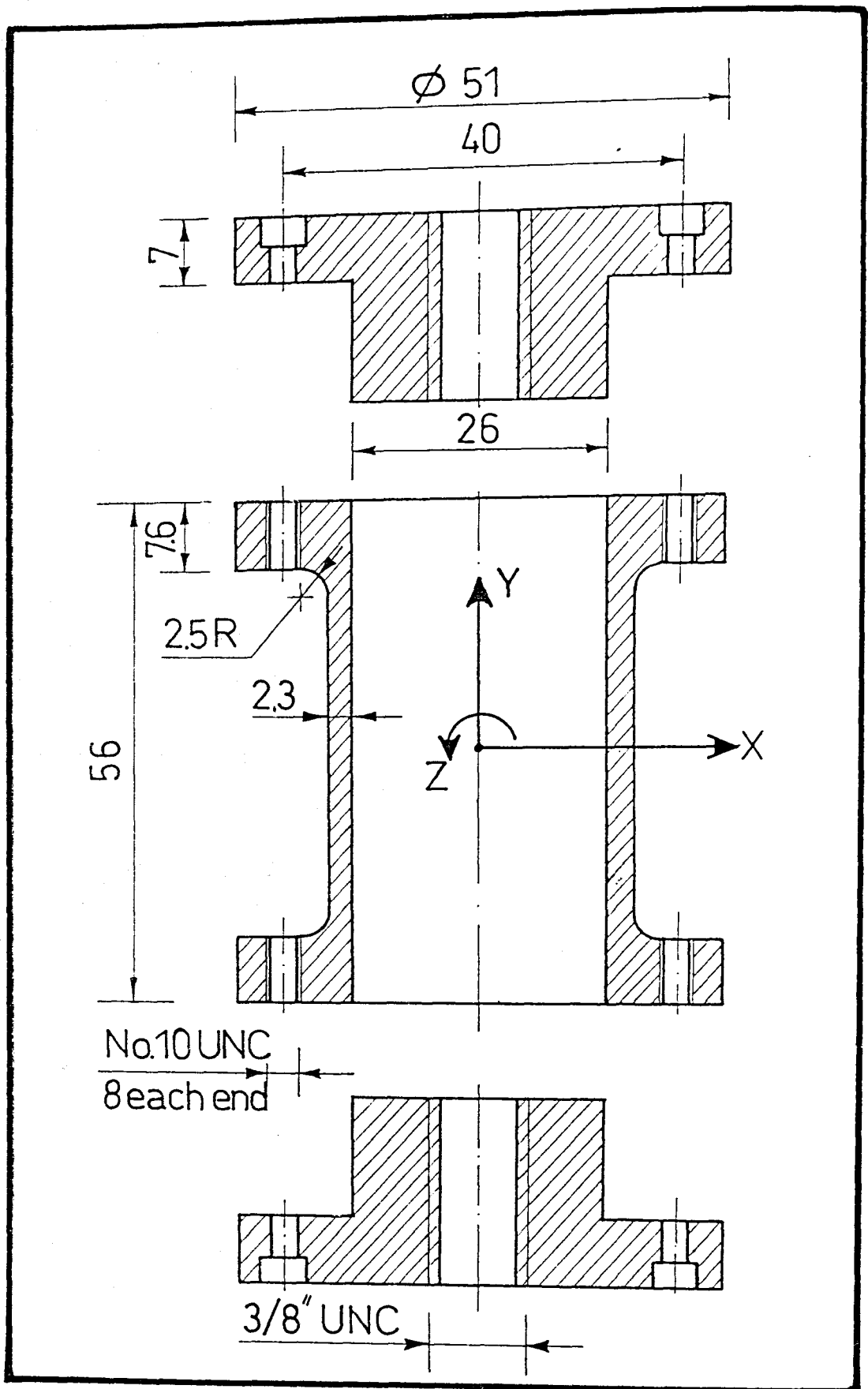


Fig 2.9 The pylon transducer designed by Berme et al, 1976

strain gauge amplifiers, have been carried out and actual outdoor tests have been undertaken by Ainscough (1991). The short pylon transducer designed by Berme et al. (1976) was used in the above system. A detailed presentation of this device follows in the next section.

2.4.5 The short Pylon Transducer designed by Berme et al. (1976)

The short pylon transducer consists of a tubular piece made of aluminium alloy (BS 6082 T4 *). The dimensions are shown in figure 2.9 with the frame configuration adopted. When the top and bottom covers shown are fixed on the tubular part, the overall length is 70 mm. The two covers allow connection with adaptors and hence with the prosthesis.

The gauging is performed on a single area with two series of full bridges, each responsible for one single component of the load acting upon the device : there is a bridge for AP shear force F_x , for axial load F_y , for ML shear force F_z , for ML bending moment M_x , for torque M_y and for AP bending moment M_z .

The two series of gauges are as close as the dimensions of the gauges permitted and the gauges are bonded using a heat curing epoxy adhesive (M-BOND 610).

The gauges responsible for monitoring bending moments and axial load are placed on the upper level and the gauges responsible for monitoring torque and shear forces are placed on the lower level (fig 2.10).

The axial load is obtained using four 90-degree 120 Ω rosettes equi-spaced around the periphery.

The torque and shear loads are monitored using two 90-degree 120 Ω rosettes for each quantity, each aligned at 45° inclination from the longitudinal axis.

* Before the introduction of the four-digit designation in June 1980, this alloy was designated as HE 30 WP

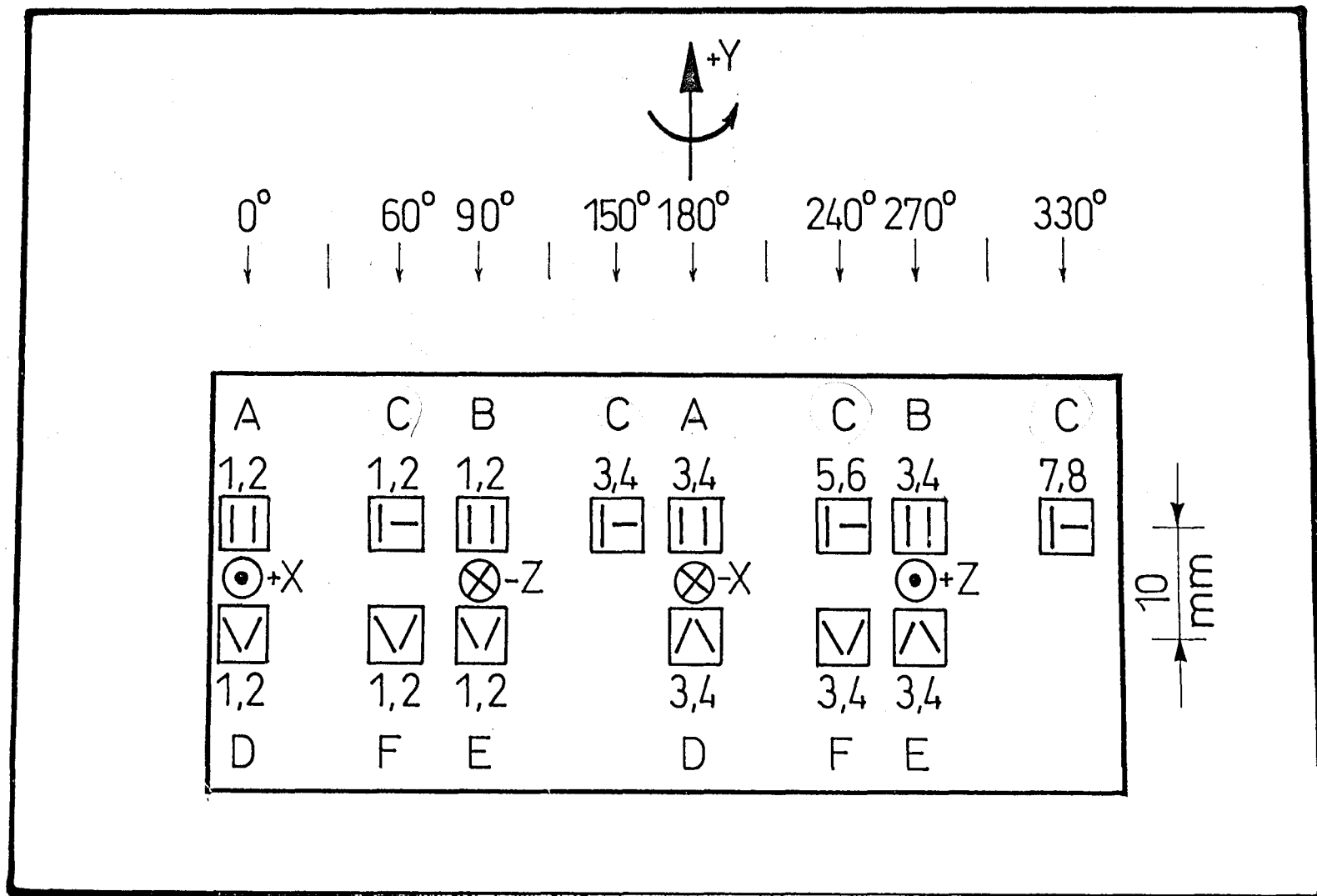


Fig 2.10 Gauging diagram of the pylon transducer
designed by Berme et al.1976

The bending moments are monitored using two standard bending-application rosettes for each quantity placed at 180° intervals around the periphery. Each full bridge consists of four resistances of $120\ \Omega$.

The wiring of all strain gauges is shown in figure 2.11 . The response of the transducer to all individual load components is presented in detail in chapter 3.

Berme et al. (1976) reported that when fitted in the prosthesis of a walking amputee, the transducer experiences loads of the following order: 100 N for shear loads, 1500 N for axial load , 150 Nm for bending moments and 20 Nm for torque.

2.5 Standards for Structural Testing of Prostheses and Design Criteria

As has been already pointed out, the reason for research in prosthetic loading data acquisition, is the need for identification of the loads applied onto the artificial legs and the production of design criteria for further improvements of the amputees' limb substitutes.

Several international meetings were convened for the presentation, grouping and publication of the international knowledge and experience in the field; the main task being the development of standards and criteria for the design and testing of modular prostheses.

The Committee on Prosthetic Research and Development (1971) reported the results of the first such meeting which was held in San Francisco under the title "Cosmesis and the Modular Prostheses". The necessity of international standards for various amputee populations was emphasised and the first definitions regarding the terms "cosmesis" and "modular prosthesis" were introduced.

It must be appreciated that at those early days of the introduction of modular endoskeletal prostheses , a certain controversy existed on whether the exoskeletal

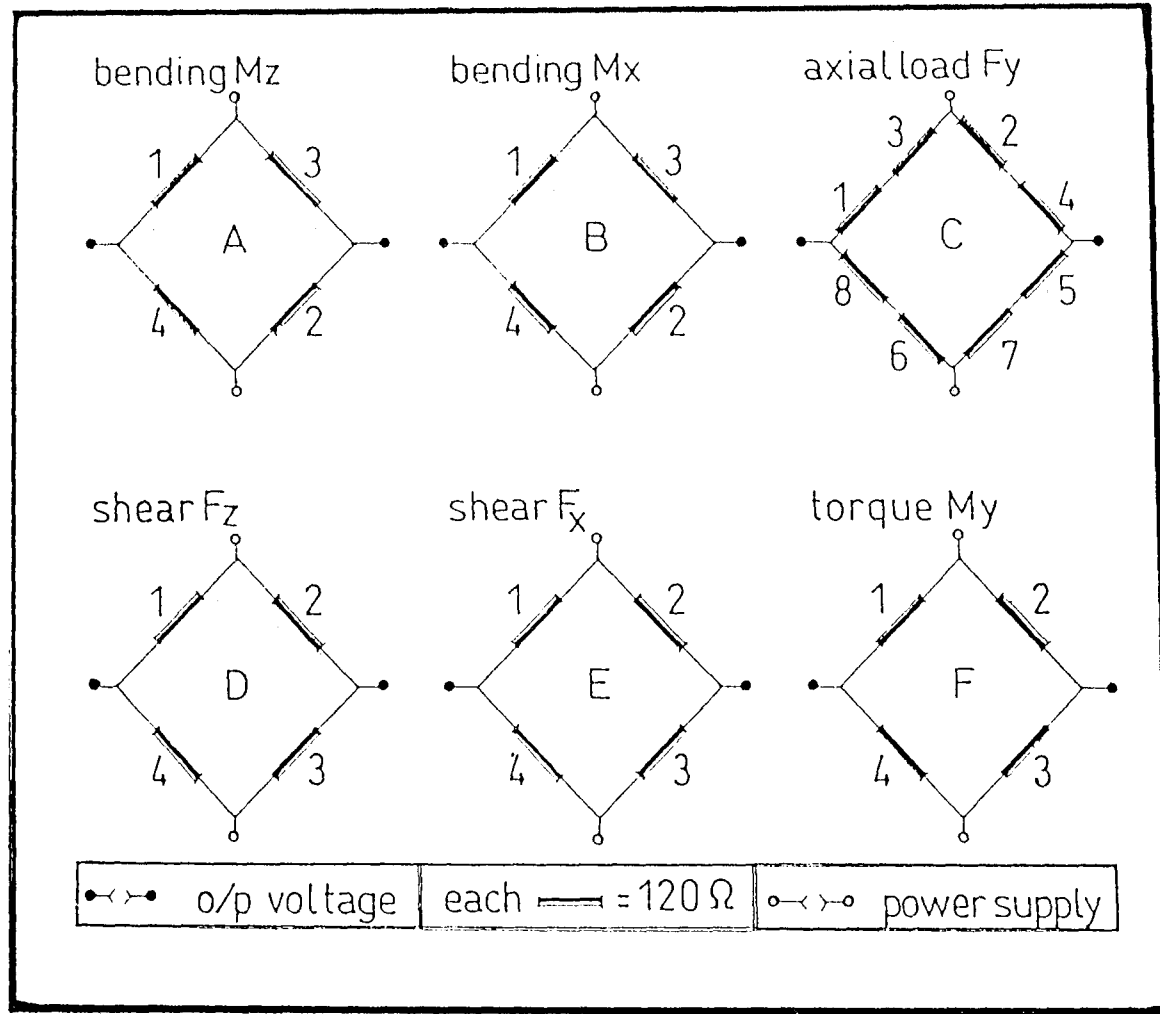


Fig 2.11 Wiring diagram of the pylon transducer
designed by Berme et al, 1976

designs could also be considered as modular or not. One important result of the above mentioned conference was the development of definitions for various terms used in prosthetics. Thus, having distinguished between modular systems and conventional systems the following definition was adopted for the term "modular" : modular is the prosthesis which has accessible a number of interchangeable components which can be assembled easily and quickly into the prosthesis. The term "cosmesis" was defined as follows : cosmesis is the combined quality of static and dynamic appearance, feel, odour and sound which enhance the acceptance of a prosthesis by an amputee.

The recognition of the need for the international use of the metric system was another important outcome.

The Department of Health and Social Security (1972) reported on the Conference held in Ascot under the title " Lower Limb Modular Prostheses ". It is reported that during this conference scientists realised that the loading data acquired in former times were not sufficient and further tests should be performed to obtain statistically better data. It was also agreed that the amputee population should be divided into various categories regarding the activity level of the subject and data for each category should be distinguishable. During this meeting the necessity to set standards for the mechanical testing of artificial limbs was recognised , since modular prostheses had started being more broadly adopted.

A first attempt to derive conclusions from experimental results was reported by the International Society for Prosthetics and Orthotics and the Department for Health and Social Security (1973). As reported, in a conference held in Dundee under the title : " Design Criteria in Lower Limb Prostheses / Amputee Performance Measurement " , three definitions were established for strength values of artificial limb design :

The static strength , relating to the most severe loading activity, excluding overloading conditions, for which no permanent deformation occurs. The dynamic strength , relating to the anticipated repetitive loading of the artificial leg. The ultimate strength , which should be set such as to allow permanent deformation without failure.

Scientists also recognised two loading conditions: the static load which is the value of the maximum load experienced during laboratory tests and describes the range of locomotor activities that the prosthesis should be able to sustain without permanent deformation and the cyclic load which is the value of the maximum load exhibited during level walking in the laboratory under comfortable speed.

It was considered important to determine quantities such as the life span of a prosthesis in order to derive data concerning the frequency and the magnitude of cyclic loads resulting in fatigue effects. Although the data were not considered to be sufficient and the statistical confidence was not still high , a first attempt for the description of proof and dynamic tests loads was performed based on 100 kg-body-mass active amputees.

It has already been mentioned earlier in this chapter , that the issue of frequency response of the recording systems had remained unresolved for several years. ISPO and DHSS (1973) however, report that the above problem was pointed out and it was agreed that frequency response is a most critical factor in affecting data of the more unusual type of activity.

The Conference " Physical Testing of Prostheses " in Heathrow (DHSS , ISPO , 1974) provided a final recommendation on the issue of frequency response of the recording systems. It was suggested that between 100 and 1000 Hz , there are not significant components

	Axial Load Newtons		Torque Newton Metres		Knee A.P. Bending Newton Metres		Knee M.L. Bending Newton Metres		Ankle A.P. Bending Newton Metres		Ankle M.L. Bending Newton Metres	
	Static	Cyclic	Static	Cyclic	Static	Cyclic	Static	Cyclic	Static	Cyclic	Static	Cyclic
Heathrow 80 Kg	2120 b/k	1060 a/k	26.7 a/k	12.5 a/k	165 b/k	90 a/k	125b/k 90a/k	80 a/k	210 b/k	110 b/k	45 b/k	30 a&b/k
Heathrow 105 Kg	2780	1390	35	17	220	120	165b/k 115a/k	105	280	145	60	45
PHP 1	2783	1391	34.8	16.4	250	118	164	85	276	144	100	50
PHP 2 All categories	2250	1300	35	20	230	120	150	80	230	140	70	60
PHP 2 Light duty	1120	980	15	-	80	70	45	40	100	95	35	30
PHP 3 as Heathrow at 105 Kg except where a figure is entered		1340		21					static thought too high			
PHP 4 Static loads as Heathrow		1333		20		100 could be higher		80		160		+40
Consensus Figures reached in Plenary Session	2500	1350	35	20	230	120	150	80	250	140	+70	+50

Table 2.1 Values for Standards for Lower Limb Prostheses,
(extracted from ISPO, 1978)

during walking and a bandwidth of 250 Hz was considered as adequate for all walking activities.

Another two important outcomes reported by DHSS and ISPO (1974) were the following : the 100-kg-body-mass amputee for production of design criteria was excessive and that an 80-kg-body-mass subject should be considered as the reference with all other results derived by appropriate factors in order to cover a range between 70 and 105 kg ; with no extrapolation allowed outside this range. It was also agreed that the ultimate strength of prostheses should also be taken into account , for reasons of amputee safety under overloading conditions and that even more data had to be acquired.

ISPO (1978) reported the important outcome of a conference held in Philadelphia under the title " Standards of Lower Limb Prostheses ". The reported work includes minimum standards for the manufacture of prosthetic components and complete prostheses as well as values for static and cyclic configurations for various loads, various categories of amputees and for the mass range of 80 to 105 kg set by DHSS and ISPO (1974). These standards have been in existence since, as guidelines in amputee locomotion testing and modular prostheses manufacture. Table 2.1 shows the evolution of the load values.

In recent years an effort has been initiated in order to include the standards for modular prostheses in the international standards. The International Standards Organisation (ISO) have nominated certain groups of scientists who meet and discuss in order to update the values proposed by the Philadelphia Standards. The documentation is not readily available. However, since the Bioengineering Unit of the University of Strathclyde was and currently is involved in most of the experimental work carried out for this purpose, the author of this thesis was able to acquire

Fig 2.12 The Kobe II loading values and configuration for testing of prostheses

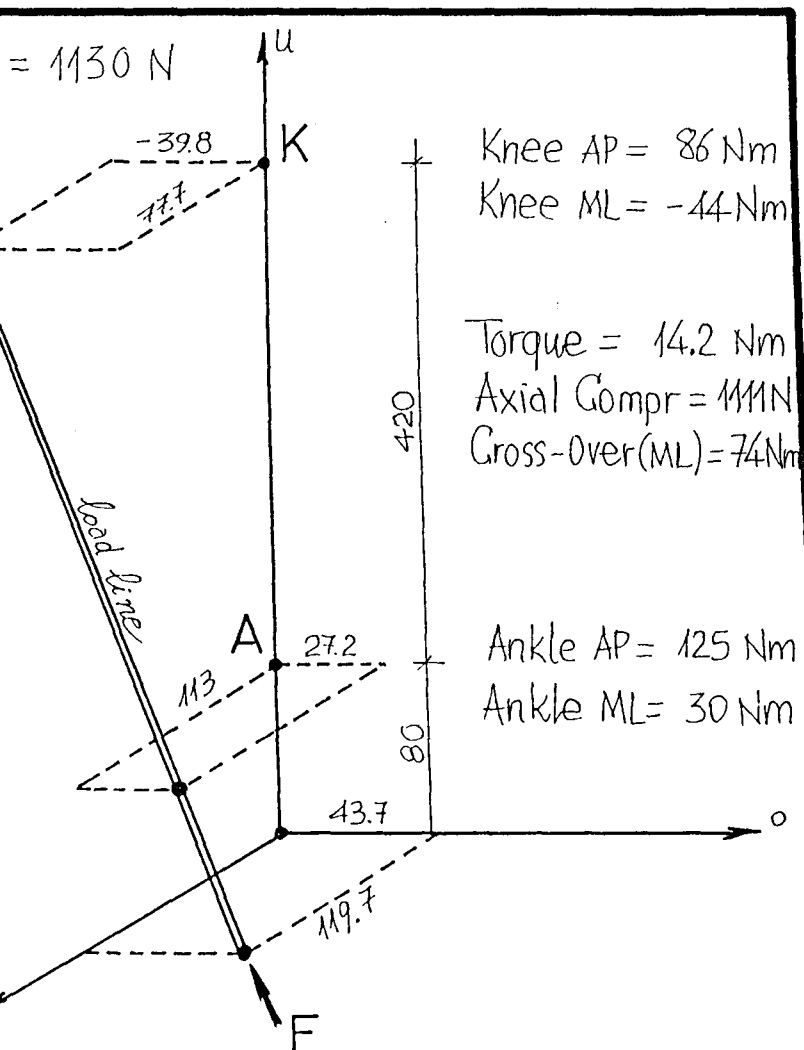


Fig 2.13 The Ottawa loading values and configuration for testing of prostheses

the loading values recommended after two meetings of the international committee.

These meetings took place in Kobe, Japan in November 1989 and in Ottawa, Canada in June 1991 (Paul, 1991) and the results are herein referred to as the "Kobe II" and "Ottawa" values.

At the former meeting the scientists presented a testing protocol and suggested loading values and configuration for the cyclic testing of prostheses (as shown in figure 2.12) . The frequency of the applied load was suggested to be initially 1 Hz and then 3 Hz. For the static tests the applied load was suggested to reach the value of 1800 N . The loading values and configuration recommended after the Ottawa meeting are shown in figure 2.13 .

From table 2.1 and figures 2.12 and 2.13 it can be appreciated that the Kobe II values are considerably lower in comparison to the Philadelphia values and that the Ottawa values are only slightly increased in comparison to the Kobe II values. The above of course applies to both static and dynamic configurations and is indicative of the following (Paul, 1991 and Krieger, 1991) :

In the conference reported by ISPO (1978) researchers produced standards derived by the maximum values of load components encountered during amputee walking activities ; these values not occurring simultaneously. The standards produced during later meetings however, were derived by a compromise between simultaneous load values and were therefore lower, in comparison to the Philadelphia standards. The reason, such a change took place, was the fact that the first testing standard values were so high that prostheses failed during testing while no such failures were reported in practice. Therefore the concept of compromise between simultaneous load values was adopted from then on.

2.6 Prosthetic Alignment

2.6.1 Introduction

Even before the development of modular endoskeletal lower limb prostheses, when the exoskeletal type of artificial leg was still widely used, the relative positioning of the parts comprising the limb substitute was found to be very important for its functional behaviour. Both the mechanical behaviour of the prosthesis and the amputee's comfort were considerably affected by alterations of the geometrical configuration adopted, even when the same components were used.

After the development of modular endoskeletal prostheses separated the two main functions of a prosthesis (namely to function and to look like a normal leg), the subject of alignment entered into a process of standardisation.

2.6.2 Terminology

The process of finally verifying that all aspects of the prosthesis (including fit , function and appearance) are satisfactory at delivery is referred to as the c h e c k -o u t .

The term f i t t i n g is used for the shaping and contouring of the inner surfaces of the socket to the outer surfaces of the stump (Haddan, 1968).

The term a l i g n m e n t , as already mentioned, refers to the inclination and position in space of the components of the prosthesis relative to each other.

In common prosthetic practice and particularly at the early stages of an amputee's rehabilitation procedure, all these terms could be used to describe the prosthetist's effort in achieving the best functional result and comfort. The terms alignment, fitting and check-out are not separate but form part of a single complex procedure, consisting of initial formation and adjustments and alterations based on

assessment made from observations of patient performance and feedback of comments.

However, once a good fit of the socket has been achieved , the prosthetist can concentrate on establishing a functional alignment and can direct the prosthetic efforts to achieving the most suitable geometrical configuration of the prosthesis. Taylor (1979) draws attention to the fact that alignment must not be used to compensate for ill-fitting sockets but that a correct stump-socket interface contact must always be established first. In such a case, one can then refer to the term alignment alone, and for practical reasons distinguish three different stages of alignment : the bench alignment, the static alignment and the dynamic alignment. As presented by British Standards (BS 7313, 1990) these terms are defined as follows :

The term *b e n c h a l i g n m e n t* refers to the initial assembly and alignment of the components of a prosthesis in accordance with their characteristics and with previously acquired data regarding the patient.

The term *s t a t i c a l i g n m e n t* refers to the process whereby the bench alignment is refined while the prosthesis is being worn by the statutory patient.

The term *d y n a m i c a l i g n m e n t* refers to the process whereby the alignment of the prosthesis is optimized by using observations of the movement pattern of the patient.

The term *a l i g n m e n t* also means the actual configuration of the prosthesis itself, after the alignment procedure has been carried out . In this case the term *a l i g n m e n t p a r a m e t e r s* can be used to refer to the parameters necessary for the qualitative description and quantitative assessment of this configuration (for definitions see section 2.7.4).

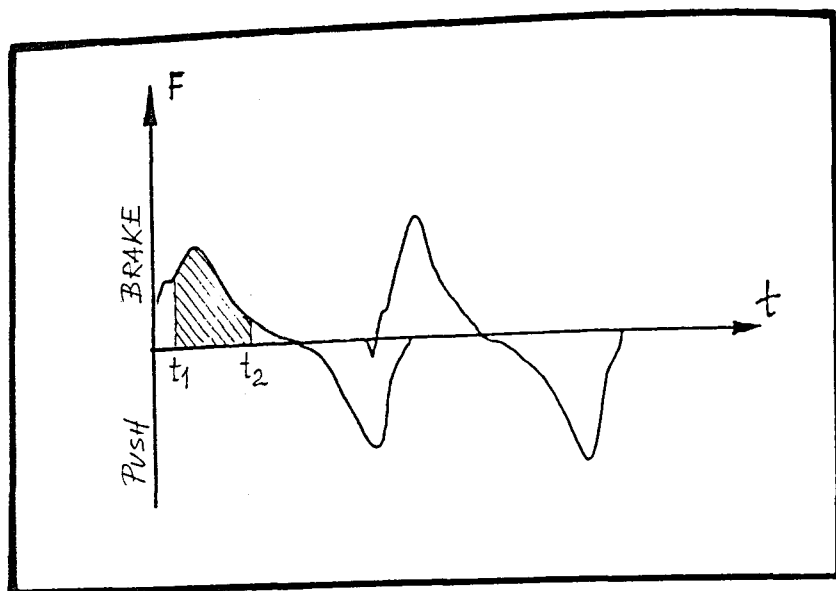


Fig 2.14 The impulse of the AP ground reaction component (adopted from Seliktar et al, 1982)

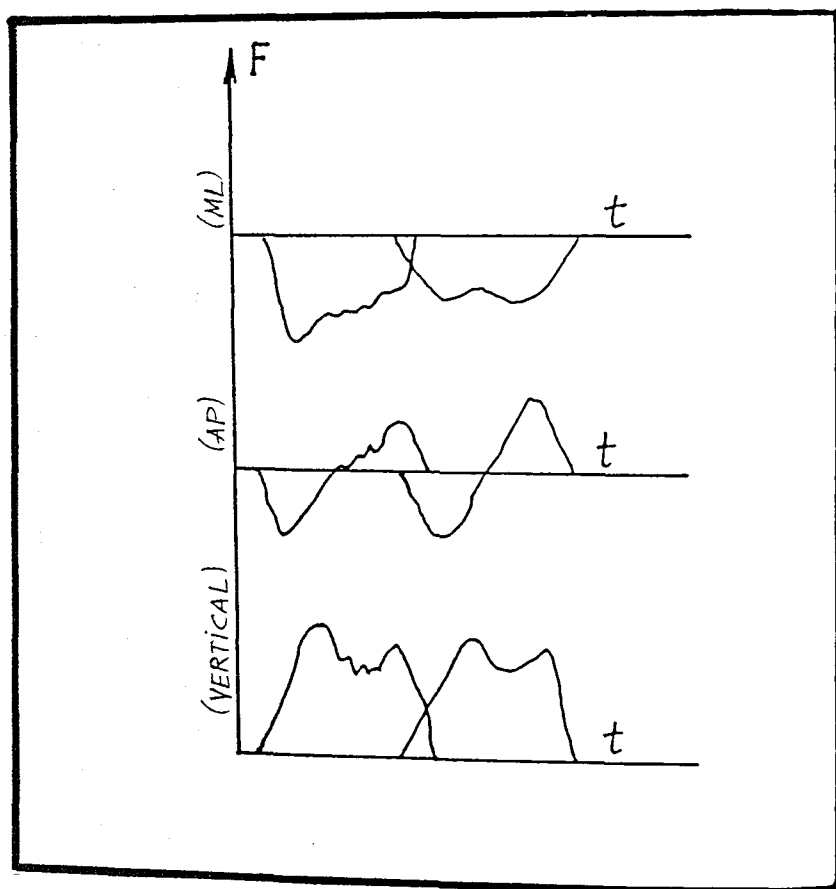


Fig 2.15 The perturbations of the ground reaction components on the prosthetic side of an amputee (adopted from Seliktar et al, 1982)

2.6.3 Studies on Optimum Alignment

The achievement of the optimum alignment for the lower limb prostheses has been studied with particular reference to the kinetics and kinematics of amputee locomotion, in order to determine criteria for the establishment of optimum alignment.

Seliktar et al. (1982) recognised that the alignment of an artificial leg depends considerably on the skills and the intuition of the prosthetist, even though some established routines do exist for this purpose. The objective of the reported work, therefore, was to produce an adequate monitoring technique which would enable the systematic alignment of the prosthesis and eventually the establishment of an optimum alignment.

Two force platforms were used for the monitoring of ground reaction force, connected to a minicomputer and closed circuit TV system for the acquisition of kinematic data. The patient was a BK amputee who worn an Otto-Bock modular prosthesis. The research team performed alignment changes on the prosthesis, in a controlled fashion, separating the effects of tilts and translations.

The recorded kinetic and kinematic data were processed and the variation of the impulses of the AP and ML reactions were studied. Figure 2.14 shows a typical output that these researchers obtained for the AP component of the ground reaction force. Thus, the braking, the pushing and the overall impulse were calculated. Seliktar et al. (1982) also reported that the alignment changes performed were reflected on the obtained impulse values, but unfortunately it was suggested that no conclusions could be drawn because of the limited amount of tests in that preliminary study. However, the researchers observed that the perturbations occurring in the pattern of the three components of the ground reaction force were highly dependent on the alignment changes (fig 2.15). It was

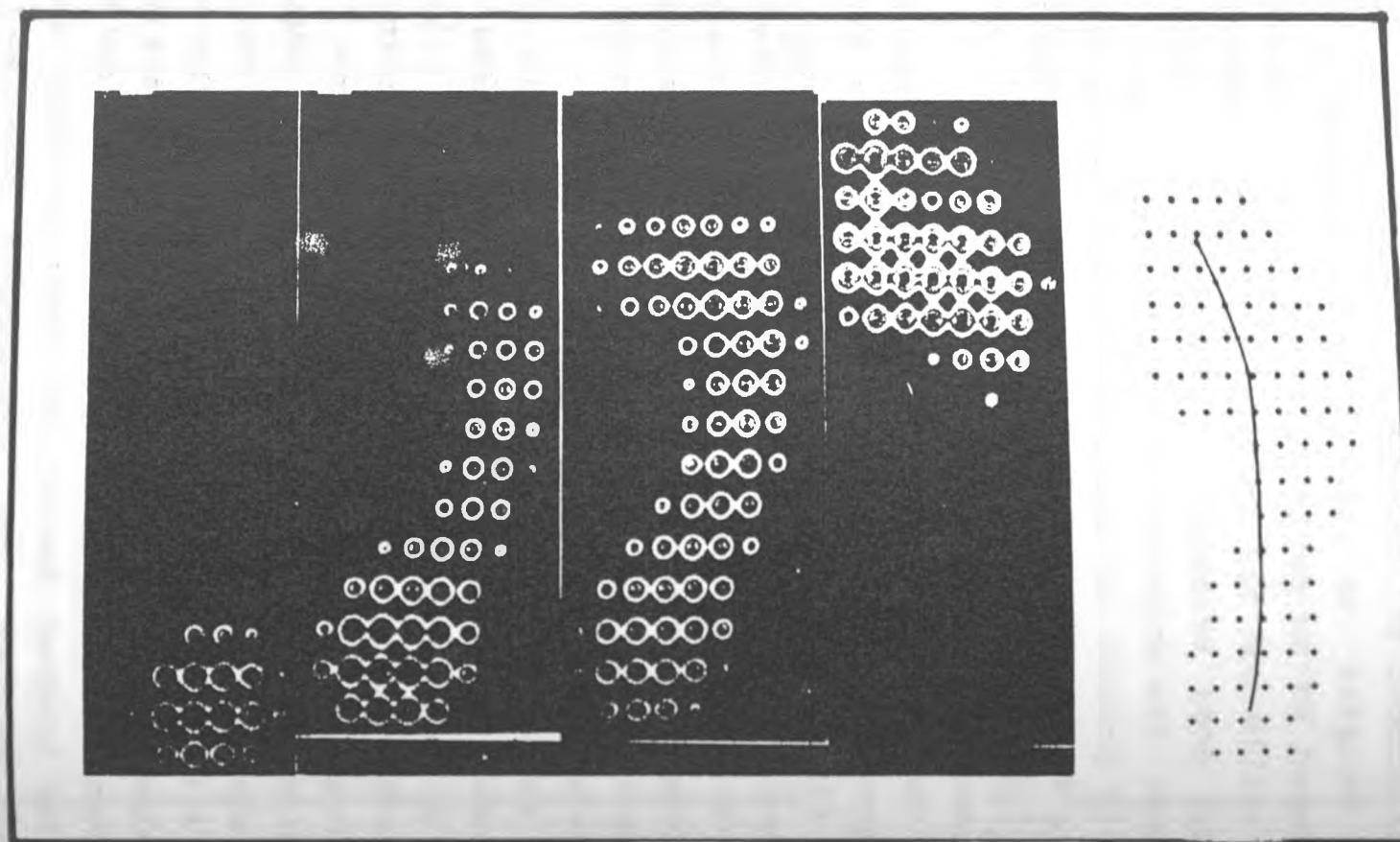


Fig 2.16 Characteristic contact phases of a normal subject
(extracted from Arcan et al, 1982)

suggested that the observed perturbations were indicative of the stability of the prosthesis. The author of this thesis noticed that the two diagrams shown displayed different conventions for the sign of the antero-posterior force.

Seliktar et al. (1982) also reported that an optimal state of alignment could be achieved by reducing the perturbation to a minimal size; this usually occurring when brought as close as possible to the time axis.

The work and results presented by these researchers is a positive experimental contribution. However, the evaluation of the gait is a problem which involves many aspects and could not be concluded with the study of one or two parameters. For instance, a particular perturbation could be the result of either a poor alignment, either a poor socket fit or both and the reported work does not comment on their distinction. A possible answer to the above comment could be the change of the socket which would allow comparative studies and thus conclusions; leading, however, to a procedure too long for clinical purposes.

Arcan et al. (1982) reported another approach. According to their theory, the quality of the alignment would be reflected on various parameters related to the centre of pressure at the foot-to-ground interface.

The reported method called the Foot-Ground-Pattern (FGP) involved a 15-meter-long modular test track which in some areas incorporated an FGP system, based on an optical pressure-sensitive sandwich. When exposed to monochromatic light the system gives an optical measurement of the local forces over a large amount of points. The output of the FGP system could be both immediately displayed and filmed.

Arcan et al. (1982) initially developed the following criteria (see fig 2.16): a) the trajectory of the centre of pressure was centered on the total FGP area, b) its shape was close to a straight line,

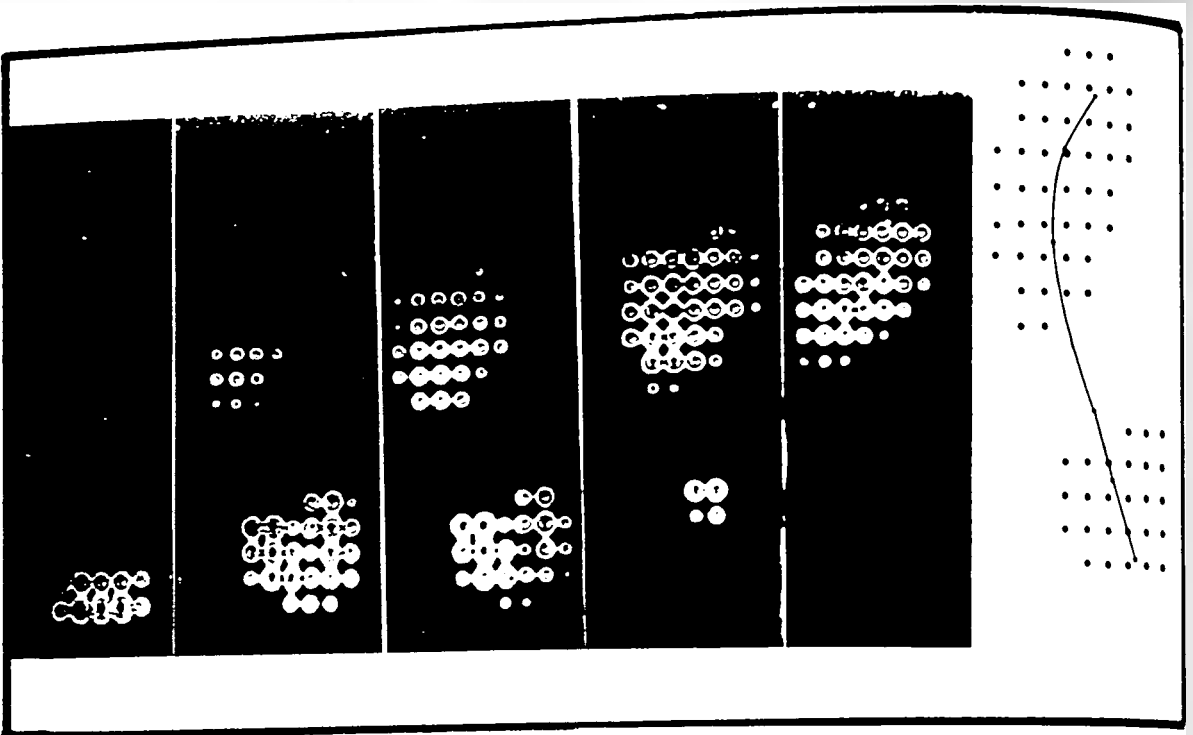


Fig 2.17 Characteristic contact phases of the prosthetic side of an AK amputee before alignment corrections (extracted from Arcan et al, 1982)

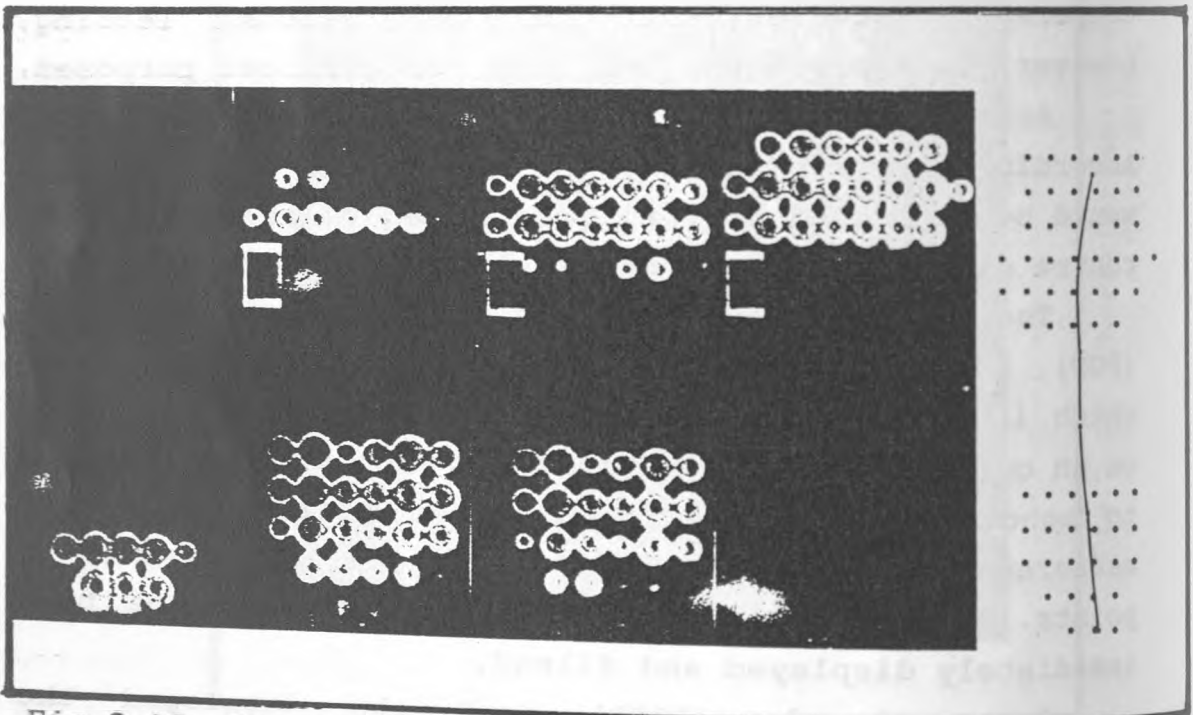


Fig 2.18 Characteristic contact phases of the prosthetic side of an AK amputee after alignment corrections (extracted from Arcan et al, 1982)

deviating medially during push-off in some cases, and c) its general direction was approximately parallel to the sagittal plane.

The services of twelve AK amputees were then enrolled and data were acquired before and after alignment changes. By comparisons of the results to the criteria, the alignment could be improved until the obtained patterns met the criteria, for both sound and prosthetic sides. Typical output patterns are shown in figures 2.17 and 2.18.

The results were considered encouraging and further experimental work was recommended. The presented method is a positive contribution at the understanding of the effect of alignment on the foot-to-ground contact mechanics, mainly because both sides of the patient are studied under the same criteria. However, until further results are acquired, the clinical usefulness of the method cannot be established and, as reported, further investigations were planned. It was also suggested that further development of the FGP system was also required because the system relied on a calibration graph which was linear in a limited range only.

Ishai et al.(1983) suggested that the major source of discomfort for the AK amputee during the swing phase of walking, is the thigh axial torque (TAT) developed at the stump-socket interface.

These researchers based the development of the method in the hypothesis that the best possible alignment should be the one resulting to minimal TAT peaks. For the evaluation of TAT, a mathematical model was developed, based on three sets of quantities :

- a) the mass, inertia and geometry of the shank, b) the knee and thigh absolute kinematics and knee flexion-extension angle and c) a set of six alignment adjustments that they defined at the knee/socket interface (3 shifts and 3 tilts) .

For the evaluation of the method a series of

simulated gait patterns was used, based on already published kinematic data from normal subjects. Applying optimization techniques to the developed model and imposing the requirement of TAT-peak minimization, Ishai et al. (1983) obtained the values of the alignment parameters they had defined and introduced in the model.

The researchers suggest that TAT, instead of being calculated could be measured by a pylon transducer and that the kinematic data should be, in future work, acquired by actual clinical tests. They also draw attention to the fact that because of lack of a rigorous definition of the interaction between TAT and patient comfort, they had to use the criterion of the TAT-peak minimization. Once established, such a definition would, as reported, allow for more complex criteria to be developed. On the other hand the optimization of the alignment would then be expanded to include other swing and stance phase considerations.

From the reported conclusions it can be appreciated that, despite the quality of the developed model, the method had to be enriched with more criteria.

A new approach to the problem was reported by Hannah et al. (1986) . The approach adopted involved kinematic data and was based on the hypothesis that optimum alignment should be the one resulting in the best kinematic symmetry between the two legs of the patient. Tests were carried out on five BK amputees one of whom was bilateral. The patients were fitted with Patellar Tendon Bearing (PTB) prostheses and during tests a set of goniometers was used to record 3-D angular data of the hips and knees on both sides. Alignment changes were performed as deviations from the initially established optimum alignment and the patients were asked to walk at their own pace on a 10-meter walkway. Data were used for the calculation of a symmetry index that had already been defined.

Fig 2.19 Fourteen different acceptable alignments by prosthetist No 1 on patient No 1 (AK) ; range of adjustment allowed by the Otto Bock system is also shown (extracted : Zahedi et al, 1986)

Hannah et al. (1986) reported that generally the hypothesis was supported and any deviation from the pre-set optimum alignment resulted in an increased asymmetry between the two sides. The most positively reported outcome of this work was that the foot dorsiflexion was found to be the most important alignment change and that the hip flexion / extension motion was the most sensitive kinematic parameter to alignment changes.

It was also suggested that further work was needed in order to investigate the importance of maintaining symmetries in some planes and joints in preference to others.

Saleh and Bostock (1988) reported a different approach. They investigated the influence of alignment changes on the ground reaction force using Kistler force platforms and created loop-diagrams of the vertical component versus the AP component.

The results obtained by five BK amputees indicated a very strong relationship between the obtained pattern and the alignment deviations from the initially pre-set optimum configuration. The authors suggested that this method could be clinically used for the achievement of the most suitable alignment by the prosthetists.

The loop-diagrams were reported to be almost as characteristic for a patient as a fingerprint. The author of this thesis believes, therefore, that no reliable reference exists for the prosthetist, unless the desirable pattern is already known. On the other hand the loop-diagram of the sound side cannot be considered as the desired pattern, since it is not independent from the performance on the artificial side. The published paper did not present any quantitative results and thus any further conclusions were disabled.

It was noted, through the literature review, that the presented works were based on the assumption that there is indeed an alignment configuration, which can

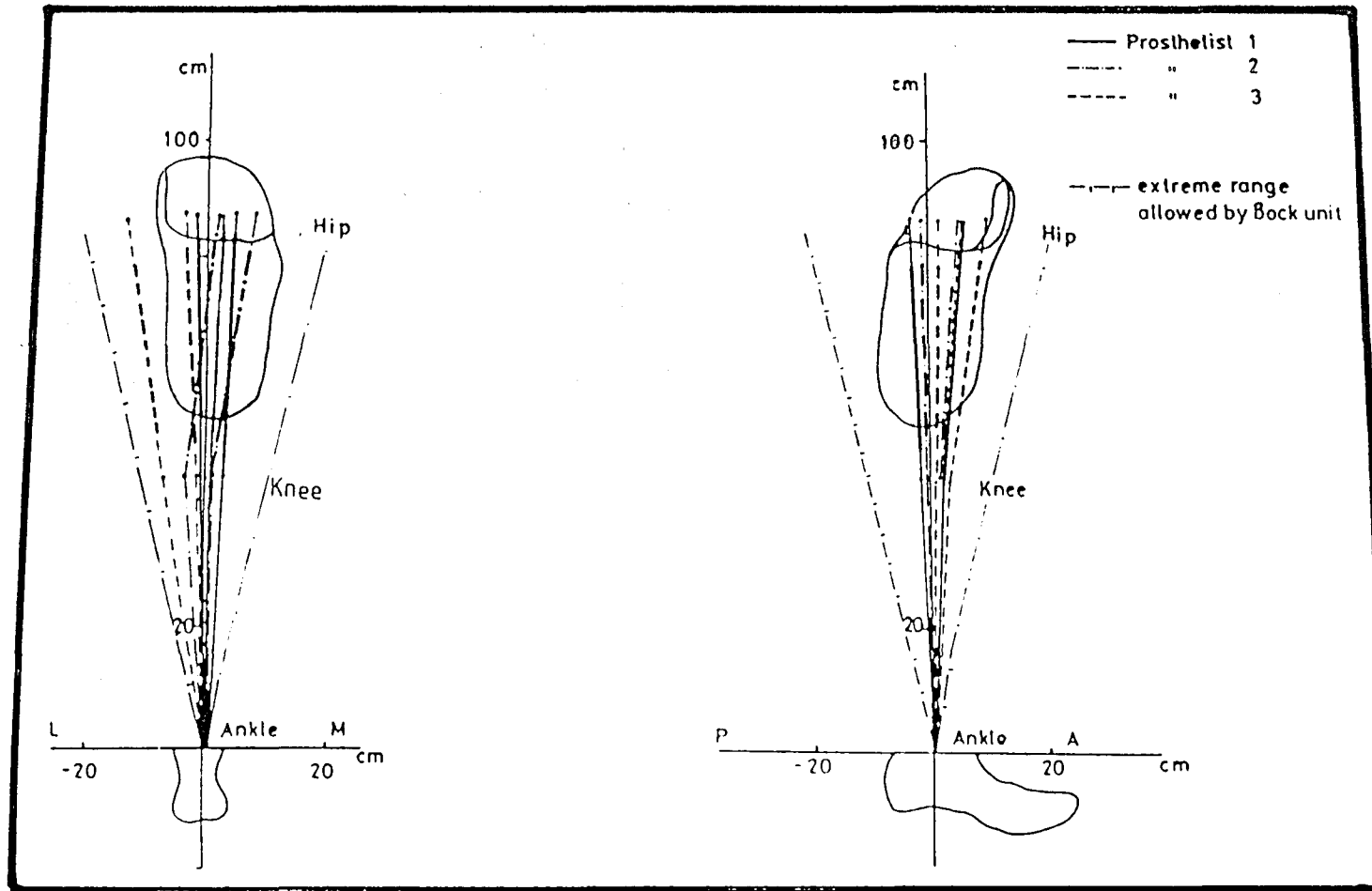


Fig 2.20 Range of alignment acceptable to patient No 1 (AK) for three prosthetists ; range of adjustment allowed by the Otto Bock system is also shown (extracted : Zahedi et al, 1986)

be considered as the optimum one . However, this assumption could only be based on strong indications that the amputees really preferred a particular alignment configuration to all other configurations ; and such published data were not available. Therefore, the assumption that an optimum alignment existed was based rather on scientific intuition than on any established feedback from amputees and prosthetists.

The first indications that an optimum alignment does not exist were obtained from the work of Solomonidis (1980) who evaluated AK modular systems. Lawes (1982) tested BK and AK amputees and also reported that there was no evidence of existence of a single and well defined optimum alignment.

Furthermore Zahedi et al. (1986, 1987) having carried out tests on twenty active BK and AK amputees, finally confirmed that a very broad range of alignment configuration (for some parameters 148 mm in shifts and 17° in tilts) was considered satisfactory and acceptable by the amputees.

The services of three prosthetists were enrolled and a total amount of 183 BK and 100 AK fittings were tried. The effect of each different prosthetist on the established range of alignment for each patient was found significant . Zahedi et al. (1986, 1987) also investigated the possibility of the prosthetist achieving an alignment repeatedly at will and reported that there was no indication for such a consideration (typical results from these studies are shown in fig 2.19 and 2.20).

Therefore, it was suggested that the task in alignment studies should be the achievement of an acceptable alignment, within the ranges considered optimum and recognised the need for an assessment method, which could assist the prosthetist in having a quantitative estimate of the alignment configuration imposed throughout the process.

The assessment of the alignment of the lower limb

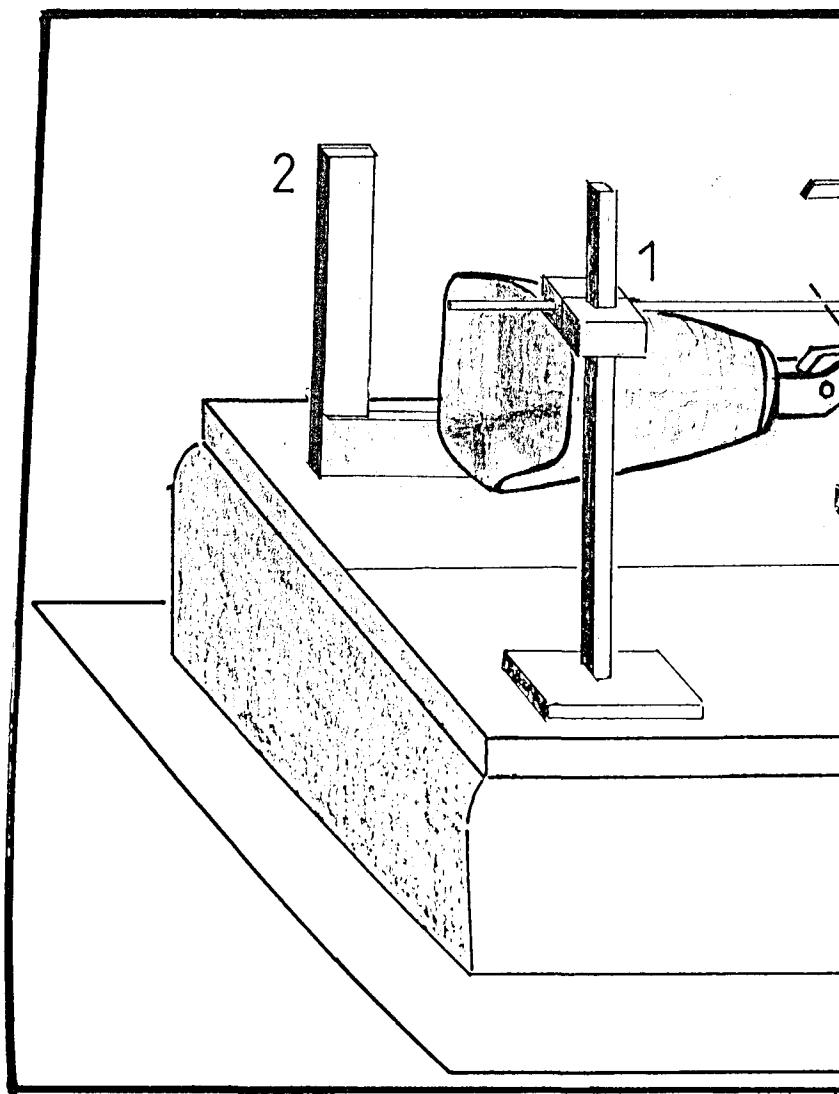
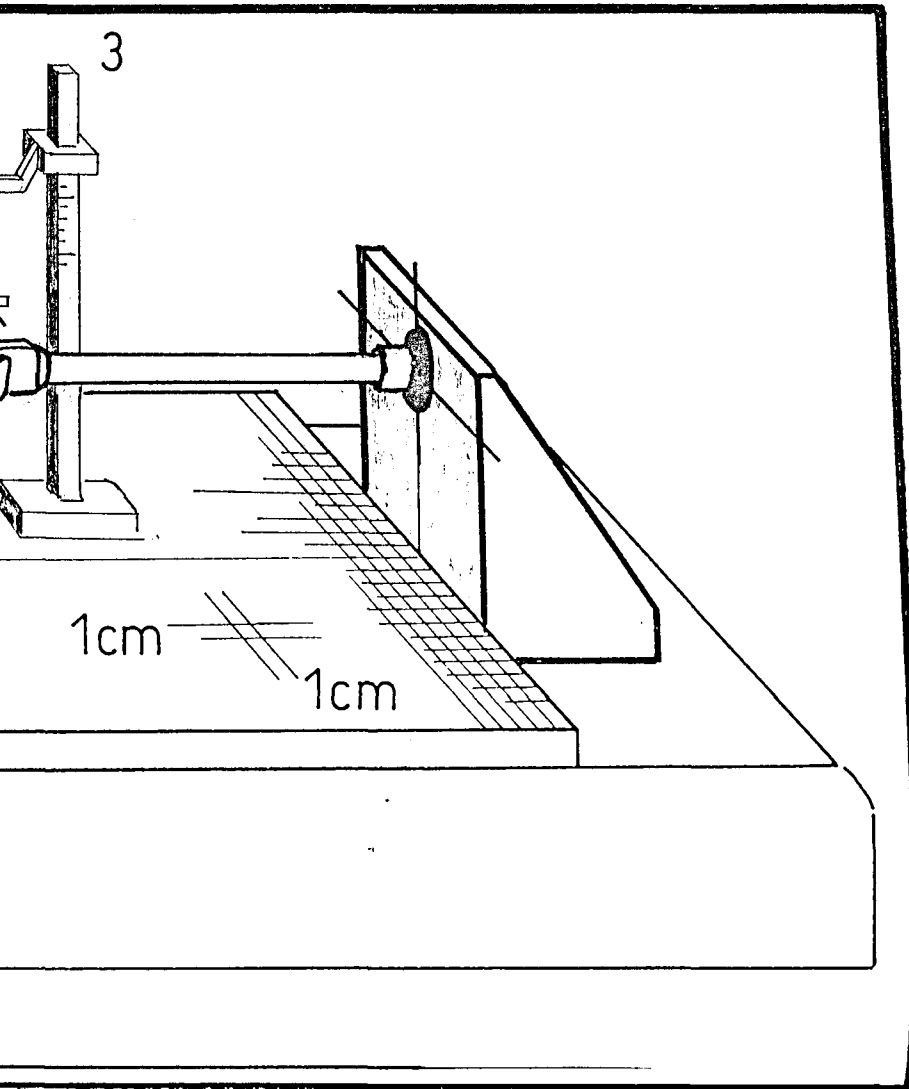


Fig 2.21 The alignment rig



of the Bioengineering Unit

prostheses is of major importance , in any studies involving the investigation of the effects of alignment on various quantities. The work of Solomonidis (1980), Lawes (1982) and Zahedi et al. (1986,1987) led to the development of the alignment rig , a device for the measurement of alignment.

2.6.4 The Alignment Rig

Zahedi et al (1983) describe the alignment rig as follows : it is a cast-iron baseplate fitted with a 120 by 50 cm horizontal perspex plate accurately marked with a grid of (1 cm x 1 cm) squares.

The prosthesis to be measured is mounted on a bracket, rigidly fixed to the baseplate (fig 2.21). The alignment parameters can be evaluated from results obtained by measurements of coordinates of all major landmarks relative to the rig frame. All points needed to describe the socket frame should be already marked onto the inner surface of the socket, having first been identified using the Socket Axis Locator (detailed description in section 2.7.2) . A specially designed device (1 in fig 2.21) can provide access to the marks and their coordinates can be measured by means of a square (2 in fig 2.21) with readings directly from the horizontal grid and a height gauge (3 in fig 2.21). The latter instruments are also used to determine the coordinates of the medial and lateral points of the knee axis on the knee unit. For the definitions of frames of reference and alignment parameters see section 2.7.4 of this chapter.

The rig measurement technique was reported (Zahedi et al, 1986) to provide a precision of ± 0.5 mm and the alignment parameters could be assessed with an overall accuracy of $\pm 1^\circ$ for tilts and ± 1 mm for shifts.

2.7 Definitions and Conventions used in this Thesis

2.7.1 Introduction

The term alignment parameters

refers to the parameters selected to represent the angular tilts and linear shifts that most alignment units implement, providing the prosthetist with the ability to perform various adjustments on the prosthesis.

For these alignment parameters to be defined , a set of frames must be allocated to each one of the major landmarks of the prosthesis. These frames are also used in order to calculate the components of the prosthetic loads at the associated landmarks (ankle, knee and hip).

Note : As will be noted, the author of this thesis has generally adopted the right hand rule for right leg prostheses and the left hand rule for left leg prostheses.

2.7.2 Frames of Reference

The frames used are all cartesian X-Y-Z frames , with the X-axis being positive towards the anterior side , the Y-axis positive upwards and the Z-axis perpendicular to the other two and positive to the lateral side (the direction of the Z-axis depends on whether the prosthesis is a right or a left side one, for reasons due to symmetry and explained later).

The definition of frames of reference for the parts of a prosthesis is generally easy to make, mainly because the components are mechanical parts with well defined dimensions and axes. The major problem in defining axes on a prosthesis is the socket. However, a method was gradually developed for the accurate determination of a socket frame of reference :

Socket

During the project for the evaluation of BK and AK prostheses a method for defining the frame of reference of the socket was conceived Lawes et al.(1976).

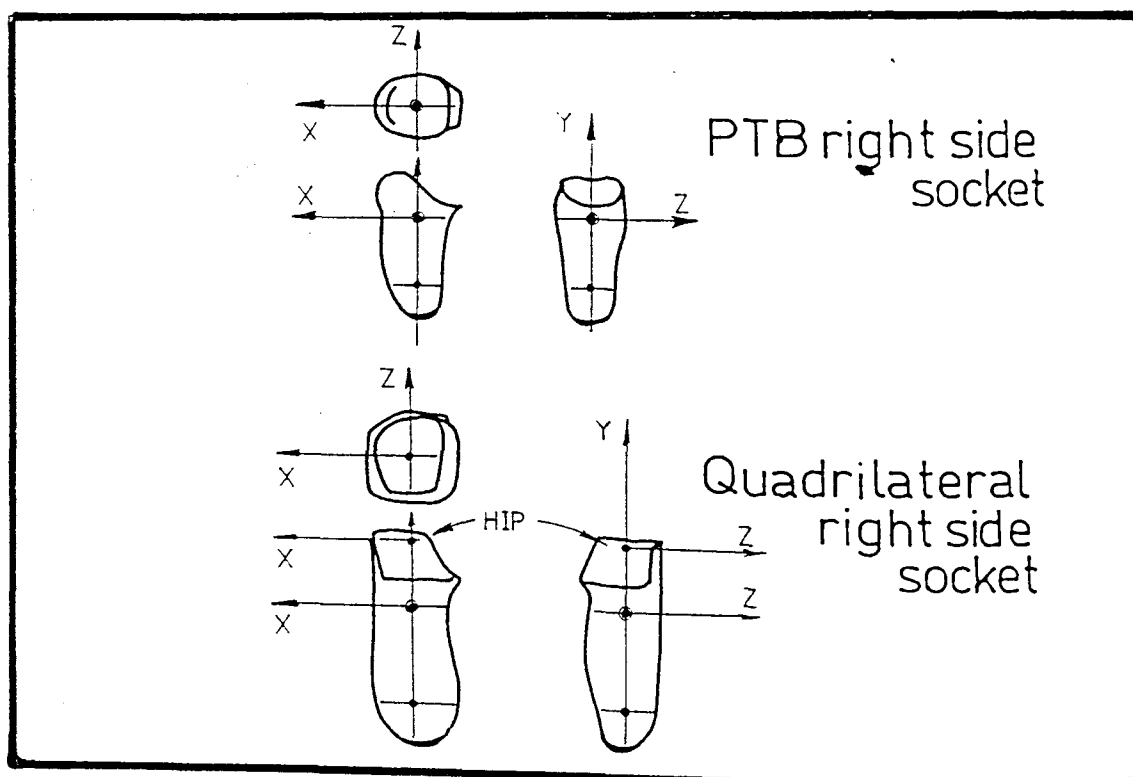
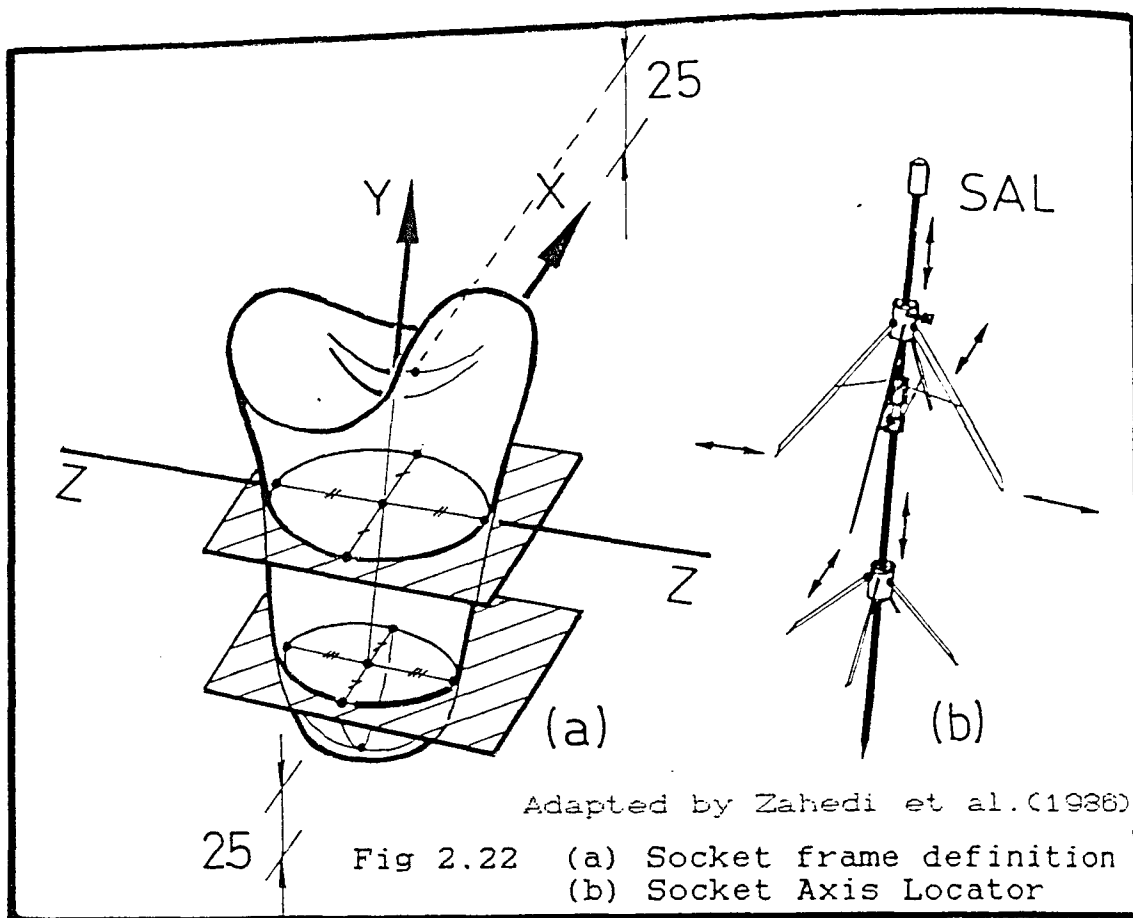


Fig 2.23 The frames for PTB and Quadrilateral type of sockets.

Adapted by Zahedi et al. (1986).

These researchers determined a frame for the sockets of the BK and AK amputees as follows (see fig 2.22). Two parallel planes were considered perpendicular to the longitudinal axis of the socket under study. The lower one was located at 25 mm proximal to the distal end of the inner socket surface and the upper at a distance of 25 mm distal to , either the patellar bar for PTB sockets (for BK prostheses) or to the posterior brim for quadrilateral sockets (for AK prostheses). Each plane was initially defined by four marks on the inner surface of the socket and their coordinates were properly measured with respect to a reference system. Then the centre point of each set of four marks was determined. The centre points of the two planes were meant to represent the Y-axis, whereas the posterior and anterior top marks represented the X-axis and the medial and lateral top marks represented the Z-axis (fig 2.22a). By an iterative procedure, the set of marks and centre points was brought to an orthonormal configuration and the three axes were uniquely defined.

Purdey (1977), using the principles of this method developed a device which could easily and accurately define the socket frame, overcoming the time consuming iterative method. Berme et al. (1978) developed this device further and reported it as the Socket Axis Locator (SAL) shown in figure 2.22b . The SAL device was later further developed by Szulc (1984) and could accurately define the Y-axis of the socket . At the same time it allowed the identification of the two sets of four points on the socket , because it was designed to be an orthonormal structure itself. Thus the XYZ frame of the socket could easily be defined, by the measurement of the coordinates of the marks, with respect to a predefined common reference (ie the frame of reference of the alignment rig).

The top centre point is taken to be the origin of the socket frame. Whereas, for a PTB socket, this point

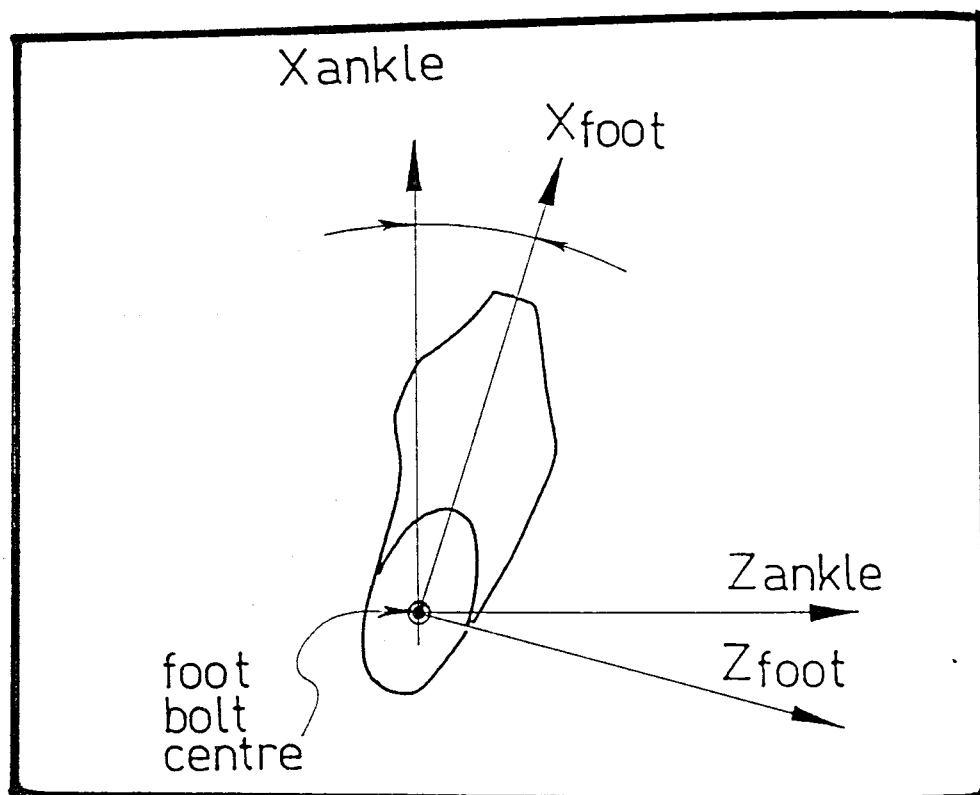


Fig 2.24 Foot and Ankle frames

is a good approximation of the anatomical joint centre (knee), for a quadrilateral socket it is distal to the anatomical joint centre (hip) and this has to be considered when the hip joint is involved in studies. This frame configuration is adopted, in this thesis, for the sockets of prostheses (fig 2.23).

Foot/Ankle

Using the point at the top surface of the SACH foot at the bolt centre, as an origin , two frames can be defined : the frame of the foot and the frame of the ankle, both sharing the same vertical Y-axis (fig 2.24) . The foot X-axis has the direction of the mid-toe, with the Z-axis being mutually perpendicular to the X and the Y axes. The ankle X-axis has the direction of progression of the gait, with the Z-axis being, again , mutually perpendicular to the corresponding X and Y ankle axes.

Knee Joint

The knee joint frame (for AK prostheses) is defined as follows : the Z-axis of the joint is the axis of the hinge, with its origin at the knee centre. The X axis is perpendicular to the Z-axis , parallel to the ground and positive forwards. The Y-axis is mutually perpendicular to the other two, positive upwards.

All frames are thus defined and using them it is possible to identify the position and orientation of any prosthetic component with respect to another. For this purpose, two different approaches can be adopted : a) considering the socket frame as the universal reference for the prosthesis everything can be described with respect to it, or b) considering the foot frame as the universal reference for the prosthesis everything can be described with respect to it.

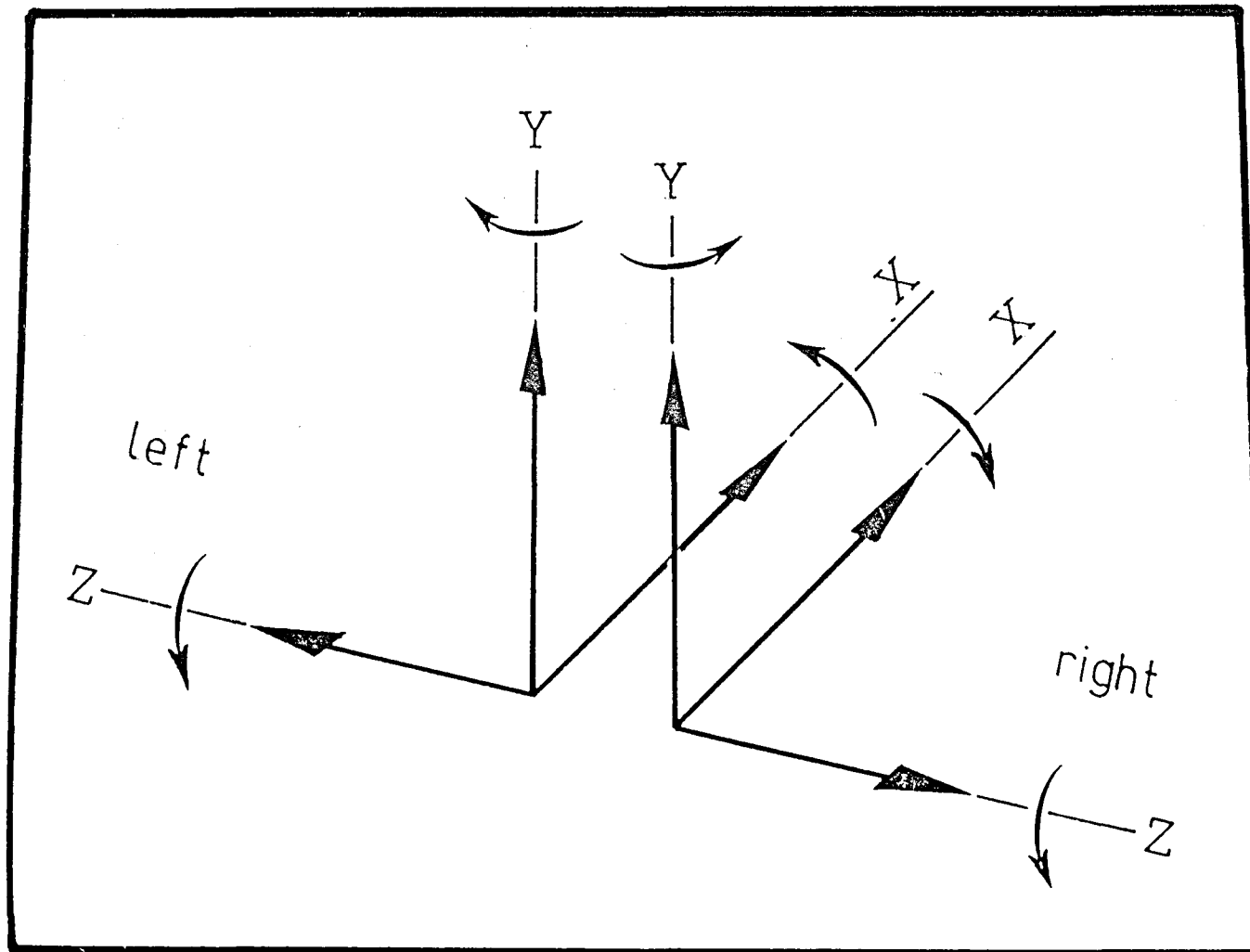


Fig 2.25 Systems of reference

It is obvious, that the same quantities, may appear with two different names, depending on which approach is used. For example, the angle shown in figure 2.24 could be referred to as toe-out angle, if the first approach is used, or as shank rotation, if the second approach is used. The reason, for these two approaches existing is that, from a medical point of view, the prosthesis has to be defined relative to the residual limb (first approach), whereas from a engineering point of view, the prosthesis, and thus the stump and the amputee's body, have to be defined relative to the foot, which is the contact through which the ground forces are transmitted to the body.

In this thesis, the second approach is adopted and the alignment parameters, described later in this chapter, are considered with the foot frame being the universal reference of the prosthesis.

2.7.3 Forces and Moments

During locomotion, or any other activity, both in normals and amputees, there are gravity, muscle and inertia forces acting on and within the body.

For loads of the same nature to have the same algebraic sign, independently of the side, two axes systems have been adopted (fig 2.25) : a right hand system for the right side and a left hand system for the left side. With the subject in the upright position, positive x-axes point forwards, positive y-axes point upwards and positive z-axes point laterally, with all positive rotational directions as shown.

As far as the loads are concerned, the following convention is important: the directions shown in figure 2.25, apply for the positive loads, when considered acting from the distal to the proximal side of a free body, and the section which is the free body's boundary could be the ground-to-foot interface, or any other transverse section along the limb.

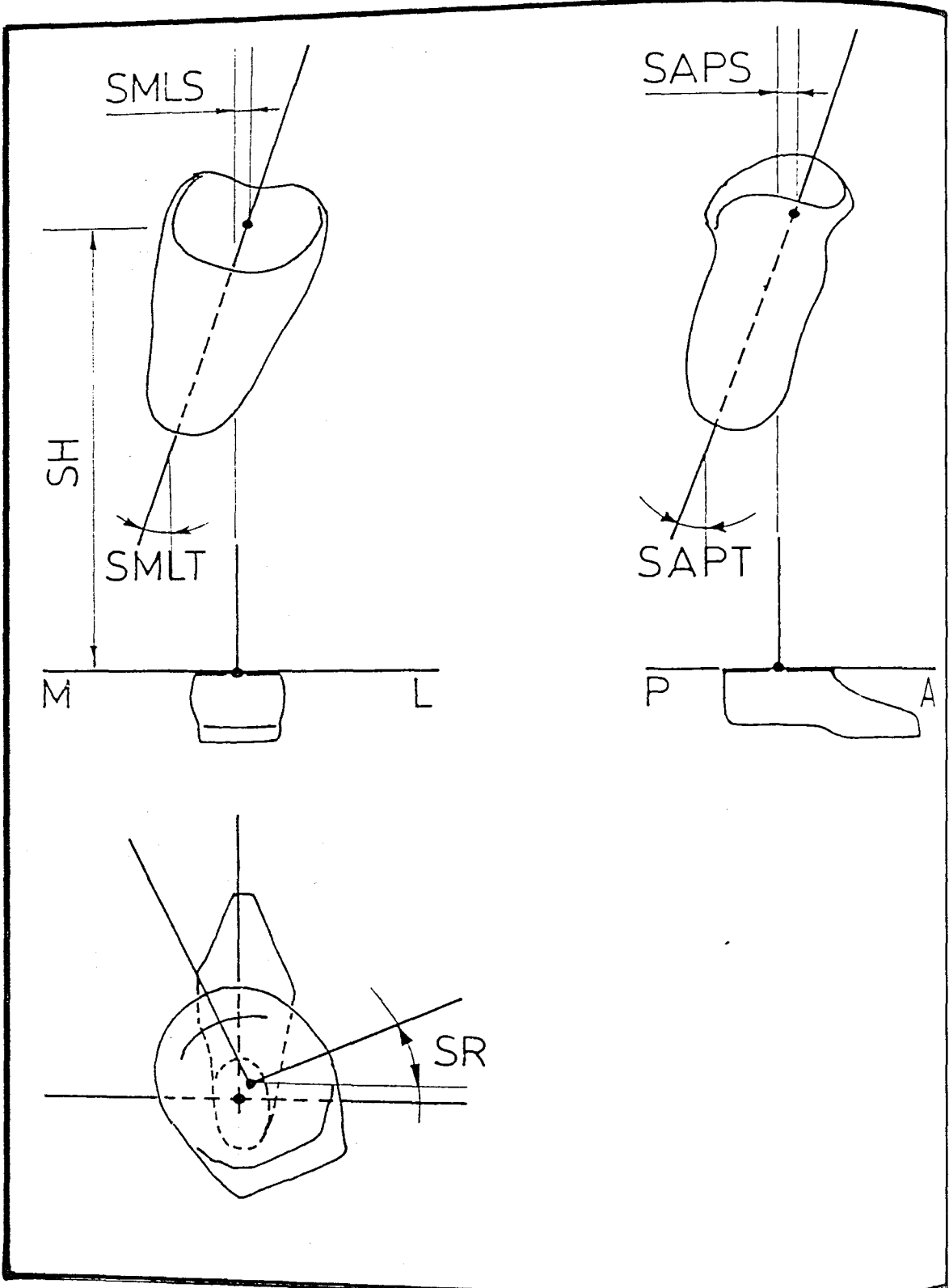


Fig 2.26 Alignment parameters for BK prostheses.

2.7.4 Alignment Parameters

Three different projections of the prosthesis are used to identify and evaluate the alignment parameters: an AP view, an ML view and a plan view.

Below the knee prostheses

Figure 2.26 shows the three views for a right side BK prosthesis. The origins of the socket frame and of the foot frame are shown. The following alignment parameters can be identified :

- the socket height (SH)
- the socket antero-posterior shift (SAPS)
- the socket antero-posterior tilt (SAPT)
- the socket medio-lateral shift (SMLS)
- the socket medio-lateral tilt (SMLT)
- the socket rotation (SR)

Since between the socket and the foot there is only the shank, the parameter SR could be also considered as a shank rotation (ie a toe-out angle, by the medical reference approach).

Above the knee prostheses

Figure 2.27 shows the three projections for a right side AK prostheses, the plan view being shown twice (ie through the knee and through the socket origins, respectively). The origins of the socket frame, of the knee frame and of the foot frame are shown. The following parameters can be identified :

- the knee height (KH)
- the knee antero-posterior shift (KAPS)
- the knee medio-lateral shift (KMLS)
- the knee medio-lateral tilt (KMLT)
- the knee rotation (KR)
- the socket height (SH)
- the socket antero-posterior shift (SAPS)
- the socket antero-posterior tilt (SAPT)
- the socket medio-lateral shift (SMLS)
- the socket medio-lateral tilt (SMLT)
- the socket rotation (SR)

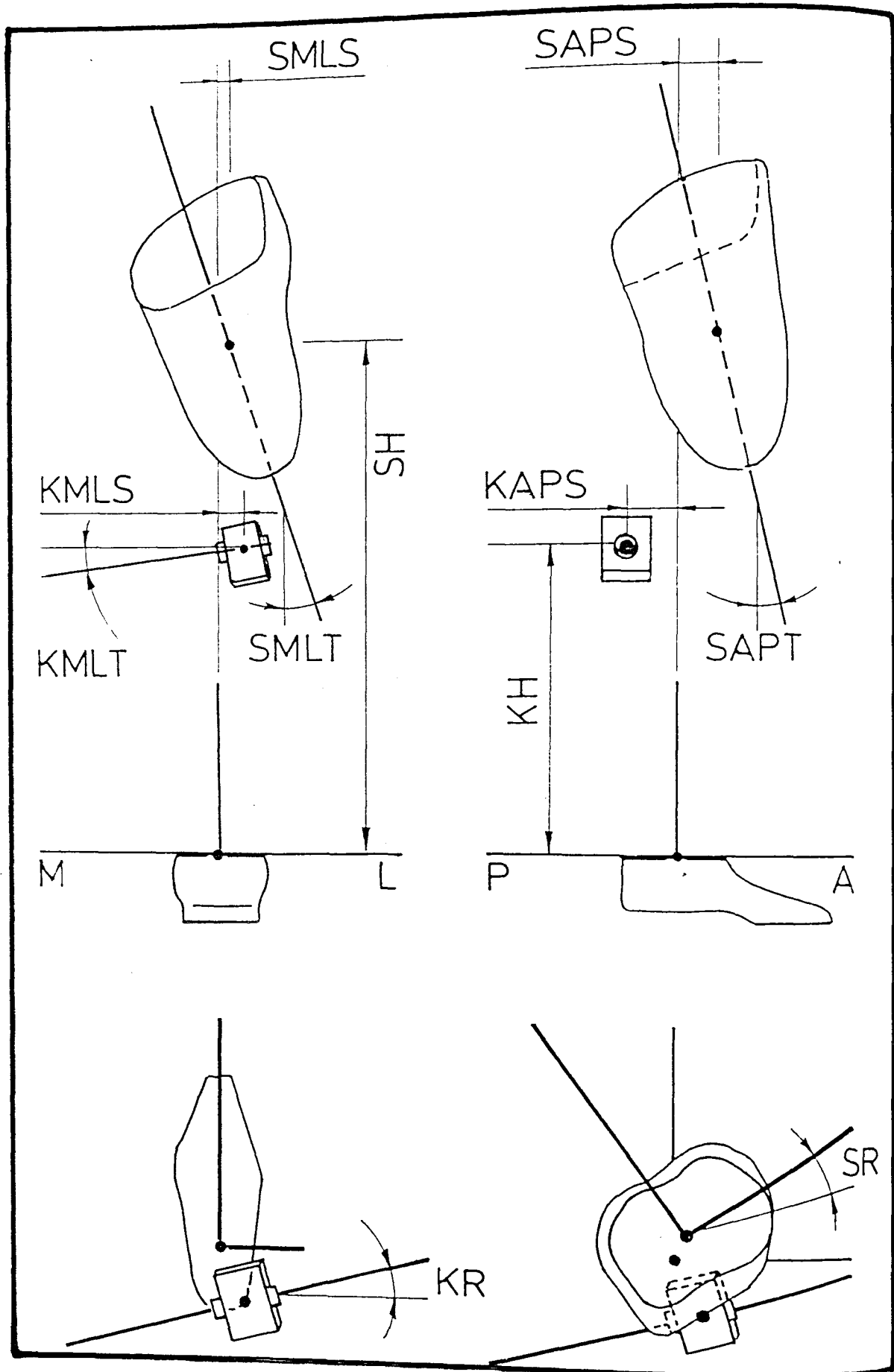


Fig 2.27 Alignment parameters for AK prostheses.

Since between the knee unit and the foot there is only the shank and no AP tilt is used on the knee unit, the parameter KR could be also considered as a shank rotation (ie a toe-out angle, by the medical reference approach).

All alignment parameters follow the sign conventions of the frames mentioned for forces and moments (fig 2.25) .

The alignment parameters can be calculated by measurements of the coordinates of the marked points of the prosthesis on the alignment rig.

2.8 The Calibration of the Pylon Transducer

2.8.1 Introduction

The short pylon transducer used throughout this study monitors all six components of the applied load. As far as calibration of transducers is concerned, two mathematical approaches, one linear and the other non-linear are advocated. The choice depends on the accuracy required for the particular application and it has been proved that the non-linear models contribute to the accuracy rather marginally (Bray et al, 1990).

A more detailed discussion on these two different approaches follows in the next sections.

2.8.2 Linear Approach

The first of the approaches described above simply assumes that each signal can be expressed as a linear combination of the components of the applied load :

$$(\text{signal})_i = \sum_{j=1}^6 m_{ij} \cdot (\text{load})_j \quad (2.1)$$

where the coefficients m_{ij} are the quantities to be determined . When $i = j$ the coefficient corresponds to a main effect and in all other cases the coefficients correspond to the five cross-effects and ideally should be zero. If the six load components are given the form

of a vector [L] and the six output signals are given the form of a vector [S] :

$$[L] = \begin{bmatrix} Fx \\ Fy \\ Fz \\ Mx \\ My \\ Mz \end{bmatrix}$$

(2.2)

$$[S] = \begin{bmatrix} SFx \\ SFy \\ SFz \\ SMx \\ SMY \\ SMz \end{bmatrix}$$

(2.3)

then using equation (2.1) the whole set of equations is the following :

$$\begin{aligned} SFx &= m_{11}Fx + m_{12}Fy + m_{13}Fz + m_{14}Mx + m_{15}My + m_{16}Mz \\ SFy &= m_{21}Fx + m_{22}Fy + m_{23}Fz + m_{24}Mx + m_{25}My + m_{26}Mz \\ SFz &= m_{31}Fx + m_{32}Fy + m_{33}Fz + m_{34}Mx + m_{35}My + m_{36}Mz \\ SMx &= m_{41}Fx + m_{42}Fy + m_{43}Fz + m_{44}Mx + m_{45}My + m_{46}Mz \\ SMY &= m_{51}Fx + m_{52}Fy + m_{53}Fz + m_{54}Mx + m_{55}My + m_{56}Mz \\ SMz &= m_{61}Fx + m_{62}Fy + m_{63}Fz + m_{64}Mx + m_{65}My + m_{66}Mz \end{aligned}$$

(2.4)

which can also be written in the simpler form :

$$[S] = [M] \cdot [L] \quad (2.5)$$

with matrix [M] being the (6 x 6) matrix of the desired coefficients m_{ij} :

$$[M] = \begin{bmatrix} m_{11} & m_{12} & m_{13} & m_{14} & m_{15} & m_{16} \\ m_{21} & m_{22} & m_{23} & m_{24} & m_{25} & m_{26} \\ m_{31} & m_{32} & m_{33} & m_{34} & m_{35} & m_{36} \\ m_{41} & m_{42} & m_{43} & m_{44} & m_{45} & m_{46} \\ m_{51} & m_{52} & m_{53} & m_{54} & m_{55} & m_{56} \\ m_{61} & m_{62} & m_{63} & m_{64} & m_{65} & m_{66} \end{bmatrix} \quad (2.6)$$

If the output signals are recorded in mV , after the amplification performed by the strain gauge amplifiers , and the loads applied are measured

in N (the 3 forces) and Nm (the 3 moments) then :

$$m_{ij} \text{ have units } (\text{mV})_i / (\text{N or Nm})_j \quad (2.7)$$

In general practice, during amputee testing, the given quantities are the output signals recorded during the amputee's activity and the quantities required for the analysis are the six components of the load applied onto the transducer for every particular moment. It is therefore necessary that equation (2.5) be solved for [L] and applied for every vector [S] recorded. Multiplying (2.5) by [M]⁻¹, the inverse of [M], the equation results in :

$$\begin{aligned} [M]^{-1} \cdot [S] &= [M]^{-1} \cdot [M] \cdot [L] \quad \text{or} \\ [M]^{-1} \cdot [S] &= [L] \quad \text{or} \\ [L] &= [C] \cdot [S] \end{aligned} \quad (2.8)$$

where [C] = [M]⁻¹ and is called the calibration matrix for the pylon transducer. This matrix [C] is of the form:

$$[C] = \begin{bmatrix} c_{11} & c_{12} & c_{13} & c_{14} & c_{15} & c_{16} \\ c_{21} & c_{22} & c_{23} & c_{24} & c_{25} & c_{26} \\ c_{31} & c_{32} & c_{33} & c_{34} & c_{35} & c_{36} \\ c_{41} & c_{42} & c_{43} & c_{44} & c_{45} & c_{46} \\ c_{51} & c_{52} & c_{53} & c_{54} & c_{55} & c_{56} \\ c_{61} & c_{62} & c_{63} & c_{64} & c_{65} & c_{66} \end{bmatrix} \quad (2.9)$$

the elements having the units of matrix [M] inverted. Since the units of [M] were (mV)_i / (N or Nm)_j, the units of the elements of [C] are (N or Nm)_j / (mV)_i. At this stage the index notation for i and j can be interchanged without any risk of confusion and thus :

$$c_{ij} \text{ have units } (\text{N or Nm})_i / (\text{mV})_j \quad (2.10)$$

The linear model approach does not take into account any elastic deformations of the device as being the reason for cross-effects and therefore is not attempting to estimate higher order terms.

If this cross-effect was to be studied, the model should consider not only single load components, but also combinations of load components, which would reveal effects due to elastic deformations. Such effects are proportional to the loads which develop them (Dubois, 1976). Therefore, if the effects mentioned above were to be studied, quadratic and rectangular terms should have been introduced in the calibration procedure and analysis. This is the principle of the non-linear approach which is discussed in the next section.

The researchers who calibrated pylon transducers (Lowe 1969 , Berme et al. 1976 , Jones 1976 , Grant - Thompson 1977, Lovely 1981, Lawes 1982, Pashalides 1989) all followed the linear approach for the calibration of the devices.

When linear regression is performed on the calibration data, for example, when the acquired output signals for an applied F_x load component are regressed against this load, six coefficients may generally be determined : m_{ij} ($i = 1$ to 6). The question then arises about which coefficients should be retained. The decision must be made on statistical grounds, without however ignoring any metrological aspects of the problem.

One approach is to ignore any cross-effects with relatively low values (Grant-Thompson, 1977). Another approach is to study the statistical results of the calibration data. Such a study was performed by Lovely (1981) who also followed a linear approach. This researcher applied a statistical approach to the calibration data acquired and derived all coefficients m_{ij} from linear regressions, using an r-square value of 95% as the threshold between acceptable and

Fig 2.28 The set-up for axial load calibration

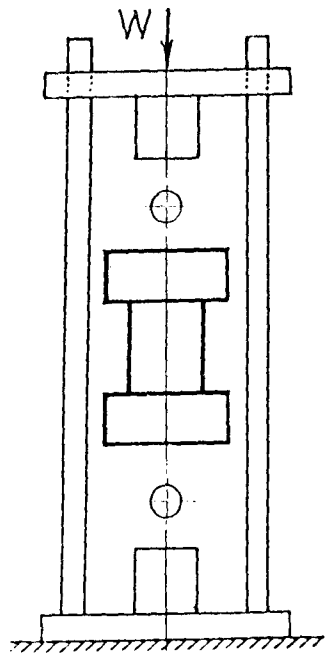
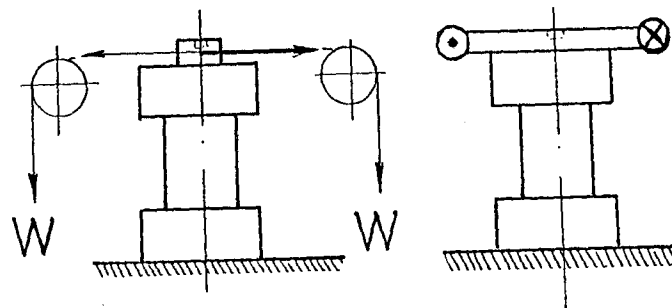
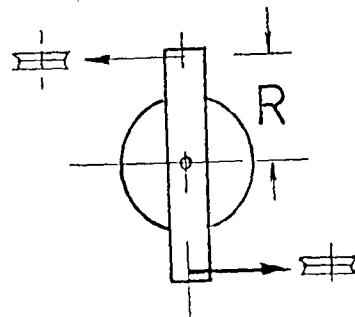


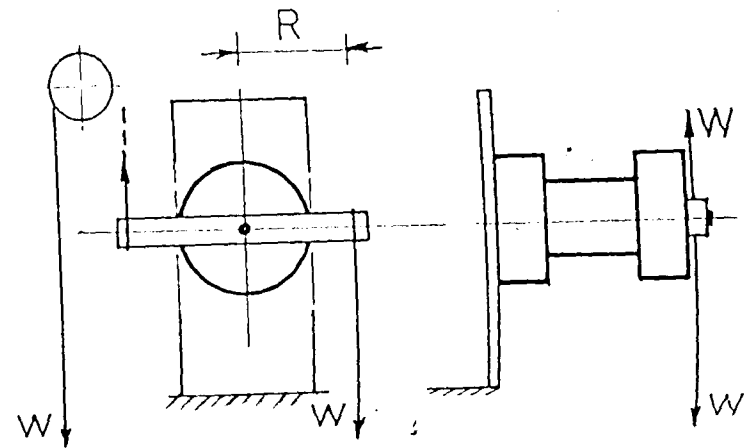
Fig 2.29 The set-up for torque calibration



(a)



(b)



non-acceptable coefficients m_{ij} . As a result of this matrix [M] was derived using only those of the cross-effect coefficients that were related to strongly linear graphs, assuming the rest to be zero.

The approach followed by Lovely (1981) was based on the following consideration : if one load component is only applied onto the transducer and all effects are expected to exhibit a linear behaviour, then any effects that do not meet this condition should be omitted. However, the author of this thesis expresses the following criticism to this approach: it is possible for cross-effects to have a poor linear fit but of significant magnitude. It is suggested here that a t-ratio or a p-value , derived from the regression of the data, would constitute a better criterion for the same decision.

The r-square value only gives information on the amount of the output signal variation explained by the applied load component (in the linear model) , whereas the t-ratio or the p-value give information on the statistical significance of the calculated regression coefficient. Therefore, it is considered statistically more sound to base any decisions on either of the last two quantities (preferably on the p-value), than on the r-square value of the regression model.

The calibration techniques, related to the assumption of linear relationships between output signals and applied load components, seek to determine the coefficients m_{ij} , by either applying one load component at a time or by applying two load components simultaneously.

In the first case by applying one load component only, all six output signals can be recorded resulting in six linear regressions, which provide the six coefficients of the corresponding column of matrix [M]. One of the coefficients is the main effect and the other five are the cross-effects. The individual setups designed and built have been reported as follows :

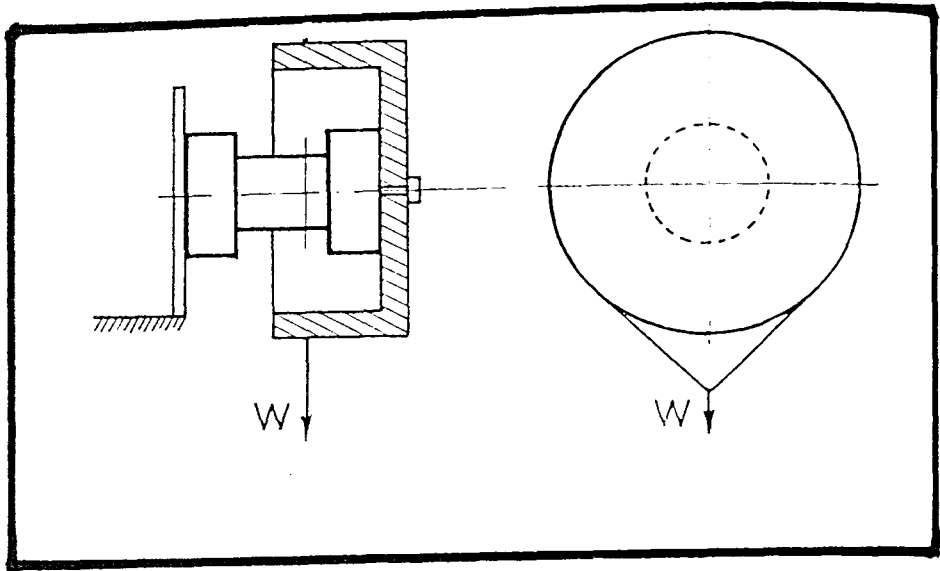


Fig 2.30 The set-up for shear force calibration

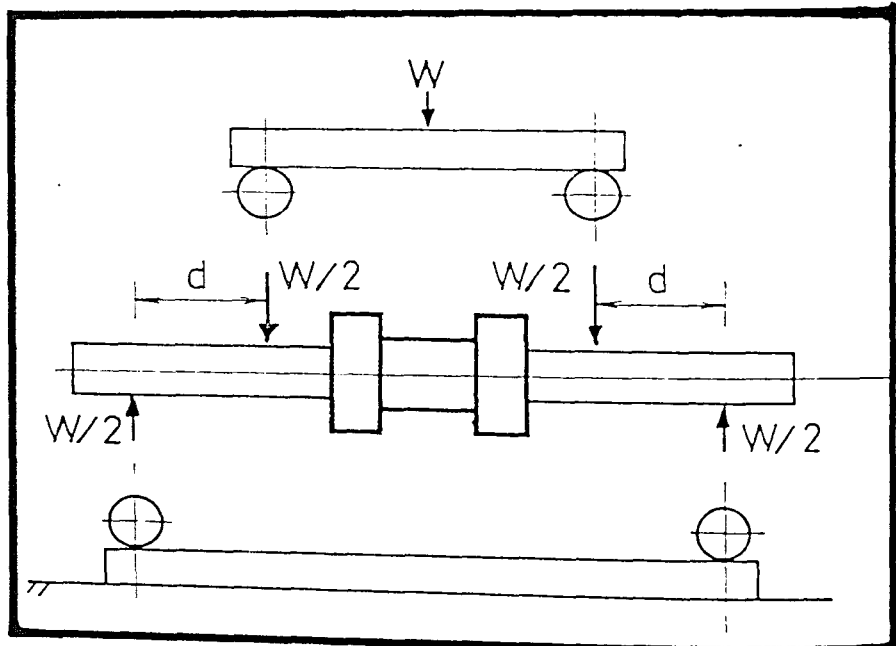


Fig 2.31 The set-up for bending moment calibration

For the axial load F_y , for example, the device shown in figure 2.28, reported by Lowe (1969), was built. Loads were applied by means of weights on the top disc, resulting in compression of the transducer. The point loading was guaranteed by the use of steel balls at the interface between pylon transducer and device.

For the torque, M_y , the transducer was fitted on a base attached to a table as shown in figure 2.29a and a specially machined bar applied the torque by means of a system of pulleys and cables. The weights (W) should be equal in order to provide a zero shear load. The pure torque applied was, thus, equal to $(2 \cdot R \cdot W)$. This device was developed and used by Grant-Thompson (1977) as well as Lawes (1982). Another version of the same device used in more recent work (Pashalides, 1989) is shown in figure 2.29b.

In the work presented by Lawes (1982) and Grant-Thompson (1977) one device for the application of pure shear force is reported, which uses the principle shown in figure 2.30. The pure shear force was applied by means of suspended weights around a drum properly fitted at one side of the pylon transducer. The positioning of the cable on the plane crossing through the instrumented periphery of the transducer attempts to eliminate any bending moment within this section.

Grant-Thompson also reported a device for the application of pure bending moment, using an Instron machine. As shown in figure 2.31, two bars were symmetrically positioned about the transducer contacting with their properly prepared ends the two tubes fitted onto the transducer at both sides. With this method a pure bending moment $(W \cdot d / 2)$ was effectively applied on the transducer.

For the case of simultaneous application of more than two load components, two devices were reported: one for combined shear force and bending moment (Lawes, 1982 and Grant-Thompson, 1977) and one for combined

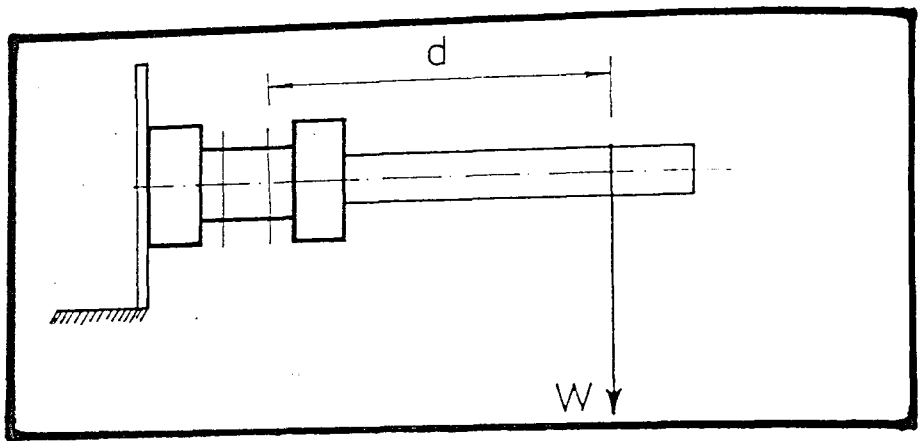


Fig 2.52 The cantilever configuration

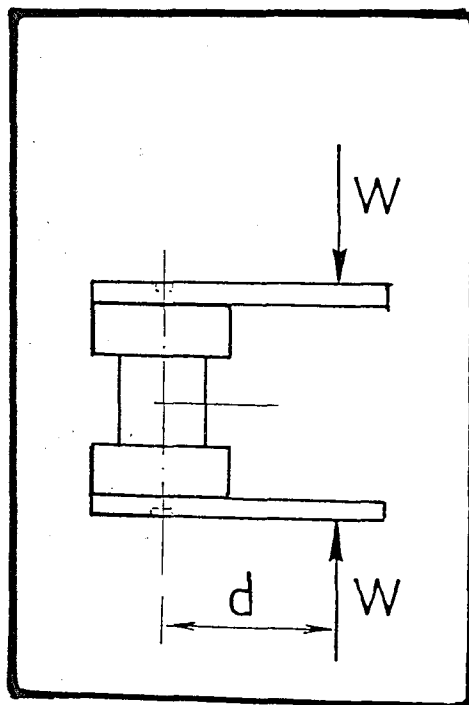


Fig 2.33 The off-axis load configuration

axial load and bending moment (Lawes, 1982).

For the first device the cantilever configuration shown in figure 2.32 was used. The weight was suspended at a distance d from the centre of the transducer. Thus except from the shear force W , a bending moment ($W \cdot d$) was also applied. The procedure just described results in the determination of the two corresponding columns of matrix $[M]$, ie. first and sixth or third and fourth. Due to linear dependence between applied shear force and bending moment, two distinct loading configurations must be tried (by change of the lever-arm of the applied load), in order to create two linearly independent equations for each pair of coefficients to be calculated.

As an example to the above a case could be considered where the dead weight is applied along the positive x - axis of the transducer ($F_x = +W$, from distal to proximal), also producing a positive M_z . Writing the first of equations (2.4) for SF_x :

$$SF_x = m_{11} \cdot F_x + m_{16} \cdot M_z = m_{11} \cdot F_x + m_{16} \cdot (F_x \cdot d)$$

but also for another value of dead weight, say W' :

$$SF_x' = m_{11} \cdot F_x' + m_{16} \cdot M_z' = m_{11} \cdot F_x' + m_{16} \cdot (F_x' \cdot d)$$

the system of m_{11} and m_{16} has a singular matrix (determinant is zero) and is therefore not solvable.

Using, however, a second position at a different distance d' and repeating the tests would result in two sets of linearly independent equations and thus solvable (even with the same weight W):

$$\begin{aligned} SF_x &= m_{11} \cdot F_x + m_{16} \cdot M_z = m_{11} \cdot F_x + m_{16} \cdot (F_x \cdot d) \\ SF_x' &= m_{11} \cdot F_x + m_{16} \cdot M_z = m_{11} \cdot F_x + m_{16} \cdot (F_x \cdot d') \end{aligned}$$

The same applies for all other output signals under this load configuration.

The principle for the device for combined axial load and bending moment is shown in figure 2.33 . The off-axis compressive load W results in a bending moment (W.d) simultaneously with an axial load W . Here again two independent equations must be compiled using two different leverarms.

2.8.3 Non-linear Approach

Various researchers have carried out and reported calibrations for force measurement transducers assuming a non-linear relationship between output signals and applied loads, suggesting that this is the approach providing the highest possible accuracy in the results. The transducers they used were multicomponent balances designed to measure loads in various non - biomedical applications. These researchers considered the effect of elastic deformations on the cross-effects and therefore introduced quadratic and rectangular terms in their analysis.

Dubois (1982) having designed a sting balance able to directly monitor the six components of a load (in an application related to force measurement for wind tunnels in aerospace studies) suggests that not only the effect of each load component to the signals must be studied, but also the effect of the interaction of every two load components. Dubois therefore suggests that a second order model should be used , which for the (signal)_i would result in the following equation:

$$(\text{signal})_i = \sum_{j=1}^6 m_i^j (\text{load})_i + \sum_{p=1}^6 \sum_{r=p}^6 n_i^{pr} (\text{load})_p (\text{load})_r \quad (2.11)$$

where coefficients m_i^j and n_i^{pr} are called sensitivity coefficients (Bray et al, 1990). The above expression implies that each signal output can actually be considered as the result of each one of the load components individually (coefficients m_i^j for linear

terms), but also of each one of all the second order load interactions (coefficients n_i^{pr} for second order terms).

Expanding the series for the output signal SFx (channel 1), for example. The full development is :

$$\begin{aligned}
 SFx = & (m_1^1 Fx + m_1^2 Fy + m_1^3 Fz + m_1^4 Mx + m_1^5 My + m_1^6 Mz) + \\
 & (n_1^{11} Fx Fx + n_1^{12} Fx Fy + n_1^{13} Fx Fz + n_1^{14} Fx Mx + n_1^{15} \\
 & Fx My + n_1^{16} Fx Mz) + (n_1^{22} Fy Fy + n_1^{23} Fy Fz + n_1^{24} \\
 & Fy Mx + n_1^{25} Fy My + n_1^{26} Fy Mz) + (n_1^{33} Fz Fz + n_1^{34} \\
 & Fz Mx + n_1^{35} Fz My + n_1^{36} Fz Mz) + (n_1^{44} Mx Mx + n_1^{45} \\
 & Mx My + n_1^{46} Mx Mz) + (n_1^{55} My My + n_1^{56} My Mz) + \\
 & (n_1^{66} Mz Mz)
 \end{aligned} \tag{2.12}$$

According to Dubois the first set of terms is uniquely due to constructive causes like insufficient structural coupling , asymetries of the machining or differences in the gauge positioning. However the second set of terms is due to the elastic deformations of the device under a particular loading configuration. It is therefore understood that the introduction of quadratic and rectangular terms attempts to approach the real strain field as much as possible.

Dubois also suggests that higher than second order terms should be included in the model, for an even better approximation , but are generally negligible, except in cases where there is either assembly play or in cases where the gauges are bonded very close to fitting parts.

The objective of a calibration procedure, in the case of this approach, is the exact determination of coefficients m_i^j and n_i^{pr} . This task demands that all

the individual load components are applied separately as well as every two load components applied separately at a time. This is an overall of twenty one ($6 + 6! / (2!4!)$) distinct loading configurations , which demand specially designed rigs. Besides the accuracy by which the loads are applied, the rig according to Dubois, should be able to apply the load configurations in the same way as the loads, expected during actual experimental use, are applied.

The final objective of a calibration is to determine the relationship between the signals acquired during tests, and the loads which must be estimated. From this point of view equation (2.11) must be written in the following form :

$$(\text{load})_i = \sum_{j=1}^6 c_i^j (\text{signal})_i + \sum_{p=1}^6 \sum_{r=p}^6 d_i^{pr} (\text{signal})_p (\text{signal})_r \quad (2.13)$$

from which the loads producing the output signals can be predicted. Coefficients c_i^j and d_i^{pr} are called exploitation coefficients (Bray et al, 1990).

The coefficients of the linear terms of equations (2.11) and (2.13) are $6 \times 6 = 36$, the same total as in the case of a simple linear approach. The additional coefficients of the second order terms are $6 \times 21 = 126$ (6 quadratic and 15 rectangular for each channel). Thus, the overall total of coefficients to be calculated is $36 + 126 = 162$.

The difficulties may arise on how to isolate some of the load components simultaneously, but also on how to process the calibration data in order to accurately derive c_i^j , d_i^{pr} and m_i^j , n_i^{pr} .

Levi (1972) used a non-linear mathematical model for calibration of machine-tool dynamometers under multi-component loading and investigated the possibilities of deriving equation (2.13) for each channel from the corresponding equation (2.11) of the

same channel. It was suggested that for the former equation to be derived the measuring device must have six channels each measuring one load component (like the short pylon transducer) . In case the device monitors less than six channels then a solution exists only if coefficients derived under non-monitored load components are zero.

This consideration brings back the distinction between pylon transducers like the short pylon transducer and transducers of the former designs, which do not detect shear forces directly.

The device used by Levi (1972) was meant to monitor only the three forces, and the performed analysis was initially based on a preliminary factorial experiment, which revealed all the significant interactions. Multiple regression was used to determine the coefficients m_i^j and n_i^{pr} for the loading configurations, which had been proved influential to the output signals. Levi suggests that for the non-linear model to be successful the operational range of the expected loads must be known (an upper boundary at least).

However , a criticism was expressed to the mathematical approach under study and reported in the same publication : although all the six individual components are independent variables, their interactions are not, because they are dependent on the first variables. In other words, the question is whether it is correct or not to consider the influence of the interactions as occurring from an independent variable. Levi (1972) claims that as far as their influence to the output signal is concerned, the second order interactions can be considered as independent variables and they can be introduced as a computational arrangement despite the fact that each product of two load components is uniquely defined by its two constituents from a mathematical point of view. This in fact is in accordance with what was stated earlier

about the effect of the elastic deformations on the output signals.

Besides the factorial design and analysis of the calibration, other methods are also suggested for the determination of the sensitivity and exploitation coefficients (Bray et al, 1990). These include multiple regression and linear algebra techniques.

It can be appreciated from the above discussion that non-linear calibration approaches provide with highly reliable results and predict the applied loads very successfully. However they are considered demanding in terms of time and equipment which may generally be very expensive and the question may arise on whether the contribution of second-order effects is such so as to justify the adoption of a non-linear model.

2.9 Summary

The measurement of prosthetic loading during various activities of the amputee is of major importance for the understanding of amputee locomotion and the development of the loading standards and design criteria for the manufacturing of modular prostheses. The intensive work carried out by several research teams, in the field, resulted in the acquisition processing and presentation of the data reported by ISPO (1978) providing an excellent reference for further work on this particular subject. These standards are occasionally updated by the ISO, who suggest new loading values for the structural testing of the prostheses.

Among the equipment produced for data acquisition, an outstanding contribution was the development of the pylon transducers, which provided for the first time, the possibility of free range measurements. An even more recent contribution was the development of the portable recording equipment for pylon transducer data, which allowed outdoor tests to take place.

The research is focusing at the moment , on further improvement of acquisition methods and reproduction of the pylon transducer signals and also on the development of new pylon transducer designs, allowing for an even broader amputee population to be tested.

The calibration of the pylon transducers has been performed by various researchers using dead-weight methods (eg Grant-Thompson , 1977 ; Lawes, 1982) and linear mathematical models. Second-order models have never been adopted in the field of prosthetics.

Throughout the studies carried out on prosthetic loading another aspect was also highlighted. As shown during the presented review, several researchers have concluded that the alignment of a prosthesis has major effect on amputee locomotion. The study on AK modular prostheses , in particular , which was carried by Solomonidis (1980) highlighted the interaction between the geometrical configuration of the artificial leg, the amputee's comfort and the loading patterns exhibited. Following this study , various researchers investigated the existence of criteria for the establishment of an optimum alignment.

However, it was later proved (Zahedi et al, 1986) that no uniquely defined optimum alignment existed and that patients and prosthetists were satisfied with a range of alignments rather than with a single one.

In prosthetic practice the prosthetist must achieve, by use of skills, intuition and feedback from the amputee, a suitable alignment. The criteria developed by researchers for the establishment of what they considered as optimum alignment can be used in the development of methods to assist the prosthetist in the accomplishment of this difficult task. The definition of alignment parameters for the quantitative assessment of the alignment configuration of a prosthesis, has facilitated the development of a methodical and mathematical approach to the subject of alignment and

also provided the basis for a common language between different disciplines. Using the defined frames of reference of a prosthesis, on the other hand, an easier and more comprehensive description of geometrical relationships of the various parts can be achieved. Thus, there is a considerable amount of knowledge and techniques that could be used for the development of methods which could assist prosthetic work.

The author of this thesis believes that since the alignment of a prosthesis is a procedure consisting of various steps, any method meant to assist the prosthetist should really be able to provide results of each particular step throughout the whole procedure ; while the prosthesis is still being worn by the subject and more prosthetic adjustments are still meant to take place.

The following chapters present the work carried out during this project. The presentation will start with a theoretical analysis required to provide a first approximation of the strain gauge response of the short pylon transducer.

CHAPTER 3

THEORETICAL ANALYSIS FOR A FIRST APPROXIMATION OF THE STRAIN GAUGE RESPONSE OF THE SHORT PYLON TRANSDUCER

3.1 Introduction

3.2 Initial Considerations and Assumptions

3.2.1 The Pylon

3.2.2 Load Components, Stresses and Strains

3.2.3 The Gauging

3.3 Study of transducer for applied Shear forces

3.4 Study of transducer for applied Axial force

3.5 Study of transducer for applied Bending moments

3.5.1 Bending Moment M_x

3.5.2 Bending Moment M_z

3.6 Study of transducer for applied Torque

3.7 Quantitative Results of the Analysis

3.8 Discussion

3.9 Conclusions

3.1 Introduction

Strain gauges used to measure loads (forces and moments) on a particular body are able to provide quantitative information about every single load component (for a detailed discussion see appendix I).

The short pylon transducer discussed in chapter 2 (Berme et al. 1976) is instrumented with six full bridges of strain gauges, each bridge being responsible for measuring one of the six components of a general load acting upon the pylon transducer, expressed in the pylon transducer reference frame.

In order to make decisions about the positioning and the wiring of the gauges, a qualitative analysis is an important prerequisite. Such an analysis is presented below.

3.2 Initial Considerations and Assumptions.

When the study presented in this chapter commenced, various considerations had to be made regarding three aspects of the problem : the actual pylon, the loading configurations meant to be studied and the gauging.

3.2.1 The Pylon

As stated in chapter 2 the aluminium alloy the pylon is made of 6082 T4 aluminium alloy (BS1474:1987). The mechanical properties of this material can be obtained by tables (Roark, 1954) :

$$\begin{aligned} \text{modulus of elasticity } E &= 68.9 \text{ MPa } (= 10 \times 10^6 \text{ psi }) \\ \text{Poisson's ratio } \nu &= 0.26 \quad \text{and} \\ \text{shear modulus } G &= \frac{E}{2(1+\nu)} = 27.3 \text{ MPa} \end{aligned}$$

The following assumptions about the pylon were made :

- a) the pylon is considered to be machined to exactly its nominal dimensions without any discrepancies in the transverse plane (ie. all cylindrical surfaces are co-axial about the device's axis),

- b) as a first approximation and recognising the limitations, the gauging area under study is considered far enough away from the ends of the device and therefore not subjected to any end-effects.

Various geometrical properties of a cross - section of the pylon transducer will be used in this study. This cross- section is considered through an instrumented periphery of the transducer. These properties are the following :

1) area $A = \pi \cdot (R_o^2 - R_i^2) = 204.5 \times 10^{-6} \text{ m}^2$,

2) second moment of inertia I (about x or z axes) =
 $= \frac{\pi}{4} \cdot (R_o^4 - R_i^4) = 20.6 \times 10^{-9} \text{ m}^4$

3) polar moment of inertia J (about y axis) =
 $= \frac{\pi}{2} \cdot (R_o^4 - R_i^4) = 41.2 \times 10^{-9} \text{ m}^4$

3.2.2 Load Components, Stresses and Strains

The loads acting upon the pylon transducer in this analysis are considered to be applied on a cross-section of the body from a lower (distal) to an upper (proximal) direction being the positive sense, according to the loading conventions discussed in chapter 2. The section was considered passing through a periphery of the pylon transducer which is instrumented with strain gauges.

For each loading configuration infinitesimal elements were considered at the boundary of each section. The stresses developed on the elements were then studied in order to derive the corresponding strains. These strains were then used to derive the strains in any other direction on the elements, if necessary, using the following equation (fig.3.1) :

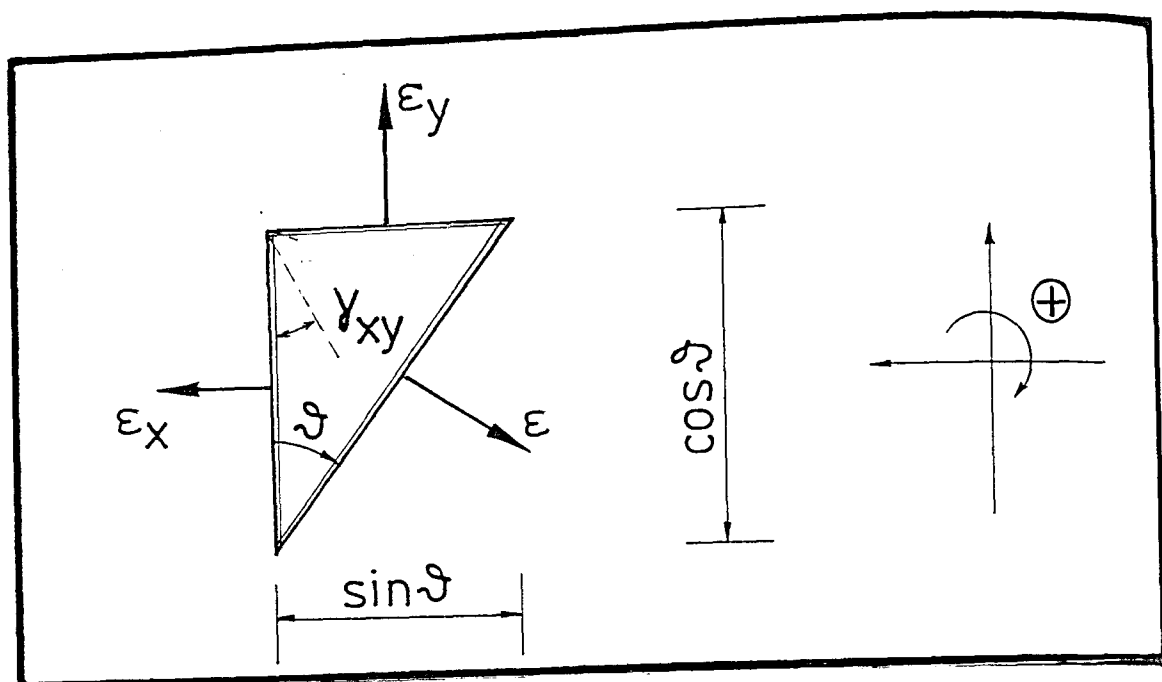


Fig 3.1 Conventions for strains on a unit element

strain gauge bridges	strain gauge type	grid area (mm ²)
for bridges A and B	EA-13-125-MK-120	2.4168
for bridge C	EA-13-062-TT-120	2.9987
for bridges D, E, F	EA-13-062-TH-120	2.1980

Table 3.1 The gauge types for the pylon transducer.

strain gauge type	grid area (mm ²)	power supply range (Volts)
EA-13-125-MK-120	2.4168	3.0 to 4.0
EA-13-062-TT-120	2.9987	3.3 to 4.5
EA-13-062-TH-120	2.1980	2.8 to 3.8

Table 3.2 The power supply ranges for the strain gauge bridges of the pylon transducer.

$$\begin{aligned} \text{strain at an angle } \theta &= \varepsilon(\theta) = \\ &= \varepsilon(x) \cos^2(\theta) + \varepsilon(y) \sin^2(\theta) + \gamma_{xy} \cos(\theta) \sin(\theta) \end{aligned} \quad (3.1)$$

One load component only was considered at a time applied as described above. The top end of the pylon transducer was assumed rigidly fixed. The loaded body was assumed to experience practically no elastic deformations, which could distort the initial geometry of the loading configuration.

3.2.3 The Gauging

The gauging was considered ideally positioned, each gauge being exactly at the particular location and orientation it was meant to be (see figure 3.2) .

The gauges* were of the types shown in table 3.1 , with a nominal gauge factor $K = 2$ and resistance of $R=120 \Omega$.

One of the objectives of the analysis was to study the status of each bridge under each loading configuration. Thus, having derived all the required strains, for a particular loading configuration the status of each bridge was studied. Ideally the only bridge being unbalanced during the application of a particular load component should be the one meant to monitor and measure this component ; all the other bridges being balanced.

As shown in figure 3.3 the recommended range for heat sink conditions for aluminium is $7.8 - 16 \text{ kWatt/m}^2$ for high accuracy of the gauges in dynamic conditions . For this range and for the grid areas shown in table 3.1 , power supply ranges were determined (see table 3.2).

In order to avoid any drifts of the output signals due to increase of the temperature and therefore

* The gauges were supplied by Measurement Group UK Ltd and are described in Catalog 500/part A of the Company

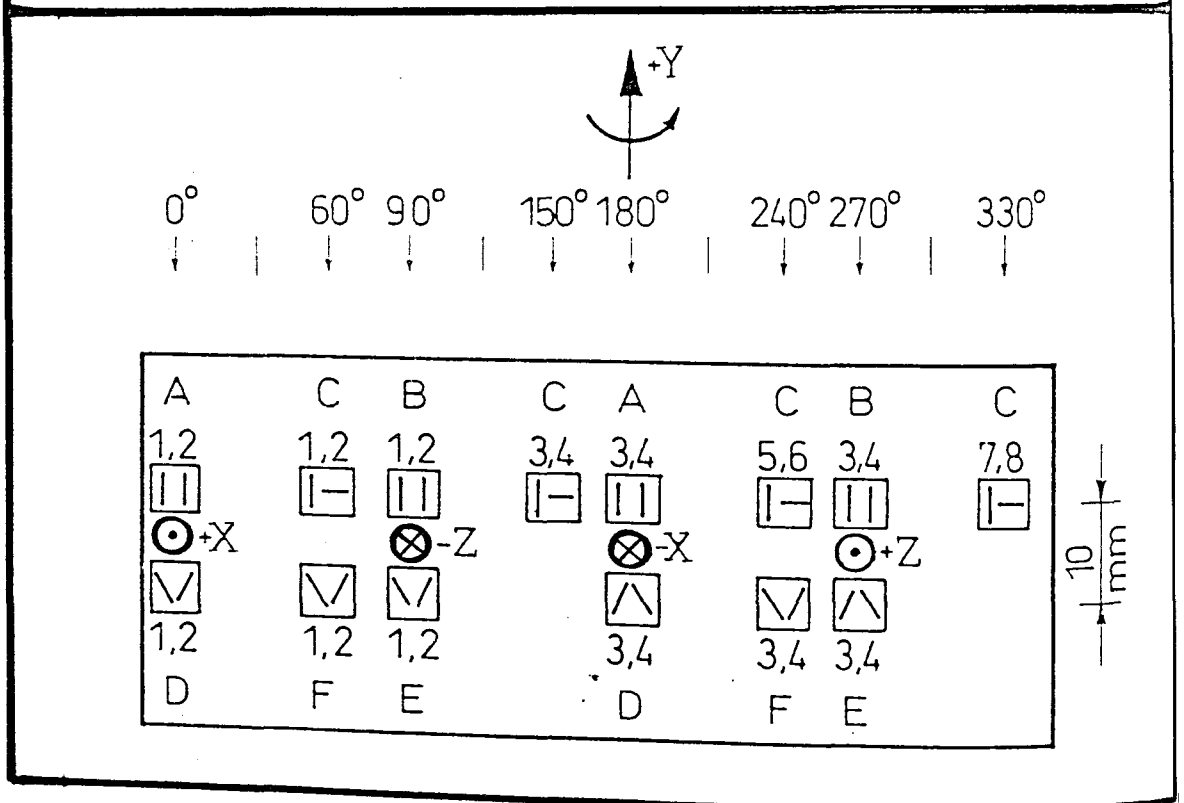
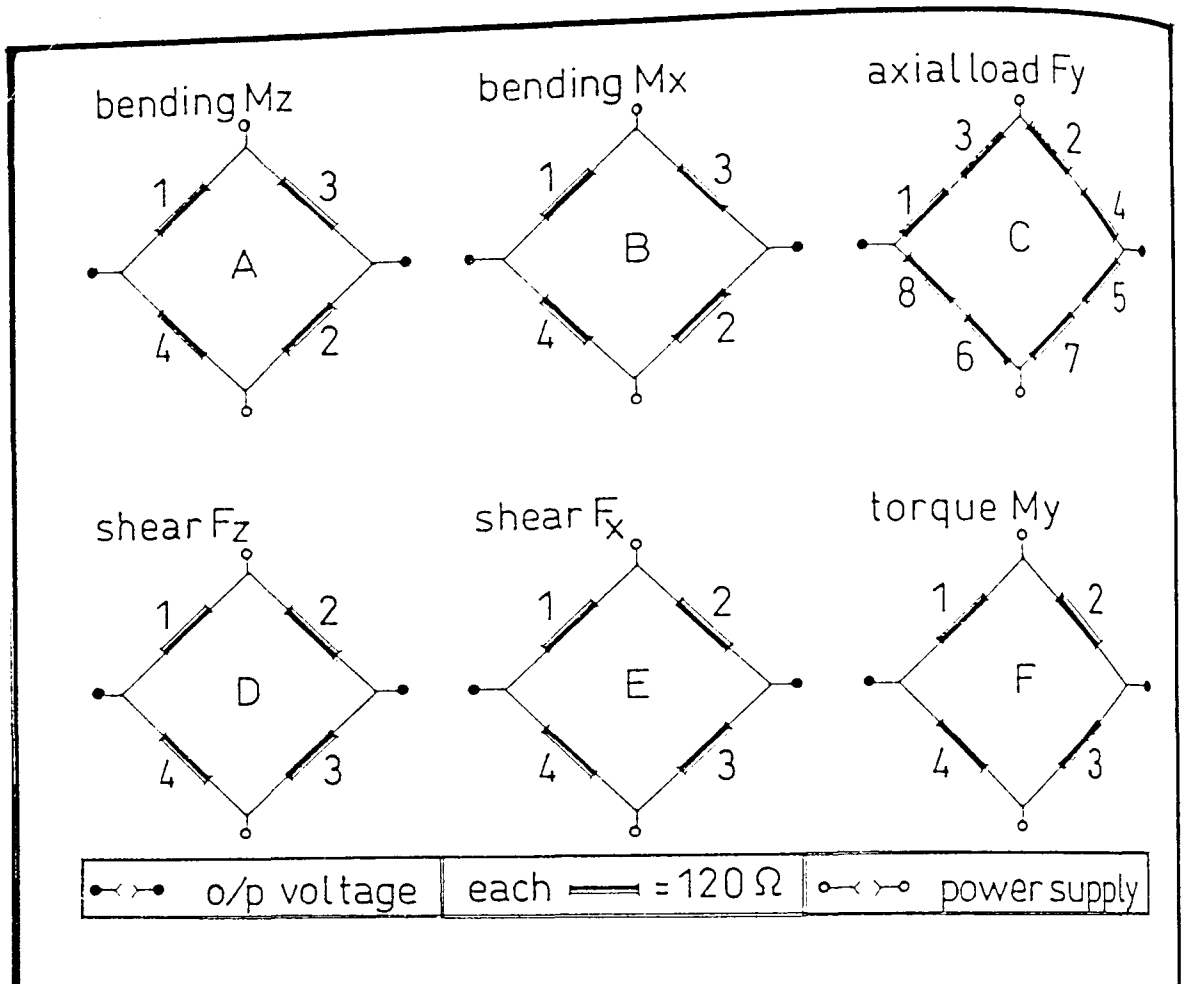


Fig 3.2 Gauging diagrams for the pylon transducer

Accuracy Requirements		EXCELLENT Heavy Aluminum or Copper Specimen	GOOD Thick Steel	FAIR Thin Stainless Steel or Titanium	POOR Filled Plastic such as Fiberglass/Epoxy	VERY POOR Unfilled Plastic such as Acrylic or Polystyrene
STATIC	High	2 — 5 3.1 — 7.8	1 — 2 1.6 — 3.1	0.5 — 1 0.78 — 1.6	0.1 — 0.2 0.16 — 0.31	0.01 — 0.02 0.016 — 0.031
	Moderate	5 — 10 7.8 — 16	2 — 5 3.1 — 7.8	1 — 2 1.6 — 3.1	0.2 — 0.5 0.31 — 0.78	0.02 — 0.05 0.031 — 0.078
	Low	10 — 20 16 — 31	5 — 10 7.8 — 16	2 — 5 3.1 — 7.8	0.5 — 1 0.78 — 1.6	0.05 — 0.1 0.078 — 0.16
DYNAMIC	High	5 — 10 7.8 — 16	5 — 10 7.8 — 16	2 — 5 3.1 — 7.8	0.5 — 1 0.78 — 1.6	0.01 — 0.05 0.016 — 0.078
	Moderate	10 — 20 16 — 31	10 — 20 16 — 31	5 — 10 7.8 — 16	1 — 2 1.6 — 3.1	0.05 — 0.2 0.078 — 0.31
	Low	20 — 50 31 — 78	20 — 50 31 — 78	10 — 20 16 — 31	2 — 5 3.1 — 7.8	0.2 — 0.5 0.31 — 0.78

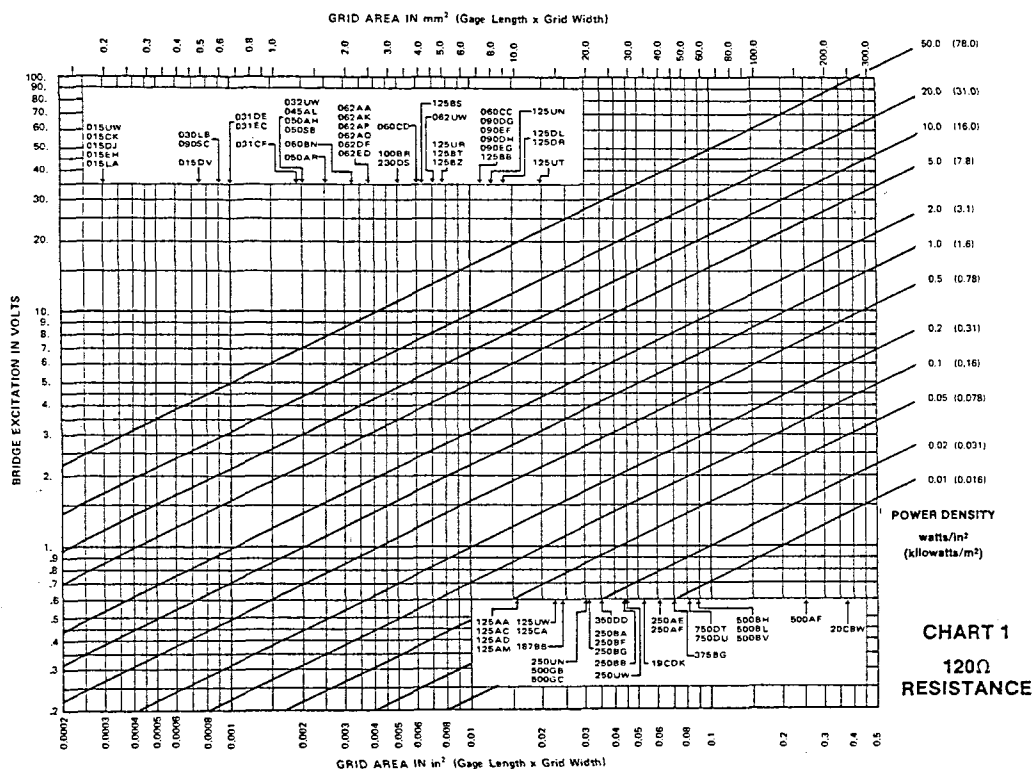
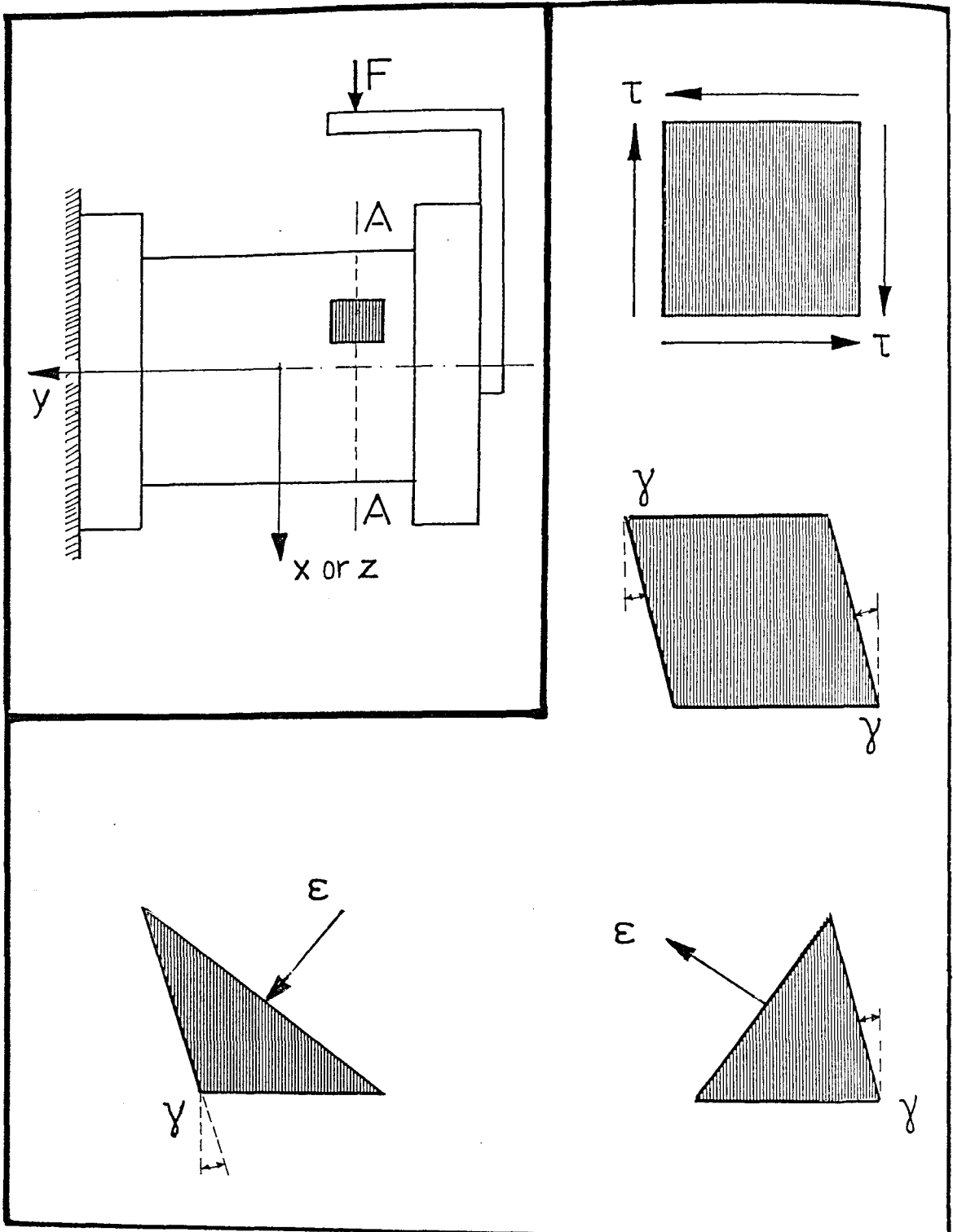


Fig 3.3 The excitation level of strain gauge bridges
(Extracted from : Measurement Group TN-502)



Note : Symmetry about x - y (or z - y) plane must be considered for stresses and strains on an element positioned on the opposite side of the transducer

Fig 3.4 Application of pure shear force

decrease of the accuracy level, a 3 Volt power supply was used for the excitation of the bridges ; using , however 6 Volts for bridge C which has double the resistance. The power supply for each bridge in Volts is denoted by Vs .

3.3 Study of transducer for applied Shear forces

Figure 3.4 shows the loading configuration for which a pure shear force F is applied through a cross-section of the pylon transducer. Despite the fact that all other cross-sections of the device are subjected to bending moments and shear force simultaneously, section A-A is only subjected to the pure shear force F.

The shear stress τ on the surface of the pylon transducer is given by the following equations, which are derived in appendix VIII :

for $0 \leq x_o \leq R_i$:

$$\tau = \frac{F}{3 \cdot t \cdot I} \frac{R_o}{\sqrt{R_o^2 - x_o^2}} \left[(R_o^2 - x_o^2)^{3/2} - (R_i^2 - x_o^2)^{3/2} \right] \quad (3.2a)$$

$$\text{where : } t = \sqrt{R_o^2 - x_o^2} - \sqrt{R_i^2 - x_o^2}$$

for $R_i < x_o \leq R_o$:

$$\tau = \frac{F \cdot R_o}{3 \cdot I} \cdot \sqrt{R_o^2 - x_o^2} \quad (3.2b)$$

In this configuration there are no normal stresses and therefore all longitudinally positioned gauges as well as all Poisson's gauges cannot (theoretically) be affected. Therefore it can be deduced from figure (3.2) that bridges A, B and C are balanced.

It is also noted that the shear stress varies with the position x_0 . This stress is :

$$\tau = \frac{F}{3 \cdot I} \cdot \frac{(R_o^3 - R_i^3)}{(R_o - R_i)} \quad (\text{maximum}) \quad (3.3)$$

at position $x_0 = 0$ and is zero at positions $x_0 = \pm R_o$. Therefore the gauges corresponding to the latter positions are not affected either. If load F is applied along the x -axis of the transducer frame bridge D is balanced and if load F is applied along the z -axis of the transducer frame, bridge E is balanced.

From the above considerations it is deduced that the only bridges which could be unbalanced under this loading configuration are : bridge F monitoring torque and the bridge monitoring the applied shear force. The gauges of bridge F are subjected to equal and opposite strains which cause resistance changes dR_F as following :

gauges $F1$ and $F4$ are subjected to a change $-dR_F$ and
gauges $F2$ and $F3$ are subjected to a change $+dR_F$

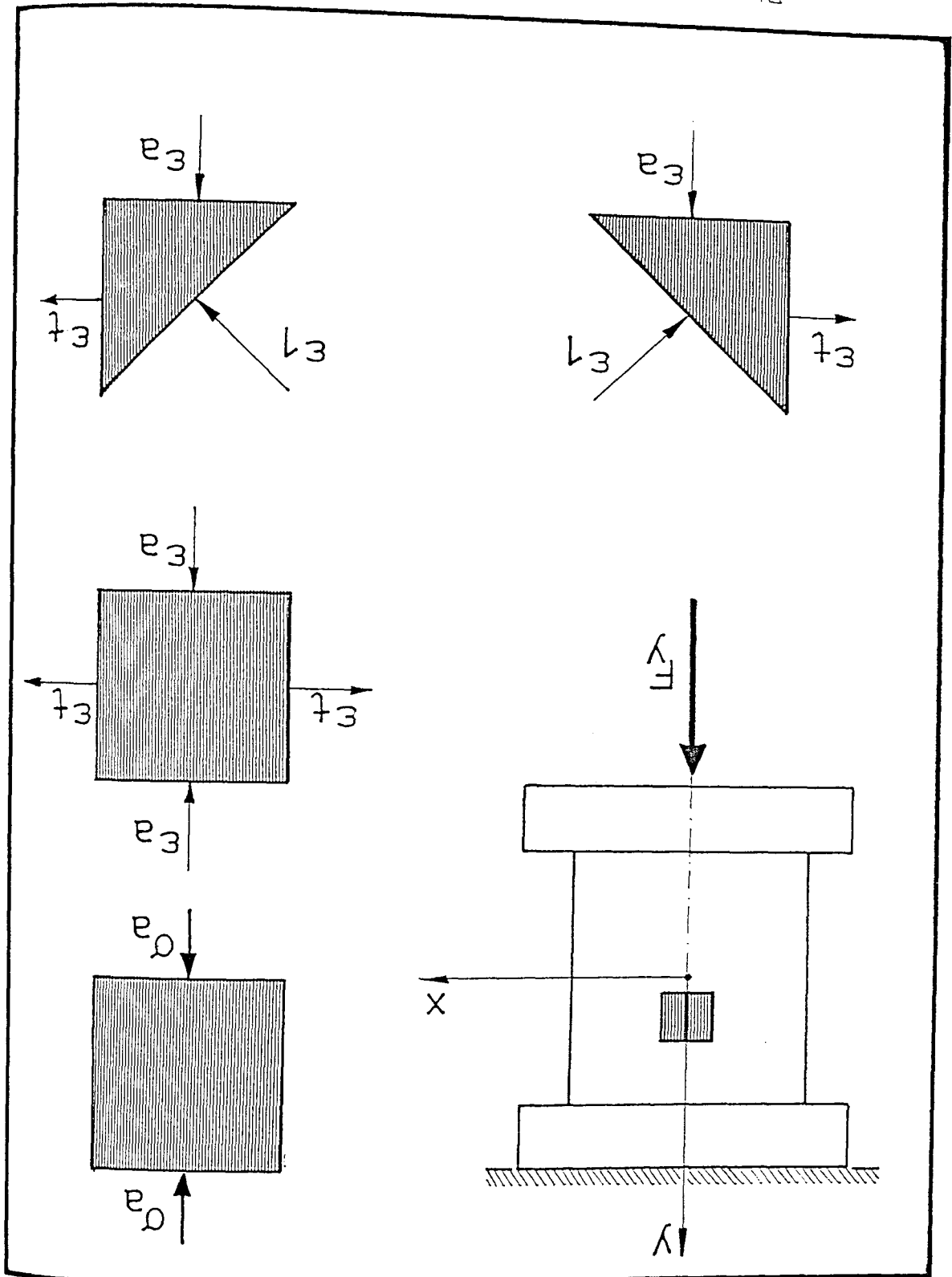
The gauges of bridge E (consider $F = F_x$) are subjected to equal and opposite strains which cause resistance changes dR as following :

gauges $E1$ and $E3$ are subjected to a change $-dR_E$ and
gauges $E2$ and $E4$ are subjected to a change $+dR_E$

From the wiring diagrams of figure 3.2, it follows that bridge F is able to compensate for the changes and remain eventually balanced, whereas bridge E is not balanced and provides an output signal V_o :

$$V_o = V_s \cdot \frac{dR_E}{R} = V_s \cdot K \cdot \epsilon \quad (3.4)$$

Fig 3.5 Application of axial force



Strain ϵ is related to the shear stress τ by the following equation :

$$\epsilon = \frac{\gamma}{2} = \frac{\tau}{2 G} \quad (3.5)$$

Thus, it is proven that for a particular shear load component applied, the only bridge which responds is the one meant to monitor it. From equations (3.3), (3.4) and (3.5) the output voltage of this bridge can be derived.

3.4 Study of transducer for applied Axial force

The axial force F_y is now considered applied as shown in figure 3.5 . In this case there is only one stress configuration and consists, as shown, of the axial normal stress σ_a . This stress causes the strains ϵ_a (compression) and $\epsilon_t = -\nu \epsilon_a$ (tension) shown .

The predominant compressive strain ϵ_a on its turn imposes a compressive strain ϵ_1 along both of the inclined directions shown :

$$\text{compressive } \epsilon_1 = \frac{1}{2} \cdot \epsilon_a \cdot (1-\nu) \quad (3.6)$$

The gauges of bridges A and B are all subjected to the same decrease of their resistance values (see figure 3.2) , due to ϵ_a . Similarly , the gauges of bridges D, E and F are also all subjected to the same decrease of their resistance values , due to ϵ_1 . Therefore, all these five bridges cannot (theoretically) respond to the application of the axial load.

The only bridge which does so is bridge C , the gauges of which are subjected to resistance changes as following :

gauges C1, C3, C5 and C7 are subjected to $-dR_C$ and
gauges C2, C4, C6 and C8 are subjected to $+\nu \cdot dR_C$

Thus, bridge C is eventually unbalanced and provides an output signal given by :

$$V_o = V_s \cdot \frac{\frac{dR_C}{R} \cdot (1+\nu)}{2 - \frac{dR_C}{R} \cdot (1-\nu)} \approx V_s \cdot \frac{dR_C}{2R} \cdot (1+\nu) \quad \text{or}$$

$$V_o = V_s \cdot (1+\nu) \cdot \frac{K}{2} \cdot \epsilon_a \quad (3.7)$$

Note that the fractional term at the denominator of the first equation, as explained in appendix I, can be neglected, resulting in a simple linear relationship.

Strain ϵ_a is related to the applied load F_y by equation :

$$\epsilon_a = \frac{\sigma_a}{E} = \frac{F_y}{AE} \quad (3.8)$$

Thus, it is proven that for a particular axial load component applied, the only bridge which responds is the one meant to monitor it.

3.5 Study of transducer for applied Bending moments

The configurations regarding purely applied bending moments will be studied separately for moments M_x and M_z , for reasons due to their influence on the various bridges.

3.5.1 Bending moment M_x

Figure 3.6 shows a bending moment M_x purely applied onto the distal end of the pylon transducer. The effect of this moment is twofold : moment M_x causes compression in the top half of the transducer (from 0° to 180°) and tension in the bottom half of the transducer (from 180° to 360°) .

Two elements have been chosen to demonstrate the

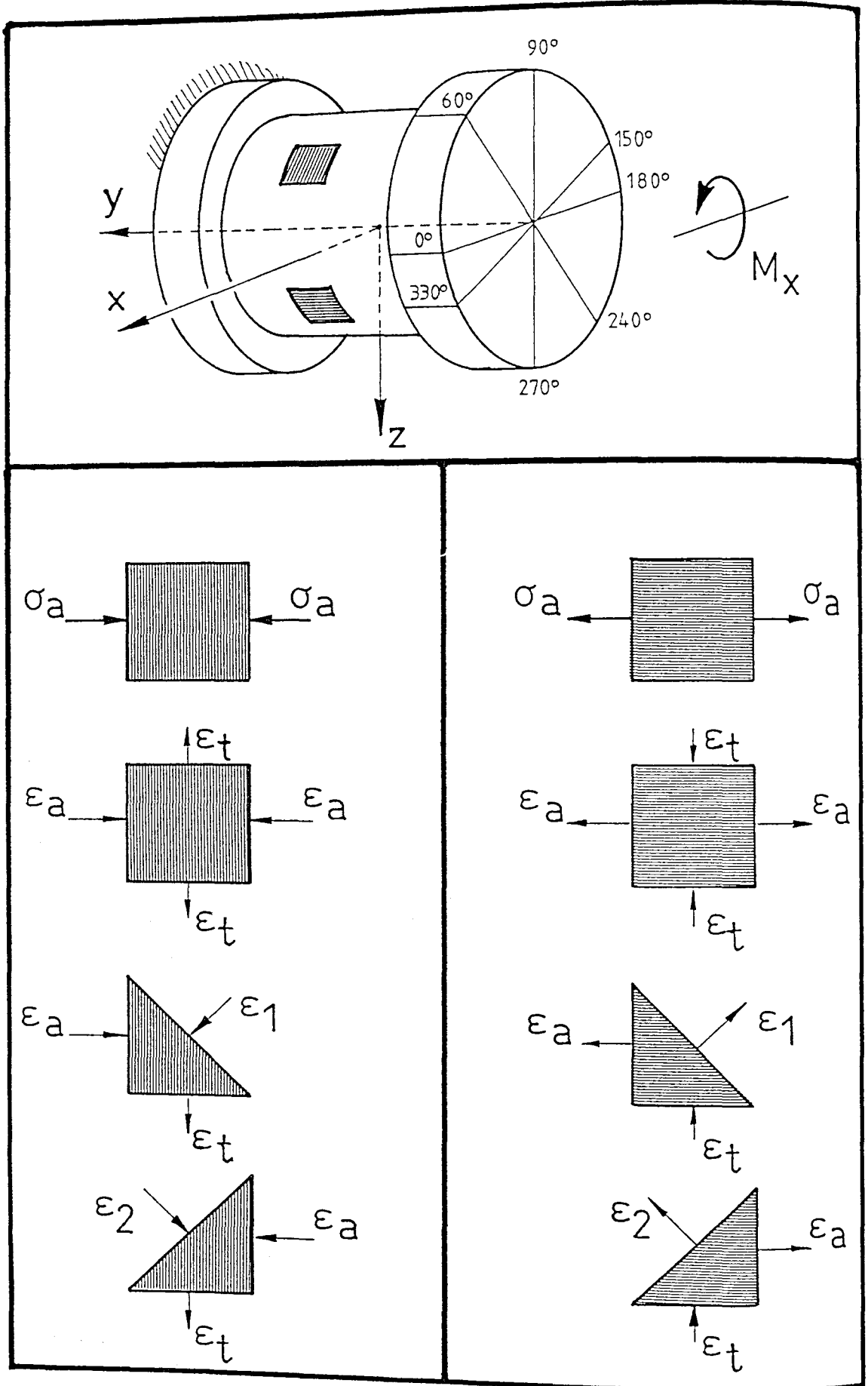


Fig 3.6 Application of bending moment M_x

stresses and strains developed ; one in the area subjected to compression , the other in the area subjected to tension. Stress σ_a in the axial direction causes the strains shown , in the axial, the transverse and the two inclined directions under study. Strain ϵ_1 and ϵ_2 are in any case equal to :

$$\epsilon_1 = \epsilon_2 = \frac{\epsilon_a}{2} \cdot (1-\nu) \quad (3.9)$$

All gauges bonded on the surface of the top half are subjected to the stress / strain configurations similar to the ones presented for the first element. All gauges bonded on the surface of the bottom half are subjected to stress / strain configurations similar to the ones presented for the second element.

However, the stresses and therefore the strains depend on the distance from the neutral plane and since the various gauges are bonded in different positions the individual stresses and strains must be considered. The individual axial stresses are all expressed in terms of the maximum value (the various locations are given here in terms of their angular position as shown) :

$$\begin{aligned} \text{for } 90^\circ : \text{compression } \sigma &= \frac{Mx}{I} Ro \\ \text{for } 150^\circ : \text{compression } \sigma_{30} &= \sigma \cdot (\sin 30^\circ) \\ \text{for } 60^\circ : \text{compression } \sigma_{60} &= \sigma \cdot (\sin 60^\circ) \\ \text{for } 270^\circ : \text{tension } \sigma &= \frac{Mx}{I} Ro \\ \text{for } 330^\circ : \text{tension } \sigma_{30} &= \sigma \cdot (\sin 30^\circ) \\ \text{for } 240^\circ : \text{tension } \sigma_{60} &= \sigma \cdot (\sin 60^\circ) \end{aligned} \quad (3.10)$$

From figure (3.2) it is appreciated that bridges A and D cannot (theoretically) respond to the applied load because their gauges are lying on the neutral plane.

However, all other bridges are affected and it must be determined which of these can compensate and

remain balanced and which cannot. Considering equations (3.9) and (3.10) and the position of the gauges of bridges E and F , the following resistance changes can be deduced:

gauges F1 and F2 are subjected to a change $-dR_F$ and
gauges F3 and F4 are subjected to a change $+dR_F$

where : $dR_F = K \cdot R \cdot \frac{\epsilon_{60}}{2} \cdot (1-\nu)$ and

gauges E1 and E2 are subjected to a change $-dR_E$ and
gauges E3 and E4 are subjected to a change $+dR_E$

where : $dR_E = K \cdot R \cdot \frac{\epsilon}{2} \cdot (1-\nu)$

In the above expressions ϵ and ϵ_{60} are the strains corresponding to the stresses σ and σ_{60} respectively .

Consulting figure 3.2 it is proved that these two bridges can compensate for the changes and are therefore balanced.

However, the gauges of bridge B are subjected to the following resistance changes :

gauges B1 and B2 are subjected to a change $-dR_B$ and
gauges B3 and B4 are subjected to a change $+dR_B$

where : $dR_B = K \cdot R \cdot \epsilon$

which proves that this bridge is not balanced and provides an output signal V_o :

$$V_o = V_s \cdot \frac{dR_B}{R} = V_s \cdot K \cdot \epsilon \quad (3.11)$$

The strain ϵ is related to the axial stress by equation : $\epsilon = \sigma / E$.

The gauges of bridge C are considered next. Theses gauges are subjected to the following resistance changes :

gauge C1 is subjected to a change : $- K \cdot R \cdot \varepsilon_{60}$
 gauge C3 is subjected to a change : $- K \cdot R \cdot \varepsilon_{30}$
 gauge C5 is subjected to a change : $+ K \cdot R \cdot \varepsilon_{60}$
 gauge C7 is subjected to a change : $+ K \cdot R \cdot \varepsilon_{30}$
 similarly,
 gauge C2 is subjected to a change : $+ K \cdot R \cdot \nu \varepsilon_{60}$
 gauge C4 is subjected to a change : $+ K \cdot R \cdot \nu \varepsilon_{30}$
 gauge C6 is subjected to a change : $- K \cdot R \cdot \nu \varepsilon_{60}$
 gauge C8 is subjected to a change : $- K \cdot R \cdot \nu \varepsilon_{30}$

From the above expressions it is proven that the longitudinal gauges of bridge C are not all subjected to stresses of equal absolute values; the same applying for the Poisson's gauges. Writing the equation for the output signal V_o , it is shown that this bridge is not eventually balanced :

$$V_o = V_s \cdot \frac{(1 - \nu^2) \cdot \left(\frac{dR^*}{R} \right)^2}{16 - (1 + \nu)^2 \cdot \left(\frac{dR^*}{R} \right)^2}$$

or because the squared fractional term in the denominator can be considered negligible :

$$V_o = V_s \cdot \frac{(1 - \nu^2)}{16} \cdot \left(\frac{dR^*}{R} \right)^2 \quad (3.12a)$$

$$\text{where : } dR^* = (\sqrt{3} + 1) \frac{dR}{2} \text{ and} \quad (3.12b)$$

$$\frac{dR}{R} = K \cdot \varepsilon = K \cdot \frac{\sigma}{E}$$

It is, therefore, proven that for a purely applied bending moment M_x , besides the corresponding bridge B, bridge C (monitoring axial load) is also unbalanced.

3.5.2 Bending moment M_z

The analysis is similar for a purely applied

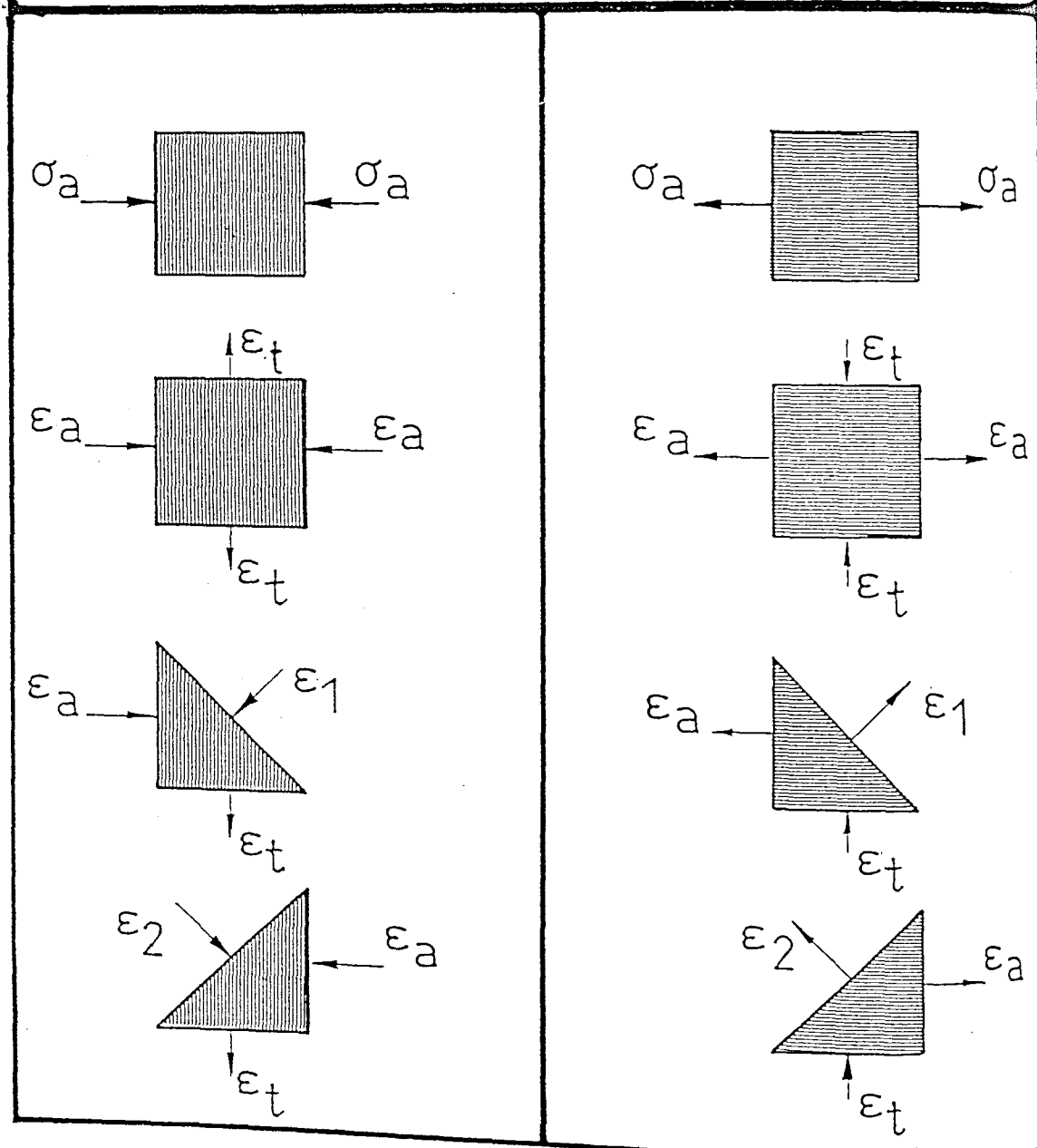
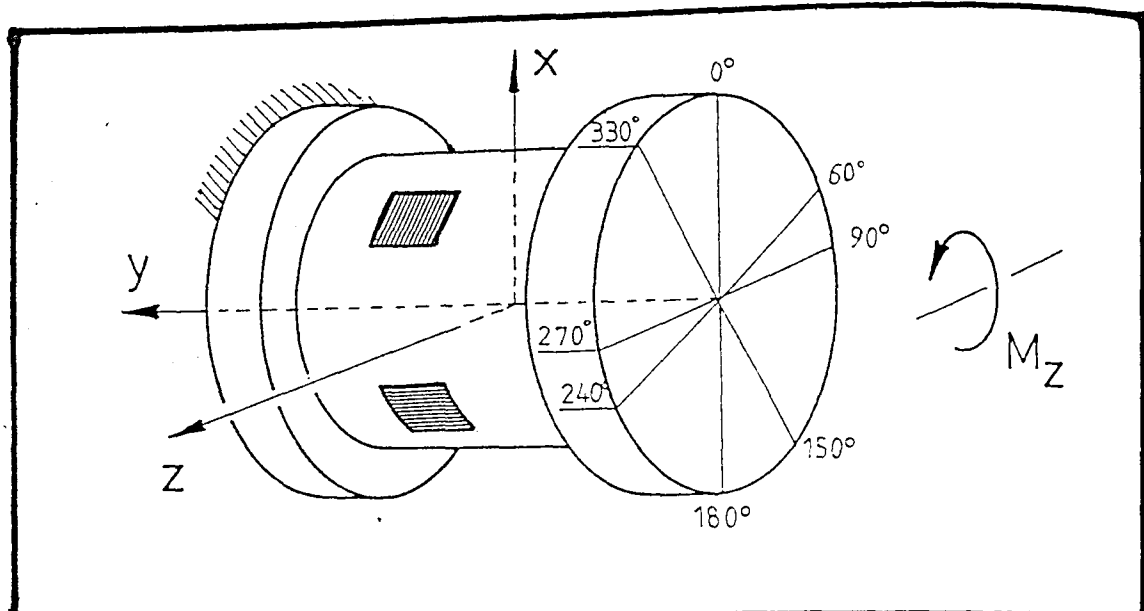


Fig 3.7 Application of bending moment M_z

bending moment M_z . As shown in figure 3.7, in this case the neutral plane passes through the angular positions of 90° and 270° .

Bridges B and E cannot (theoretically), therefore, respond to the applied load. Bridges D and F are, however, affected but can compensate for the effects and remain eventually balanced.

Bridge A meant to monitor the applied bending moment is not balanced and provides an output signal V_o :

$$V_o = V_s \cdot \frac{dR_A}{R} = V_s \cdot K \cdot \varepsilon \quad (3.13)$$

The strain ε is related to the applied load by equation : $\varepsilon = (M_z \cdot R_o) / EI$.

Like in the previous configuration, here again bridge C is not balanced. However, there is a difference due to the resistance changes that occur this time on the gauges. The individual resistance changes can be expressed, using the same notation, as follows:

gauge C1 is subjected to a change : $- K \cdot R \cdot \varepsilon_{30}$
gauge C3 is subjected to a change : $+ K \cdot R \cdot \varepsilon_{60}$
gauge C5 is subjected to a change : $+ K \cdot R \cdot \varepsilon_{30}$
gauge C7 is subjected to a change : $- K \cdot R \cdot \varepsilon_{60}$
gauge C2 is subjected to a change : $+ K \cdot R \cdot \nu \varepsilon_{30}$
gauge C4 is subjected to a change : $- K \cdot R \cdot \nu \varepsilon_{60}$
gauge C6 is subjected to a change : $- K \cdot R \cdot \nu \varepsilon_{30}$
gauge C8 is subjected to a change : $+ K \cdot R \cdot \nu \varepsilon_{60}$

Writing again the equation for the output signal V_o , as provided in appendix I, it is shown that this bridge is not eventually balanced for this configuration either. The output voltage is given again by equation (3.12a), where :

$$dR^* = (\sqrt{3} - 1) \frac{dR}{2} \quad (3.14)$$

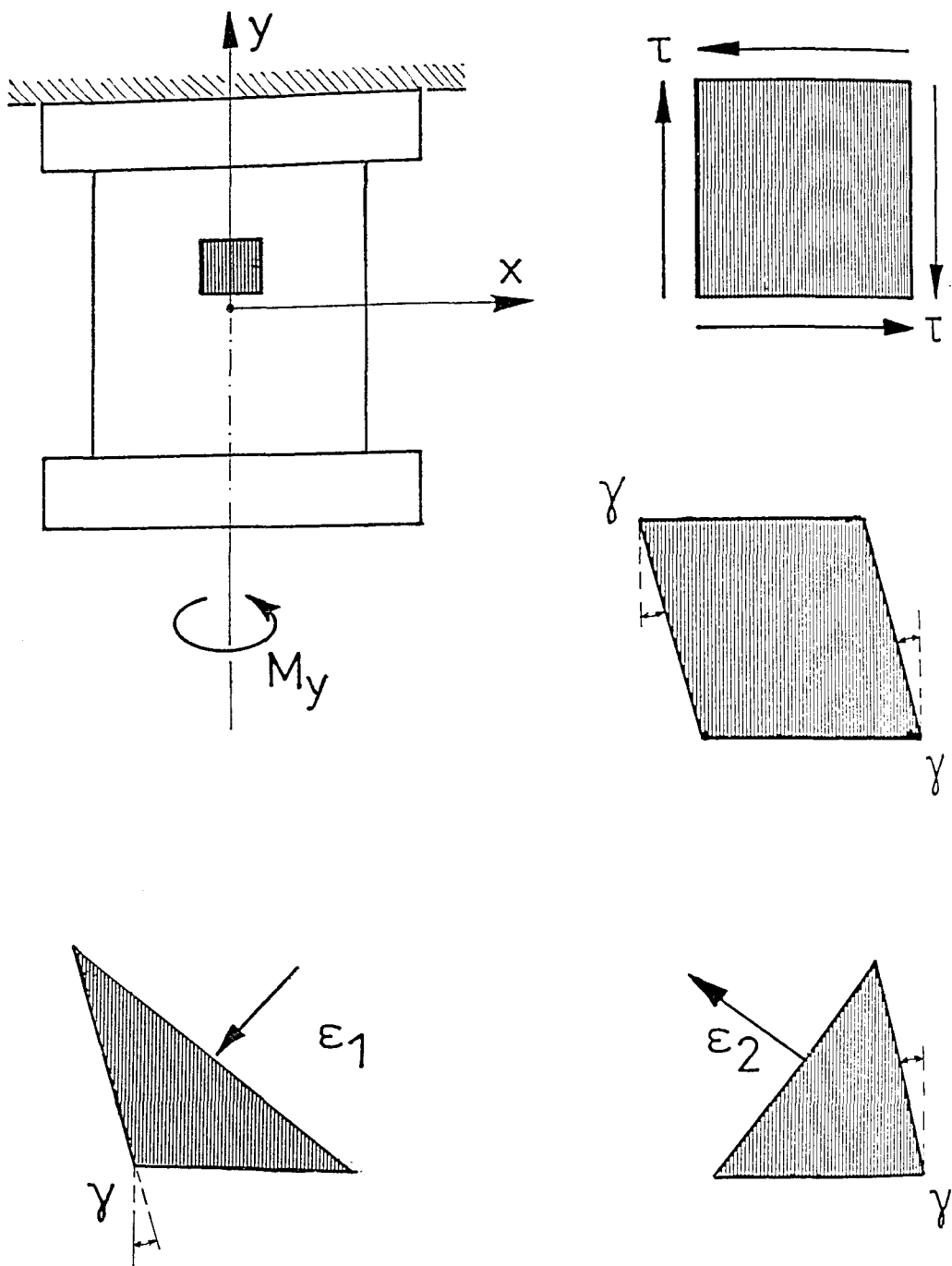


Fig 3.8 Application of torque M_y

In this case the value dR^* is different (in fact lower) than the one derived for bending moment M_x .

It is, therefore, proven that for a purely applied bending moment M_z , besides the corresponding bridge A, bridge C (monitoring axial load) is also unbalanced.

3.6 Study of transducer for applied Torque

In this case, the stress configuration purely consists of the shear stress τ . Therefore, all gauges in longitudinal and transverse directions are not (theoretically) subjected to any stress at all. Thus, bridges A, B and C are balanced.

As shown in figure 3.8 only the gauges oriented at an angle from the y-axis are subjected to strain and therefore the gauges under study for this case are the gauges of bridges D, E and F.

The shear stress τ applied on the element produces a shear strain γ as shown. At the inclined directions the strains are equal and opposite and their value is :

$$\begin{aligned} \text{(compression)} \quad \epsilon_1 &= \gamma / 2 \\ \text{(tension)} \quad \epsilon_2 &= \gamma / 2 \end{aligned} \tag{3.15}$$

The gauges of bridges D, E and F are subjected to the following changes of their resistance :

gauges D1 and D4 are subjected to a change $+dR_D$ and
 gauges D2 and D3 are subjected to a change $-dR_D$
 gauges E1 and E4 are subjected to a change $+dR_E$ and
 gauges E2 and E3 are subjected to a change $-dR_E$
 gauges F1 and F3 are subjected to a change $+dR_F$ and
 gauges F2 and F4 are subjected to a change $-dR_F$

where : $dR_D = dR_E = dR_F = K \cdot R \cdot (\gamma / 2)$

$$\text{and} \quad \gamma = \frac{\tau}{G} = \frac{M_y \cdot R_o}{J \cdot G} \tag{3.16}$$

From the wiring diagrams shown in figure (3.2) it is appreciated that bridges D and E compensate for the effect of the developed strain, and are eventually balanced. However , bridge F results to an output signal V_o , given by the familiar formula :

$$V_o = V_s \cdot \frac{dR_F}{R} = V_s \cdot K \cdot \frac{\gamma}{2} \quad (3.17)$$

Thus, it is proven that for a purely applied torque the only bridge which responds is bridge F.

3.7 Quantitative Results of the Analysis

In the study presented in the previous sections equations were derived relating the o/p signal of each bridge to the load component applied onto the pylon transducer. These equations will here be used to quantify the effect of various load components on the bridges, namely to determine the sensitivity of the bridges to the applied loads.

- 1) applied shear force F (along x or z axes) = 100 N
 shear stress τ (from eq. 3.3) = 0.974 MPa
 strain ϵ_1 (from eq. 3.5) = 17.839×10^{-6}
for the corresponding channel only :
 output signal V_o (from eq. 3.4) = 107.0 μ Volts
 sensitivity = 1.070 μ Volts / N
 sensitivity for unit power supply = 0.357 μ Volts / N

- 2) applied axial load F_y = 1000 N
 stress σ_a (from eq. 3.8) = 4.890 MPa
 strain ϵ_a (from eq. 3.8) = 70.972×10^{-6}
for the corresponding channel only :
 output signal V_o (from eq. 3.7) = 536.5 μ Volts
 sensitivity = 0.537 μ Volts / N
 sensitivity for unit power supply = 0.090 μ Volts / N

- 3) applied bending moment $M_x = 100 \text{ Nm}$
stress σ (from eq. 3.10) = 74.272 MPa
strain $\epsilon = 1077.968 \times 10^{-6}$
for the corresponding channel :
output signal V_o (from eq.3.11) = 6467.8 μVolts
sensitivity = 64.678 $\mu\text{Volts} / \text{Nm}$
sensitivity for unit power supply = 21.559 $\mu\text{Volts}/\text{Nm}$
and for channel 2 (F_y) :
relative change dR^*/R (from eq. 3.12) = 2945×10^{-6}
output signal V_o (from eq.3.12) = 3.033 μVolts
sensitivity = 0.030 $\mu\text{Volts} / \text{Nm}$
sensitivity for unit power supply = 0.0051 $\mu\text{Volts}/\text{Nm}$
- 4) applied bending moment $M_z = 100 \text{ Nm}$
stress $\sigma = 74.272 \text{ MPa}$
strain $\epsilon = 1077.968 \times 10^{-6}$
for the corresponding channel :
output signal V_o (from eq.3.13) = 6467.8 μVolts
sensitivity = 64.678 $\mu\text{Volts} / \text{Nm}$
sensitivity for unit power supply = 21.559 $\mu\text{Volts}/\text{Nm}$
and for channel 2 (F_y) :
relative change dR^*/R (from eq.3.14) = 789.13×10^{-6}
output signal V_o (from eq.3.12) = 0.2177 μVolts
sensitivity = 0.0022 $\mu\text{Volts} / \text{Nm}$
sensitivity for unit power supply = 0.0004 $\mu\text{Volts}/\text{Nm}$
- 5) applied torque $M_y = 30 \text{ Nm}$
shear stress τ (from eq. 3.16) = 11.141 MPa
shear strain γ (from eq. 3.16) = 408.095×10^{-6}
for the corresponding channel only :
output signal V_o (from eq. 3.17) = 1224.3 μVolts
sensitivity = 40.810 $\mu\text{Volts} / \text{Nm}$
sensitivity for unit power supply = 13.603 $\mu\text{Volts}/\text{Nm}$

3.8 Discussion

The study presented in this chapter was carried out in order to determine in qualitative and quantitative terms the effect that various load

components have on the strain gauge bridges of the short pylon transducer (Berme et al.1976). The analysis was based upon the assumptions presented in section 3.2.

A shear force (either F_x or F_z), an axial load F_y and a torque M_y , when applied individually produced an output signal of the corresponding bridges only. However, bending moments did not only produced output signals of the corresponding bridges, but also an output signal of the bridge corresponding to load F_y (channel 2).

The effect of the two bending moments on channel 2 is not the same: the bridge of channel 2 was proved to be more sensitive to bending moment M_x and less sensitive to bending moment M_z . The former sensitivity for unit power supply was calculated to be $0.0051 \mu\text{Volts/ Nm}$ and the latter was calculated to be $0.0004 \mu\text{Volts/ Nm}$.

The sensitivity of channel 2 for axial load F_y and for unit power supply was calculated to be $0.090 \mu\text{Volts/ N}$. Thus, the effect that the two bending moments have on channel 2 can be given the following interpretations :

sensitivity ratio ($0.0051 / 0.090$) $\cong 0.057$ or
 apparent axial load $F_y = 0.057 \text{ N} / (\text{Nm of } M_x)$ and
 sensitivity ratio ($0.0004 / 0.090$) $\cong 0.004$ or
 apparent axial load $F_y = 0.004 \text{ N} / (\text{Nm of } M_z)$

It can be appreciated that the effect of M_z and M_x on channel 2 can practically be considered negligible. Even if the antero-posterior bending moment reaches the typical value $M_z = 100 \text{ Nm}$ (at the ankle level of a prosthesis) the apparent F_y load will only be 0.40 N and even if the medio-lateral bending moment reaches the typical value $M_x = 10 \text{ Nm}$ (at the ankle level again) the apparent F_y load will only be 0.57 N . It can therefore be concluded that these theoretical effects

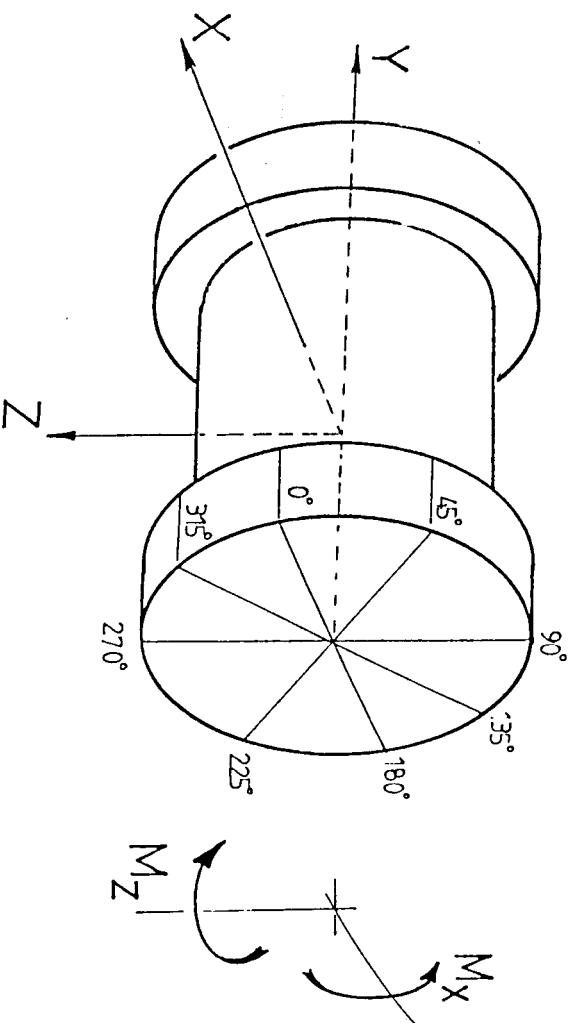
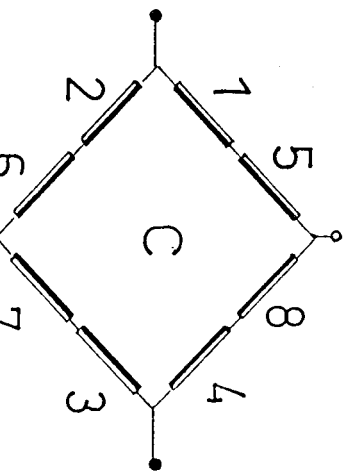
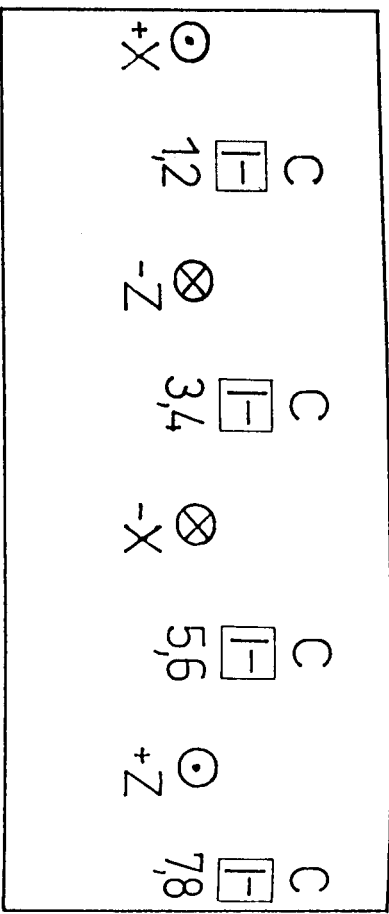
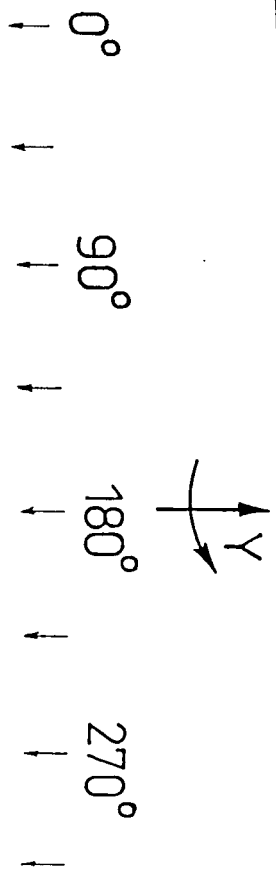


Fig 3.9 Suggested gauging design and bending-moment loading configurations



can be practically considered negligible.

Gauging design which would eliminate the observed cross- sensitivity, is shown in figure 3.9 . During the application of a pure bending moment, bridge C is unbalanced because the two resistance ratios of its gauges are not equal :

$$\frac{R_{C1} + R_{C3}}{R_{C1} + R_{C3} + R_{C6} + R_{C8}} \neq \frac{R_{C2} + R_{C4}}{R_{C2} + R_{C4} + R_{C5} + R_{C7}} \quad (3.18)$$

On the other hand, due to the existence of the Poisson's gauges, the above ratios could only be equal if the resistance changes caused by the loading configuration were equal and opposite for each one of the numerators and denominators shown.

Figure 3.9 shows a bridge configuration that fulfills the above condition. All gauges are symmetrically positioned about axes x and z , ie. at 45° , 135° , 225° and 315° . Furthermore the gauges are differently connected. For this configuration the two resistance ratios are :

$$\frac{R_{C1} + R_{C5}}{R_{C1} + R_{C5} + R_{C2} + R_{C6}}, \quad \frac{R_{C4} + R_{C8}}{R_{C4} + R_{C8} + R_{C3} + R_{C7}} \quad (3.19)$$

When an M_x bending moment is applied (say in the positive sense as shown), gauges C1 and C3 experience the same compression and gauges C5 and C7 equal in magnitude tension (accordingly for the Poisson's gauges). As a result the absolute resistance change is dR for all longitudinal gauges and $(\nu \cdot dR)$ for all Poisson's gauges. The ratios (3.19) can now be evaluated :

$$\text{left hand-side ratio} = \frac{(R - dR) + (R + dR)}{R - dR + R + dR + R + \nu dR + R - \nu dR}$$

$$\text{right hand-side ratio} = \frac{(R + \nu dR) + (R - \nu dR)}{R + \nu dR + R - \nu dR + R - dR + R + dR}$$

$$\text{and both ratios equal to } \frac{2R}{4R} = \frac{1}{2}$$

The two ratios are equal and thus no output signal will be produced. The bridge will compensate for the changes and will remain balanced.

The same stands for an applied bending moment M_z . As shown the gauges are again in areas which favour the balance of the bridge.

3.9 Conclusions

The conclusions from the work presented in this chapter are as follows :

- 1) The short pylon transducer has by-design two very small cross-sensitivities, between applied bending moments and bridge C (of channel 2), which are practically negligible.
- 2) A new design is suggested that eliminates these minor cross-effects and favours the balance of bridge C even during application of bending moments; maintaining however the sensitivity of the bridge to the corresponding axial load F_y .
- 3) For the work presented in this thesis a 3 Volt power supply was justified for each bridge except channel 2, for which supply of 6 Volts was chosen.
- 4) As a theoretical reference, sensitivity values for all channels have been calculated. These values could be later compared with the ones derived by the actual calibration of the transducer presented in the next chapter.

CHAPTER 4

THE CALIBRATION OF THE SHORT PYLON TRANSDUCER

4.1 Introduction

4.2 Followed approach

4.3 The Calibration using the Instron machine

4.3.1 Introduction

4.3.2 Shear load Calibration

4.3.3 Axial load Calibration

4.3.4 Bending moment Calibration

4.3.5 Torque Calibration (system Mark I)

4.3.6 Torque Calibration (system Mark II)

4.4 Results and Discussion

4.6 Conclusions

4.1 Introduction

During experimental use the output signals of the pylon transducer must be converted into meaningful mechanical quantities (forces and moments). Therefore the transducer must be calibrated. The principle is to apply known loads onto a mechanical system containing the transducer in such a way as to load the directions of interest and then record the outputs signals ; the objective being the compilation of a mathematical relationship between them.

For the pylon transducer there are six mechanical quantities of interest, namely the shear forces (F_x and F_z), the axial load (F_y), the bending moments (M_x and M_z) and the torque (M_y), all expressed in the transducer's frame of reference (the pylon transducer is described in details in chapters 2 and 3).

Ideally, each of the six channels would respond (i.e produce a non-zero output signal) when and only when a load corresponding to that particular channel is applied (this is called a main effect). In practice, however, even under the existence of one single load component, all six channels may respond, introducing therefore the study of other effects in the calibration procedure (cross-effects). These effects are due to inherent characteristics of the device, which could be:

- a) Asymetries of the device due to machining errors and/or
- b) Misalignment of the gauges on the device.

Cross - effects may also be due to :

- c) elastic deformations caused by the particular loading configuration.

Therefore, the issue arises on which calibration procedure to follow and also which mathematical approach to adopt in order to obtain a relationship between the output signals and the applied loads. The various approaches and techniques related to the above issues have been discussed in the literature review.

For the calibration of the short pylon transducer and the validation of the derived calibration matrix

(chapter 5) the author initially decided to use an Instron machine. This method was later proved, both from the tests and the literature, not as reliable as the well established dead-weight techniques. However, at the time, such problems were not anticipated and the work on the material testing machine proceeded.

4.2 Followed Approach

The approach followed for the calibration of the transducer consists of the following points :

- a) The linear model would be initially adopted, ie the objective of the calibration would be the determination of matrix $[M]$ and then the calculation of matrix $[C]$.
- b) All loads would be purely applied allowing, thus, for the determination of each one of the effects individually.
- c) All output signals would be regressed against the applied load component and the decisions about the retention or elimination of coefficients m_{ij} would be based on their p-values.
- d) The derived calibration matrix must be validated and therefore known loads should be applied on the pylon transducer and estimated by the matrix.
- e) Investigation regarding the use of a second order model for the calibration of the short pylon transducer should be conducted and comparative results between the two models should be acquired.

The method of calibration of the pylon transducer using the Instron machine is discussed in detail in the next section.

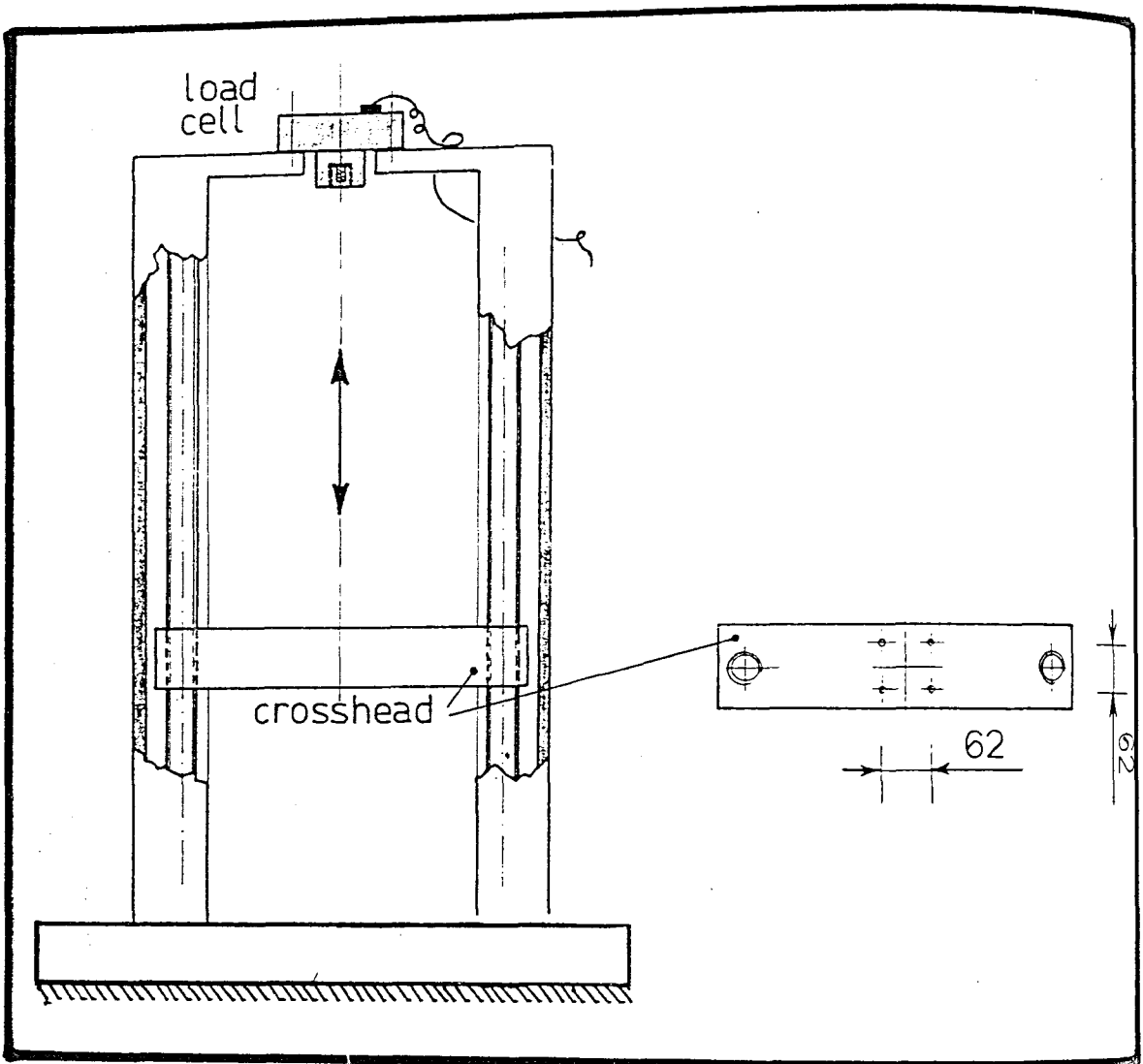


Fig 4.1 The Instron machine

4.3 The Calibration using the Instron machine

4.3.1 Introduction

The Instron machine shown in figure 4.1 has a cross-head which can be subjected to controllable motion in the vertical direction and on which the pylon transducer may be mounted. An interface plate had to be designed for this latter purpose (see appendix II) . On the other hand, the various loads had to be applied by means of appropriately designed componentry , mechanically connecting the transducer to the load cell which is responsible for the assessment of the applied loads. These components had to ensure the absence of any off-axis loading that the Instron machine cannot be subjected to.

All six loads (F_x , F_y , F_z , M_x , M_y , M_z) were to be individually applied and signals were to be recorded with a multimeter at the output of the strain gauge amplifiers. Wiring connections of the system and gain settings of the amplifiers are given in appendix IX, and the bridge voltage supplies are given in chapter 3.

4.3.2 Shear Load Calibration (figs 4.2 a and b)

For the calibration tests, concerning the shear forces F_x and F_z , the machined interface plate (1), was mounted onto the cross-head of the Instron. A base (2) was then fitted on top of the plate, providing support for the transducer to be mounted with its longitudinal axis horizontally.

The load cell of the Instron was a 0-100 kg tension / compression load cell* and was fitted with a threaded cone (3) for point loading.

The transducer was connected by means of a bolt to a specially machined bracket (4) provided with a small locator (5) to secure proper contact with the cone (3). This bracket had to be properly aligned against the

* The type of the cell could not be identified.

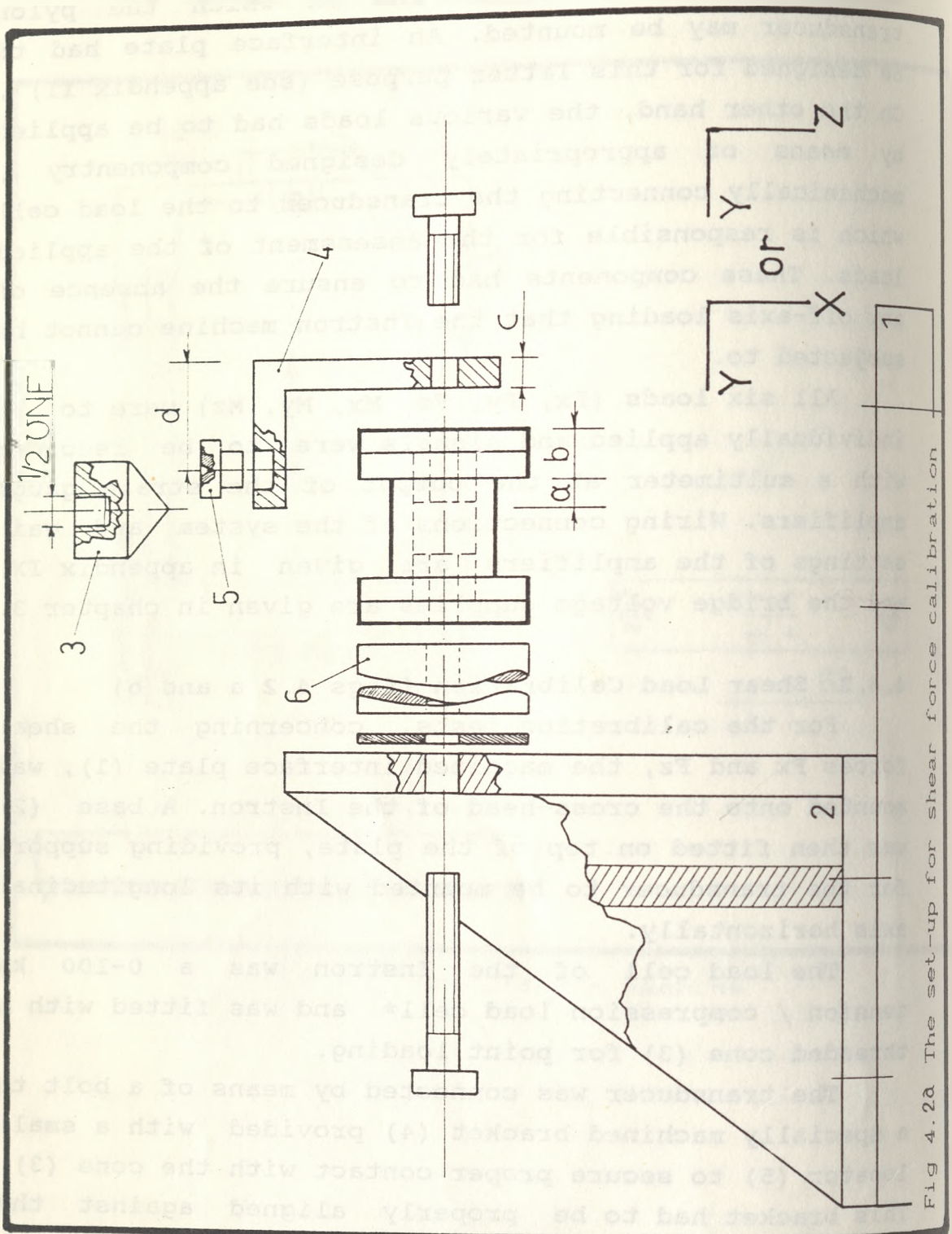


Fig 4.2a The set-up for shear force calibration

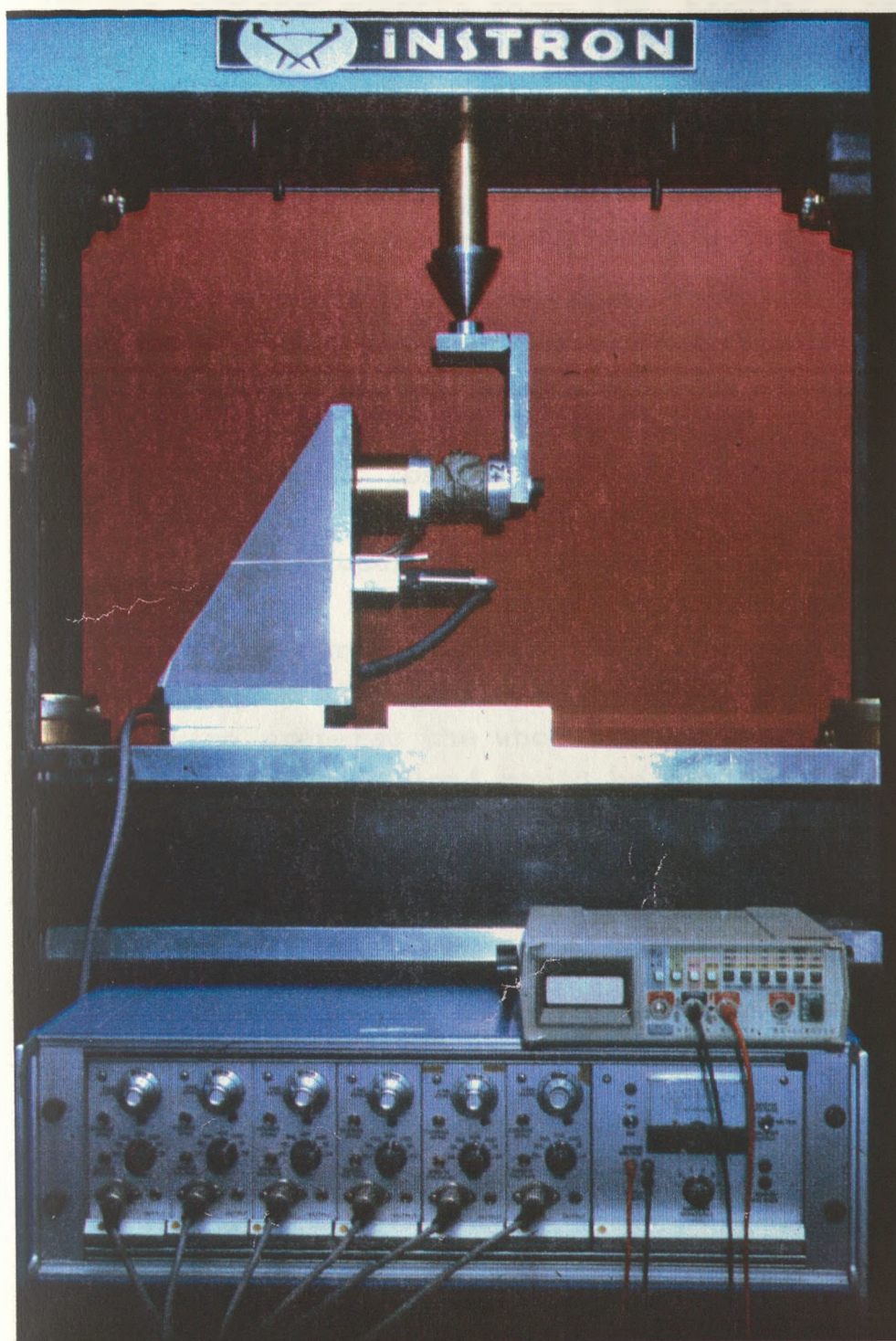


Fig 4.2b The set-up for
shear force calibration

transducer frame, at the required angular position, depending on whether Fx or Fz loads was to be applied. The transducer had also to be aligned itself against the base (2) depending on the same condition.

The bracket (4) was designed so that the locator (5) was centered exactly above the bending - detecting gauges, which were at distance "a" from the top flange of the pylon transducer. If no bending moment was to be created, the following equation had to be fulfilled during the design :

$$(d - c) = (a + b)$$

The a s s u m p t i o n was made that the very small leverarm between the load line and the lower gauge level was producing a negligible bending moment at that level. The maximum bending moment would only be 1.47 Nm (for a 15 kg shear load).

The spacers (6) were selected in order that the system of transducer and bracket could be exactly below the cone (3), to ensure that both cone (3) and locator (5) centres coincided with the vertical axis of the Instron machine.

Having prepared the whole setup and by moving the cross-head upwards, load could be applied on the pylon transducer, purely along the shear force direction , as required.

The bridges were then balanced and the Instron load was increased up to 15 kg, by increments of 1 kg, using a cross-head speed of 0.01 mm/min. When the maximum load was reached, the load was reduced to zero using steps of 1 kg. The loading - unloading cycle was then repeated once more. Then the transducer was rotated by 180° and the same procedure was followed, applying this time a shear load in the opposite sense. Readings were taken in every single step for all six channels, thus recording the main response of the channel under load, as well as the five cross-effects resulting on the other channels.

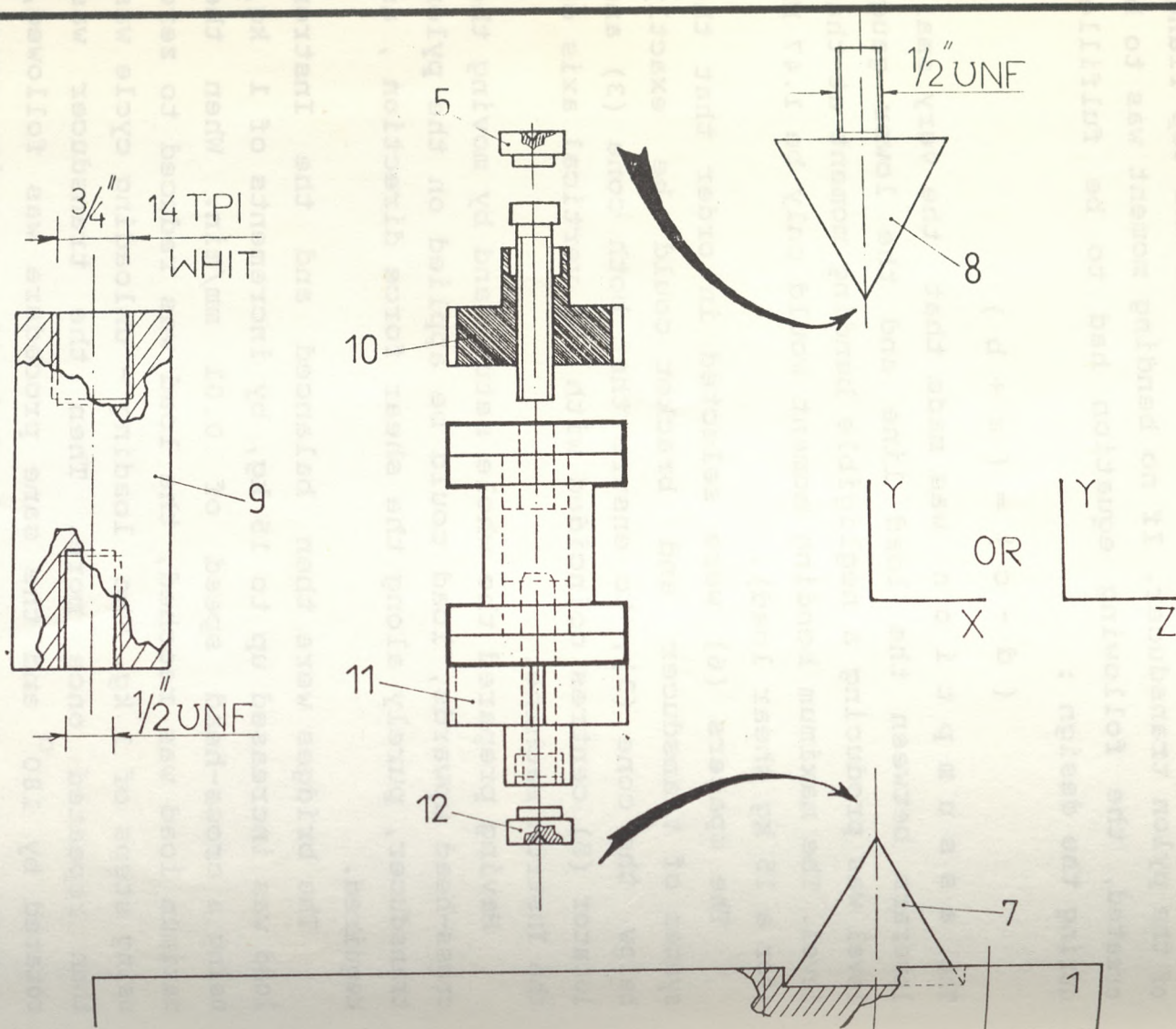


Fig 4.3a The set-up for axial load calibration

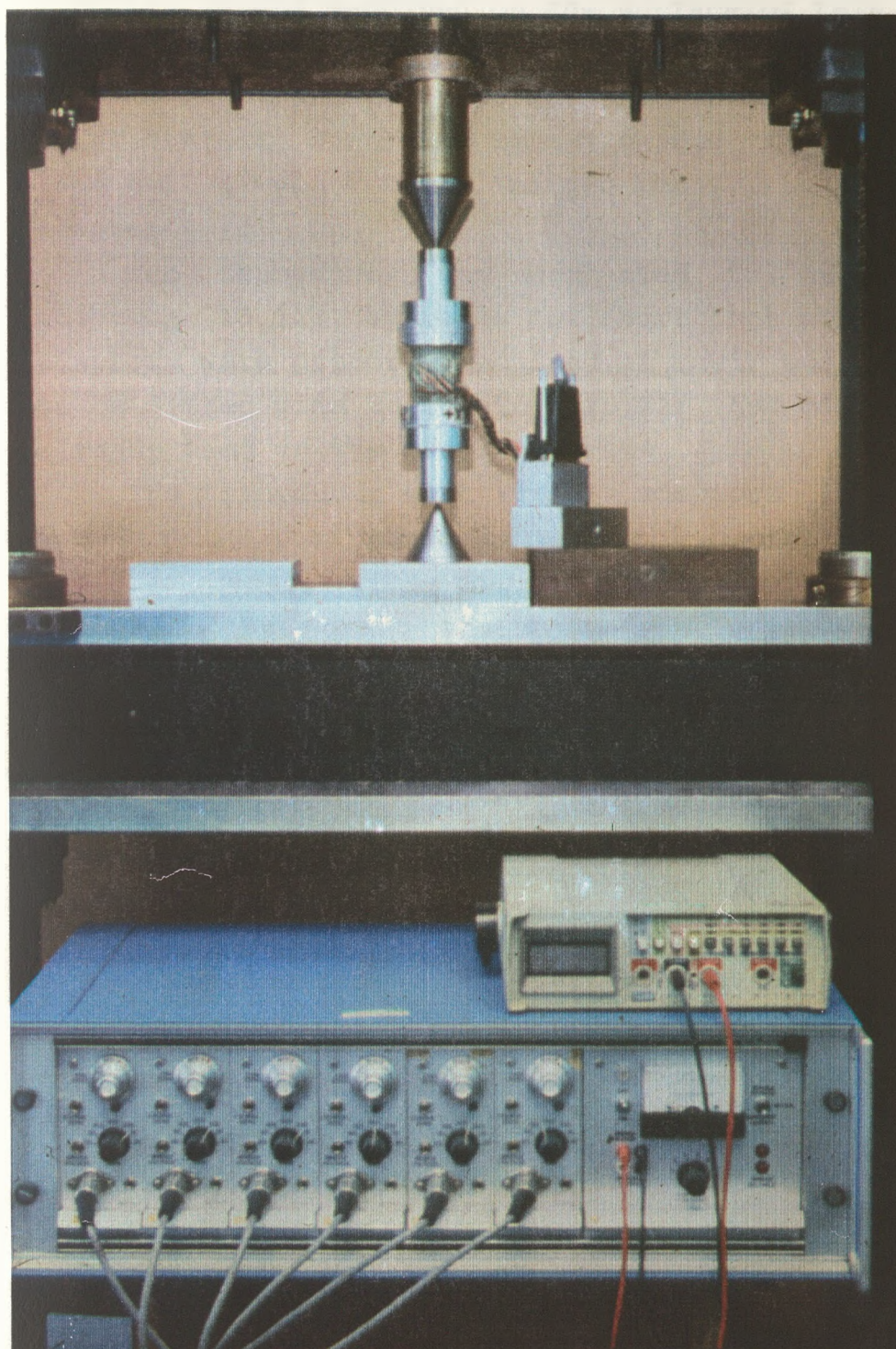


Fig 4.3 b The set-up for
axial load calibration

4.3.3 Axial Load Calibration (figs 4.3 a and b)

For the calibration tests, concerning the axial load F_y the interface plate (1) was mounted on the cross-head of the Instron machine. The plate was this time provided with a conical component (7) fitted in a circular recess machined on the surface of this plate, accurately centered with the Instron axis.

Another threaded cone (8) was used for the top point contact, connected to the 0-5000 kg compression load cell (type : FMR / Instron Ltd) , by means of an adaptor (9).

The transducer was connected to two identical adaptors (10,11) by means of short foot bolts. These adaptors were properly machined at their ends, so that to be fitted with two locators (5,12), one of which was already used in the previous tests.

The transducer with its two adaptors and locators was finally positioned between the contact points of the two cones, with the load cell under zero load as shown. By moving the cross-head upwards an axial load was applied to the transducer. This procedure was carried out twice. The cross-head speed was 0.05 mm/min and the load was applied within a range of 0-100 kg with steps of 10 kg. All six output signals were recorded for each step. For this test load was applied in the positive sense only.

4.3.4 Bending Moment Calibration (figs 4.4 a and b)

For the calibration tests concerning bending moments M_x and M_z , two bars were used to implement a four-point-bending configuration. The top bar (13) was connected to the load cell by means of an adaptor similar to component (9) of the previous test. This bar was provided with two sharp protruding edges for point contact with the transducer system. The bottom bar (14) was mounted on the cross-head by means of a pair of specially machined plates (shown in fig 4.4b only) , which held the set-up in a symmetrical position

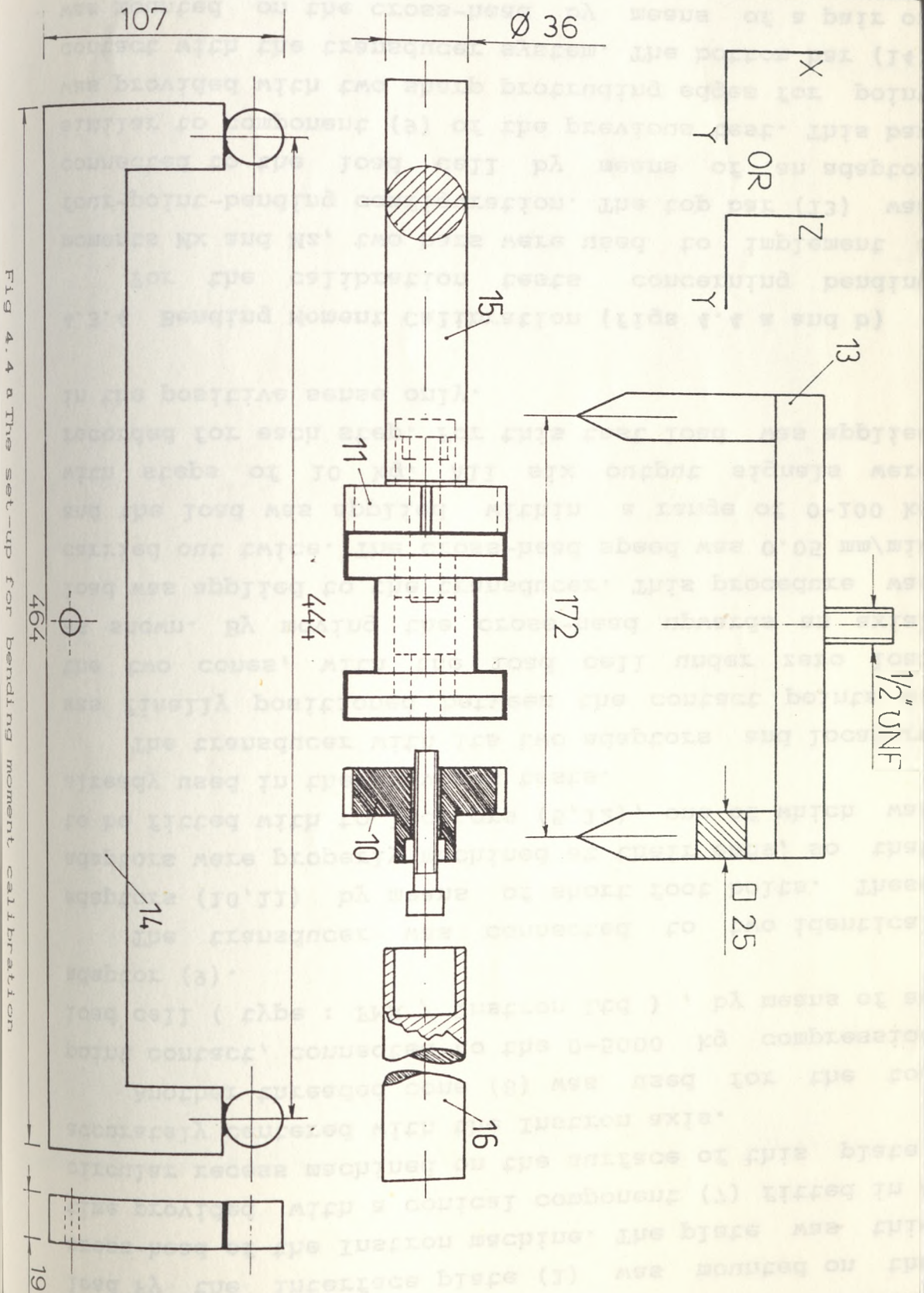


Fig 4.4 a The set-up for bending moment calibration

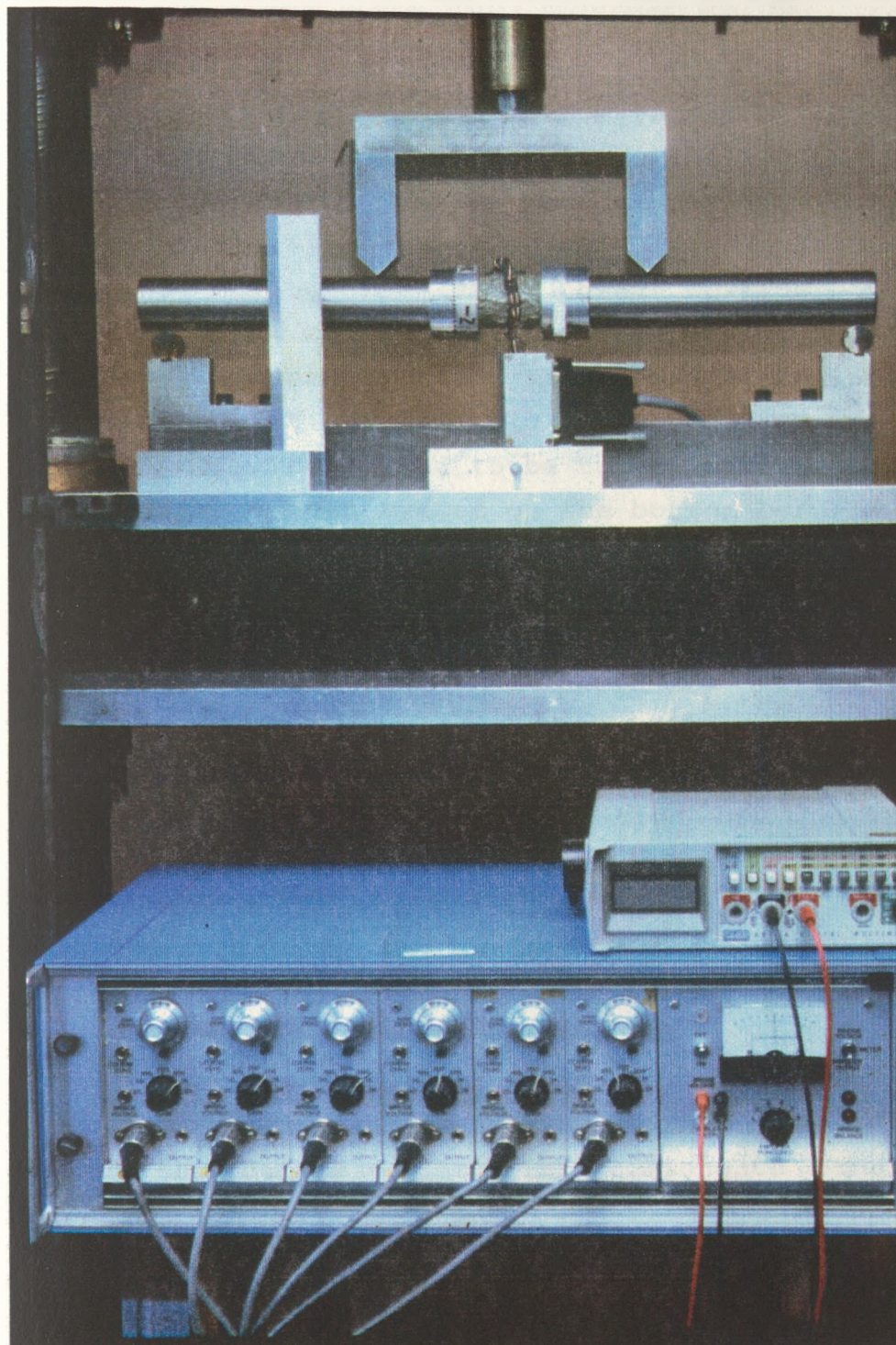


Fig 4.4b. The set-up for bending moment calibration

relative to the small centre hole shown , with a pin. This bar was provided with two cylindrical edges for point contact with the transducer system.

The transducer was fitted with its two adaptors (10,11) as before, but with no locators this time and was aligned against the adaptors' lateral slots (these slots are also mentioned later). Two cylindrical bars were machined (15,16) having a recess at one end onto which the adaptors were fitted . Finally the transducer system was positioned on the top of the edges of the bottom bar (14).

By moving the cross head upwards, four-point bending could be established, resulting, because of structural symmetry, to the application of a pure bending moment.

Special care had to be taken during positioning of the transducer system on the bottom bar, in order to ensure that either of the frame configurations shown is achieved. For the above task slots, like the one shown on adaptor 11 , were used. The slots were machined at 90° intervals around the periphery of the adaptors (10,11). These slots were initially meant to provide with location for a small spirit level which would guarantee the correct orientation of the transducer frame. However, this method was not considered reliable and later alignment was achieved by using a graduated square resting on the surface of the cross - head . The lateral slot of either adaptors was aligned with the correct reading on the square. This reading had to be equal to the height of the transducer longitudinal axis from the surface of the cross-head, as resulted from the dimensions of the components involved. As shown , this distance was :

$$107 + (36 / 2) = 125 \text{ mm.}$$

Under four-point full contact, the leverage creating the bending moment was the horizontal distance

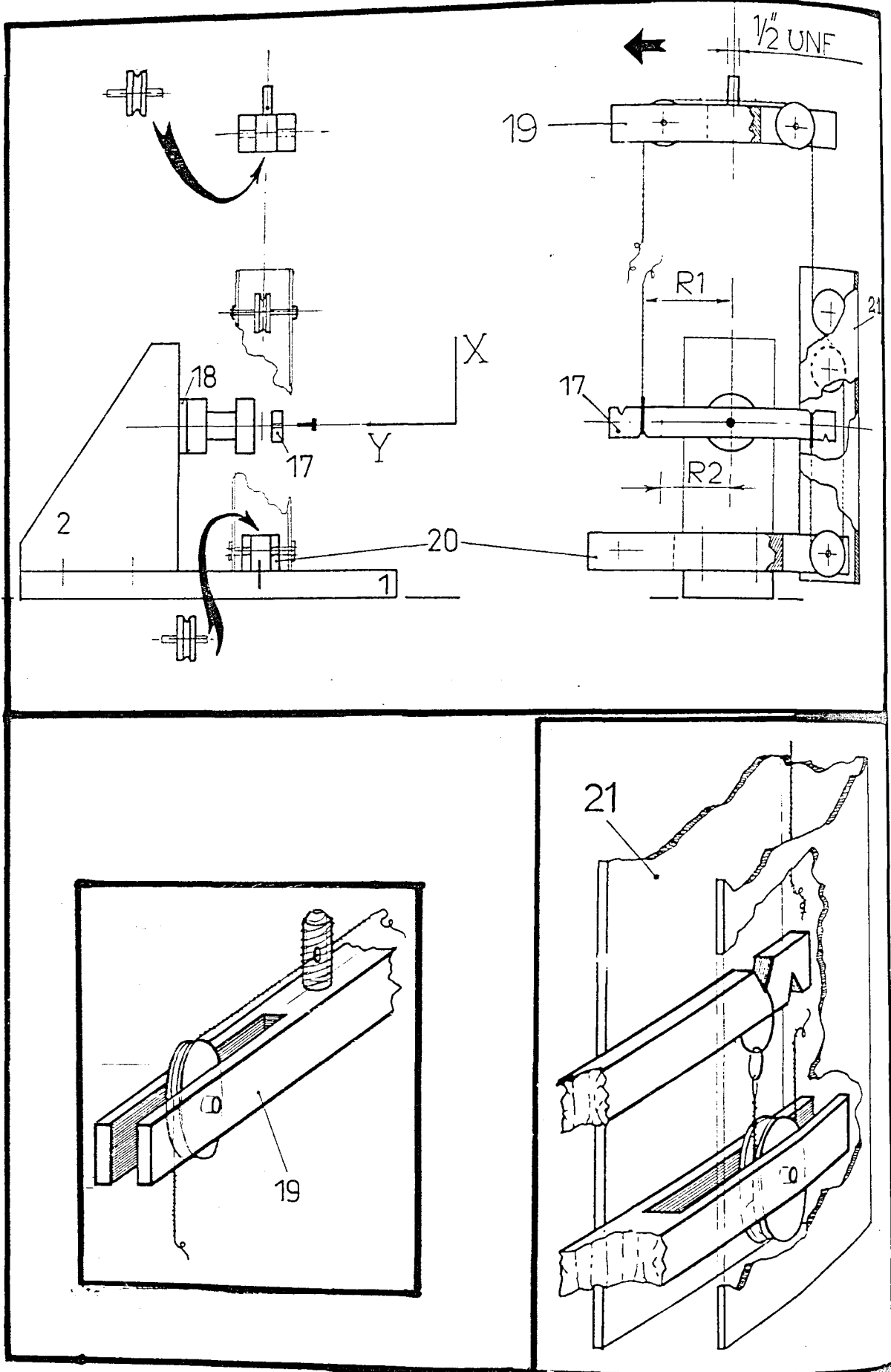


Fig 4.5 The set-up for torque calibration (system Mark 10) and two structural details of the system

between upper and lower contact points on each side. From the dimensions shown, that leverage was calculated to be :

$$(444 - 172) / 2 = 136 \text{ mm.}$$

To ensure the secure location of the system , an initial Instron load of 20 kg was applied. The bridges were balanced under that initial load and the load was increased up to 70 kg by increments of 10 kg. Then unloading started down to 20 kg again with the same steps. The cycle was repeated once more. Readings were taken for every step for all six channels again.

The load cell in those tests was the 0-5000 kg compression load cell, and the speed of the cross-head had a value of 0.5 mm/min.

4.3.5 Torque Calibration (system Mark I)

The set-up presented in this section corresponds to the first attempt (Mark I) for torque calibration in the Instron machine (fig 4.5).

A system of pulleys had to be developed. The transducer was fitted with a bar (17) appropriately grooved to accept the cable applying the load. The transducer fitted with this bar was mounted onto the base (2), as for the shear calibration tests, the difference being, that this time no spacers were used but only a double - sided emery cloth disc (18) to ensure immobility at the interface.

The pulley system consisted of two parts :

- a) the top part was a set of two pulleys mounted on a specially machined bar (19) connected, by means of a bolt and an adaptor , to the load cell . The cable had to be already passed through the small hole drilled on the threaded part of the bar and was resting on these two pulleys at both sides of the bar.

- b) the bottom part consisted of an horizontal bar (20) mounted on the bottom plate (1) by means of two screws, fitted with one pulley on the side required and a lateral rig (21) mounted on the horizontal bar (20) and fitted with two other pulleys at appropriate locations to ensure correct direction of the application of the load.

The cable was attached to the bar of the transducer (17) by means of rings as shown in fig 4.5. In the beginning, the cable was loose, applying no load on the transducer. Moving the cross - head downwards, the cable could gradually be stretched, resulting to equal and opposite forces at the two sides of the transducer bar. The pure torque developed could be determined by the Instron and the radial distance R_1 .

An initial Instron load of 10 kg was applied. Then the bridges were balanced and the load was increased up to 30 kg by steps of 2 kg. After having reached the maximum value, the load was gradually reduced to 10 kg using the same steps. The cycle was repeated once more.

For this test the load cell was the 0-100 kg tension/compression load cell and the cross-head speed adopted was 0.05 mm/min. The application of an opposite sense torque was achieved by changing the position of the lower part of the pulley system to the other side of the bar (20) and attaching the cable to the opposite grooves of the transducer bar (17) located at a radial distance $R_2 = 100$ mm. Then again two loading cycles were performed and readings taken.

4.3.6 Torque Calibration (system Mark II)

For the torque calibration of the pylon transducer in the Instron machine a second set-up was designed and machined called here Mark II. The reason for this new set-up to be designed was the fact that the first one was not considered reliable. As the results and the discussion, presented in the next sections, will prove,

Fig 4.6a The set-up for torque calibration (system Mark II)

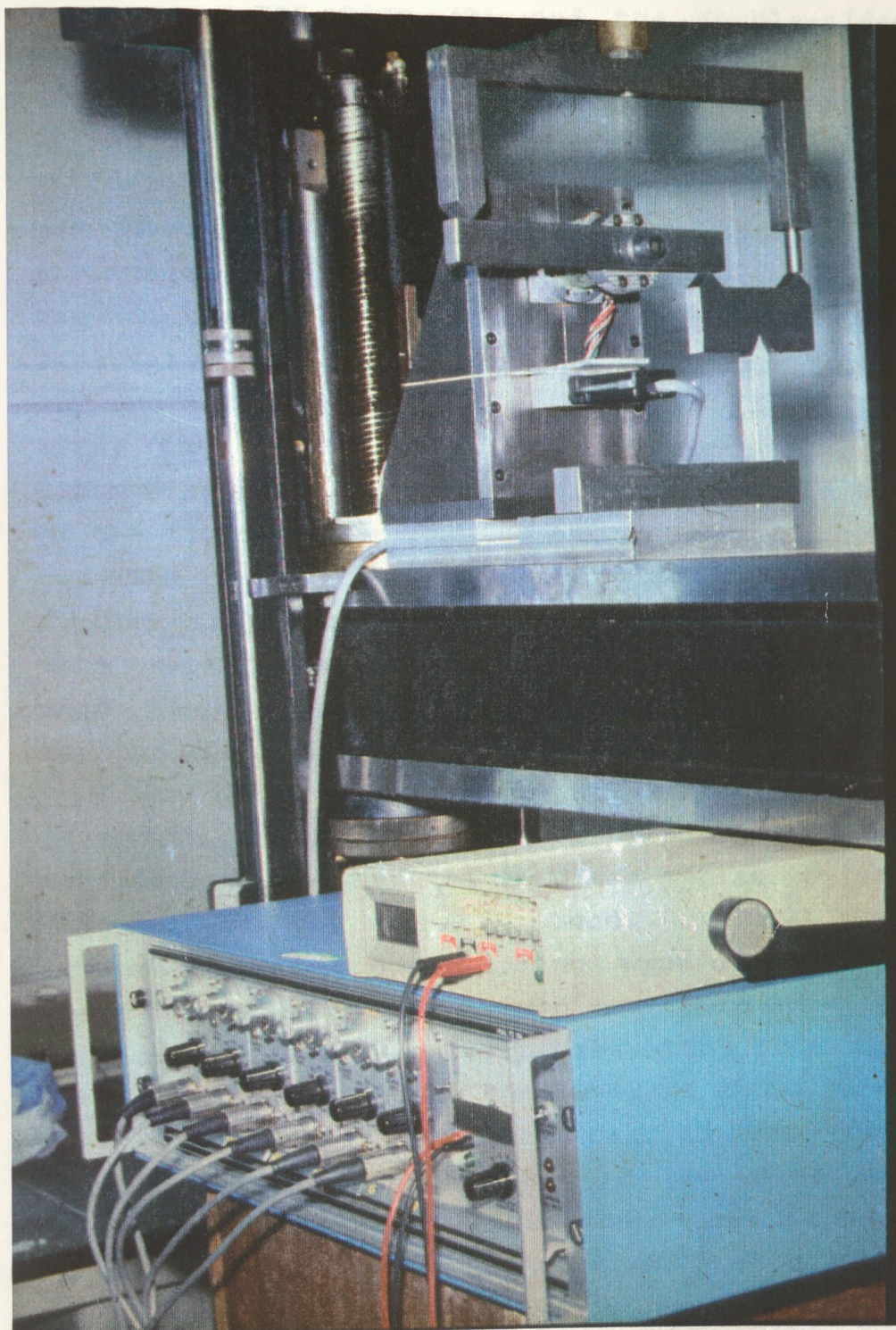


Fig 4.6 b The set-up for torque calibration (system Mark II)

system Mark I did not eventually apply pure torque only. In this section system Mark II is presented (see figs 4.6 a and b).

The pylon transducer is mounted as before on the cross-head of the Instron machine, using the interface plate (1), the base (2) and the double-sided emery cloth disc (18). A transverse bar (22) was fitted at the free end of the transducer. A top bar (23), similar to the one used in the bending tests, was mounted onto the 0-100 kg load cell by means of an adaptor. This bar was provided on one end with a threaded cylindrical protrusion (24) as shown. The design was meant to provide the following condition : when the cylindrical protrusion was fully screwed into the top bar (23) and contact was established between top and transverse bars, the bottom sides of the protrusion (24) and transverse bar (22) were level (as shown in the detail of the figure) .

The set-up was also provided with the bottom bracket (25) mounted on the plate (1). The top end of this bracket was machined as a knife shaped edge. This edge was used to provide a bevel function to an appropriately machined plate (26).

The idea was to create a lever by means of which inversion, in the sense of one of the forces , could be achieved. Thus, when the load was applied by the upward movement of the cross - head, the two equal load components were counteracting each other in terms of shear force. The only load applied onto the pylon transducer was a pure torque resulting from the Instron load and the breadth of the leverarm shown ($R = 170\text{mm}$).

Before any tests were carried out, the bottom surfaces of components (22) and (24) were checked to ensure that they are level. When slight discrepancies were observed fine adjustments of the treaded protrusion were made. The tests were conducted in the same way as for system Mark I, but no pre-load was needed this time. The loading range was 0 - 30 kg with

increments of 5 kg. The loading-unloading cycle was performed twice. It was also performed twice for the opposite sense. This configuration was obtained by mounting the top bar (23) and the bottom bracket (25) on the other side, also rotating the transverse bar (22) to match the inverted set-up.

4.4 Results and Discussion

Since all loads were purely applied in one direction only, the o/p signals recorded from the strain gauge amplifiers during each test, corresponded to one main effect and five cross-effects, caused by the particular load applied.

These signals were recorded in mV, against the corresponding Instron load in kg and were averaged using the values obtained during the two loading cycles, for positive and negative loading senses (except of course from axial load tests, where positive loading sense was only involved).

For the net (when pre-load was used) value of Instron load L , the corresponding loads applied on the pylon transducer frame, for each one of the presented configurations were calculated as follows :

for shear force	:	$F_x, F_z = \pm 9.81 \cdot L$	(N)
for axial load	:	$F_y = 9.81 \cdot L$	(N)
for bending moment	:	$M_x, M_z = \pm 9.81 \cdot 0.136 \cdot L / 2$	(Nm)
for torque (Mark I)	:		
positive sense	:	$M_y = 9.81 \cdot 0.160 \cdot L / 2$	(Nm)
negative sense	:	$M_y = -9.81 \cdot 0.200 \cdot L / 2$	(Nm)
for torque (Mark II):	:	$M_y = \pm 9.81 \cdot 0.170 \cdot L / 2$	(Nm)

The data of the calibration tests are presented in appendix II, together with the calibration graphs.

The coefficients m_{ij} of matrix $[M]$ shown in equation (4.6) can be derived by regression of the data (fitting a straight line : $\text{signal}_i = m_{ij} \cdot \text{load}_j$) .

The Minitab software in the main frame VAX was used to fit the straight lines to the data, for all main and cross effects .

coef. m_{ij}	mean (mV _i / N, Nm _j)	st. dev. (mV _i / N, Nm _j)	p-value	r-square (%)
under load Fx				
m11	0.9848200	0.0006890	0.000	99.997
m21	0.0000000	0.0000000	*	*
m31	0.0038843	0.0004841	0.000	50.539
m41	0.0000000	0.0001289	1.000	0.000
m51	- 0.0380110	0.0016720	0.000	89.131
m61	0.0190720	0.0008722	0.000	88.361
under load Fy				
m12	0.0038723	0.0001772	0.000	95.784
m22	- 0.2525250	0.0001490	0.000	99.999
m32	- 0.0005428	0.0001666	0.000	33.586
m42	0.0026477	0.0000999	0.000	97.099
m52	- 0.0024028	0.0001125	0.000	95.602
m62	0.0025153	0.0000937	0.000	97.167
under load Fz				
m13	0.0317630	0.0022480	0.000	76.017
m23	- 0.0116220	0.0006055	0.000	85.396
m33	0.9413640	0.0008570	0.000	99.995
m43	0.0266560	0.0026020	0.000	62.489
m53	- 0.0576790	0.0031030	0.000	84.581
m63	0.0000000	0.0000000	*	*
under load Mx				
m14	- 0.2218210	0.0058330	0.000	98.434
m24	0.3526600	0.0358700	0.000	80.776
m34	0.1792300	0.0134700	0.000	88.501
m44	-10.6126000	0.0567000	0.000	99.934
m54	0.1846800	0.0049100	0.000	98.399
m64	0.0640590	0.0021970	0.000	97.367
under load My				
m15	2.1945600	0.0479700	0.000	99.007
m25	- 0.0792610	0.0048680	0.000	86.045
m35	0.4388900	0.0131100	0.000	96.304
m45	- 0.0020180	0.0010490	0.061	7.917
m55	-18.6183000	0.0523000	0.000	99.966
m65	0.4624000	0.0169300	0.000	97.261
under load Mz				
m16	0.0190800	0.0136900	0.177	7.790
m26	- 0.0678100	0.0370800	0.080	12.694
m36	0.2886060	0.0039500	0.000	99.571
m46	- 0.0143110	0.0062330	0.031	18.647
m56	- 0.1536730	0.0024600	0.000	99.415
m66	5.4099100	0.0289100	0.000	99.934
* Not determined values due to zero signal output				

Table 4.1 Statistical analysis of the calibration data

Firstly the results of the first six tests are presented (ie. for F_x , F_z , F_y , M_x , M_z and M_y using Mark I). The results from the regression of these data are exhibited in table (4.1) and consist of the following : the mean values of the coefficients , the standard deviations of the coefficients, the p-values of the coefficients and the r-square values of the fitted lines. .

As shown in the table the fitted lines explain more than 99.9 % (r-square) of the variation of the main effects. The anticipated statistical significance of the derived coefficients is proved by the zero p-values (three decimal places only).

As far as the cross-effects are concerned, besides the coefficients which are zero (ie. m_{21} , m_{63}), the coefficients exhibiting a high p-value (> 0.05) can also be considered negligible. Generally the null hypothesis is that the coefficients are zero and for this latter set of coefficients the hypothesis has been proved statistically correct . Therefore the coefficients m_{41} , m_{45} , m_{16} , m_{26} and m_{46} are considered zero. Obviously, these last coefficients also exhibited very low t-ratio (not shown) , which was less than the value provided by tables for a level of 95 % .

Most of the coefficients of the cross-effects however, are non-zero, and they exhibit p-values which do not allow the null hypothesis to be established, and therefore they must be taken into account as derived. These coefficients, as expected, also exhibited t-ratios higher than the values provided by tables. At the same time, as shown, the r-square values are not high (or even very poor for some coefficients).

Although these latter regression lines exhibited poor linearity it was not considered statistically correct to assume that the corresponding coefficients are zero and therefore they were taken into account with their calculated values.

The observation which led to the design of system

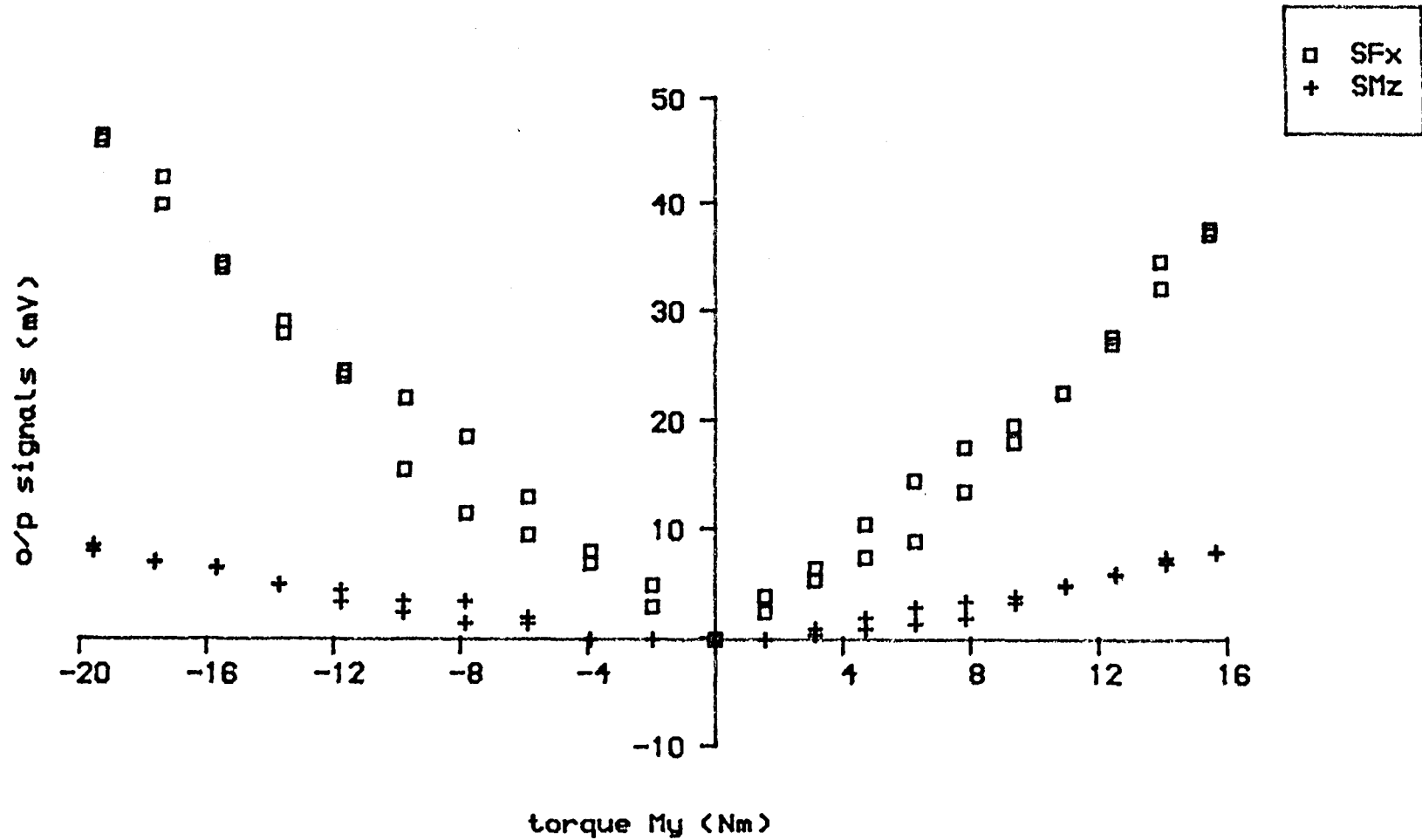


Fig 4.7 The o/p signals of channels 1 and 6 For applied torque My using the system Mark I

Mark II and the replacement of system Mark I was the following : as can be seen in figure 4.7 (or even in table II.6 in appendix II), the output signal of channel 1 (SFx) exhibited a peculiar set of values, which were always positive. Similar was the behaviour exhibited by the output signal of channel 6 (SMz).

By inspection of the set-up Mark I (figure 4.5) it was realised that due to friction in the path followed by the cable through the system of pulleys, the two branches of the cable did not eventually transmit the same force; the branch which was directly connected to the transverse bar was transmitting a greater force. Thus, both in the case of positive and negative torque application, there was a residual shear load always positive along the Fx direction, eventually resulting to a subsequent bending moment Mz also positive.

The regression of the data for these two output signals showed that the slopes in the two quadrants were almost equal and opposite . In table 4.1 only the positive values are shown . These are coefficients m15 and m65.

After these observations instead of improving the existing set-up, a new one was decided to be built, which would eliminate the use of cables and pulleys completely. The resulting set-up was system Mark II.

The calibration data acquired using system Mark II are shown in table II.7, in appendix II. In table 4.2 the results of the regression of the data are shown.

It can be appreciated from figures 4.8 and 4.9 (or even from table II.7 in appendix II) that the obtained data did not meet the expected qualities. The new system Mark II created more problems. By inspection of the data plotted in figures 4.8 and 4.9 the following can be seen :

The two forces applied onto the horizontal bar are not equal and therefore there is always a negative residual shear force Fx (same problem as with system

coef. m_{i5}	mean (mV_i / Nm My)	st.dev. (mV_i / Nm My)	p-value	r-square (%)
under load My				
m15	- 1.245380	0.081290	0.000	94.751
m25	- 0.188125	0.007083	0.000	96.314
m35	1.719500	0.130600	0.000	86.530
m45	0.789070	0.062350	0.000	85.575
m55	-18.197400	0.162600	0.000	99.785
m65	- 0.641800	0.020850	0.000	98.645

Table 4.2 Statistical analysis of the calibration data obtained using system Mark II .

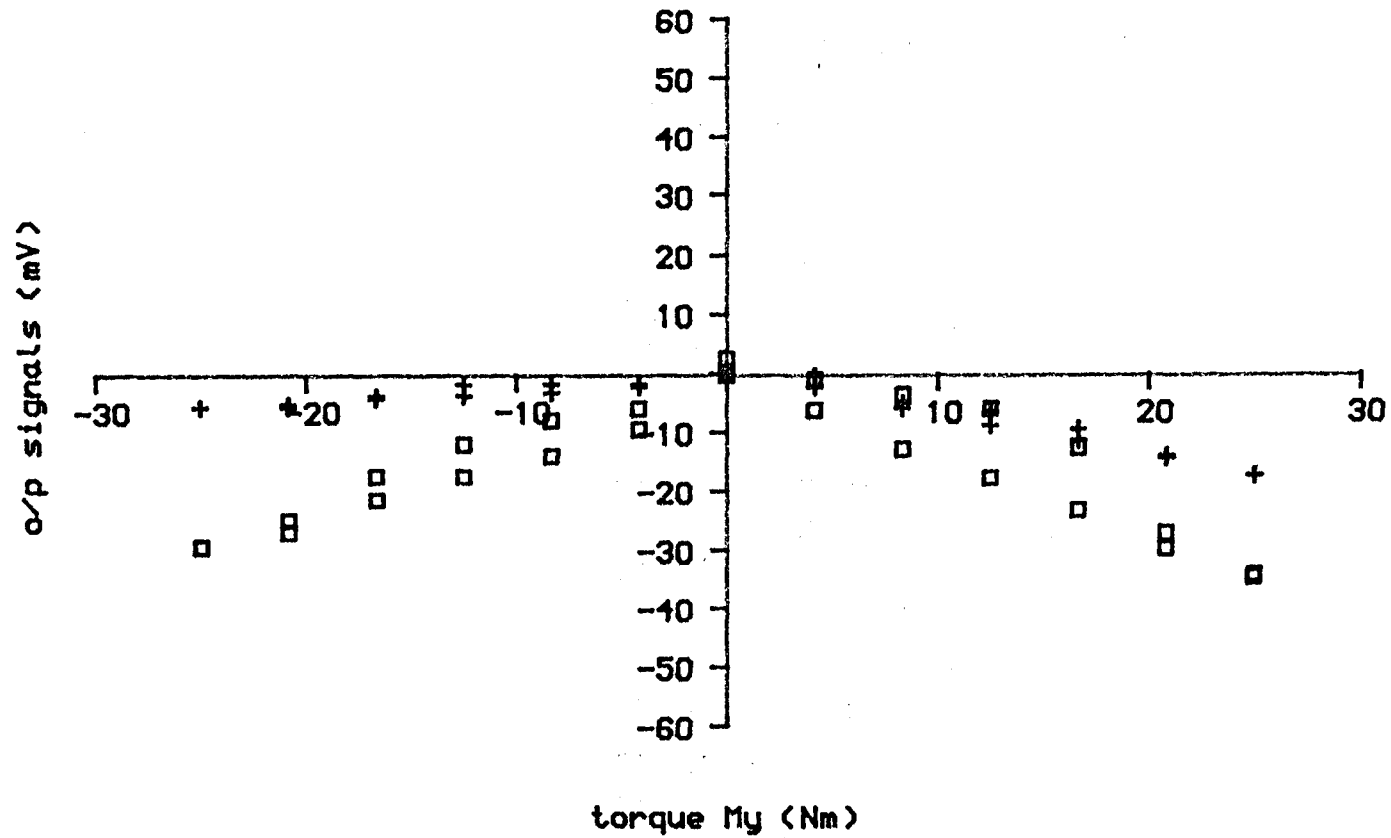


Fig 4.8 The o/p signals of channels 1 and 6 For applied torque My using the system Mark II

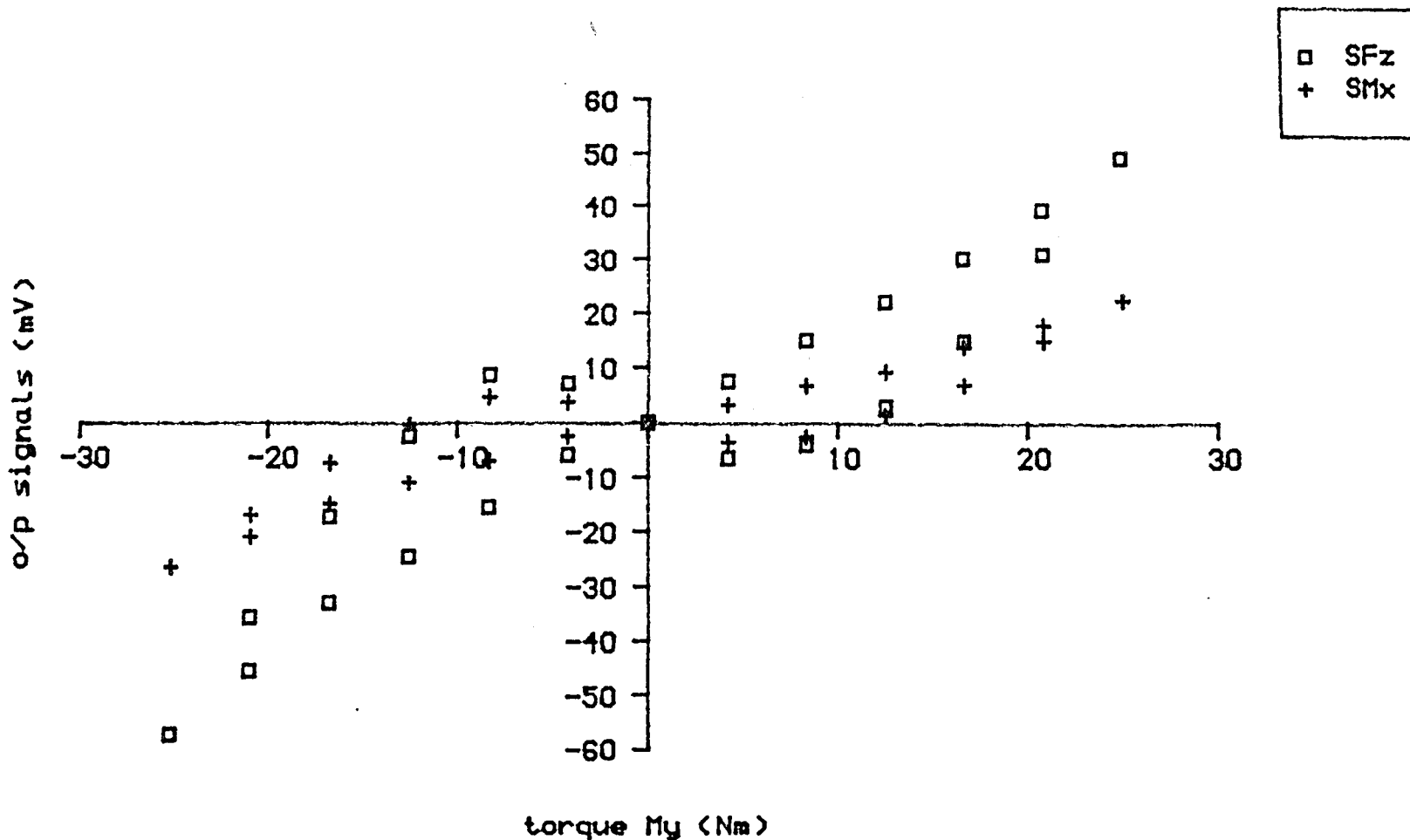


Fig 4.9 The o/p signals of channels 3 and 4 For applied torque My using the system Mark II

Mark I), creating subsequently a residual bending moment M_z . This is indicated by the fact that the signals of channels 1 and 6 keep the same sign for both positive and negative torque values. Furthermore, in the case of the system Mark II, there are also significant signals from channels 3 and 4 corresponding to shear force F_z and bending moment M_x (fig 4.9). It is possible that the output signal of channel 3 (SF_z) is due to friction effect between the knife edges and the horizontal bar. This unwanted effect produces subsequently an unwanted bending moment M_x . The fact that this latter effect is due to friction can be proved by the change of algebraic sign of the output signals during the loading / unloading cycles.

The coefficients shown in table 4.2 are derived by regressing the data over the whole range, except coefficients m_{15} and m_{65} which, like in the case of the system Mark I, correspond to the positive range only.

The use of the Instron machine or any commercial testing machine for calibrating the short pylon transducer was put under question, at least for the torque and bending moment tests. Despite the important advantages that such a method could provide there was a major drawback that affected the quality of the procedure and results : due to the structural constraints of the Instron machine, the applied loads could not follow the elastically deformed material of the contacted components, thus creating friction effects, which introduced unknown load components.

It must be mentioned that a further effort to solve these was made : the author thought of re-designing some of the components introducing ball bearings in all contact points. However, this idea was discouraged by bearing manufacturers, mainly because the testing conditions, for the particular application are static.

Thus, it was finally decided that the matrix $[M]$ should be derived in the future using dead-weight

0.990226	0.000000	0.000000	-0.3798	0.2568	0.1172
0.014487	-0.259765	0.000000	0.2549	-0.1823	-0.3208
0.000000	0.000000	0.950245	0.0722	-1.0020	0.3866
0.000000	0.000000	0.000000	-12.0048	0.0000	0.0000
0.000000	0.000000	0.000000	0.0000	-19.6490	0.0000
0.000000	0.000000	0.000000	0.0000	0.0000	5.8686

Table 4.3 Matrix [M] derived using dead-weights methods
(Solomonidis, 1989). Units: (mV_i / N or Nm_j)

1.00987	0.00000	0.00000	-0.031950	0.013200	-0.020166
0.05632	-3.84963	0.00000	-0.083533	0.036453	-0.211564
0.00000	0.00000	1.05236	0.006333	-0.053667	-0.069330
0.00000	0.00000	0.00000	-0.083300	0.000000	0.000000
0.00000	0.00000	0.00000	0.000000	-0.050893	0.000000
0.00000	0.00000	0.00000	0.000000	0.000000	0.170400

Table 4.4 The matrix [C] = [M]⁻¹ (Solomonidis, 1989)
Units : (N or Nm_i / mV_j)

methods, at least for the torque and bending moment tests, as used by former researchers (Solomonidis, 1989). The tests presented in this chapter and the acquired data and results provided a rich experience but could not be used with confidence. The matrix [M] derived during former work, using dead-weights methods (Solomonidis, 1989), was thus to be used for the rest of this project work as more reliable. This matrix [M] is shown in table 4.3 . The calibration matrix [C] is shown in table 4.4 .

It can be appreciated that the main diagonal of matrix [M] shown in table 4.3 compares well with the diagonal coefficients m_{ij} derived using the Instron machine. However, as expected, there are many differences between the coefficients of the cross-effects. What must be noted, here, is the fact that the coefficients of the main diagonal for both cases can be now comparable with the theoretical values derived in chapter 3 (section 3.7). The sensitivities derived in that chapter for the six channels, when multiplied by the gain settings , can be compared to the experimentally derived main effects as shown in table 4.5 . It is obvious that the coefficients derived with dead-weights method are much more close to the theoretically derived ones.

4.6 Conclusions

The work presented in this chapter provided many conclusions, which are presented in this final section.

1) The choice was made to use an Instron machine for the calibration of the short pylon transducer, applying one load components at a time and adopting the linear approach for the calibration model. Coefficients m_{ij} were derived, with the decision based on the p-values of the statistical analysis. Despite the fact that the Instron machine provides the user with the most controllable way of load application, it was proved

	theoretical coefficient (see section 3.7 in chapter 3)	coefficients derived with the following methods	
		dead-weight	Instron
channel	mV / (N or Nm of the corresponding load)		
1 (Fx)	1.0700	0.9902	0.9848
2 (Fy)	-0.2685	-0.2560	-0.2525
3 (Fz)	1.0700	0.9502	0.9414
4 (Mx)	-12.9360	-12.0048	-10.6126
5 (My)	-20.4050	-19.6490	-18.6183
6 (Mz)	6.4678	5.8686	5.4099

Table 4.5

A comparative presentation of the
sensitivity coefficients of the main effects
(all figures rounded with 4 decimal cases)

that it also introduces undesirable and unquantifiable friction effects which put the accuracy of some of the tests under question.

2) For the patient tests involved in this project the calibration matrix [C] derived by former researchers (Solomonidis , 1989) using dead - weights methods will be used (table 4.4) . This matrix corresponds to a matrix [M], the main diagonal of which is very closely comparable with the theoretical sensitivity coefficients derived in chapter 3.

3) The useful experience drawn by this work proved that the dead-weight method should be used in the future for calibrating the pylon transducer, but a new specially designed rig is needed. This rig should make use of the useful loading principles adopted by former researchers and described in the force measurement literature (see for example Bray et al. 1990) and should allow the application of pure load components independently, with a predefined and constant geometry.

The following chapter presents the work that the author carried out in order to develop a method for validation of calibration matrices.

CHAPTER 5

VALIDATION OF THE CALIBRATION MATRIX

5.1 Introduction

5.2 Development of the required Device

5.2.1 Initial Considerations

5.2.2 Mathematical Considerations

5.2.3 Description of the Device

5.3 Preparation of the Device and Setup

5.4 Testing Procedure and Program for Analysis of Data

5.5 Tests and Results

5.6 Discussion and Conclusions

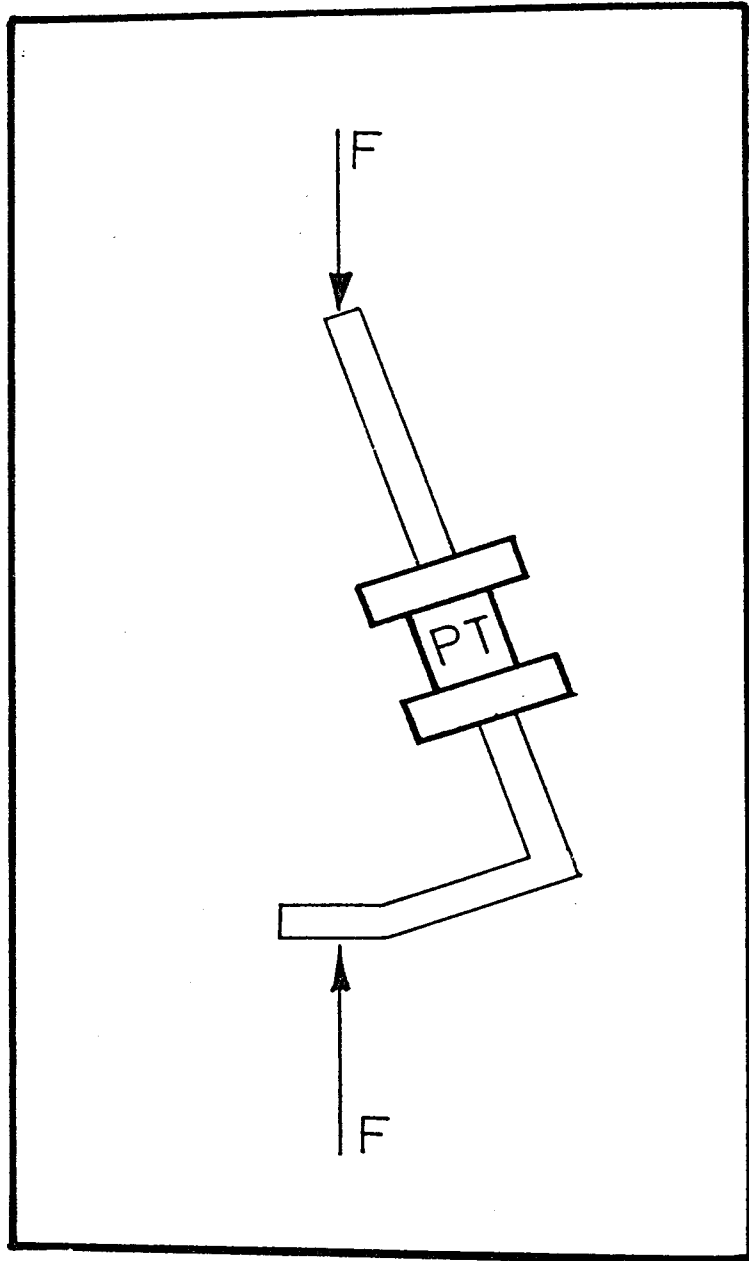


Fig 5.1 Application of known loads on the pylon transducer (PT)

5.1 Introduction

When a calibration matrix is obtained through calibration tests, it is always necessary to check its prediction ability, by applying known loads on the transducer. This procedure is known as the validation of the calibration matrix.

The calibration matrix for the pylon transducer used in this thesis is presented in chapter 4 , in table 4.4 and was derived by former researchers, using dead-weights calibration methods.

For the validation tests a device was required that would allow various known loading configurations to be applied on the transducer. It was initially thought that the device should resemble the shank of a BK amputee (as shown in fig 5.1). This first idea was however abandoned because such a device would only allow a certain set of configurations to be applied. Finally, another more versatile device was conceived. This device would be fitted with the pylon transducer and would be attached to the Instron machine.

Application of compressive forces onto the device would result in a set of six load components on the transducer. Since the geometry of the structure would be known, the six components could also be known. The output signals of the transducer could then be used with the calibration matrix to predict the applied load components and thus validate the matrix.

As mentioned in the introduction and conclusions of chapter 4 , the use of the Instron machine does have some disadvantages. The reader must bear in mind that the device presented in this chapter was developed before the calibration tests on the Instron machine were accomplished and proved these disadvantages.

5.2 Development of the required Device

5.2.1 Initial Considerations

Since it was decided that the Instron machine would be used for the validation tests , several

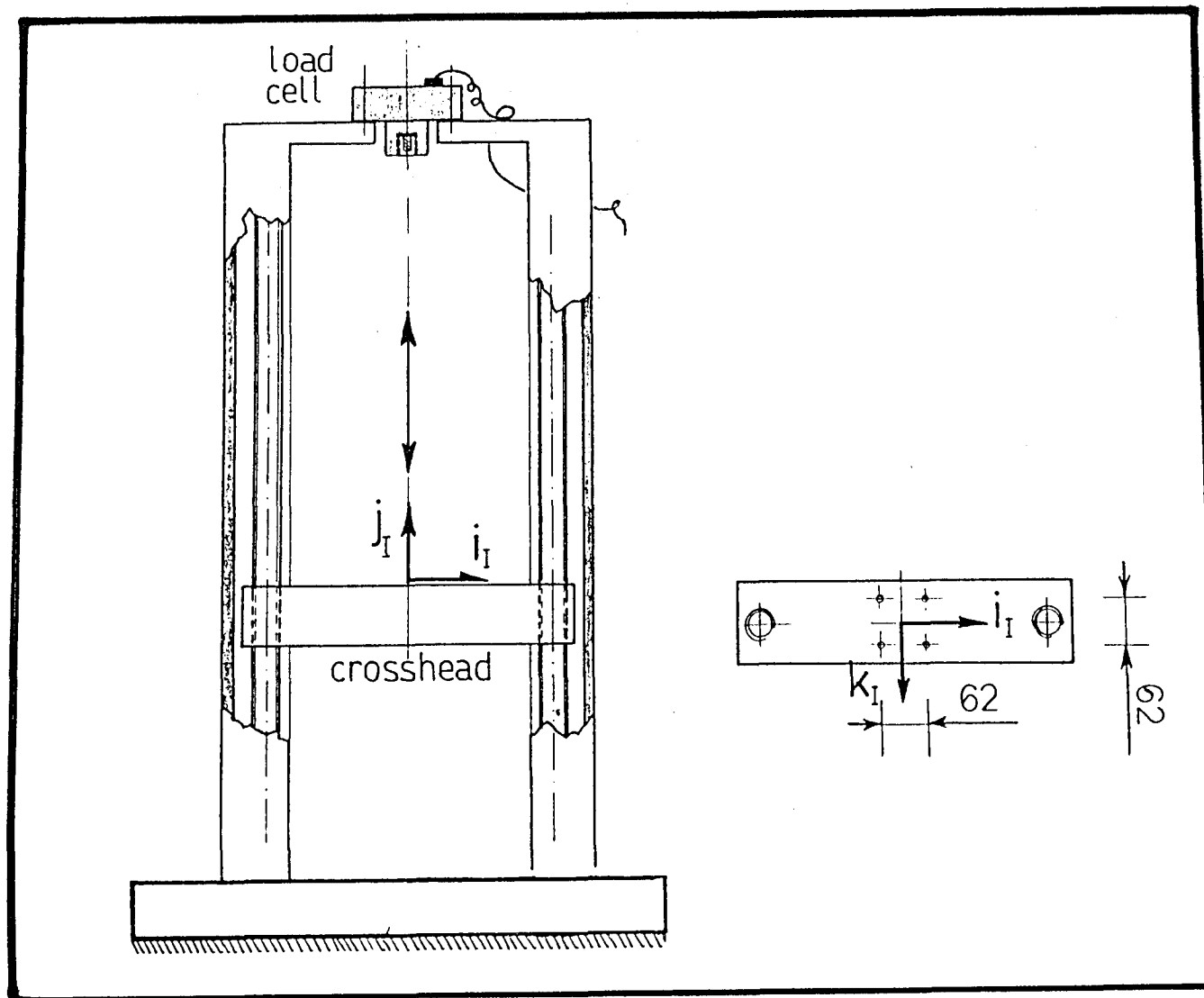


Fig 5.2 The Instron machine and its frame of reference

considerations were to be taken into account for the development of the device, in order to ensure that important technical requirements were to be met. These requirements are the following :

a) As already stated, in chapter 4 concerning the calibration of the pylon transducer, the Instron machine cannot sustain off-axis loads.

b) The device should be designed under the geometrical constraints imposed by the Instron machine itself.

c) The device should be provided with an upper adaptor matching the load cell to be used and incorporating a hinge joint to eliminate unwanted bending moment on the load cell.

On the other hand, several requirements concerning the pylon transducer had also to be met :

d) The device should be designed in such a way so as to be possible to create three forces and three moments through the application of one single load, namely the Instron load.

e) The pylon transducer has been given load limits for all the six channels and therefore the device and the method followed had to respect them, in order not to exceed the transducer's elastic limit or destroy the strain gauges.

f) For the validation to be as reliable as possible, the mode by which the loads were to be applied on the pylon transducer should be similar to the mode of the loads applied in practice.

And finally, regarding the device itself, one more requirement had to be met:

g) It had to be of adequate strength but light, easy to use and at the same time rigid enough for unwanted deflections to be practically eliminated.

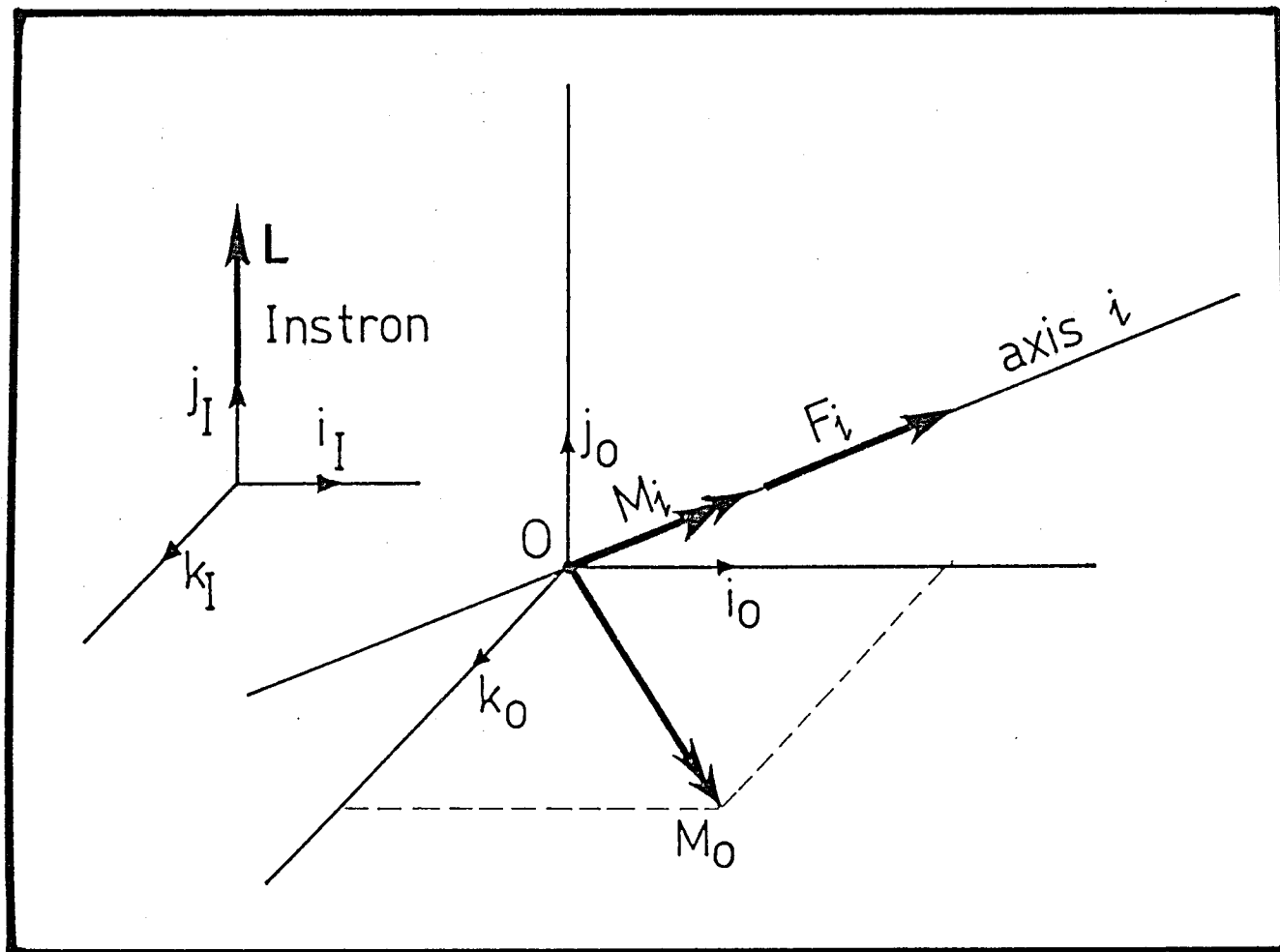


Fig 5.3 The force and moment developed by an Instron load L along and about an axis i

5.2.2 Mathematical Considerations

The design of the device was initiated with mathematical considerations, in an attempt to fulfil requirement (d), which was considered to be a key one for the tests to be carried out. A step - by - step description of the mathematical and design considerations is presented below.

The Instron machine can only provide and assess a single load, namely the force applied along the direction of its main axis (fig 5.2). Such a force can be described in terms of the Instron frame shown in figure 5.2 as follows :

$$\vec{L} = 0 \cdot \vec{i}_I + L \cdot \vec{j}_I + 0 \cdot \vec{k}_I = L \cdot \vec{j}_I \quad (5.1)$$

Referring to figure (5.3) it is understood that : on any other axis i in the 3-D space, having direction cosines l_i, m_i, n_i with respect to the Instron frame, this load \vec{L} will have a component \vec{F}_i with magnitude:

$$F_i = l_i \cdot 0 + m_i \cdot L + n_i \cdot 0 = m_i \cdot L \quad (5.2)$$

On the other hand, considering a point O , with respect to which the origin of the Instron is described by (r_x, r_y, r_z) the moment \vec{M}_O of the Instron load \vec{L} will be given by :

$$\vec{M}_O = \det \begin{vmatrix} \vec{i}_O & \vec{j}_O & \vec{k}_O \\ r_x & r_y & r_z \\ 0 & L & 0 \end{vmatrix} = r_x L \vec{k}_O - r_z L \vec{i}_O \quad (5.3)$$

If the axis i mentioned above, is again considered to pass through O , the moment \vec{M}_i about this axis is then a component of \vec{M}_O , with magnitude :

$$M_i = n_i (r_x L) - l_i (r_z L) \quad (5.4)$$

To partially fulfil the requirement (g) , the decision was taken that the device will provide r_x and r_y working only on the Instron $X_I Y_I$ plane ($r_z = 0$).

Thus, for the axis i referred , the Instron force \vec{L} results in the following loads :

$$\begin{aligned} \text{a force with magnitude } F_i &= m_i L \\ \text{a moment with magnitude } M_i &= n_i r_x L \end{aligned} \quad (5.5)$$

If all the axes of the pylon transducer are meant to be subjected to a force and a moment simultaneously, it is obvious by inspecting (5.5) , that every pylon axis had at least :

- (a) to be inclined with respect to Y_i ($m_i \neq 0$)
 - (b) to be inclined with respect to Z_i ($n_i \neq 0$), (5.6)
- with $r_x \neq 0$

To perceive more clearly the way these inclinations could be achieved, a further mathematical analysis was required.

For a frame to be inclined with respect to another, it is required that it is rotated in space, thus changing its orientation with respect to the reference.

For the system of transducer and Instron it was thought that the most easy to assess and analyse way of implementing these rotations, would be to design componentry directly mounted onto the transducer, which would provide the possibility of successive re-orientations of the frame of the transducer, within the Instron reference frame.

On the other hand, to assess the angular displacements more easily, it was thought that these displacements should be rotations about the Instron axes (absolute angles) and not about any current axes of the transducer's frame.

Thus, the rotations available were :

- 1) by angle ϑ_x about X_I
- 2) by angle ϑ_y about Y_I
- 3) by angle ϑ_z about Z_I

As shown in details in appendix V , for rotations of frames, the rotation matrices in every case are :

$$R_{\vartheta x} = \begin{bmatrix} 1 & 0 & 0 \\ 0 & \cos\vartheta_x & -\sin\vartheta_x \\ 0 & \sin\vartheta_x & \cos\vartheta_x \end{bmatrix} \quad (5.7)$$

$$R_{\vartheta y} = \begin{bmatrix} \cos\vartheta_y & 0 & \sin\vartheta_y \\ 0 & 1 & 0 \\ -\sin\vartheta_y & 0 & \cos\vartheta_y \end{bmatrix} \quad (5.8)$$

$$R_{\vartheta z} = \begin{bmatrix} \cos\vartheta_z & -\sin\vartheta_z & 0 \\ \sin\vartheta_z & \cos\vartheta_z & 0 \\ 0 & 0 & 1 \end{bmatrix} \quad (5.9)$$

For any combination of these rotations the final matrix describing the total effect, with respect to the reference frame is the product of the matrices $R_{\vartheta x}$, $R_{\vartheta y}$, $R_{\vartheta z}$ multiplied from the right to the left ; with the matrix corresponding to the first rotation being the right most.

It was considered easier to start with the pylon transducer's frame parallel to the Instron axes, with origin located at the point with coordinates : $(R_x , R_y , 0)$.

Since the pylon is a cylindrical device provided with two threaded flanges along its y_p axis, it was

also considered easier to start with a rotation about this axis, which effectively. would be a rotation about the axis Y_I . The next rotation was chosen to be a rotation about the axis X_I .

The reason for this choice was the fact that this rotation when superimposed to the first one (about Y_I) results in direction cosines m and n for all pylon axes ; and as can be seen from conditions (5.6) , these two direction cosines are necessary so that all pylon axes experience a force and a moment. This is the resulting orientation matrix :

$$R_{\vartheta_X} \circ R_{\vartheta_Y} = \begin{bmatrix} \cos\vartheta_Y & 0 & \sin\vartheta_Y \\ \sin\vartheta_X \sin\vartheta_Y & \cos\vartheta_X & -\cos\vartheta_Y \sin\vartheta_X \\ -\sin\vartheta_Y \cos\vartheta_X & \sin\vartheta_X & \cos\vartheta_X \cos\vartheta_Y \end{bmatrix} \quad (5.10)$$

If a rotation about Z_I was chosen instead, the resulting matrix would not provide the necessary direction cosines m and n to all pylon axes :

$$R_{\vartheta_Z} \circ R_{\vartheta_Y} = \begin{bmatrix} \cos\vartheta_Z \cos\vartheta_Y & -\sin\vartheta_Z & \sin\vartheta_Y \cos\vartheta_Z \\ \sin\vartheta_Z \cos\vartheta_Y & \cos\vartheta_Z & \sin\vartheta_Y \sin\vartheta_Z \\ -\sin\vartheta_Y & 0 & \cos\vartheta_Y \end{bmatrix} \quad (5.11)$$

Since the necessary direction cosines could be achieved with the rotation about axes Y_I and X_I there was no need to implement a third rotation. With these two rotations the transducer's final orientation matrix is given by (5.10) .

The next step was to design componentry to implement the chosen angular displacements ϑ_Y and ϑ_X .

5.2.3 Description of the Device

The device was designed within the geometrical constraints of the Instron machine (requirement (b) of

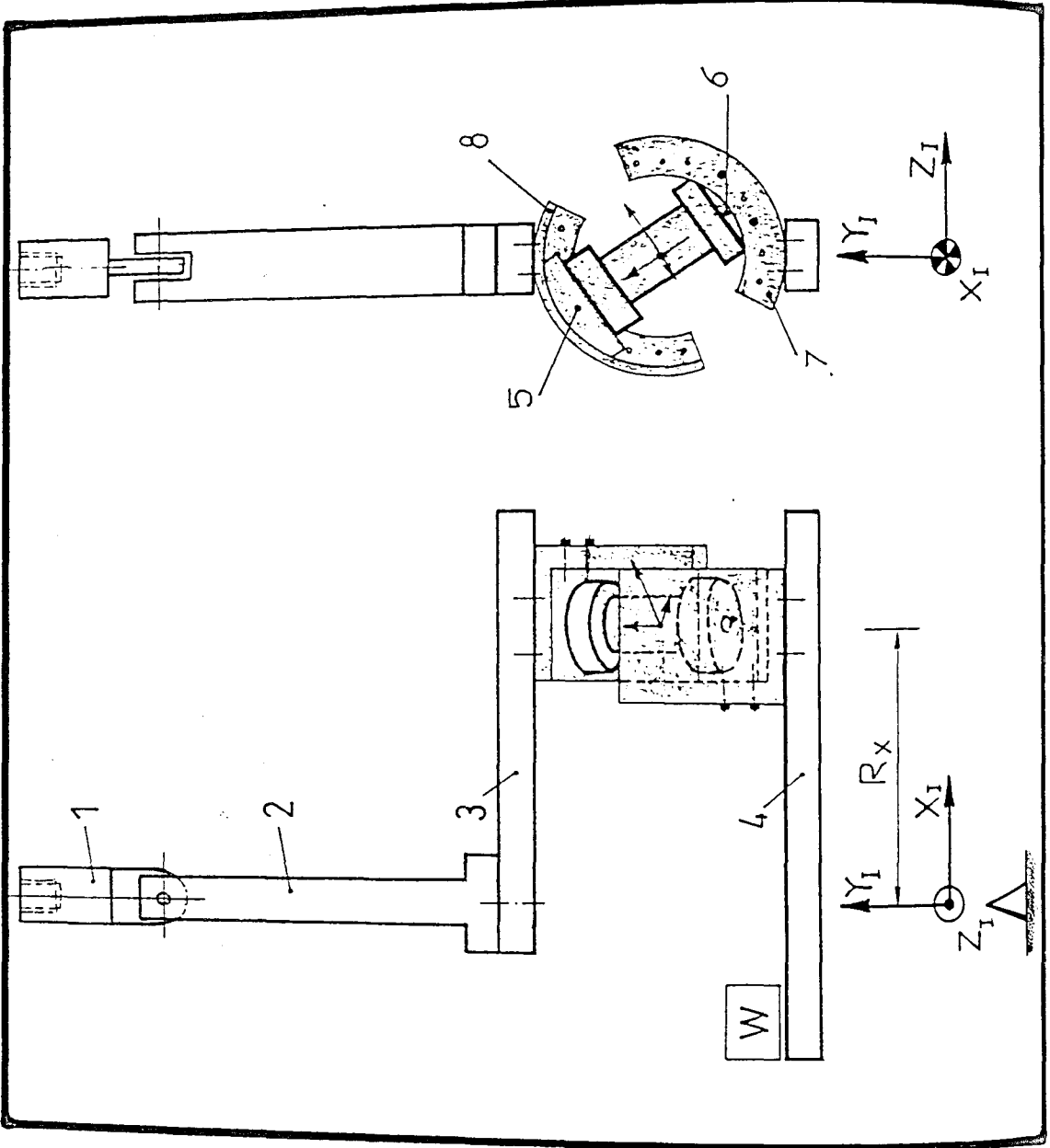


Fig 5.4 General assembly of the device fitted with the pylon transducer

section 5.2.1) and all components were meant to be machined from aluminium alloy to keep the total weight to a minimum (requirement (g) of section 5.2.1).

During actual tests with the pylon transducer the loads applied are always loads transmitted onto the pylon in a distributed mode through the flanges. Therefore, the device had to be designed as closely as possible to this principle (requirement (f) of section 5.2.1).

The analytical description of the componentry is presented in appendix III. A brief description is only given below . Figure 5.4 shows therefore a front and lateral view of the whole device fitted with the pylon transducer. The X-Y-Z frame of the Instron machine is shown below the device where the load L is applied along Instron Y-axis. The transducer is shown in a general orientation at a distance R_x from the origin of the Instron frame of reference. A top hinged adaptor is also shown, which was used to match and suspend the device from the load cell (requirement (c) of section 5.2.1).

Since the Instron machine should not be subjected to off-axis loads (requirement (a) of section 5.2.1), any tests should be carried out with the centre of gravity of the whole device exactly below the suspension point. Therefore, the lower horizontal bar was provided with a small base accepting counterbalance weights W, in order to bring the system level into balance regardless of its tendency (weight W is omitted from the lateral view in figure 5.4).

For the Instron load to be applied, the cross-head was fitted with the base and cone used for the axial load calibration (see figure 4.10 in chapter 4).

5.3 Preparation of the Device and Setup

First of all the values of quantities R_x , ϑ_y and ϑ_x have to be decided. The user has the following options : for R_x a range of 0-200 mm with increments of

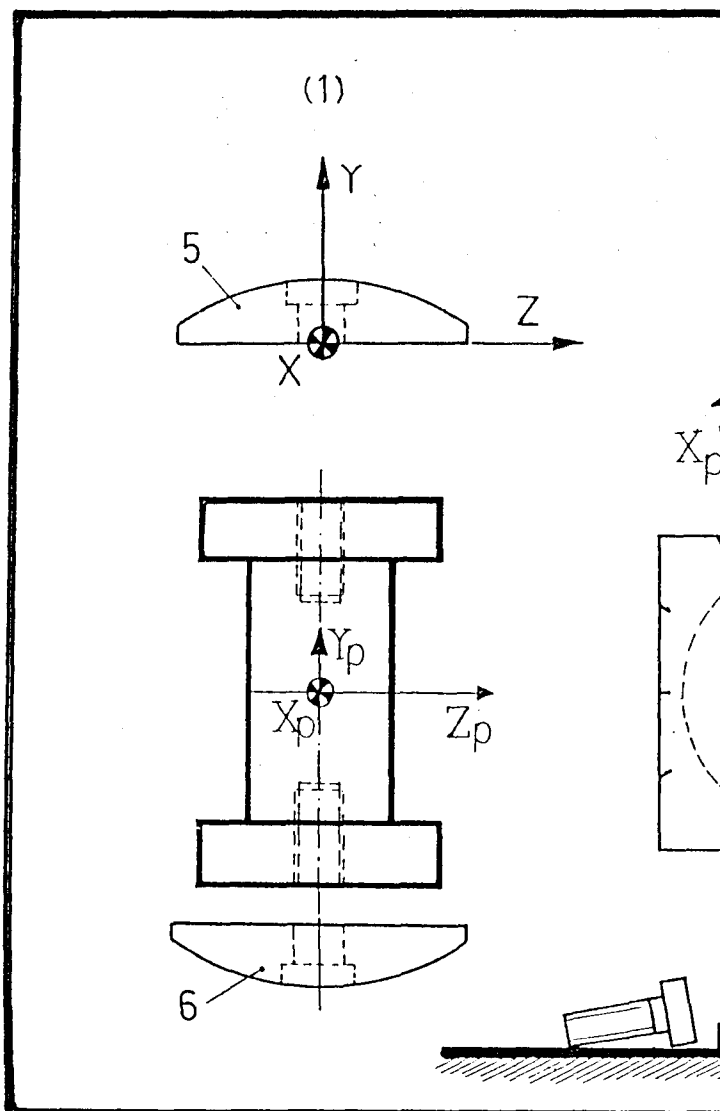
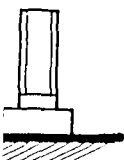
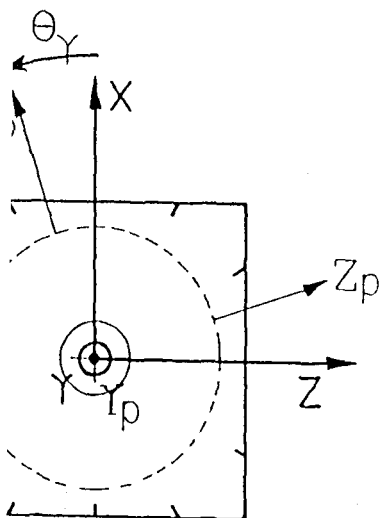


Fig 5.5 The implementation

$$(1) + \theta_Y \rightarrow (2)$$

(2)



of angle θ_Y

20 mm , for ϑ_y a range of 0-360 degrees with increments of 30 degrees and for ϑ_x a range of 0-90 degrees with increments of 18 degrees.

The algebraic sign of the quantities depends on the actual way the components are assembled. In any case , the signs of ϑ_x and ϑ_y have to follow the mathematical convention of the right hand rule.

It is important to notice that R_x is a coordinate of the pylon transducer's origin within Instron frame, but r_x in equations (5.5) is a coordinate of the Instron origin within the initial transducer's frame. Therefore, for equations (5.5) to be used , r_x must be considered as :

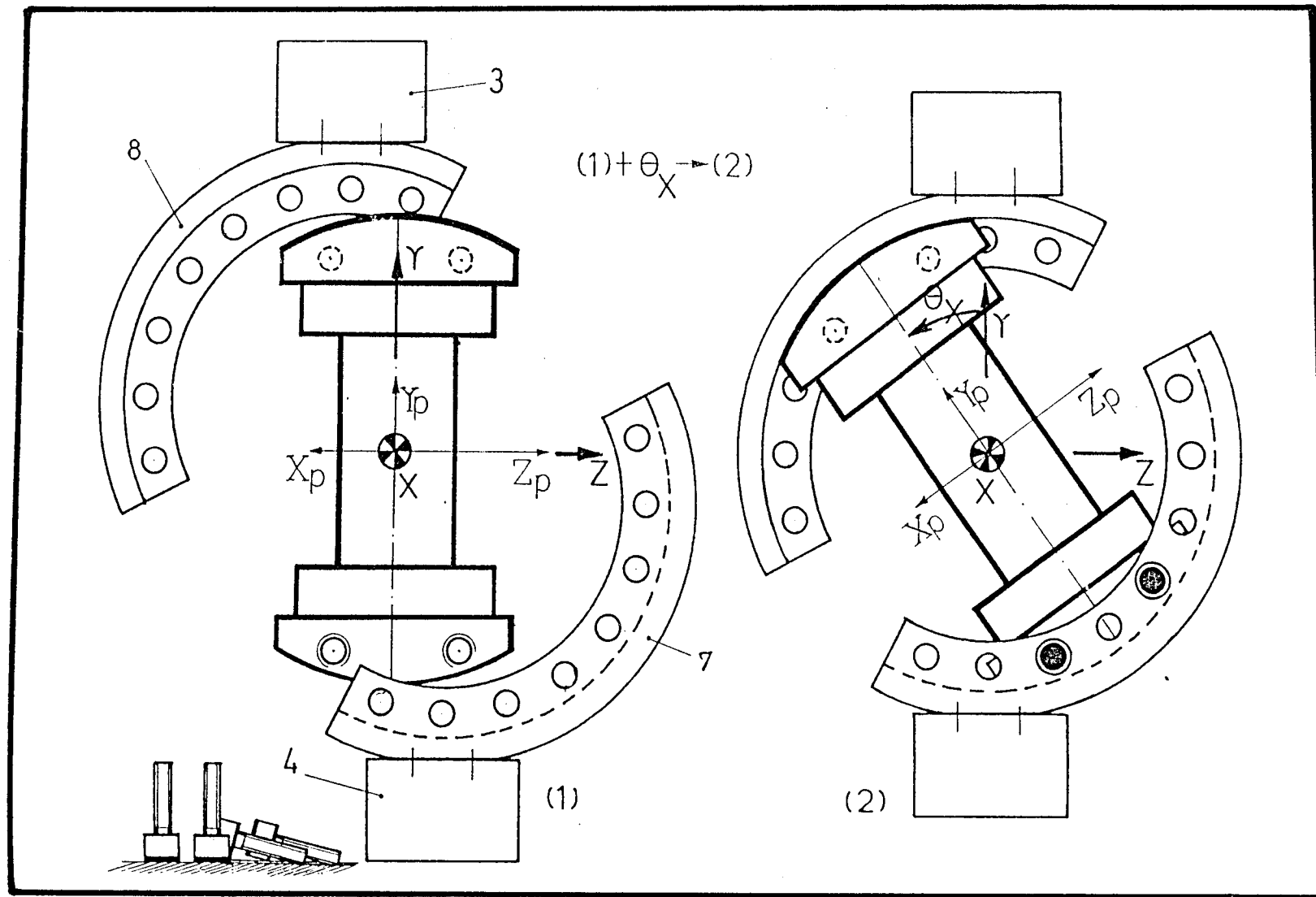
$$r_x = - R_x \quad (5.12)$$

The components needed for the assembly of the device are shown numbered in figure 5.4.

Initially the pylon transducer has to be fitted with components (5) and (6) by means of small foot bolts. The orientation of the transducer against these two components has to match the value of ϑ_y chosen. Figure 5.5 shows the transducer with components (5) and (6) in the initial position 1 and a plan view of the final position 2, where the pylon frame is simply rotated by ϑ_y , against the reference which corresponds to the Instron frame. Thus ϑ_y is implemented.

Having chosen the value for R_x , then components (7) and (8) must be fixed on the horizontal bars, using eight 1/4" UNC cap screws and the pairs of tapped holes corresponding to the chosen value of R_x . Thus, the distance R_x is implemented.

It is very important for the next step, that exactly at this stage, components (5) and (6) are with their sides parallel and their lateral holes on opposite sides (not shown) . The system resulting from this step is shown in figure 5.6 between the components (7) and (8) already mounted onto the bars.

Fig 5.6 The implementation of angle θ_x

This position is the initial position for the next step and is called position 1. To implement angle ϑ_x , the system of the pylon is fixed to the components (7) and (8) by means of four 1/4" UNC cap screws, in an angular position corresponding to the value of ϑ_x decided. The final configuration described as position 2, involves the transducer frame with a 3-D orientation with respect to the reference, which corresponds to the Instron frame.

The preparation is completed with the suspension of the system from the hinged load cell adaptor and the balancing of all the device, by means of small lead plates implementing weight W (see fig 5.4).

For the load to be applied, the plate and the cone must also be fixed on the cross-head of the Instron machine.

The transducer is then connected to the Strain Gauge Amplifiers. The bridge voltages and gain settings are the same as for the calibration. Wiring connections are described in appendix IX.

For every particular combination of R_x , ϑ_y and ϑ_x the loads on the transducer change, no matter if the Instron load L remains the same; and therefore, before every test is carried out, none of applied loads should higher than the maximum accepted values (requirement (e) of section 5.2.1).

It can be appreciated that the developed device provides multi-position loading configurations and not multi-component loading configurations. The load components applied onto the pylon transducer are not independent, but all relate to the Instron load L, with a relationship dictated by the geometry of the device (ie. the values of R_x , ϑ_x and ϑ_y).

In the next section the testing procedure and the development of the related computer program are presented.

5.4 Testing Procedure and Program for Analysis of Data

Before any series of tests , the developed program provides information on the maximum Instron load allowed for all parameter sets ie. R_x , ϑ_y , ϑ_x .

The program specifies the corresponding direction cosines for all the axes of the pylon transducer frame with respect to the Instron frame and calculates the Instron load allowed for every channel, taking under consideration the following load limits: 100 N for F_x and F_z , 1000 N for F_y , 100 Nm for M_x and M_z and 30 Nm for M_y . When a channel is not subjected to a load (for example when $\vartheta_x = 0$ then $F_x = F_z = M_y = 0$) , the program, for simplicity, assumes a limit of 1000 N or Nm accordingly.

Having obtained the maximum values for all channels, the lowest one must be recorded ; the reason being that since all channels are simultaneously loaded, the channel to dictate the Instron load must be the one appearing to be the most highly stressed for the particular configuration. The same routine is to be followed for as many sets of R_x , ϑ_y , ϑ_x as required

An Instron load equal or lower to the corresponding maximum allowed value must be applied on the device and the readings from the amplifiers and the Instron load are recorded. At this point, the testing for this particular geometrical configuration is over and the preparation of the set-up for another test may start. Then again the Instron load has to be equal or lower to the corresponding maximum allowed value .

Having carried out all tests required, then the program can be re-run. The input data in this case are: the applied Instron load and the output signals of the amplifiers for every geometrical configuration.

The program then, using the formulae (5.5) calculates the load components applied by the Instron on every direction of the transducer's frame. Then the program using the calibration matrix calculates the predicted load components for every loading

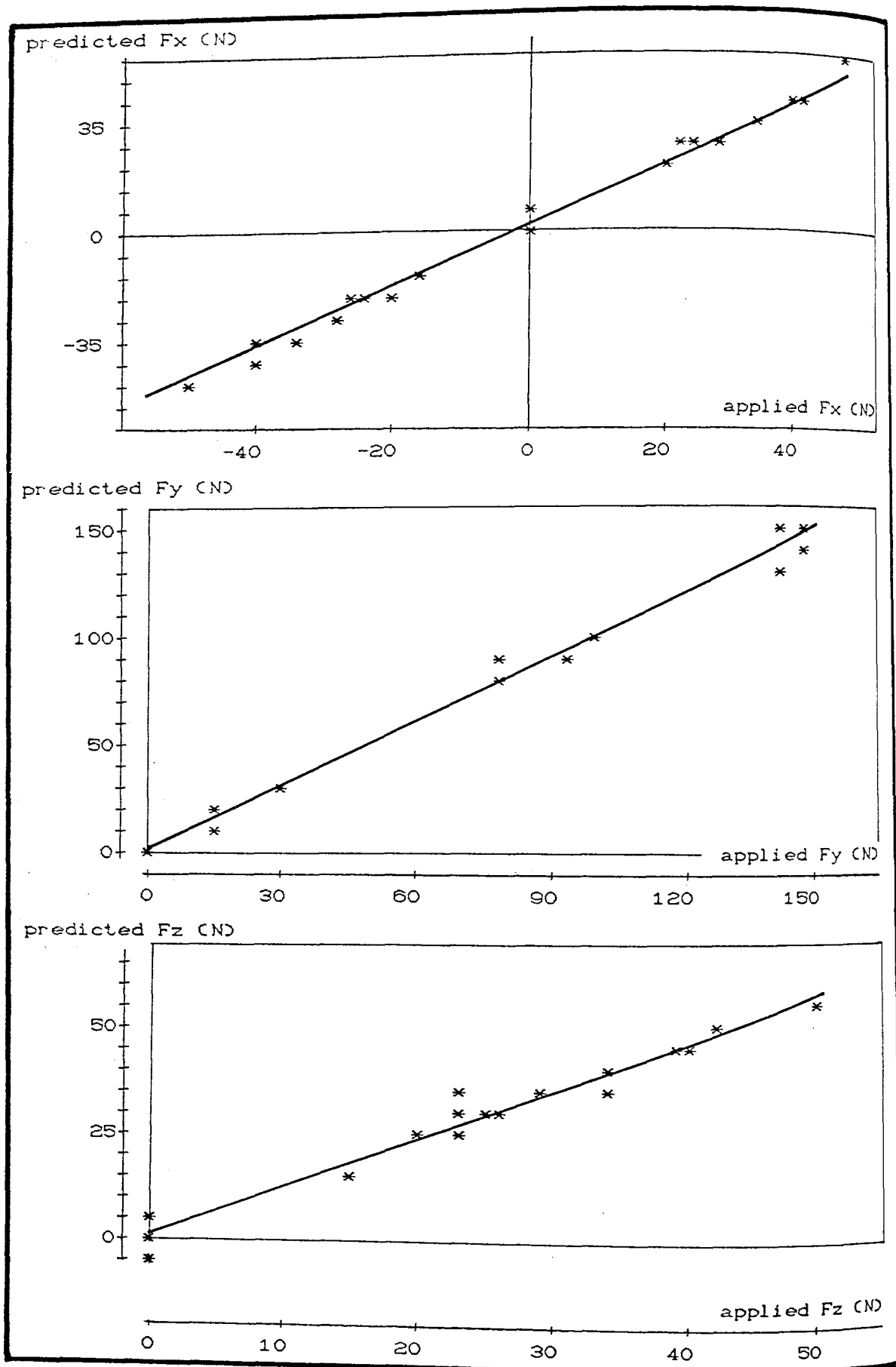


Fig 5.7 Predicted and applied forces

configuration. Finally, by comparing the applied and predicted values, the program supplies comparative results. The program developed is shown in appendix XIII.

Having followed the testing procedure as presented, twenty-four tests were carried out. These tests and their results are presented in the next section.

5.5 Tests and Results

The tests were planned to be carried out at a constant distance $R_x = 100 \text{ mm}$. The values of angles ϑ_y and ϑ_x were chosen to meet all the possible combinations within the following ranges : -90° to 90° for ϑ_y and 0° to 90° for ϑ_x .

Twenty-four different loading configurations were thus tried. Analytical data from these tests are shown in appendix III.

The results are presented in this section in a way so that inferences about the prediction ability of the calibration matrix [C] can be drawn. In figures 5.7 and 5.8 the predicted load values are plotted against the actual applied load components.

The ideal pattern would be a straight line with unit slope and zero intercept. As shown in the diagrams the predicted and the actual values exhibit a pattern similar to the expected one. A quantitative evaluation of the patterns shown can be obtained by linear regression of the data. The results from such regressions are as follows :

$$\begin{aligned} (\text{predicted } F_x) &= 1.7004 + 1.00048 \cdot (\text{applied } F_x) && \text{in N} \\ (\text{predicted } F_y) &= 0.7690 + 1.00915 \cdot (\text{applied } F_y) && \text{in N} \\ (\text{predicted } F_z) &= 1.1100 + 1.11669 \cdot (\text{applied } F_z) && \text{in N} \\ (\text{predicted } M_x) &= -0.0196 + 0.95368 \cdot (\text{applied } M_x) && \text{in Nm} \\ (\text{predicted } M_y) &= -0.1799 + 0.98400 \cdot (\text{applied } M_y) && \text{in Nm} \\ (\text{predicted } M_z) &= 0.0991 + 0.98597 \cdot (\text{applied } M_z) && \text{in Nm} \end{aligned}$$

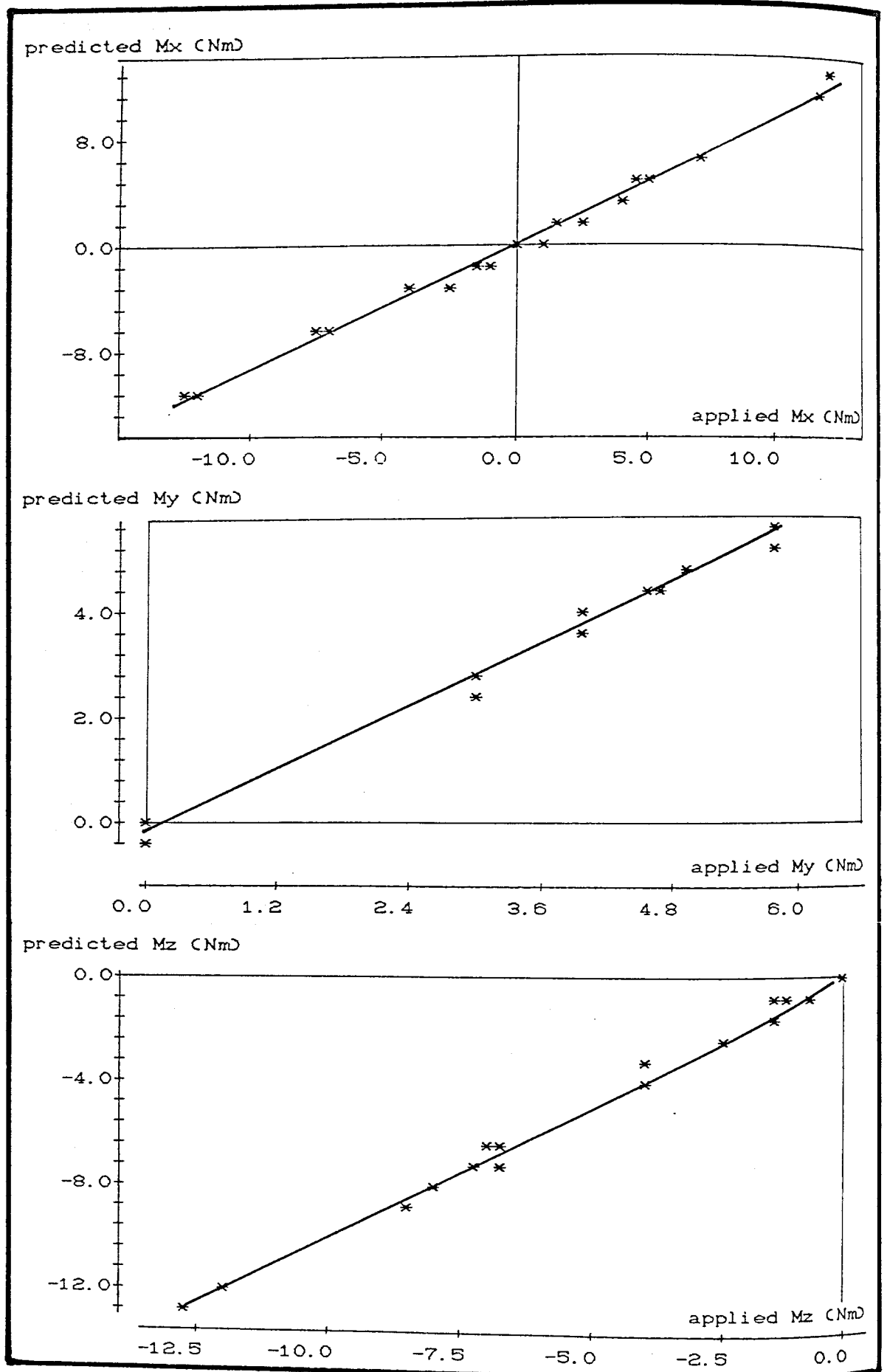


Fig 5.8 Predicted and applied moments

Indeed the slopes are close to unity and the intercepts are close to zero. On the other hand, as indicated by the r-square values (not shown) , these equations satisfy the plotted data by more than 99.5 %, the only exception being the equation for Fz where the value for r-square is poorer (98.1 %) .

However, the interpretation presented above is not complete , unless some more statistical information is provided, by calculating the percentage error. However, this was not considered appropriate for all the data acquired because many of the applied load components appear with very small values and thus percentage errors could be misleading. As can be seen in figure 5.8 for example the torque component appears with very small values. Therefore this component was excluded from the statistical analysis. For the rest of the load components. The calculated errors are shown in table 5.1 .

The final section deals with a discussion of the presented work and a series of conclusions drawn from the method and the tests.

5.6 Discussion and Conclusions

The work presented in this chapter was conducted in order to establish a method by which various users of the pylon transducer could validate the calibration matrices they use.

The method proved to be a useful tool for this purpose and provided comparative results that former pylon transducer studies lacked. However , the author recognised a drawback which is reported here.

As explained earlier, the applied Instron load cannot exceed a certain value imposed by the most highly stressed of the channels. Thus, channels which can afford higher loads are not tested within their full range and therefore the acquired data for these channels are limited in terms of their magnitude. Nevertheless , as discussed in the introduction , the

load component	calculated prediction error
for Fx over 20 N	5.3 %
for Fy over 50 N	3.5 %
for Fz over 20 N	16.9 %
for Mx over 10 Nm	4.4 %
for Mz over 10 Nm	2.4 %

Table 5.1 The prediction errors resulted from the validation tests

reported method and the device have disadvantages related to the use of the Instron machine and therefore the global character of the drawn inferences is affected. A solution to this problem could be the following.

In chapter 4 it was suggested that a calibration rig is needed to be designed and manufactured. Such a rig could also allow all six load components to be individually applied, providing the researcher the ability to validate a calibration matrix within the full loading ranges. Such loading configurations would then be multi-component loading configurations and the pylon transducer would not need to be mounted in different orientations.

Conclusions can be, finally, drawn as follows :

1) The validation tests for the calibration matrix under study resulted in the calculation of the prediction errors, which however cannot be attributed to the calibration matrix with confidence, for reasons discussed above. These results were the following : for the axial compression F_y and the moments M_x and M_z were relatively low (3.5% , 4.4% and 2.4% respectively), and for the shear force F_x 5.3% . The error for shear force F_z was found very large (16.9%), and could relate to the poor linearity of the cross-effects noticed during calibration (see figure II.10 in appendix II). However, shear force F_z is not an important determinant during amputee locomotion.

2) The device developed allows only for multi-position loading configurations to be tested. This introduces the problem of not testing all channels in their full loading range. Besides, the use of the Instron machine introduces uncertainty about the obtained results.

3) The calibration rig mentioned in chapter 4 can be used to solve the above problem. It must provide the

researcher the ability of independent application of the six load components, so that it allows for multi-component loading configurations to be tested for the purpose of matrix validation.

The next chapter presents work carried out in order to investigate the possibility of using a second-order calibration model.

CHAPTER 6

INVESTIGATION FOR A SECOND-ORDER MODEL FOR THE CALIBRATION OF THE PYLON TRANSDUCER

6.1 Introduction

6.2 Description of Set-up and Tests

6.3 Processing of Data

6.4 Results

6.4.1 The Sensitivity Coefficients

6.4.2 The Exploitation Coefficients

6.4.3 Predictions

6.5 Discussion

6.6 Conclusions

6.1 Introduction

The second - order calibration model has been presented in detail in section 2.8 of chapter 2 . Since no relevant studies are available for the application of such a model on the short pylon transducer , this chapter deals with a first investigation in this field.

The work presented in this chapter has many practical similarities with the work presented in chapter 5.

Second - order calibration models are used in other scientific disciplines, where the main and cross effects of various transducers are to be evaluated with accuracy. Several experimental techniques and processing methods have been established for this purpose.

The main concern of the researchers was to build appropriate calibration rigs in order to be able to apply all the load components required for a full calibration. Two well known rigs for this purpose were reported by Dubois, 1974, 1976, 1978, 1982 and Bray, 1978 and Ferrero et al. 1986. These rigs allow the application of six independent load components in all possible combinations and therefore provide the experimenters with data the processing of which can result in the determination of individual (ie first order) or interaction (ie second order) effects.

As discussed in section 2.8 of chapter 2 , not all load configurations produce significant output signals and decisions must be made on which coefficients to omit and which to retain. Referring to equations (2.11) and (2.13) presented in chapter 2 , it can be appreciated that, because of the number of the coefficients, the experimental procedure must be well planned in advance and any decisions must be based on statistical analysis.

Various researchers have planned their tests in terms of a factorial experiment meant to point out all significant first and second order effects. Such a

method is well described in the work presented by Zompi and Levi (1978). The multiple regression technique has also been used for the development of the sensitivity and exploitation equations (Verrini and Levi, 1968). This method is better known as stepwise regression and its principle is the selection of retained variables according to their correlation coefficients with the dependent variable and their F-value . If the F-value exceeds a given significance level then the corresponding variable is included in the model and when no more variables are to be included the procedure stops and the equation constitutes the final regression equation.

According to the literature, second-order effects can be determined using dead-weight techniques (see references above). The analysis presented in this chapter, however, is based on the multiple regression of data acquired from the pylon transducer using the loading system described in chapter 5.

6.2 Description of Set-up and Tests

The device developed for the validation of the calibration matrix of the pylon transducer provides the possibility of a large number of multi-position loading configurations. This device (see figure 5.4) has been designed to produce on the pylon transducer six load components by simply applying an Instron compression load.

However, the large number of data needed for the compilation of second-order equations would result in very lengthy experimental work because of the time needed for the assembly of the components between tests. Thus, an improvement of the method was needed which would allow for several different configurations to be tested; all sharing the same initial assembly.

Figures 6.1 a and b show how this was achieved. Having assembled the components in a particular configuration, the device can then be tilted and

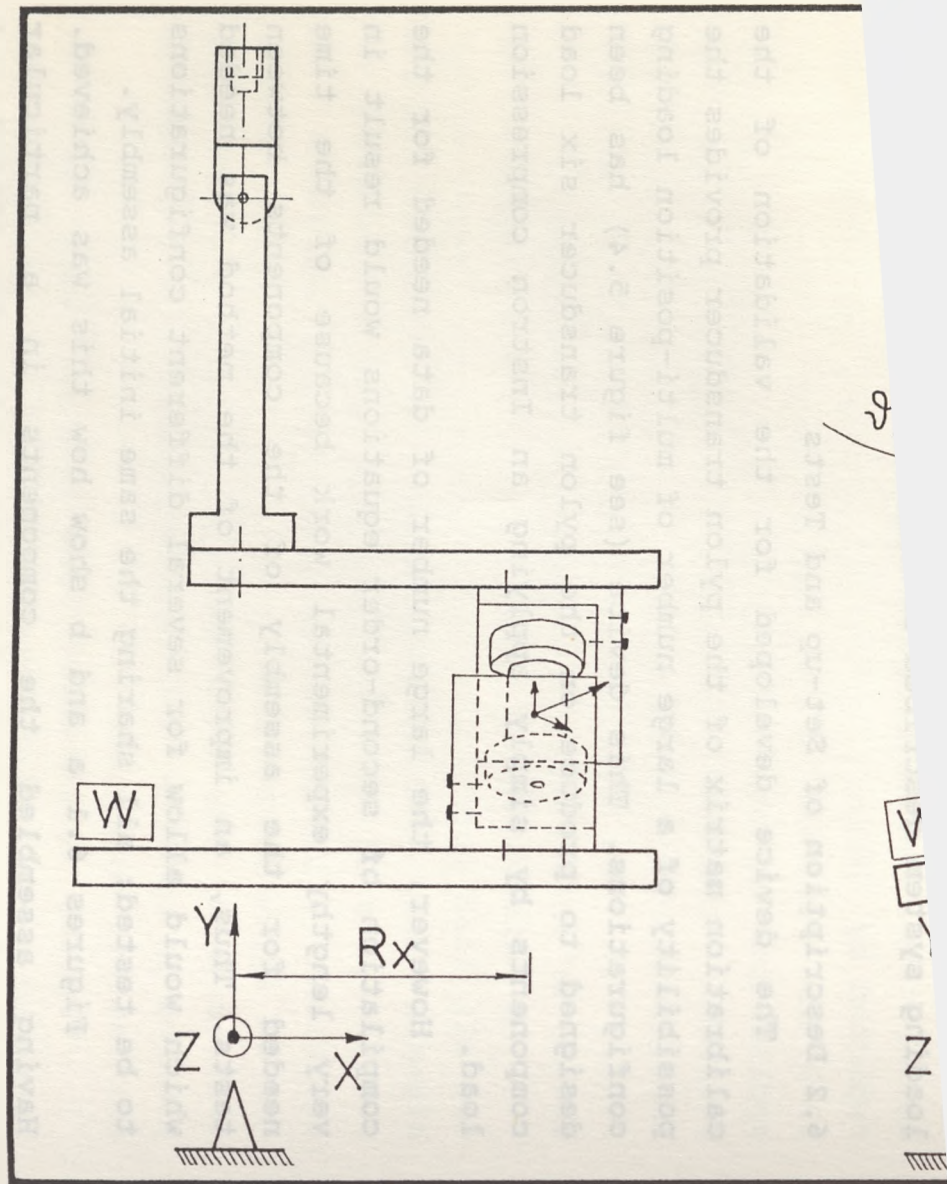
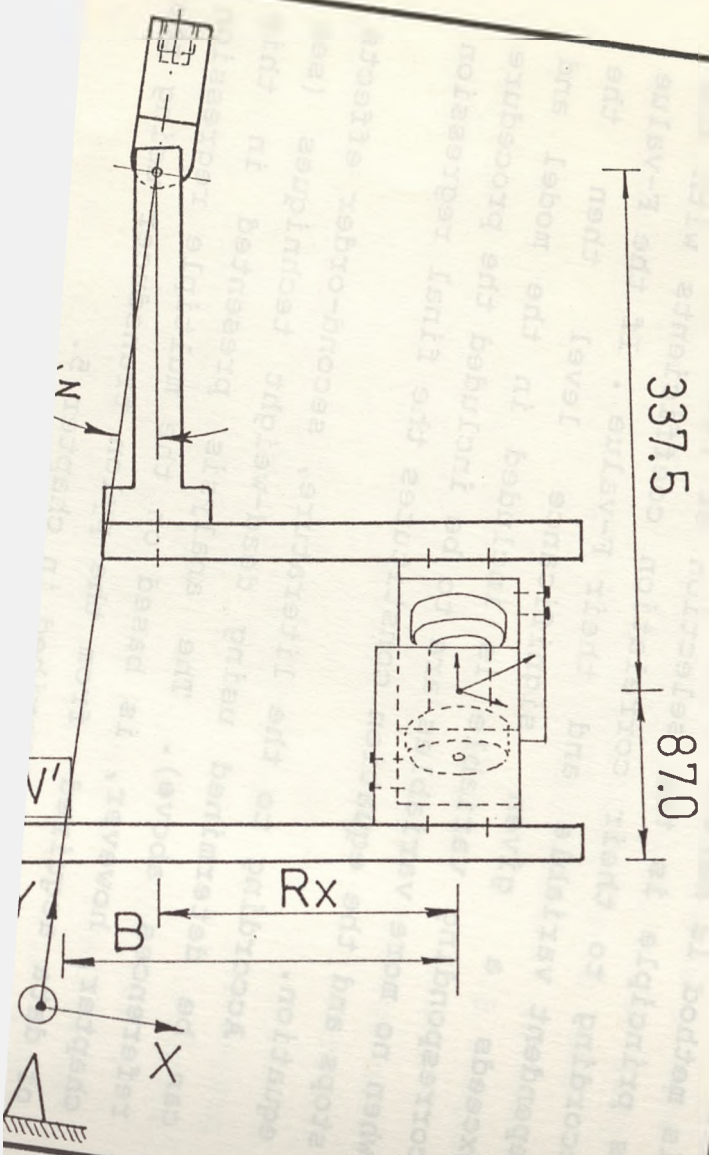


Fig 6.1a The set-up used for



for the tests

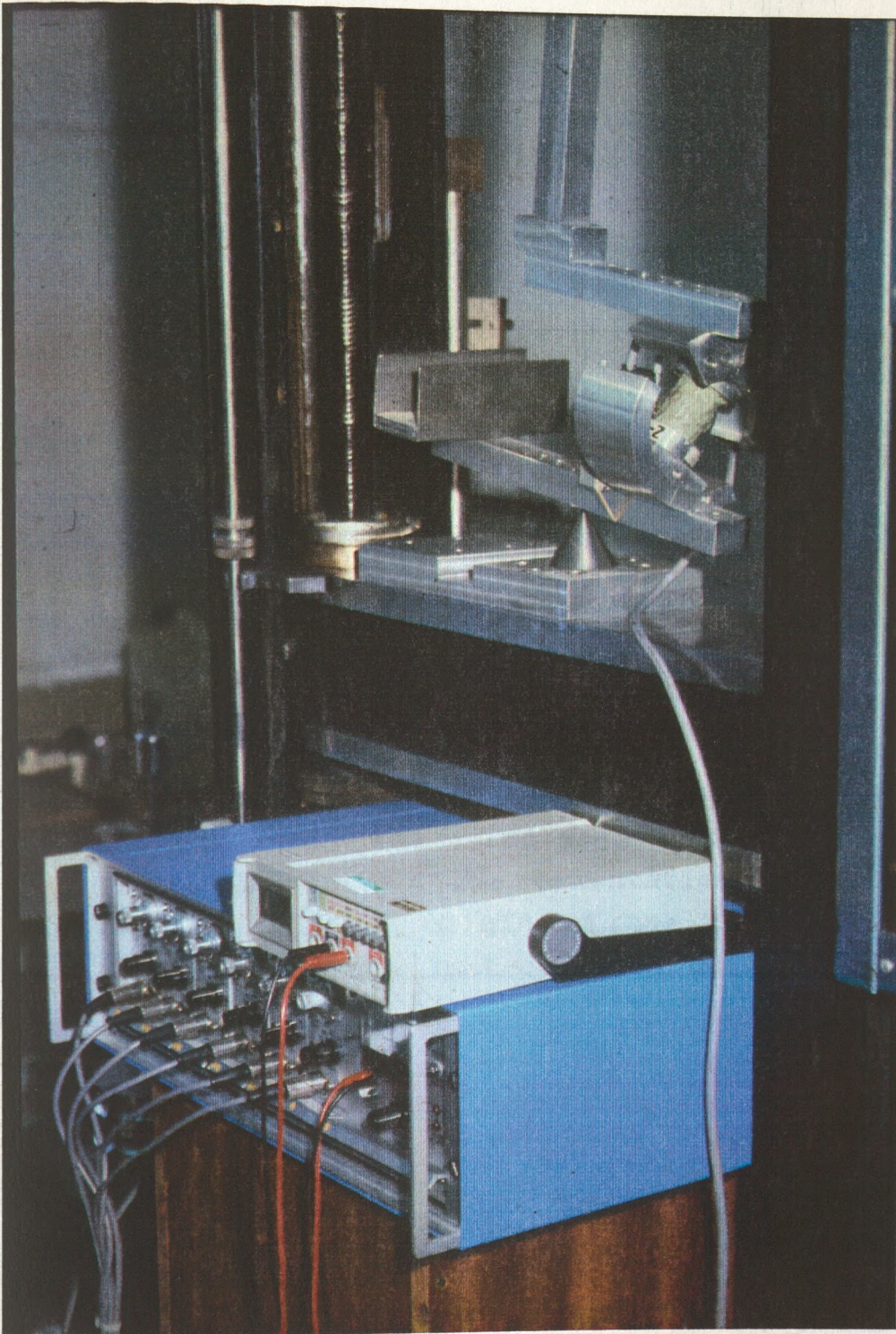


Fig 6.1b The set-up used for the tests (note that $\theta z < 0$)

balanced (weight W') at various inclinations described by angle ϑ_z about the top hinge joint. While the initial set-up of the components remains unchanged, the choice of different angular positions results in different multi-position configurations and therefore in an equal number of sets of data.

Before tilting the device, the orientation of the pylon transducer frame of reference, with respect to the Instron frame of reference is given by equation (5.10) as a function of the parameters ϑ_y and ϑ_x . After having tilted the device by ϑ_z the final orientation matrix will include this angular parameter and can be calculated (see appendix V). This matrix is:

$$\begin{bmatrix} (c_z \cdot c_y - s_x \cdot s_y \cdot s_z) & (-s_z \cdot c_x) & (c_z \cdot s_y + c_y \cdot s_x \cdot s_z) \\ (s_z \cdot c_y + c_z \cdot s_x \cdot s_y) & (c_z \cdot c_x) & (s_z \cdot s_y - c_z \cdot c_y \cdot s_x) \\ (-s_y \cdot c_x) & (s_x) & (c_x \cdot c_y) \end{bmatrix} \quad (6.1)$$

where c and s denote cosine and sine respectively and x , y and z denote the three angles ϑ_x , ϑ_y and ϑ_z .

In addition to the orientation matrix the new coordinates of the origin of the transducer's frame with respect to the Instron frame of reference can be calculated :

$$\begin{aligned} \text{x-coordinate} &= R_x \cdot c_z + 337.5 \cdot s_z & (\text{in mm}) \\ \text{y-coordinate} &= R_x \cdot s_z - 337.5 \cdot c_z + 424.5 & (\text{in mm}) \\ \text{z-coordinate} &= 0 & (6.2) \end{aligned}$$

As described in chapter 5, the values of R_x , ϑ_y and ϑ_x can be measured on the components themselves. For the assessment of the newly introduced ϑ_z the same principle was used : a scale marked on the lower

horizontal bar could provide the value of parameter B (fig 6.1) which is directly related to the angle ϑ_z by equation :

$$\vartheta_z = \arctan \left[\frac{(B - R_x) \text{ in mm}}{424.5 \text{ mm}} \right] \quad (6.3)$$

The program described in chapter 5 was therefore modified in order to include the new developments. The user run the program providing the values of parameters R_x , ϑ_y , ϑ_x and B and obtained the maximum allowed Instron load for each configuration as already described in chapter 5. Then the various tests were carried out and the output signals of the transducer were recorded. Besides the introduction of angle ϑ_z in the analysis the set up and method was identical to the one used in chapter 5.

Using the above method, 92 different loading configurations were tested. These tests together with the 24 tests presented in chapter 5 formed a set of 116 tests in total. Then one file was created for all the sets of applied load components (116 sets of 6 components each) and another file for all the corresponding sets of output signals (116 sets of 6 signals each). These two files constituted an adequate base for multiple regression to be performed. The data acquired from these tests are presented in appendix XI.

6.3 Processing of Data

The processing of the data was performed using the Minitab statistical package. It was decided that 103 tests would only be used ; allowing the remaining 13 tests to be used as predictors for the equations compiled.

The objective of the multiple regression was to calculate the linear, quadratic and rectangular coefficients of the sensitivity and exploitation

equations (2.11) and (2.13) shown in chapter 2 . The processing consisted of the following stages :

- 1) Read-in the 103 sets of loading data , ie 103 rows x 6 columns
- 2) Compile all the second-order loading products, ie another block of 103 rows x 21 columns
- 3) Read-in the column of the corresponding output signals of the first of the channels, ie 103 values of signal SFx
- 4) Perform a multiple regression between SFx and the 27 columns of loading data
- 5) Note which columns of loading data have, in the obtained regression equation, a p-value higher than 0.05 and consider them insignificant
- 6) Exclude observations with high standard residual values (absolute value of st.resid > 2.5)
- 7) Repeat the regression of SFx against the significant columns of loading data only
- 8) Repeat stages 5 to 7 until the regression results in significant predictors only and no high standard residual values

The above procedure must be repeated another five times, in order to derive all the sensitivity coefficients for all six channels. Finally it must be repeated another six times with the role of loading data and output signals inversed, in order to derive the exploitation coefficients for the six load components.

6.4 Results

The multiple regression resulted in two sets of results presented in this section : a) the sensitivity coefficients which explain how each load component or combination of two load components influence the output signals of the six channels and b) the exploitation coefficients which explain how each output signal or

combination of two signals indicate the applied load along each one of the six directions.

In this section comparisons are also made with the corresponding coefficients derived by using the linear calibration model. The comparisons refer to the elements of matrices [M] and [C] presented in chapter 4 as derived by former researchers using dead-weight techniques (Solomonidis,1989). For these two matrices see tables 4.3 and 4.4 respectively.

As already mentioned, a set of 13 tests was used for predictions. The results from these prediction are also presented in this section.

6.4.1 The Sensitivity Coefficients

The derived sensitivity equations were as follows:

$$\begin{aligned} SFX = & 0.985 Fx - 0.267 Mx + 0.345 My - 0.000159 Fx Fy \\ & +0.000032 Fy Fy - 0.00181 Fz My + 0.00524 Mx Mz \\ & +0.0132 MyMy \end{aligned} \quad (6.4)$$

$$\begin{aligned} SFY = & 0.014 Fx - 0.257 Fy + 0.327 Mx - 0.273 My \\ & -0.294 Mz - 0.000624 Fx My + 0.00464 My My \\ & +0.00123 MzMz \end{aligned} \quad (6.5)$$

$$\begin{aligned} SFZ = & 0.956 Fz + 0.402 Mz \\ & +0.000180 Fx Fx - 0.00232 Fx My \\ & -0.000132 Fy Fz + 0.000974 Fy Mx \\ & +0.0031 Fz My - 0.0125 My My \\ & +0.00616 MzMz \end{aligned} \quad (6.6)$$

$$\begin{aligned} SMX = & -0.0151 Fy + 0.0551 Fz - 11.2 Mx - 0.155 My \\ & -0.000165 FxFz - 0.00596 FxMx - 0.00116 FyMx \\ & -0.00389 FyMy - 0.000794 FyMz - 0.00114 FzMx \\ & +0.00674 MxMx + 0.0149 MyMy - 0.0237 MyMz \end{aligned} \quad (6.7)$$

$$\begin{aligned} SMY = & 0.0248 Fy - 19.6 My - 0.000120 Fy Fy \\ & +0.00563 Fz My \end{aligned} \quad (6.8)$$

$$\begin{aligned} SMZ = & 0.0177 Fx + 0.0113 Fy - 0.165 Mx + 0.0479 My \\ & +5.79 Mz - 0.000097 Fx Fx - 0.000088 Fx Fy + \end{aligned}$$

In the equation for	the coefficient of	is for the 2nd order model	and for the 1st order (linear) model
SFx	Fx	0.98462	0.99023
	Mx	-0.26660	-0.37980
	My	0.34497	0.25680
	Mz	*	0.11719
SFy	Fx	0.01412	0.01449
	Fy	-0.25707	-0.25977
	Mx	0.32744	0.25490
	My	-0.27306	-0.18230
	Mz	-0.29449	-0.32080
SFz	Fz	0.95597	0.95024
	Mx	*	0.07220
	My	*	-1.00200
	Mz	0.40173	0.38662
SMx	Fy	-0.01513	*
	Fz	0.05513	*
	Mx	-11.24080	-12.00480
	My	-0.15477	*
SMy	Fy	0.02478	*
	My	-19.64270	-19.64900
SMz	Fx	0.01771	*
	Fy	0.01130	*
	Mx	-0.16548	*
	My	0.04785	*
	Mz	5.79002	5.86855

* the values for these coefficients are zero

Table 6.1 The comparison of the sensitivity coefficients

$$\begin{aligned}
&+0.000016 F_y F_y - 0.000122 F_y F_z + 0.00137 F_y M_x \\
&+0.00131 F_y M_z + 0.00633 M_x M_z + 0.00513 M_y M_y \\
&+0.00453 M_y M_z + 0.00592 M_z M_z
\end{aligned}$$

(6.9)

The above coefficients have units :

$$mV / N , \quad mV / Nm , \quad mV / N \cdot Nm \quad \text{or} \quad mV / Nm \cdot Nm$$

accordingly and refer to the output signals of the strain gauge amplifiers. Statistical details about the obtained coefficients are exhibited in appendix XI.

Table 6.1 shows a comparative juxtaposition of the above coefficients with the ones derived using the linear model (see matrix [M] in table 4.3). It can be appreciated that first order coefficients could only be compared.

6.4.2 The Exploitation Coefficients

The derived exploitation equations were as follows:

$$\begin{aligned}
FX = & 1.02 SF_x - 0.0262 SM_x + 0.0170 SM_y \\
& -0.000461 SF_y SF_y - 0.000111 SM_x SM_y \\
& +0.000088 SM_x SM_z
\end{aligned} \tag{6.10}$$

$$\begin{aligned}
FY = & 0.0577 SF_x - 3.89 SF_y - 0.119 SM_x + 0.0438 SM_y \\
& -0.204 SM_z + 0.000058 SM_x SM_x
\end{aligned} \tag{6.11}$$

$$\begin{aligned}
FZ = & 1.05 SF_z - 0.0672 SM_z \\
& -0.000179 SF_x SF_x - 0.000128 SF_x SM_y \\
& -0.000272 SF_y SM_x + 0.000160 SF_z SM_y \\
& +0.000031 SM_y SM_y - 0.000186 SM_z SM_z
\end{aligned} \tag{6.12}$$

$$\begin{aligned}
MX = & 0.00569 SF_y + 0.00458 SF_z - 0.0885 SM_x \\
& +0.000523 SM_y + 0.000023 SF_y SF_y \\
& -0.000032 SF_y SM_x + 0.000056 SF_y SM_z \\
& +0.000011 SF_z SM_x + 0.000004 SM_y SM_y \\
& +0.000011 SM_y SM_z
\end{aligned} \tag{6.13}$$

and

In the equation for	the coefficient of	is for the 2nd order model	and for the 1st order (linear) model
Fx	SFx SMx SMy SMz	1.02040 -0.02619 0.01700 *	1.00987 -0.03195 0.01320 -0.02017
Fy	SFx SFy SMx SMy SMz	0.05768 -3.89463 -0.11916 0.04382 -0.20424	0.05632 -3.84963 -0.08353 0.03645 -0.21156
Fz	SFz SMx SMy SMz	1.05012 * * -0.06716	1.05236 0.00633 -0.05367 -0.06933
Mx	SFy SFz SMx SMy	0.00569 0.00458 -0.08849 0.00052	* * -0.08330 *
My	SFy SMy	-0.00475 -0.05078	* -0.05089
Mz	SFx SFy SMy SMz	-0.00125 0.00957 0.00046 0.16756	* * * 0.17040

* the values for these coefficients are zero

Table 6.2 The comparison of the exploitation coefficients

$$\begin{aligned}
MY = & -0.00475 \text{ SFy} - 0.0508 \text{ SMy} + 0.000007 \text{ SFx SFx} \\
& +0.000051 \text{ SFx SMx} - 0.000055 \text{ SFy SFy} \\
& -0.000074 \text{ SFy SMy} + 0.000023 \text{ SFy SMz} \\
& -0.000014 \text{ SFz SMy} - 0.000082 \text{ SFz SMz} \\
& -0.000007 \text{ SMx SMy} - 0.000009 \text{ SMx SMz} \quad (6.14)
\end{aligned}$$

$$\begin{aligned}
MZ = & -0.00125 \text{ SFx} + 0.00957 \text{ SFy} + 0.000458 \text{ SMy} \\
& +0.168 \text{ SMz} + 0.000015 \text{ SFx SFx} \\
& -0.000065 \text{ SFy SFz} - 0.000017 \text{ SFy SMx} \\
& +0.000015 \text{ SMx SMz} - 0.000022 \text{ SMz SMz} \quad (6.15)
\end{aligned}$$

The above coefficients have units :

$$N / mV , \quad Nm / mV , \quad N / mV \cdot mV \quad \text{or} \quad Nm / mV \cdot mV$$

accordingly. Statistical details about the exploitation coefficients are also exhibited in appendix XI.

Table 6.2 shows a comparative juxtaposition of the exploitation coefficients with the coefficients derived using the linear model (see matrix [C] in table 4.4). Here again first order only coefficients could be compared.

6.4.3 Predictions

The derived exploitation equations were used to predict the loads applied onto the pylon transducer during the thirteen tests carried out for this purpose. Predictions of the above loads were also made using the calibration matrix [C] derived by the linear model.

The loading configurations involved in these tests were chosen to resemble the push - off configuration of an amputee (see figure 5.1). Thus, these configurations only involved components Fx , Fy and Mz which are the major components in human locomotion . Components Fz , Mx and My were not applied.

The absolute values of the predictions are shown in tables 6.3 and 6.4. Table 6.3 shows the predicted

Fx (N)			Fy (N)			Mz (Nm)		
applied	2nd order pred.	1st order pred.	applied	2nd order pred.	1st order pred.	applied	2nd order pred.	1st order pred.
0.00	0.68	-0.16	196.20	191.18	187.80	19.62	18.25	19.37
-4.62	-5.00	-5.86	97.99	98.53	96.71	11.36	10.68	11.23
-9.23	-9.86	-10.85	195.98	194.57	190.98	22.71	21.24	22.53
-18.41	-17.58	-18.83	195.33	192.94	189.22	25.75	24.27	25.71
-27.46	-27.85	-29.29	194.27	190.40	186.57	28.69	26.98	28.58
-36.34	-41.56	-43.19	192.81	184.05	180.20	31.54	29.38	31.10
-54.40	-59.40	-60.72	289.21	275.35	269.57	47.32	43.58	46.69
-44.99	-43.63	-45.53	190.97	183.59	179.55	34.28	32.18	34.08
-67.48	-66.07	-67.80	286.46	271.79	265.82	51.42	47.51	50.95
0.00	-0.94	-1.15	294.30	292.84	287.89	29.43	27.62	29.53
-13.85	-14.27	-14.76	293.97	292.40	287.26	34.07	31.80	33.98
-27.61	-28.31	-29.17	293.00	293.34	287.96	38.62	36.67	39.19
-41.19	-42.06	-43.13	291.40	291.01	285.45	43.04	39.99	42.77

Table 6.3 The predictions of the two models for the applied Fx, Fy and Mz

values of the F_x , F_y and M_z for both models as well as the corresponding values which were actually applied (shown in bold characters). Table 6.4 similarly shows the predicted values for the two models and the actually applied load values (all zero and shown in bold characters).

All above results are considered in the following discussion.

6.5 Discussion

The discussion in this section will first deal with the second-order coefficients, then with the first order coefficients and finally with the predictions and the comparisons.

A first observation of the coefficients derived with the second-order model for the sensitivity and exploitation equations (equations 6.4 to 6.15) shows that the multiple regression introduces a certain number of second-order coefficients.

The output signals of channels 1 and 3 measuring shear forces (ie signals SF_x and SF_z) are shown to be sensitive to combinations of shear stress - producing load components (like $F_x F_x$, $F_x M_y$, $F_z M_y$, $M_y M_y$) but also in combinations of bending moments (like $M_x M_z$, $M_z M_z$).

The output signal of channel 2 measuring the axial compressive load (ie signal SF_y) is shown to be sensitive to loading combinations involving torque (like $M_y F_x$ and $M_y M_y$). This signal is also shown to be sensitive to the presence of bending moment M_z (both on its own and as $M_z M_z$). For this latter remark one can refer to the conclusions drawn in chapter 3 regarding the sensitivity of this particular channel in moment M_z by design.

The output signals of channels 4 and 6 measuring bending moment (ie signals SM_x and SM_z) are shown to be sensitive to a considerable amount of combinations involving axial compression load F_y (like $F_y F_x$, $F_y F_z$, $F_y M_x$, $F_y M_y$, $F_y M_z$ as well as $F_y F_y$). These two channels

Fz (N)			Mx (Nm)			My (Nm)		
applied	2nd order pred.	1st order pred.	applied	2nd order pred.	1st order pred.	applied	2nd order pred.	1st order pred.
0.00	-4.32	-1.72	0.00	-0.30	0.28	0.00	0.24	0.37
0.00	-2.43	-1.51	0.00	-0.04	0.19	0.00	0.24	0.22
0.00	-6.34	-2.82	0.00	-0.35	0.30	0.00	0.27	0.45
0.00	-6.94	-2.37	0.00	-0.45	0.27	0.00	0.27	0.51
0.00	-9.37	-3.63	0.00	-0.52	0.27	0.00	0.35	0.62
0.00	-14.03	-6.98	0.00	-0.63	0.22	0.00	0.53	0.80
0.00	-23.86	-8.45	0.00	-1.32	0.35	0.00	0.29	1.14
0.00	-11.05	-2.79	0.00	-0.63	0.27	0.00	0.36	0.74
0.00	-21.54	-3.38	0.00	-1.47	0.31	0.00	0.03	1.10
0.00	-7.15	-1.27	0.00	-1.19	-0.07	0.00	0.06	0.60
0.00	-9.38	-1.59	0.00	-1.42	-0.14	0.00	0.05	0.72
0.00	-11.22	-0.98	0.00	-1.75	-0.30	0.00	-0.13	0.70
0.00	-13.97	-1.62	0.00	-1.82	-0.25	0.00	-0.15	0.77

Table 6.4 The predictions of the two models for the applied Fz, Mx and My

were also shown to be sensitive to combinations of bending moments and of these moments with torque (like $M_x M_z$, $M_x M_x$, $M_z M_z$, $M_z M_y$).

Finally the output signal of channel 5 measuring torque (ie signal S_{My}) was shown to be sensitive to only two loading combinations : one involving axial compression ($F_y F_y$) and one involving shear stress-producing loads ($F_z M_y$).

Similar remarks can be made for the second-order effects corresponding to the exploitation coefficients used to convert output signals into predicted applied load components.

For the first-order coefficients the situation is clearly shown in tables 6.1 and 6.2 . The second-order model and the first-order (linear) model exhibit many similarities. Besides few exceptions , where the two models do not both have coefficients (asterisks in tables), the rest of the values shown allow for two very important and positive remarks : a) there are not any differences at all regarding the algebraic signs of the values provided by the two models and b) all values of main and cross effects compare very closely. As far as the linear coefficients are concerned the two models can therefore be considered highly comparable.

The prediction ability of the second-order model and of the linear model for all six components has been presented in tables 6.3 and 6.4. These two tables show that despite the presence of second-order terms, the prediction ability of the second-order model does not in general improve in comparison to the prediction ability of the linear model. In fact, it can be noted that in many cases the two models provided predictions of a rather ambiguous nature : whereas in some cases the second-order model predicted applied loads better, in other cases the linear model did so and in the case of the non-applied F_z component the linear model offered much better predictions.

The principle of second-order calibration models

by the use of strain-gauge transducers and was not in the intention of this chapter to prove its validity. The presented work only aimed in an introductory investigation of the subject as towards its use for prosthetic loading measurements. The discrepancies and ambiguities observed during this study should be considered as motivation for further work, and by no means as a negative proof. Second-order effects may be looked into in the future, but as shown from the presented work their contribution may not be considered practically significant enough to justify the exchange of the simple linear model with the more complex second-order one. As other researchers have found out " it is hardly likely that the contribution of second-order effects is sizeable, from a technical point of view " (Bray et al ,1990) . However, despite the above comment, it is the author's opinion that the second-order effects should be investigated using a future calibration rig, simply to verify the above comment for the particular application.

6.6 Conclusions

The presented work and discussion can be summarised in the form of the following conclusions :

- 1) A second-order model was derived in this chapter by multiple regression on data acquired from 103 multi-position tests. The linear coefficients of this model proved to be very closely comparable to the ones provided by the already known linear model, derived with dead-weight method by former researchers (Solomonidis, 1989).

- 2) The second-order coefficients introduced in the sensitivity and exploitation equations (eq 6.4 to 6.15) implied that the transducer may be also sensitive to combinations of load components, in the sense explained

in section 2.8 of chapter 2 (sensitivity to elastic deformations). However, predictions performed by the second-order model and the linear model compared closely and therefore the contribution of the second-order effects cannot be considered practically significant.

3) If confidence in the determination of second-order effects is required in the future , then dead-weight techniques should be adopted following the principles discussed in chapter 2 and using the rig suggested in chapters 4 and 5.

The next chapter deals with the mathematical modelling of lower limb prostheses and their adjustability.

CHAPTER 7

MODELLING OF THE ADAPTORS AND OF THE STRUCTURE OF A LOWER LIMB PROSTHESIS

7.1 Introduction

7.2 Technical and Prosthetic Considerations

7.3 Initial Steps in the Study of the Adaptors

7.4 First Attempt to Model an Adaptor Analytically

7.4.1 Analysis

7.4.2 The Experimental Set-up and Method

7.4.3 Results

7.5 First Attempt to Calibrate an Adaptor

7.5.1 The Experimental Set-up and Method

7.5.2 Results

7.6 Further Considerations of the Adaptors

7.7 Mathematical Modelling of a Prosthesis

7.8 Discussion

7.9 Conclusions

7.1 Introduction

The use of the pylon transducer as a prosthetic loading measuring device can expand in the field of prosthetic alignment studies. The transducer could in fact provide data, enabling the researchers to establish criteria for the achievement of suitable alignment configurations.

The alignment of an artificial leg has been found to be very important in the mechanical behaviour of the prosthesis and thus for the walking performance and comfort of the amputee. The term `a l i g n m e n t` signifies the relative geometrical position of the various components of the prosthesis. In quantitative terms, the alignment of a prosthesis has been expressed as a set of parameters - shifts, tilts and rotations - concerning the socket (for a BK prosthesis), the knee and socket (for an AK prosthesis) and the knee, hip and socket (for a Hip Disarticulation prosthesis) relative to the foot.

The assessment of the alignment, in other words, the quantitative evaluation of the alignment parameters, is currently carried out by measurements of the prosthesis. These measurements are performed on the alignment rig described in section 2.6 , after the dynamic alignment session has been completed and without the necessity of prosthetist or patient being present.

The lack of a mathematical model, which could be easily brought into a program form, makes impossible both the immediate measurement of the alignment and the establishment of the inverse procedure, which in many cases is highly desirable. For example :

- a) it is not possible to instantly measure the imposed alignment configuration , at the same time as the adjustments are made on the joints and
- b) it is not possible to predict which adjustments should be made in order to obtain a predefined alignment configuration, for purposes of research or

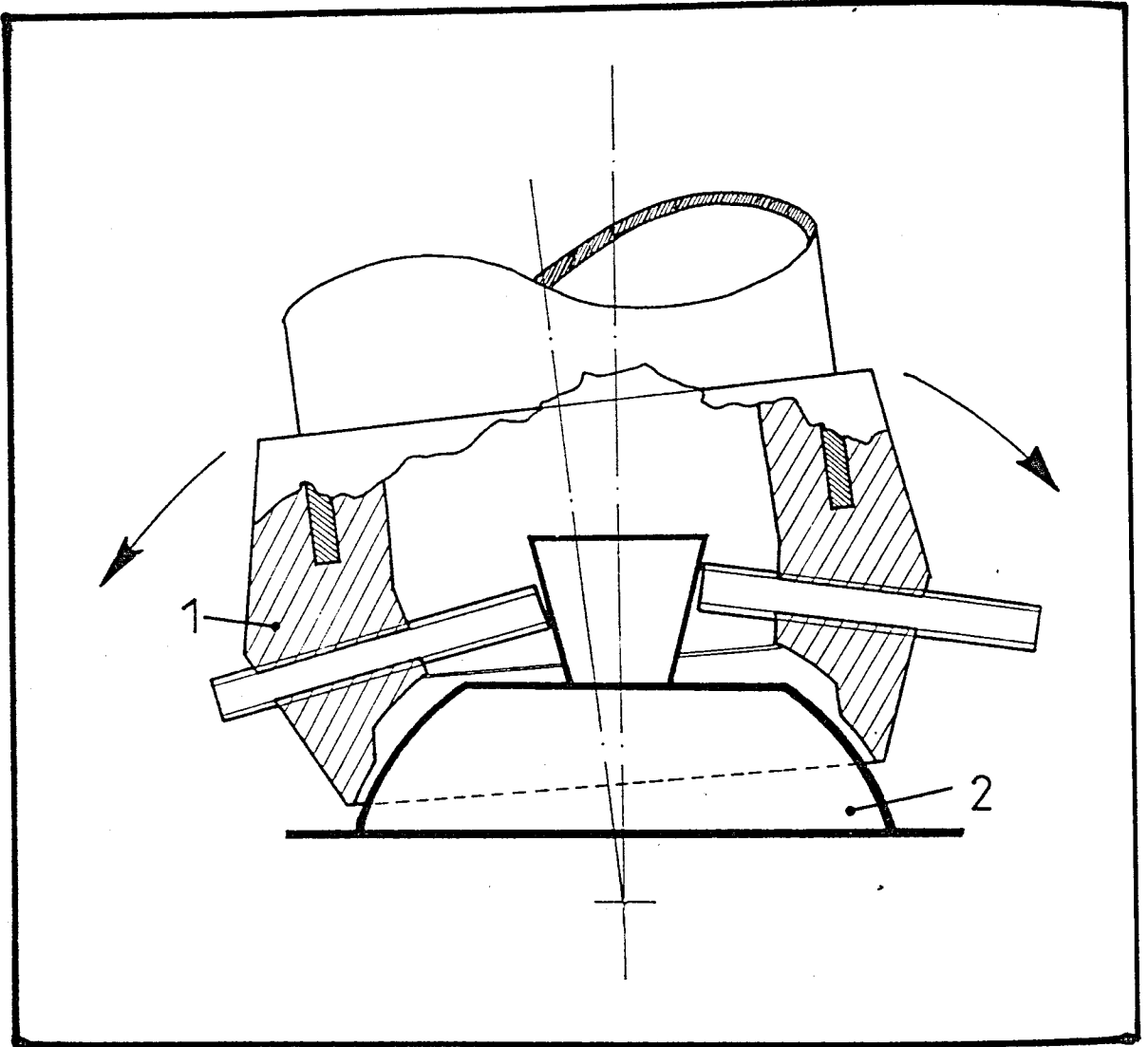


Fig 7.1 An Otto Bock adaptor for the ankle joint.

clinical applications.

The development of a method for the immediate measurement of the alignment is presented in chapter 8. A preliminary investigation in the area of the inverse problem is presented in appendix X .

The present chapter presents the work carried out in order to establish the prerequisite modelling mentioned above; and concerns an Otto Bock prosthesis. This modelling is based upon the study of the functional behaviour of the alignment adaptors of such a prosthesis.

7.2 Technical and Prosthetic Considerations

The alignment adjustments on an Otto Bock modular prosthesis are made by means of adaptors built in at all joints of the prosthesis. All possible adjustments are by means of simple rotations only and every particular combination leads to the establishment of a set of shifts, tilts and axial rotations, defining the alignment of the artificial leg.

The adjustments made are angular displacements in the sagittal plane (AP), the frontal plane (ML) and the transverse plane. The adaptors which had to be studied in this work were those providing the possibility of AP and ML adjustments.

The principle used for these adjustments to be achieved is the same for both planes. Figure 7.1 shows an ankle adaptor for an Otto Bock modular prosthesis. As shown, the accurately machined cup-shaped surface of the upper part (1) is allowed to slide onto the spherical surface (dome) of the lower part (2) of the adaptor. The upper part can be locked in any particular orientation (AP, ML, or both) by means of two pairs of set screws, which are tightened against the pyramid - shaped protrusion of the lower part. When a particular alignment adjustment is to be carried out, in order to change the geometrical relationship between adjacent components in one

plane, say the AP plane, the prosthetist must loosen one of the set screws on the other plane (ML) and then adjust the screw of the plane in which the geometry is to be altered. After the adjustment is over, both screws belonging to the plane of interest are tightened up, as well as the one initially loosened on the other plane; the latter screw is always tightened last. As can be appreciated from figure 7.1, when a pair of set screws is adjusted, the proximal component tends to lean over towards the side of the screw, which is the farthest in against the pyramid, consequently increasing its angular distance from the other side.

The problem which arose in this study was that, whereas the transverse rotational adjustments, if any, can be measured directly by means of an appropriately implemented protractor, the AP and ML adjustments, just described, cannot be measured, because of the indirect way in which they are imposed. However, since the AP and ML angular changes are achieved by means of the set screws fitted on the adaptor, a relationship established between screws and angular position would allow the knowledge of the angular adjustment imposed by means of these screws ; and of course, it could be possible to use these angular adjustments for the calculation of the corresponding alignment parameters of the prosthesis, after this change.

7.3 Initial Steps at the Study of the Adaptors.

The need for the establishment of a relationship between the adaptor screws and the angular adjustments imposed has already been explained. An analytical approach was initially tried in order to determine a formula for the solution of the problem. This study is presented in the next section.

This approach involved measurements of the geometry of an Otto Bock ankle adaptor. Both parts, i.e the pyramid component and the tubular rim, were

measured. A new set of screws was then machined. These four screws were, obviously, the same kind as those provided by Otto Bock (metric M8). The only difference was that the new ones were much longer (length 30 mm) and machined at both their ends to produce a uniform length with the two end surfaces smooth and perpendicular to the screw axis, thus providing good contact and reliable reference for measurements.

Since the geometry of both parts of the adaptor and the length of the screws was known, the next thing to be sought was a geometrical relationship between the angular position of the proximal component and the protruding length of the screw responsible for the tilt imposed. This screw was considered to be the screw over which the proximal component leans.

For a better perception of the way in which such a relationship could be established, it was necessary that the two parts of the adaptor were accurately drawn on two different transparencies hinged by means of a drawing pin on a board. The pin was located at a point corresponding to the geometrical centre of the spherical surface of the pyramid component (the drawing was as already shown in figure 7.1). By moving the transparency depicting the proximal component around the centre (see arrows), while holding the other one stable, the changes of the relative position of the two parts were made much clearer.

7.4 First Attempt to Model an Adaptor Analytically

7.4.1 Analysis

The measurements of the adaptor's geometry resulted in data, concerning the position of all the important points of the adaptor. Of particular interest was the position of the centre of the spherical surface (point C).

In figure 7.2, a simplified version of the adaptor is shown, with the proximal tubular part in a non-

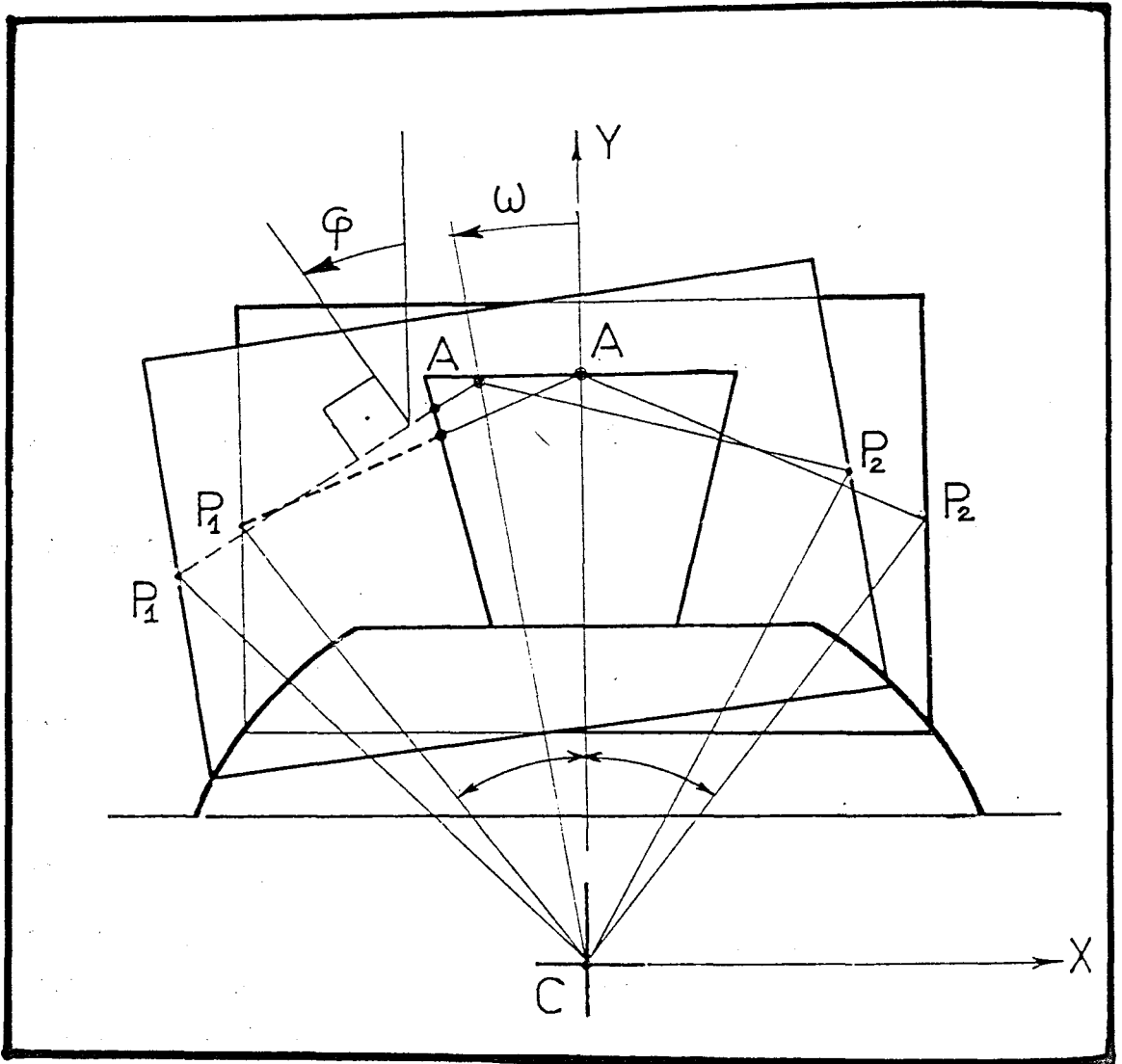


Fig 7.2 Simplified drawing of an Otto Bock adaptor for the ankle joint.

tilted (ie neutral) and a tilted orientation. The axis of the responsible screw is shown with broken line. The points of interest are :

- the centre of the spherical surface C ,
- the imaginary points P_1 and P_2 corresponding to the intersection of the two axes of the screws with the internal surface of the rim ,
- the point A where the two axes of the screws intersect each other .

The two triangles ACP_1 and ACP_2 fulfilled the following :

$$\begin{aligned}\hat{ACP}_1 &= \hat{ACP}_2 = 28^\circ \\ CP_1 &= CP_2 = CA = 30 \text{ mm} \\ P_1P_2 &= 28 \text{ mm}\end{aligned}\tag{7.1}$$

at any orientation of the top component, since they both belong to this component. Therefore the coordinates of point P_1 with respect to the frame shown can be expressed as :

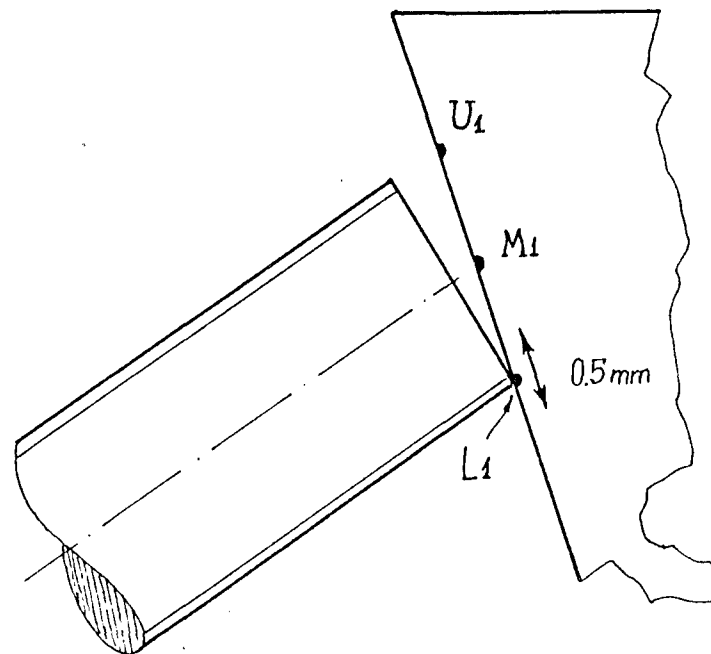
$$\begin{aligned}X_{P1} &= -30 \sin(28^\circ + \omega) \text{ mm} \quad \text{and} \\ Y_{P1} &= 30 \cos(28^\circ + \omega) \text{ mm}\end{aligned}\tag{7.2}$$

Any angle ϕ relates to ω as follows :

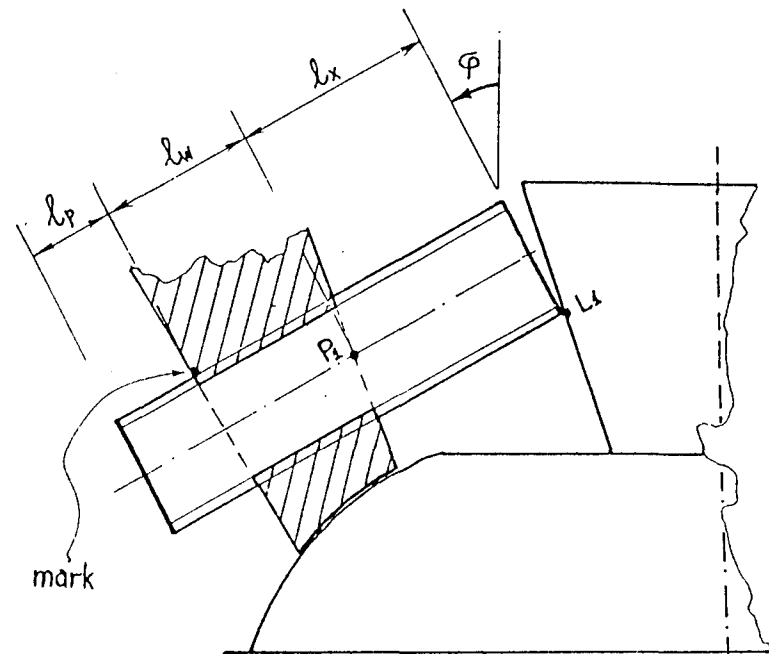
$$\phi = 14^\circ + \omega\tag{7.3}$$

Also the two screws did not contact the pyramid with the same point throughout the range of movement. The responsible screw, for a particular tilt ω , contacted it with its lower edge, whereas the other screw with its upper edge (see fig 7.1). The ends of both screws were flat against the pyramid only at the $\omega = 0^\circ$ neutral position.

Therefore, the coordinates of three more points (for the responsible screw) were measured, with respect to the same frame of reference . These points were the lower, upper and middle contact points of the screw



(a)



(b)

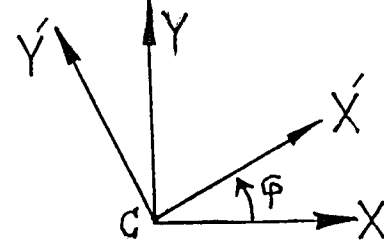


Fig 7.3 Detail of an adaptor adjustment screw.

edge with the pyramid side. This is clearly depicted in figure 7.3a, for the screw which is responsible for the tilt ω . The coordinates were measured to be :

$$X_{L1} = -6.9 \text{ mm and } Y_{L1} = 25.7 \text{ mm} \quad (7.4a)$$

$$X_{U1} = -8.1 \text{ mm and } Y_{U1} = 30.5 \text{ mm} \quad (7.4b)$$

$$X_{M1} = -7.5 \text{ mm and } Y_{M1} = 28.1 \text{ mm} \quad (7.4c)$$

and the assumption was made that they were independent of the angle ω . In fact this was proved (graphically) to be true : these points were moving along the side of the pyramid for various angles ω within a range of $\pm 0.25 \text{ mm}$.

Having determined all the above quantities, the following consideration was made :

Any angle ω could be related to the length l_x (see figure 7.3b) and the latter could be derived by measuring the protrusion length l_p , knowing of course the total length l_t of the screw under study, as well as the length l_w in the wall of the rim (constant). The relationship sought could be established simply by considering the coordinates of points P_1 and L_1 in a suitable frame. This frame, as shown, was considered to be a frame rotated from the initial one by $\phi = 14^\circ + \omega$; offering therefore an X' -axis parallel to the axis of the thread.

Equations (7.2) and (7.4a) could thus be used to derive the coordinates of points P_1 and L_1 in the new frame, as follows :

$$\begin{aligned} X'_{P1} &= -30 \sin(14^\circ) = -7.26 \text{ mm} \\ Y'_{P1} &= 30 \cos(14^\circ) = 29.11 \text{ mm} \end{aligned} \quad \text{and}$$

$$\begin{aligned} X'_{L1} &= - (6.9 \cos \phi) + (25.7 \sin \phi) \text{ mm} \\ Y'_{L1} &= (6.9 \sin \phi) + (25.7 \cos \phi) \text{ mm} \end{aligned} \quad (7.5)$$

Thus :

$$\begin{aligned} l_x &= l_t - l_p - l_w \quad \text{and} \\ l_x &= - (6.9 \cos \phi) + (25.7 \sin \phi) + 7.26 \end{aligned} \quad (7.6)$$

Equation (7.6) had to be solved for ω and the following substitutions were used :

$$\begin{aligned} (\text{with : } \phi &= 14^\circ + \omega) \\ \tan (\phi/2) &= t \\ \cos \phi &= (1 - t^2) / (1 + t^2) \\ \sin \phi &= 2 t / (1 + t^2) \end{aligned} \quad (7.7)$$

With the above substitutions , equation (7.6) becomes a second degree equation which can then be solved for t . The angle ω was then derived as follows :

$$\omega = 2 \cdot \tan^{-1} \left[\frac{-b - \sqrt{b^2 - 4 \cdot a \cdot c}}{2 \cdot a} \right] - 14^\circ \quad (7.8)$$

$$\begin{aligned} \text{where : } a &= l_x - 7.26 - 6.9 = l_x - 14.16 \\ b &= - 2 \cdot 25.7 = - 51.40 \\ c &= l_x - 7.26 + 6.9 = l_x - 0.36 \end{aligned} \quad (7.9)$$

Equation 7.8 was the relationship desired in order to calculate the tilts imposed, knowing the length l_x of the screw.

The length l_x was derived indirectly by using a graduated specially prepared ruler to measure the protrusion length l_p (fig 7.3b). Knowing also that l_w is equal to 6.25 mm and that the screw total length l_t , after machining, is equal to 28.75 mm, the following equation was derived :

$$\begin{aligned} l_x &= l_t - l_w - l_p = 28.75 - 6.25 - l_p \\ l_x &= 22.50 - l_p \end{aligned} \quad (7.10)$$

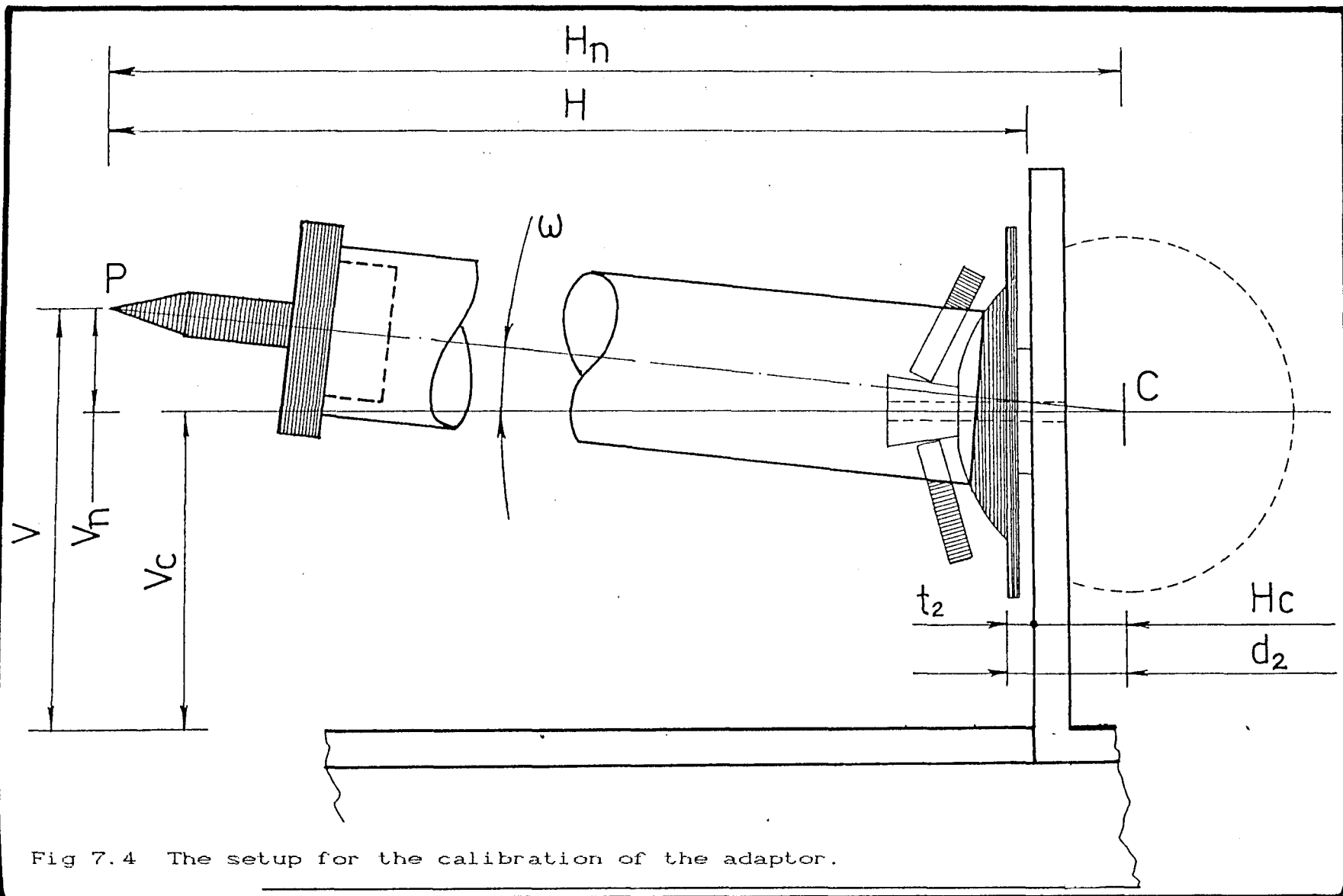


Fig 7.4 The setup for the calibration of the adaptor.

Equations (7.8) to (7.10) were then applied to the adaptor several times, for various adjustments l_x .

The values of ω obtained by equation 7.8 were meant to be compared to the actual tilts imposed by the adjustments made on the adaptor.

For the measurement of the actual tilts the following method was developed.

7.4.2 The Experimental Set-up and Method

The adaptor under study was mounted on the alignment rig as shown in figure 7.4, by means of a foot bolt. The AP plane of the adaptor was vertical to the surface of the rig, with the posterior side facing upwards.

Because of the spherical shape of the distal part of the adaptor, any angular adjustment was considered as a rotation taking place about the centre C of the spherical surface. The proximal end of the tube was provided with a specially machined pointer having its top point P lying on the axis of the tube. By means of the adaptor screws it was possible to change the angular position of point P with respect to point C within the rig frame shown. By using the measuring equipment associated with the alignment rig, it was also possible to record this position in terms of vertical and horizontal distances from point C.

The position of point C was the first to be identified. This was done by simply applying geometrical formulae to the spherical part of the ankle adaptor, taking into account the dimensions of the adaptor (see fig 7.5) :

$$\begin{aligned}
 d_2 &= \frac{(l_2^2 - l_1^2) / 4 - h^2}{2h} \\
 d_1 &= d_2 + h \\
 R &= \sqrt{(l_2/2)^2 + d_2^2}
 \end{aligned}
 \tag{7.11}$$

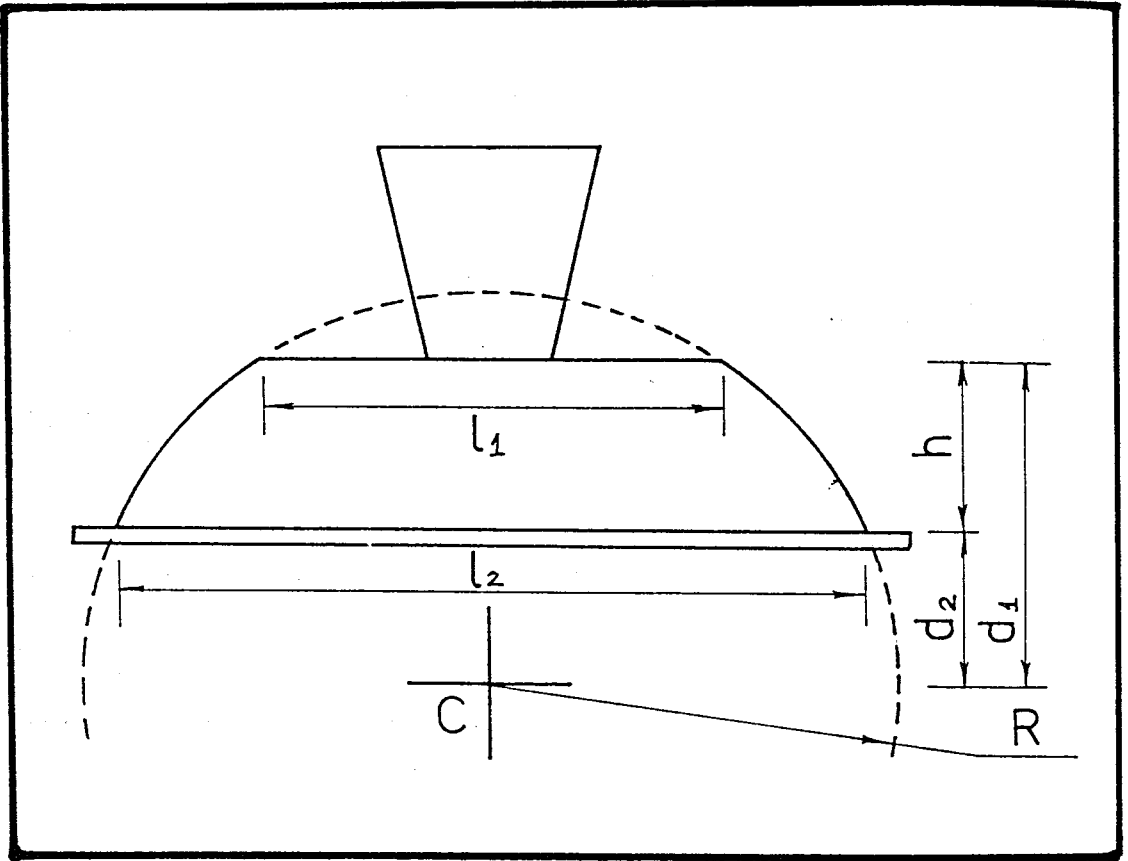


Fig 7.5 Geometry of the distal part of an ankle adaptor.

where : $l_1 = 23.50 \text{ mm}$, $l_2 = 39.50 \text{ mm}$, $h = 7.10 \text{ mm}$
and thus, $d_2 = 14.20 \text{ mm}$, $d_1 = 21.30 \text{ mm}$, $R = 24.30 \text{ mm}$
(7.12)

It was therefore possible to establish the position of point C within the rig frame. It was then possible to relate any vertical and horizontal coordinates of point P to point C and calculate the angular position ω of point P in the frame located at point C :

$$\omega = \tan^{-1} \left(\frac{\text{net Vertical displacement}}{\text{net Horizontal displacement}} \right) = \frac{V_n}{H_n} \quad (7.13)$$

where : $V_n = V - V_c$ and $H_n = H - H_c$

Whereas V_c is the height of the foot bolt axis from the rig surface, H_c has to be calculated (see fig 7.4) as :

$$H_c = d_2 - t_2 \quad (7.14)$$

A series of measurements was carried out recording V and H as well as the corresponding protrusion length l_p , mentioned above .

Having carried out these measurements the experimental values of the angle ω could be compared to the values derived by equation (7.8) .

7.4.3 Results

The values of ω resulting from equation (7.8) (ie. the theoretical values) were plotted against the corresponding screw length l_x . The resulting graph (fig 7.6) showed a very good linear relationship between ω and l_x .

The linear regression of the data performed by the Minitab software available in the main frame VAX resulted to the following equation :

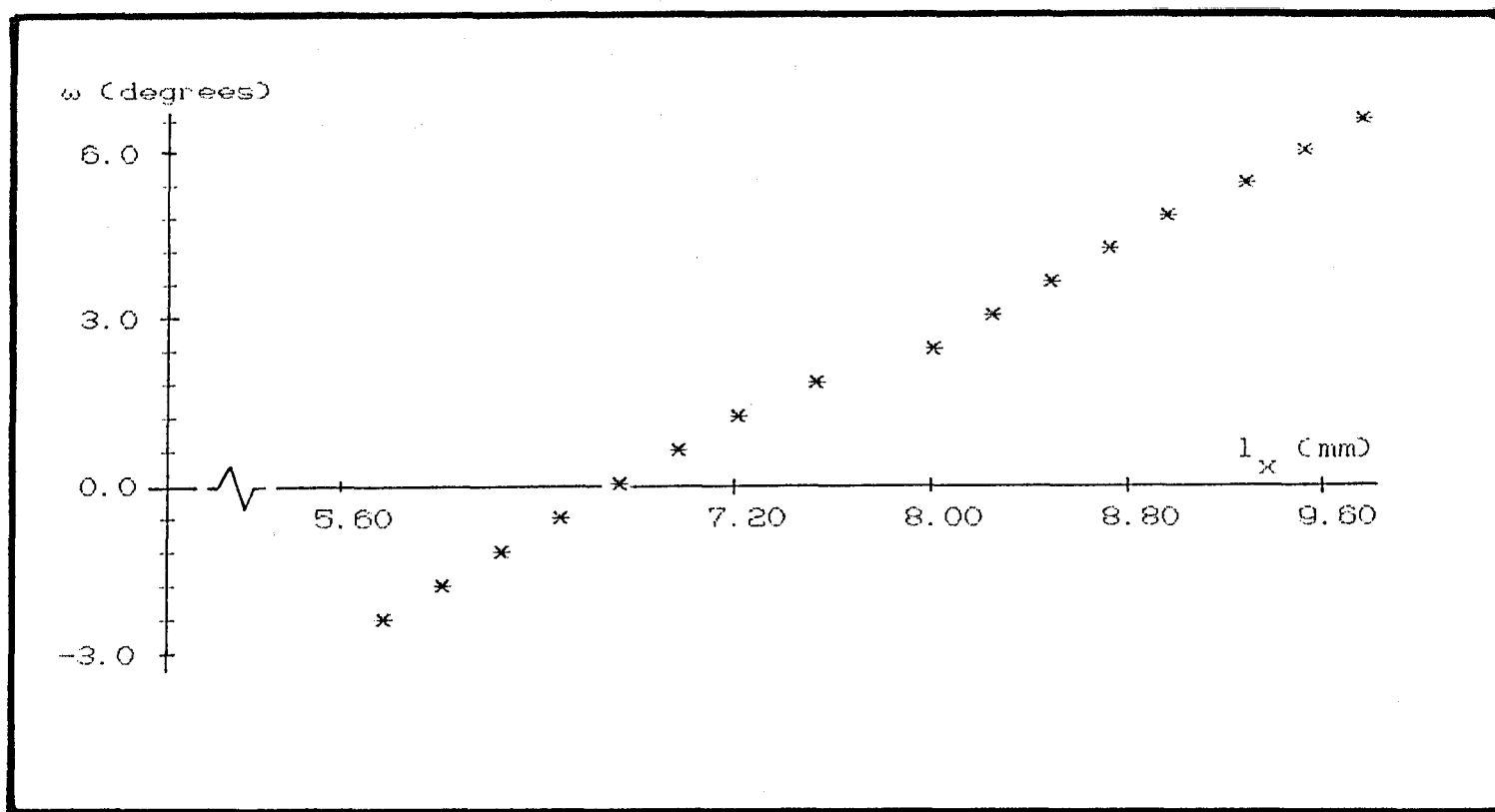


Fig 7.6 Graph for the results of the analytical model

$$\omega = -14.6159 + 2.15598 l_x \quad (7.15)$$

with r-square = 99.9 %

Thus, the analytical model expressed by equation (7.8) could then be replaced by the regression model (7.15) .

The comparison of the theoretical values of ω to the experimental values of ω did not give a positive result. The theoretical values derived by either of the equations (7.8) or (7.15) were always found to be less than the experimental ones . The differences were of the order of 1° .

These results were considered not satisfactory at all and this approach was abandoned. The reason for the observed discrepancies was thought to be the fact that this mathematical model, derived theoretically, could not describe properly the actual behaviour of the adaptor. In practical terms, the behaviour of the adaptor might depend on unpredictable factors introduced by the change of the contact point at the side of the pyramid for different angles ω . The assumption which was made, that this point was always the same, might have been wrong. On the other hand the high degree of measurement accuracy that this method initially relied on in association with the fact that all the components are metal castings was considered to be another reason for the discrepancies and for the failure of this approach.

However, the results obtained by this method showed that the relationship between any imposed tilt ω and the corresponding value of a parameter related to the screw length was distinctly linear. This important conclusion was the base for further work.

The linear relationship sought had to be established by more practical means and derived directly from the adaptor's behaviour by directly calibrating the adaptor screws against the tilts. This work is described in the next section.

l (mm)	ω (degrees)	ω (degrees)	ω (degrees)
16.00	0.00000	0.00000	-0.00001
15.75	0.39217	0.41321	0.40638
15.50	0.85157	0.90062	0.86858
15.25	1.40484	1.32090	1.25852
15.00	1.93468	1.75510	1.70249
14.75	2.39450	2.18096	2.19581
14.50	2.94010	2.83434	2.61278
14.25	3.33338	3.29234	3.01168
14.00	3.82550	3.78732	3.66196
13.75	4.44914	4.20663	4.16875
13.50	4.94177	4.73338	4.66456
13.25	5.34383	5.31099	5.20638
13.00	5.72753	5.75573	5.61654
12.75	6.37089	6.09088	6.07171
12.50	6.85128	6.71437	6.59235
12.25	7.20783	7.06927	7.05373
12.00	7.55007	7.40167	7.35690

Table 7.1 Data obtained by the
calibration for the AP plane

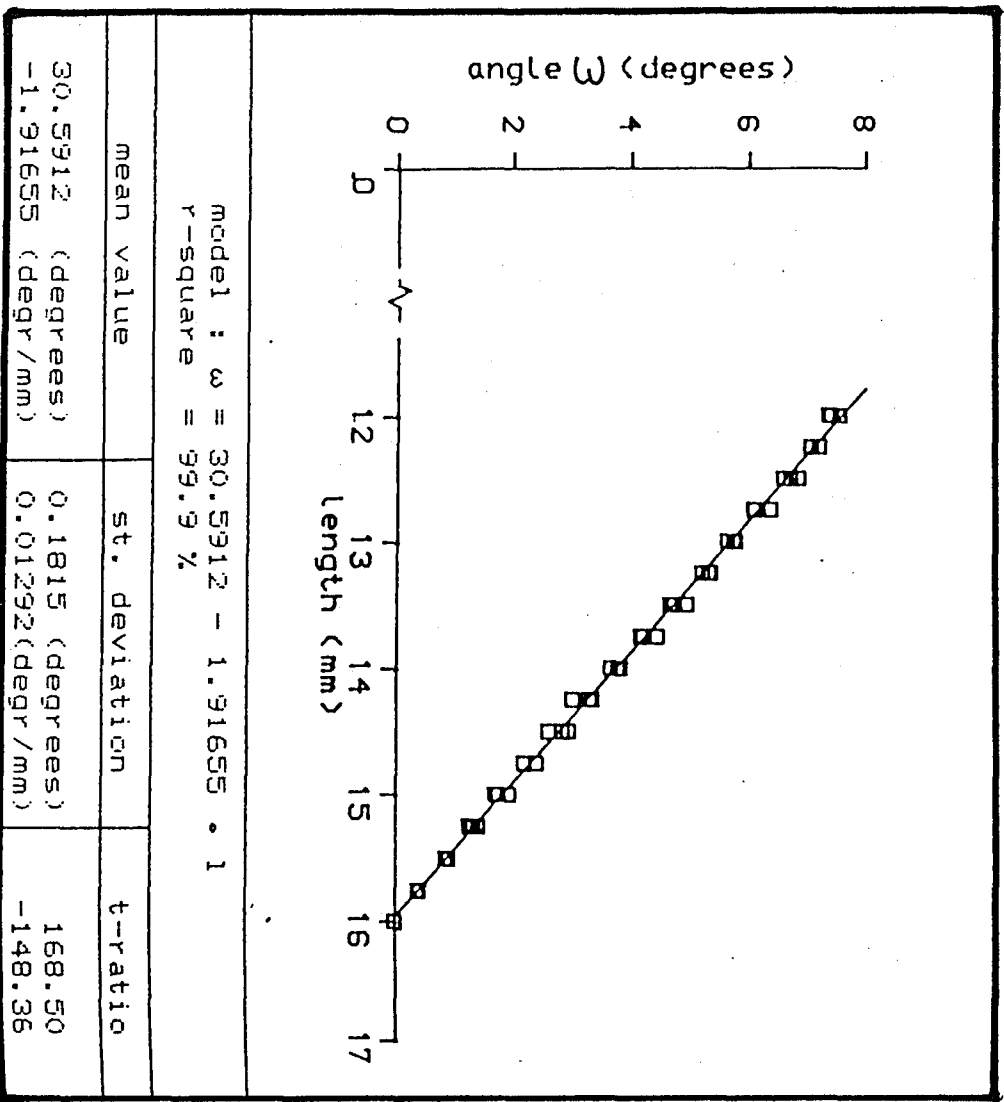


Figure 7.7 Regression results for the AP plane.
(with zero ω (ML) tilt)

7.5 First Attempt to Calibrate an Adaptor

7.5.1 The Experimental Set-up and Method

The same adaptor was considered. The four screws of the adaptor were again replaced by the set of newly machined ones and the relationship sought was this time the one between protrusion length (called l) and angular tilt ω .

The protrusion length, shown in figure 7.3b , was to be measured as before. The posterior screw was considered as being the responsible one for AP changes and the lateral one for ML changes.

The adaptor under study was mounted on the alignment rig , as shown in figure 7.4 . The method for measuring the imposed tilt ω was the same as described above.

Measurements started from a fully horizontal position ($V = V_c$) . Then the angular position of the tube was increased by small steps. Various adjustments were made and the corresponding angular displacements ω were derived. Adjustments were stopped just before the functional limit of the adaptor (in order to avoid end-effects). This procedure was repeated twice.

7.5.2 Results

Having carried out these measurements for the first time, the data were processed and using Minitab software a regression line was fitted in order to derive the expected linear equation.

Indeed, the graph relating l and ω was , as expected an almost straight line . The fitted line satisfied the data by 99.8% .

Table 7.1 shows the results obtained for this first calibration on the AP plane and in figure 7.7 the corresponding calibration graph.

The equation obtained for the adaptor's behaviour was :

$$\omega = 30.5912 - 1.91655 l \quad (7.16)$$

where : l is in (mm) and ω in degrees .

l (mm)	ω (degrees)	ω (degrees)	ω (degrees)
16.25	0.00000	0.00000	0.00000
16.00	0.35756	0.40647	0.33905
15.75	0.79654	0.78516	0.75699
15.50	1.21467	1.13866	1.16847
15.25	1.72331	1.53106	1.61959
15.00	2.24163	2.15912	2.19900
14.75	2.68002	2.68416	2.65963
14.50	3.14448	3.09114	3.01914
14.25	3.81266	3.79178	3.62400
14.00	4.15989	4.13487	4.03422
13.75	4.71519	4.62026	4.55295
13.50	5.23296	5.13467	5.16212
13.25	5.71127	5.66050	5.66051
13.00	6.29590	6.24310	6.19798
12.75	6.67174	6.65176	6.69807
12.50	7.15290	7.15046	7.13168
12.25	7.77908	7.87647	7.68519

Table 7.2 Data obtained by the calibration for the ML plane

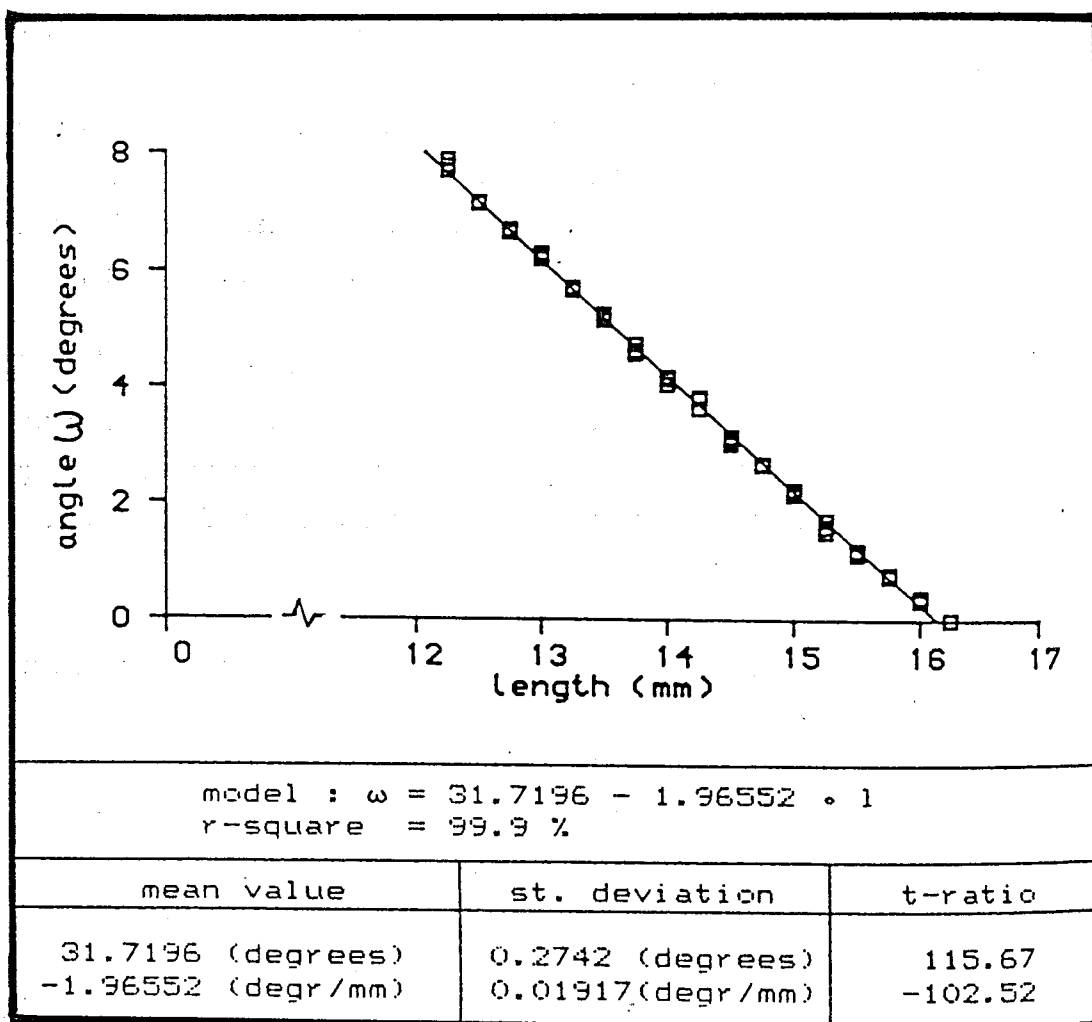


Figure 7.8 Regression results for the ML plane.
(with zero ω (AP) tilt)

Solving the equation (7.16) for l it becomes :

$$l = 15.9616 - 0.5218 \omega \quad (7.17)$$

implying that for zero tilt the length should be $l = 15.9616$ mm . As it was anticipated, this value is actually very close to the value $l = 16.00$ mm measured during the tests.

Further proof of satisfactory prediction ability for the model was sought. Thus, statistical predictions were carried out. These predictions proved that the model could provide predictions of the tilt ω , which were falling in intervals of $\pm 0.12^\circ$, for a level of 95% .

These very satisfactory results enhanced and proved the initial idea about the relationship between the responsible adaptor screw and the tilt , imposed by means of it, on the adjacent component.

If the adaptors of an artificial leg could be simulated by linear equations describing their functional behaviour, then perhaps the simulation of the whole alignment procedure could be obtained.

7.6 Further Considerations on the Adaptors

Having investigated the behaviour of an adaptor and proved that it is possible to predict the angular adjustments imposed within acceptable limits, some more issues were considered.

a) It is necessary to establish whether or not the same regression model can apply to both AP and ML planes of the adaptor.

b) It is also necessary to establish whether or not any interaction exist between AP and ML adjustments imposed on the same adaptor. Such interactions could change the functional behaviour of the adaptor in one plane depending on the adjustment already established in the other.

l index	ω values AP plane (degr)	ω values ML plane (degr)
1	0.0000 0.0000 0.0000	0.0000 0.0000 0.0000
2	0.3922 0.4132 0.4064	0.3576 0.4065 0.3390
3	0.8516 0.9006 0.8686	0.7965 0.7852 0.7570
4	1.4048 1.3209 1.2585	1.2147 1.1387 1.1685
5	1.9347 1.7551 1.7025	1.7233 1.5311 1.6196
6	2.3945 2.1810 2.1958	2.2416 2.1591 2.1990
7	2.9401 2.8343 2.6128	2.6800 2.6842 2.6596
8	3.3334 3.2923 3.0117	3.1445 3.0911 3.0191
9	3.8255 3.7873 3.6620	3.8127 3.7918 3.6240

l index	ω values AP plane (degr)	ω values ML plane (degr)
10	4.4491 4.2066 4.1687	4.1599 4.1349 4.0342
11	4.9418 4.7334 4.6646	4.7152 4.6203 4.5529
12	5.3438 5.3110 5.2064	5.2330 5.1347 5.1621
13	5.7275 5.7557 5.6165	5.7113 5.6605 5.6605
14	6.3709 6.0909 6.0717	6.2959 6.2431 6.1980
15	6.8513 6.7144 6.5924	6.6717 6.6518 6.6981
16	7.2078 7.0693 7.0537	7.1529 7.1505 7.1317
17	7.5501 7.4017 7.3569	7.7791 7.8765 7.6852

Source	d. f	S. squares	Mean square	f -ratio	f (95%) (table)
length 1	16	576.7803	36.0488	4506.10	1.7945
plane 1	1	0.0602	0.0602	7.525	3.9820
inter. 16	16	0.3704	0.0232	2.900	1.7945
error 68	68	0.5469	0.0080		
TOTAL 101	101	577.7578			

Table 7.3 The analysis of variance for the ω values, for the two different planes AP and ML.

Further measurements were first carried out on the same initial adaptor and on the AP plane again, resulting in very satisfactory repeatability, and proving that once a regression is derived carefully for one adaptor it can accurately predict its behaviour in the corresponding plane. This concerns of course the slope of the regression model since the intercept depends on the overall screw length which could be different in various applications. Nevertheless, the derivation of a tilt ω is a subtraction between initial and final values, in which the intercept is eliminated.

More measurements were carried out using the same setup and the same adaptor, but this time, investigating the behaviour of the adaptor in the ML plane. The results obtained exhibited again the same quality of linearity ie. 99.9 % of the variation was explained by the regression model. These results are exhibited in table 7.2 and figure 7.8 . The model was :

$$\omega = 31.7196 - 1.96552 l \quad (7.18)$$

However , issue (a) expressed above was still unresolved and therefore the necessary step was considered to be the analysis of the variance performed on the data obtained in the two planes (table 7.3).

The length l is expressed by indices corresponding to its seventeen different levels, common for the two planes. The data of the ML plane have been shifted along the dimension of the length l , in order to be comparable with the corresponding data of the AP plane. This did not affect the result at all since the quantity under study is the slope of the fitted lines.

As can be seen in the results the change in plane led to a regression model which was significantly different from the initial one ($f = 7.525 > 3.982$) and therefore there is strong indication that the behaviour of the adaptor in the two planes should be expected

l (mm)	ω (degrees)	ω (degrees)	ω (degrees)
16.25	0.00000	0.00000	0.00000
16.00	0.43588	0.22622	0.54799
15.75	0.73507	0.69040	0.81664
15.50	1.15986	1.07304	1.13154
15.25	1.64495	1.67253	1.62192
15.00	2.03279	2.16564	2.18151
14.75	2.61076	2.53150	2.63875
14.50	3.22279	3.09466	3.02256
14.25	3.73012	3.67727	3.77599
14.00	4.08476	4.10156	4.18410
13.75	4.68658	4.61113	4.65427
13.50	5.27391	5.20181	5.26607

Table 7.4 Data obtained by the calibration for the ML plane with pre-established AP tilt

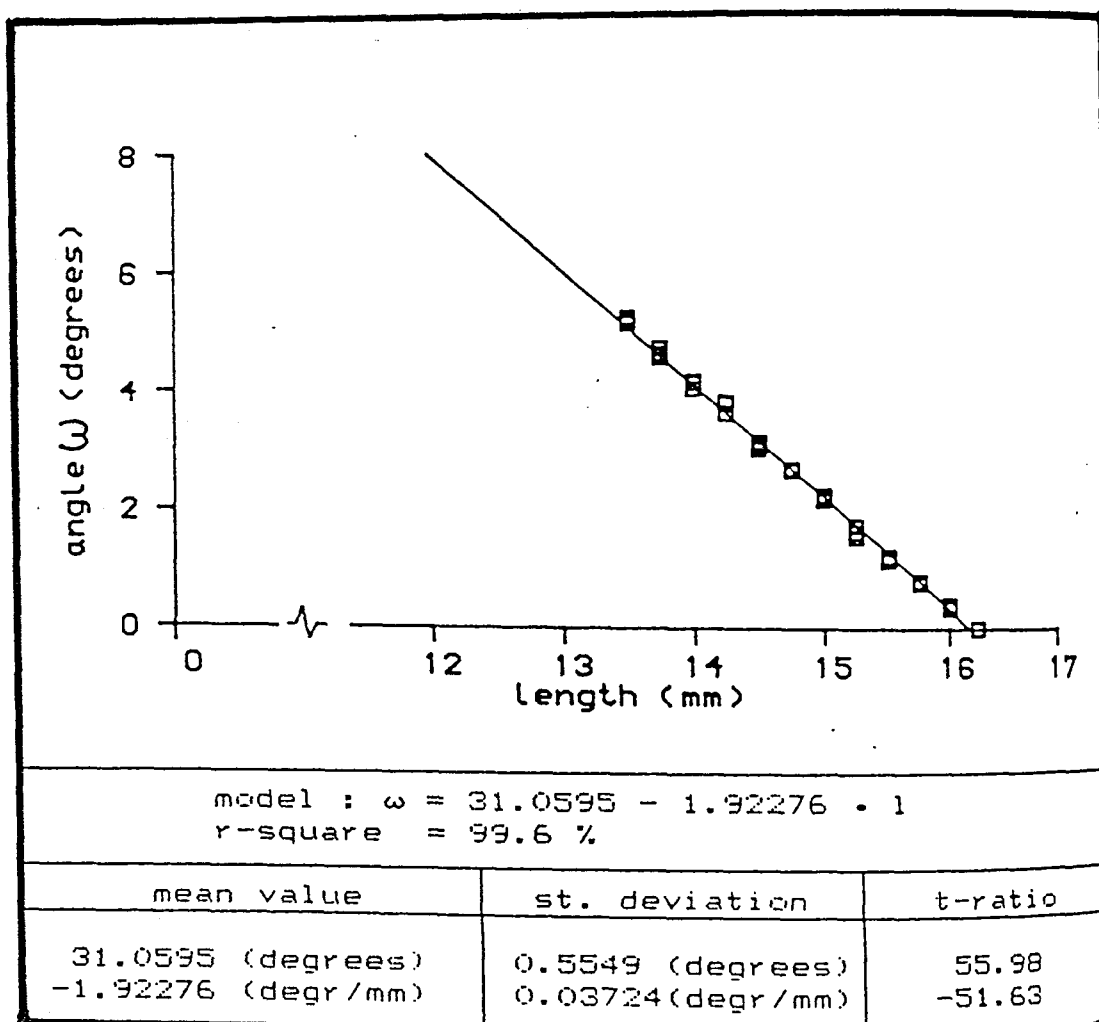


Figure 7.9 Regression results for the ML plane, with non-zero ω (AP) tilt.

to be different (also see the f - values for the interaction).

More generally that was the case for various adaptors tested. Every one of those adaptors exhibited a linearity in its behaviour described by a different slope, implying therefore, that the adaptors had to be treated individually. The reason was thought to be the fact that the cast adaptors had dimensional discrepancies from the nominal values , serious enough to jeopardise any similarity in terms of mathematical modelling.

The decision was taken therefore that all the adaptors should be calibrated individually and furthermore each functional plane (AP or ML) should be calibrated individually.

Since, during prosthetic practice, an alignment adjustment in the AP plane of an adaptor can be followed by an ML one of the same adaptor, or vice versa, it was necessary to investigate whether any interaction existed between the functional behaviour of the adaptor in one plane (see issue b above) and the adjustments made on the other. All the experimental work so far on planes AP and ML was done with no tilt existing on the other plane.

Since results for the plane ML had already been obtained (table 7.2) for zero tilt at the AP plane, for the interaction to be investigated another set of results was required, this time, with non-zero tilt at the AP plane. This set of results was obtained on the ML plane for a non-zero tilt at the AP plane equal to 4.7° . These results are shown in table 7.4 and figure 7.9 . As can be seen the range of function in this case is limited because of the functional constraint imposed on the adaptor by the already established AP tilt (ie. the arc of the spherical surface, over which the proximal component can move, is now shorter).

For issue (b) to be answered , the same analysis

l index	ω (ML) $\omega(\text{AP})=0$ (degr)	ω (ML) $\omega(\text{AP})\neq 0$ (degr)
1	0.0000	0.0000
	0.0000	0.0000
	0.0000	0.0000
2	0.3576	0.4359
	0.4065	0.2262
	0.3390	0.5480
3	0.7965	0.7351
	0.7852	0.6904
	0.7570	0.8166
4	1.2147	1.1599
	1.1387	1.0730
	1.1685	1.1315
5	1.7233	1.6450
	1.5311	1.6725
	1.6196	1.6219
6	2.2416	2.0328
	2.1591	2.1656
	2.1990	2.1815

l index	ω (ML) $\omega(\text{AP})=0$ (degr)	ω (ML) $\omega(\text{AP})\neq 0$ (degr)
7	2.6800	2.6108
	2.6842	2.5315
	2.6596	2.6388
8	3.1445	3.2228
	3.0911	3.0947
	3.0191	3.0226
9	3.8127	3.7301
	3.7918	3.6773
	3.6240	3.7760
10	4.1599	4.0848
	4.1349	4.1016
	4.0342	4.1841
11	4.7152	4.6866
	4.6203	4.6111
	4.5529	4.6543
12	5.2330	5.2739
	5.1347	5.2018
	5.1621	5.2661

Source	d. f	S. squares	Mean square	f -ratio	f (95%) (table)
length 1	11	197.1497	17.9227	4168.1	1.9946
ω (AP)	1	0.0005	0.0005	0.1163	4.0426
inter.	11	0.0357	0.0032	0.7442	1.9946
error	48	0.2084	0.0043		
TOTAL	71	197.3943			

Table 7.5 The analysis of variance for the values of ω (ML), for zero and non-zero ω (AP).

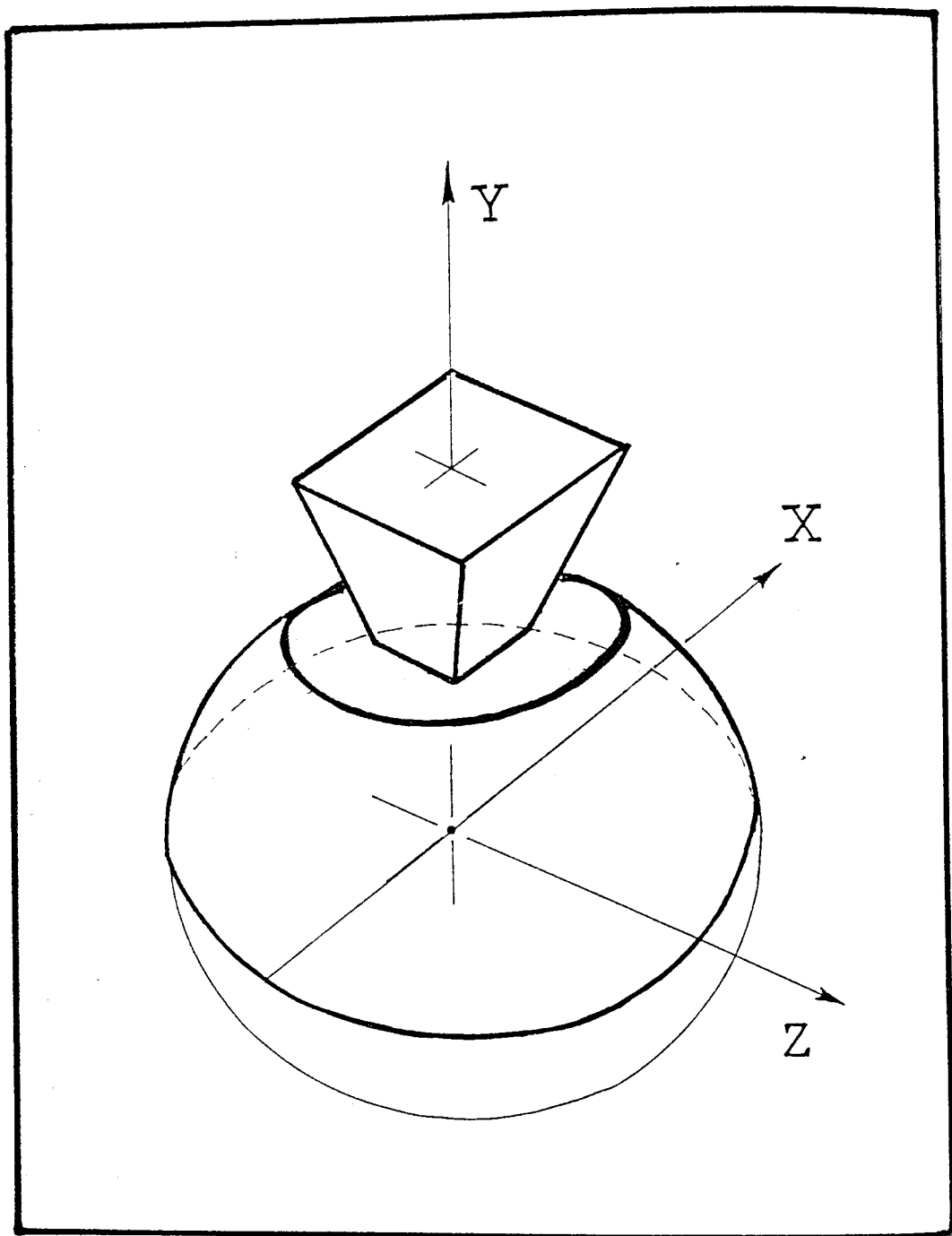


Fig 7.10 Frame configuration for the adaptors.

as before was carried out : the data of tables 7.2 and 7.4 were subjected to an analysis of their variance and as shown in table 7.5 the differences were found to be not significant ($f = 0.1163 < 4.0426$) and therefore the regression model derived for the ML plane with zero AP tilt could be considered to represent the behaviour in this plane for all cases (also see the f-values for the interaction).

The reason for this positive result was thought to be the narrow functional range provided by the adaptor (approximately $\pm 8^{\circ}$) .

Therefore, the behaviour of the adaptor in the two planes was considered independent and the two linear models for AP and ML could be used, as derived from the tests, regardless of the order of the adjustments and the value of any already established tilt.

7.7 Mathematical Modelling of a Prosthesis

Provided that any angular adjustment at any adaptor of an Otto Bock modular prosthesis can be calculated by a linear model the next point to be considered was the simulation of the adaptors' mechanical behaviour by rotations about the axes of 3-D frames allocated at the centres of these adaptors.

Such frames were considered at all adaptors as following (fig 7.10) :

the origin of the frame was taken at the centre of the spherical surface of the adaptor, the Y-axis being positive upwards (ie. towards the proximal direction), the X-axis positive forward and Z-axis positive from left to right; these two later axes being parallel to the corresponding sides of the pyramid. In the case where the adaptor is positioned as shown , positive Y-axis passes through the pyramid base centre , whereas in the case where the adaptor is upside down (eg for the knee unit) it is the negative Y-axis which passes through the pyramid base centre.

Thus, an AP angular adjustment could be considered

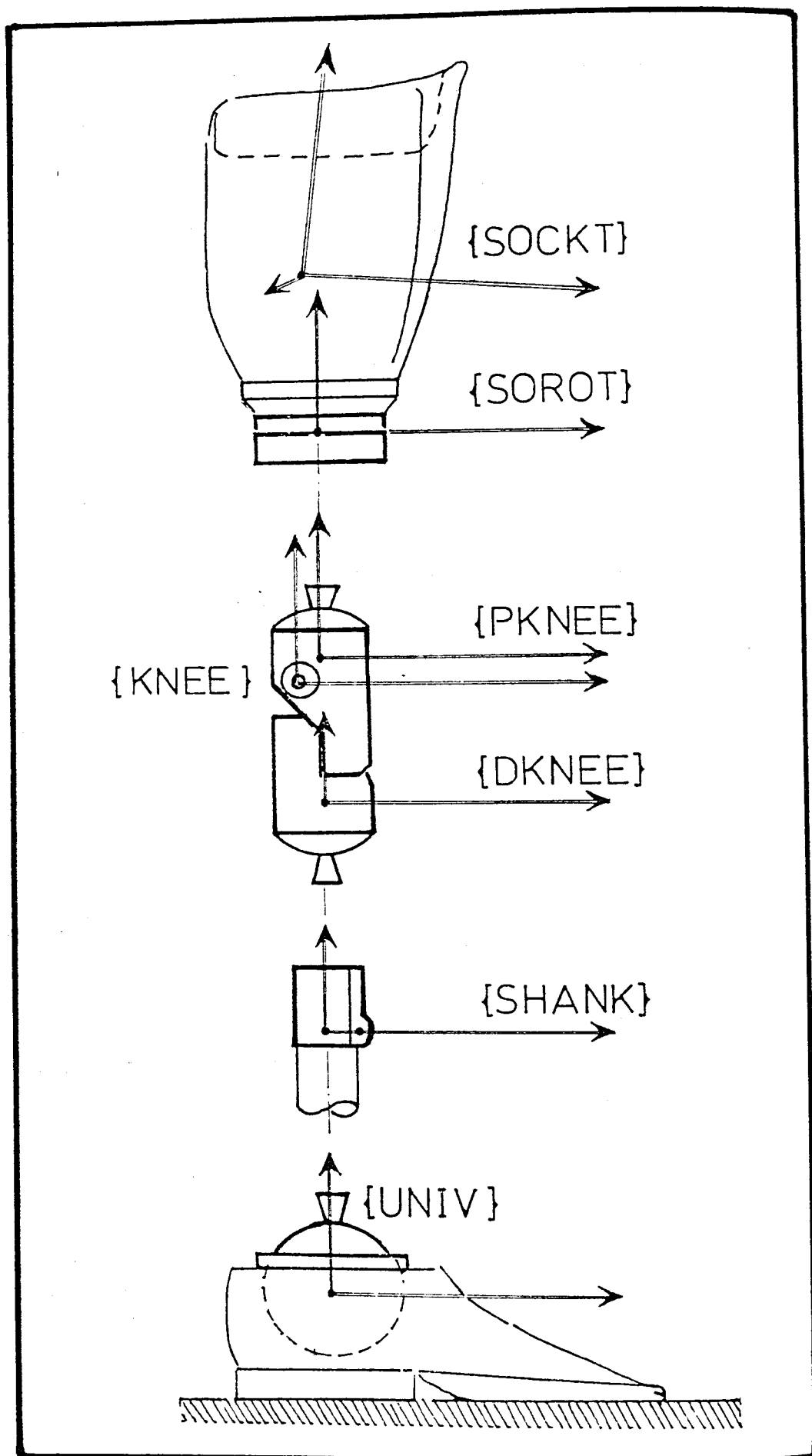


Fig 7.11 Frame configuration for an AK prosthesis.

as a rotation about the Z-axis , and an ML adjustment could be considered as a rotation about the X-axis.

The same sort of frames (although without pyramid considerations) were also adopted for the rotatable adaptors, those providing the possibility for transverse angular adjustments. In this case the angular adjustments could be considered as rotations about the Y-axis.

Thus, all prostheses could be represented by a set of XYZ frames positioned in the space according to the prostheses' general geometry.

In this study, AK prostheses only were considered, since the BK prostheses are only a partial application of the same principles. Hip disarticulation prostheses were not considered either, because the same principles could be used for as many further joints as needed. AK prostheses seemed a good compromise from this point of view.

In figure 7.11 the system of frames used for an AK prosthesis is shown. It is a lateral view of a right side prosthesis and, as can be seen, besides the adaptors already studied, frames have also been allocated to the rotatable adaptors of the shank and the socket. A frame is also provided to the socket itself. Whereas all frames are shown in a neutral orientation (no tilts and rotations) , the socket frame has a general orientation depending on the in-built flexion-extension and adduction-abduction, but with the corresponding adaptor neutrally adjusted.

This overall neutral position, depicted in figure 7.11, will from now onwards be referred to as the Initial Reference Position (IRP) . In general in an IRP the distal knee frame may have an already built-in flexion, called $d\omega$, discussed later. The frames shown are the :

- socket frame (SOCKT);
- socket rotatable adaptor frame (SOROT);

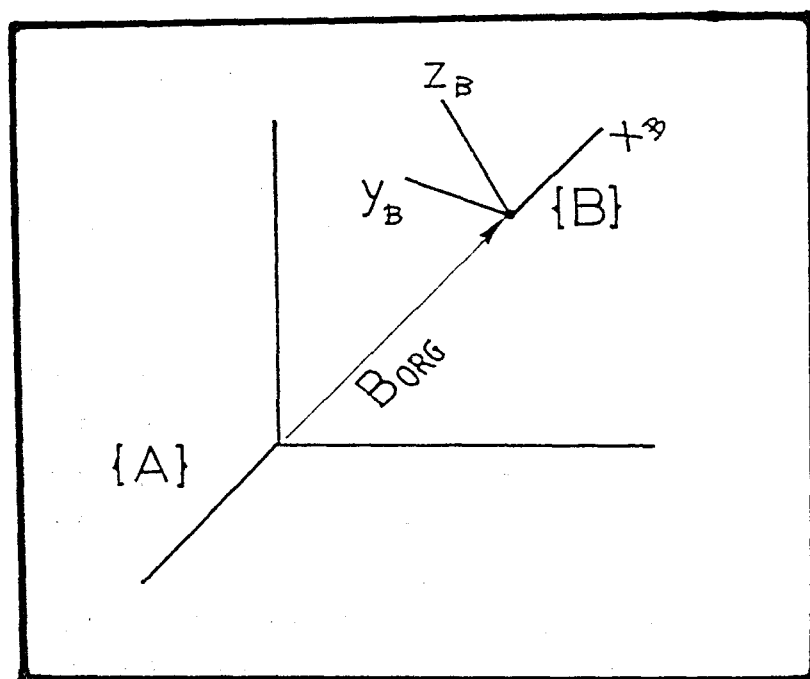


Fig 7.12 Mathematical description of a frame.

- proximal knee adaptor frame (PKNEE);
- knee frame (KNEE);
- distal knee adaptor frame (DKNEE);
- shank rotatable adaptor frame (SHANK);
- foot frame (FOOT) and finally
- frame of the universal reference (UNIV).

The shank frame (SHANK) can be considered shifted along the axis of the shank down to the reference frame (UNIV), and thus sharing the same origin with the latter one.

Starting from this position the origin and orientation of all the frames could be described, with respect to the distal most one (reference UNIV), for any set of adjustments (angles ω_1 to ω_8 shown), with any sequence, following the mathematical analysis discussed in the next section.

The mathematical background needed for the modelling is discussed in appendix V. Since all alignment adjustments can be seen as rotations about a given axis, the paragraph of this appendix describes this procedure.

The description of a frame {B}, with respect to another frame {A} ,is given by a matrix [T], which is a (4 x 4) matrix of the form (fig 7.12) :

$$[T] = \left[\begin{array}{ccc|c} (x_B)x & (y_B)x & (z_B)x & (B_{ORG})x \\ (x_B)y & (y_B)y & (z_B)y & (B_{ORG})y \\ (x_B)z & (y_B)z & (z_B)z & (B_{ORG})z \\ \hline 0 & 0 & 0 & 1 \end{array} \right] \quad (7.19)$$

where: $(x_B)x, y, z$ are the projections of the unit vector $\vec{x_B}$ of frame {B} on the axes x, y, z of frame {A},
 $(y_B)x, y, z$ are the projections of the unit vector $\vec{y_B}$ of frame {B} on the axes x, y, z of frame {A},
 $(z_B)x, y, z$ are the projections of the unit vector $\vec{z_B}$ of frame {B} on the axes x, y, z of frame {A},
 $(B_{ORG})x, y, z$ are the coordinates of the origin of frame {B} on the axes x, y, z of frame {A}.

The last row $(0, 0, 0, 1)$ is added for reasons related to the homogeneity needed during the operations.

The first three columns of the top left 3×3 submatrix can also be considered as the direction cosines of the unit vectors $\vec{x_B}, \vec{y_B}, \vec{z_B}$, with respect to frame {A}.

Using the formulae V.15 to V.19 from appendix V, all the matrices describing the adjustments can be derived. The information needed to determine each one of these matrices comprises the location and orientation of the axis of rotation as well as the amount and direction of the angular displacement.

For this latter consideration and referring to figure 7.11 the following can be deduced :

a) For angular adjustments ω_1 and ω_2 the rotation axes are the Z and X axes of frame {UNIV} respectively and the angles are determined by the calibration models of the corresponding adaptor screws.

b) For angular adjustments ω_3 and ω_4 the rotation axes are the Z and X axes of frame {DKNEE} respectively. At the moment of angular adjustment ω_3 or ω_4 , the frame {DKNEE} can be found in any general location and orientation as a result of previous alignment changes and therefore the frame mentioned here is meant to be the c u r r e n t {DKNEE} frame and not of course the

initial one. In this case again, the angles are determined by the calibration models of the corresponding adaptor screws.

c) For angular adjustments ω_5 and ω_6 the rotation axes are the Z and X axes of the c u r r e n t {PKNEE} frame and the angles are determined again by the calibration models of the corresponding adaptor screws.

d) For angular adjustment ω_7 the rotation axis is the Y-axis of the c u r r e n t {SHANK} frame, since this frame could have also been subjected to previous angular changes and the angle can be determined simply by measuring on a self-drawn protractor stuck on the shank distal to the rotatable adaptor.

e) For angular adjustment ω_8 the rotation axis is the Y-axis of the c u r r e n t {SOROT} frame, since this frame could have also been subjected to previous angular changes and the angle can be determined simply by inspecting the in-built Otto Bock protractor of the socket rotatable adaptor.

Therefore, when a particular alignment adjustment is performed, the matrix describing this adjustment can be derived using the c u r r e n t geometry and can be used to determine the new frames resulting from it. It is obvious that not all frames are affected by all possible adjustments. The changes ω_1 and ω_2 affect all frames proximal to the ankle. The changes ω_3 and ω_4 affect all the frames proximal to the {DKNEE} frame, itself i n c l u d e d . The changes ω_5 and ω_6 affect all the frames proximal to the {PKNEE} frame (the latter not included). The change ω_7 affects all the frames proximal to the {SHANK} frame (the latter not included) and change ω_8 affects only the socket frame {SOCKET}. The frame of universal reference {UNIV} is not affected by any angular adjustment .

Once all frames are determined by the calculation of their transforms, for the final or any intermediate alignment configuration, the alignment parameters can be quantified.

If the knee and socket frames {KNEE} and {SOCKET} are described with respect to the universal reference by (4x4) matrices called for simplicity [K] and [S] , the alignment parameters of the prosthesis are (for the definitions see the figures in chapter 2) :

$$\begin{aligned}
 \text{Knee AP Shift} &= \text{KAPS} = K(1,4) \\
 \text{Knee ML Shift} &= \text{KMLS} = (+1) \cdot K(3,4) \\
 \text{Knee Height} &= \text{KH} = K(2,4) - (H_C + t_1) \\
 \text{Knee ML Tilt} &= \text{KMLT} = (+1) \cdot \arctan \left(\frac{-K(2,3)}{K(3,3)} \right) \\
 \text{Knee Rotation} &= \text{KR} = (+1) \cdot \arctan \left(\frac{K(1,3)}{K(3,3)} \right) \\
 \text{Socket AP Shift} &= \text{SAPS} = S(1,4) \\
 \text{Socket ML Shift} &= \text{SMLS} = (+1) \cdot S(3,4) \\
 \\
 \text{Socket Height} &= \text{SH} = S(2,4) - (H_C + t_1) \\
 \text{Socket AP Tilt} &= \text{SAPT} = \arctan \left(\frac{-S(1,2)}{S(2,2)} \right) \\
 \text{Socket ML Tilt} &= \text{SMLT} = (+1) \cdot \arctan \left(\frac{-S(3,2)}{S(2,2)} \right) \\
 \text{Socket Rotation} &= \text{SR} = \\
 &= (+1) \cdot \left[\arctan \left(\frac{-S(1,3)}{S(3,3)} \right) - \arctan \left(\frac{-K(1,3)}{K(3,3)} \right) \right]
 \end{aligned} \tag{7.20}$$

The quantity $(H_C + t_1)$ corrects the heights of the frame origins so that they refer to the foot frame which is actually the reference for the alignment parameters. Factor (+1) relates to the fact that the presented prosthesis is a right side one. Its meaning will be explained in the next chapter.

The mathematical modelling of the prosthesis finds eventually its implementation in a program able to follow and simulate any alignment session. This program is presented in the discussion covered in section 8.5 of the next chapter.

However, in order to take advantage of the

model developed , it is necessary to determine the prosthesis' general geometry as well as the calibration models for its adaptors. This discussion is presented in the next chapter.

7.8 Discussion

The main objective of the work presented in this chapter was to establish a relationship between the tilt imposed on an Otto Bock adaptor and a parameter related to the set screw.

When an analytical method was initially used to derive this relationship, the obtained results were not considered satisfactory. However, calibration of an adaptor provided very reasonable results.

It was shown that both approaches resulted eventually in a linear model; the only difference being that the model derived by calibration was much better in terms of prediction ability.

Despite the apparent algebraic differences between the two models, one can appreciate that they are closely comparable. Considering equation 7.16 :

$$\omega = 30.5912 - 1.91655 l$$

and the fact that $l = l_p = 22.50 - l_x$ (from eq 7.10) it can be derived that :

$$\omega = -12.5312 + 1.91655 l_x \quad (7.21)$$

Equation (7.21) is comparable with equation (7.15) derived from the theoretical results .

The above considerations are a further proof that there is a linear relationship as the one sought and is a functional characteristic of the Otto Bock adaptors.

The adopted model, however, must be the one derived by the calibration of the adaptors for the reasons explained in section 7.4

The developed model has a very high ability for

predictions, but there is one aspect of the problem that should be discussed further.

During the tests of the adaptors it was noted that the tubular rim of the proximal component was relatively flexible, thus introducing the following complication :

if the effort of tightening the set screws was not maintained relatively uniform throughout the tests, then the changing shape of the rim surface would jeopardize the measurements of the screw length, for which it is the reference. Furthermore, if the effort applied was not relatively the same during the calibration of the adaptors and the actual use , then the equation derived from the calibration might not reflect the behaviour of the adaptor during other tests, due to the different screw readings.

In order to maintain this effect as uniform as possible throughout the tests, an effort was made to tighten all set screws using the same effort. Ideally this should have been done by setting the screws at a specific torque using an appropriate torque wrench * .

The successful calibration of the adaptors was the first step in the modelling of an Otto Bock modular prosthesis. The next step was the allocation of 3-D frames for each adaptor as well as for the knee and socket. The use of 3-D transforms allows the simulation of the alignment procedure.

The simulation method and the development of the corresponding program are the subject of the next chapter.

7.9 Conclusions

From the experimental work and the statistical analysis presented in this chapter the following conclusions can be drawn :

* The torque values recommended by Otto Bock for this purpose are between 14 and 16 Nm.

1) There is a highly linear relationship (value of r -square $> 99\%$) between the tilt imposed on an Otto Bock adaptor and the protrusion length of the corresponding set screw ; this screw being longer than that provided by the manufacturer.

2) This relationship is generally different for AP and ML planes, but adjustments made on one plane do not affect the relationship on the other.

3) These relationships can constitute the models describing the functional behaviour of the adaptors and can be determined by calibrating the adaptors in the two planes.

4) The effort of tightening the set screws must be kept as uniform as possible in order to avoid discrepancies in the measurement of the screw length

5) Besides the modelling of the adaptors, the modelling of an AK Otto Bock modular prosthesis was also developed, based on 3-D frame transforms.

6) The models of the adaptors and the prosthesis together can provide the ground to built software procedures for simulation of alignment in prosthetic practice, which could assist the prosthetist's decision making.

The next chapter presents the simulation method and the computer program developed.

CHAPTER 8

A NEW METHOD FOR THE ASSESSMENT OF ALIGNMENT OF LOWER LIMB PROSTHESES

8.1 Introduction

8.2 Adaptor screws and Measuring Device

8.3 Measurement of the adaptors

8.4 Measurements on the Prosthesis

8.4.1 Preparation of the prosthesis

8.4.2 Procedure followed

8.4.3 Data acquired from the measurements

8.4.4 Final results from the measurements

8.5 Simulation of the Alignment Procedure

8.5.1 The computer software

8.5.2 The prosthetic procedure

8.6 Simulated Alignment Sessions for Evaluation of the New Method

8.6.1 Introduction

8.6.2 Simulated alignment session No 1

8.6.3 Simulated alignment session No 2

8.6.4 Simulated alignment session No 3

8.6.5 Simulated alignment session No 4

8.7 Discussion

8.8 Conclusions

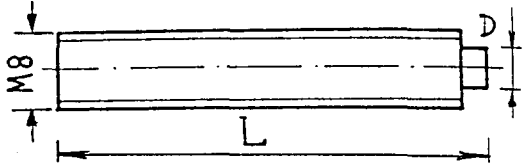
No	screw length (mm)	contact diameter (mm)		
1	28.28	5.50	screw length mean value 28.320 mm st.deviation 0.026 mm minimum 28.280 mm maximum 28.370 mm	
2	28.32	5.56		
3	28.37	5.54		
4	28.32	5.48		
5	28.30	5.50		
6	28.28	5.50		
7	28.31	5.47		
8	28.31	5.50		
9	28.30	5.43		
10	28.36	5.51	contact diameter mean value 5.4894 mm st.deviation 0.0368 mm minimum 5.4100 mm maximum 5.5600 mm	
11	28.33	5.50		
12	28.34	5.47		
13	28.33	5.41		
14	28.31	5.50		
15	28.31	5.50		
16	28.35	5.46		

Table 8.1 Statistical description of the new set of adaptor screws

8.1 Introduction

In order that a prosthesis be entirely described in terms of its system of frames, several measurements have to be carried out. These measurements concern the position of the different frames, with respect to a reference frame.

Another set of measurements needed is that one concerning the mechanical behaviour of the adaptors of the prosthesis, carried out as described in section 7.5 (calibration of adaptors).

For the measurements concerning the geometry of the prosthesis and the calibration of the adaptors, the alignment rig described in section 8.4 was used.

For the measurements concerning the detailed geometry of the adaptors and knee unit, a Coordinate Measuring Machine (CMM) was used. These measurements were of high importance, because it was by means of them that the centres of all three adaptors were geometrically determined (see ankle, distal knee and proximal knee adaptor in fig 7.11).

The prosthesis chosen to work on was an AK Otto Bock modular prosthesis belonging to a well built male amputated on the right side.

8.2 Adaptor screws and Measuring Device

A whole set of twelve new set screws was properly machined, the objective being to provide a uniform length L and also the same contact diameter D . Data for this set of screws are shown in table 8.1. These screws were to replace the short ones provided by Otto Bock.

A new device was designed and machined for the accurate measurement of the protrusion length of the screw. This device is shown in figure 8.1 fitted on an adaptor screw to measure its protrusion length l . The pyramid (p) component and the wall (w) of the tubular rim are also shown. The set screw is shown tightened up against the pyramid through the wall of the rim.

The measuring device consists of two parts. The

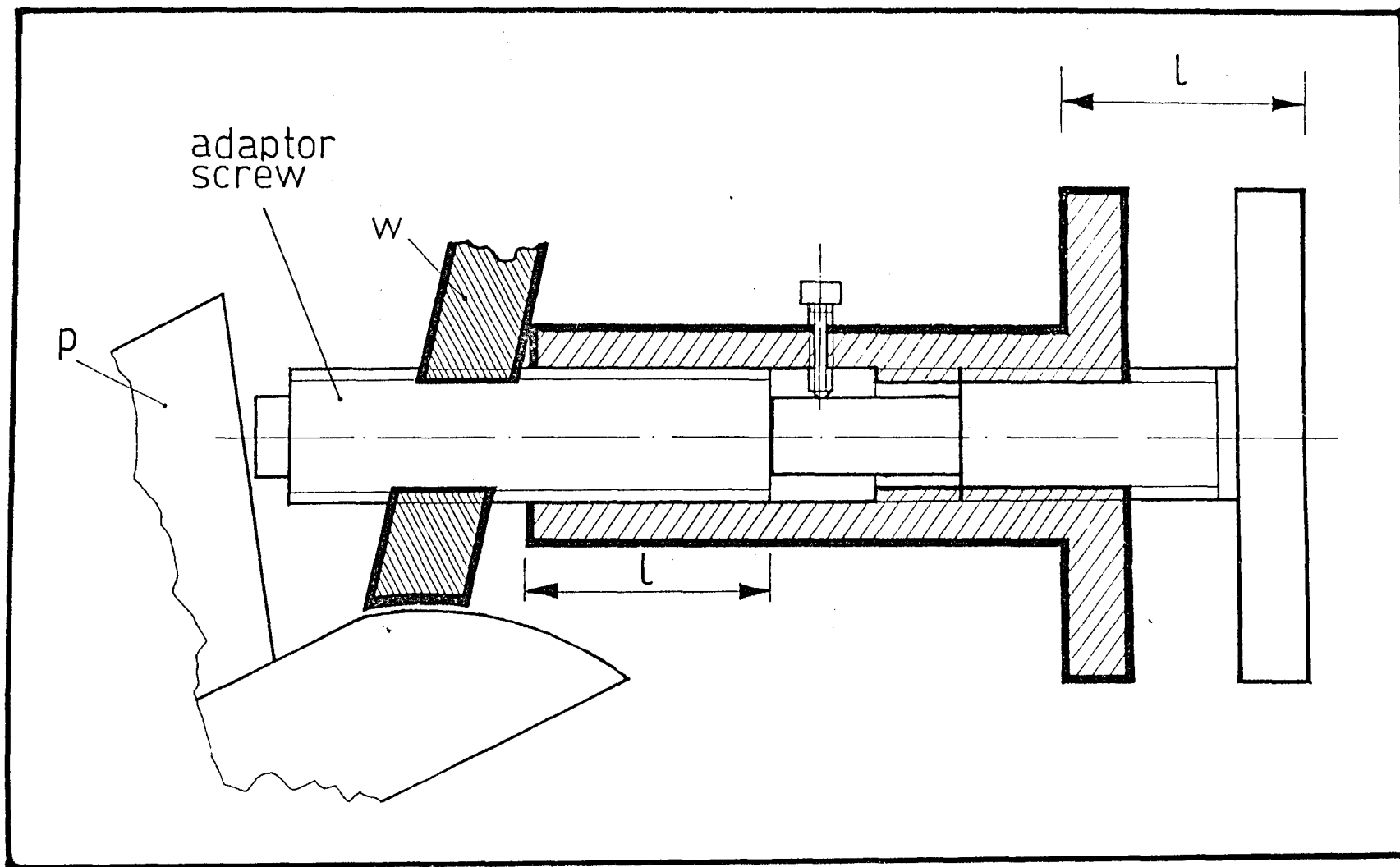


Fig 8.1 The device for the measurement of the protrusion length of the screws.

Measurements for a constant screw length (mm)

14.693	14.672	14.692	14.689	14.669	14.677
14.674	14.690	14.673	14.691	14.677	14.676
14.672	14.671	14.689	14.669	14.712	14.675
14.676	14.669	14.667	14.672	14.663	14.668
14.701	14.690	14.667	14.679	14.676	14.676

Statistics

Number of measurements = 30
 Mean value = 14.679 mm
 Median = 14.676 mm
 Standard deviation = 0.011 mm
 Minimum value = 14.663 mm
 Maximum value = 14.712 mm

Histogram of the data

Midpoint	Count	
14.665	3	***
14.670	8	*****
14.675	9	*****
14.680	1	*
14.685	0	
14.690	6	*****
14.695	1	*
14.700	1	*
14.705	0	
14.710	1	*

Consistency
 of measurement = (measured value) \pm 0.022 (mm)
 (level of 95%)

Table 8.2 Analysis for the measuring consistency of the new device

external part shown shaded, is tubular and provided with a top flange. The internal surface of this part is threaded at its top half. Laterally there is a small security screw perpendicular to the axis of the device.

The internal part of the device is cylindrical and also provided with a top flange matching with that of the external part. This cylindrical component is threaded and can be screwed into the external part, until it meets the top machined surface on the set screw. It can then be secured in location by means of the small lateral security screw.

Because of the design of the device, when the device is mounted on the set screw as shown, the external dimension between the two flanges is equal to the protrusion length of the screw as demonstrated in figure 7.3. Measuring the external dimension between the two flanges, by means of a digital micrometer, the screw protrusion length is assessed.

The digital micrometer has a sensitivity of ± 0.0005 mm and the device provides a measurement precision of ± 0.022 mm, as shown in table 8.2 , for 95% probability level.

8.3 Measurement of the Adaptors

Equipment used

The Coordinate Measuring Machine (CMM) is an electronic machine provided with a robust surface table on which the component to be measured is positioned (fig 8.2) . It is also provided with a system which has the capability of motion in an X - Y - Z frame, with three independent degrees of freedom. This system is connected to a personal computer and works over the surface table within quite a broad range. This three dimension system of the CMM is provided with an end-effector which can reach any position (x,y,z) within the range with a resolution of 0.001 mm. The end-effector is fitted with a special crystal probe. The actual function of this electronic probe is to send

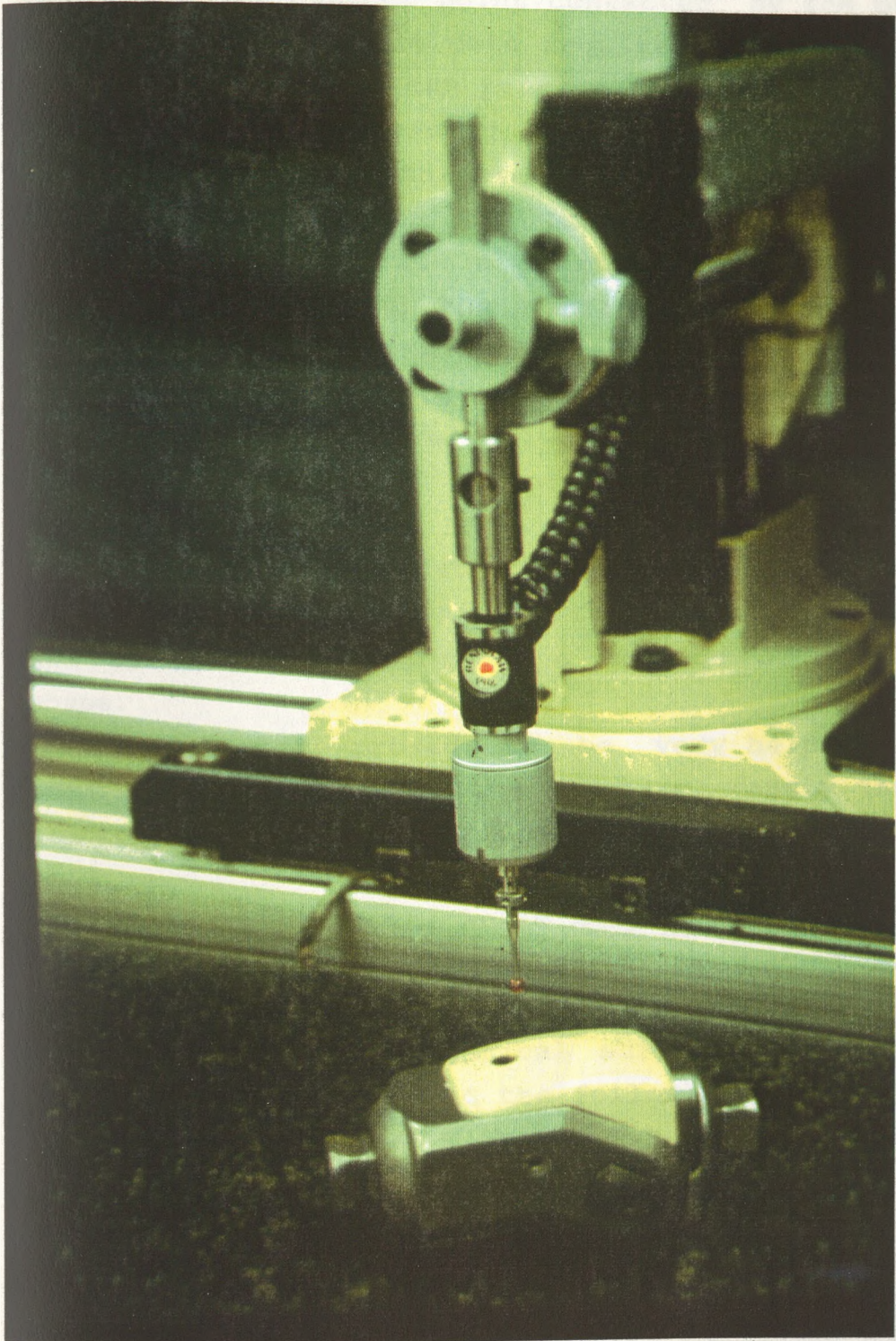


Fig 8.2b Knee unit measured on CMM

a signal to the computer whenever it is touched ; the computer then records the corresponding coordinates of the probe's position (x,y,z) and thus, the coordinates of the point contacted are stored.

The software is then ready to receive the coordinates of another point contacted by the probe in order to store all the data required. Special routines provided by the menu can process the data in order to derive results concerning the particular body under study (diameters, distances etc.)

For example when the probe is approaching the spherical portion of a particular component and successively touching the surface on several points, the appropriate routine processes the data acquired and provides the user with the radius of the spherical surface, which otherwise would be not accurately identified, because of the complicated geometry of the particular component.

In another application the user could obtain the distance between two points, for example the external and the internal point of a surface of complicated shape.

This machine proved to be very helpful in the accurate measurement of the adaptors, namely the ankle adaptor, and the two adaptors of the knee unit.

Measurement of the Ankle Adaptor

The ankle adaptor was shown in figure 7.5. The dimension required was the distance d_2 between the lower level of the spherical surface and its centre point C. The CMM measured the following : $l_1 = 24.115$ mm , $l_2 = 39.861$ mm , $h = 6.935$ mm and using the following equation , d_2 was calculated :

$$d_2 = \frac{(l_2^2 - l_1^2) / 4 - h^2}{2 h} = 14.689 \text{ mm}$$

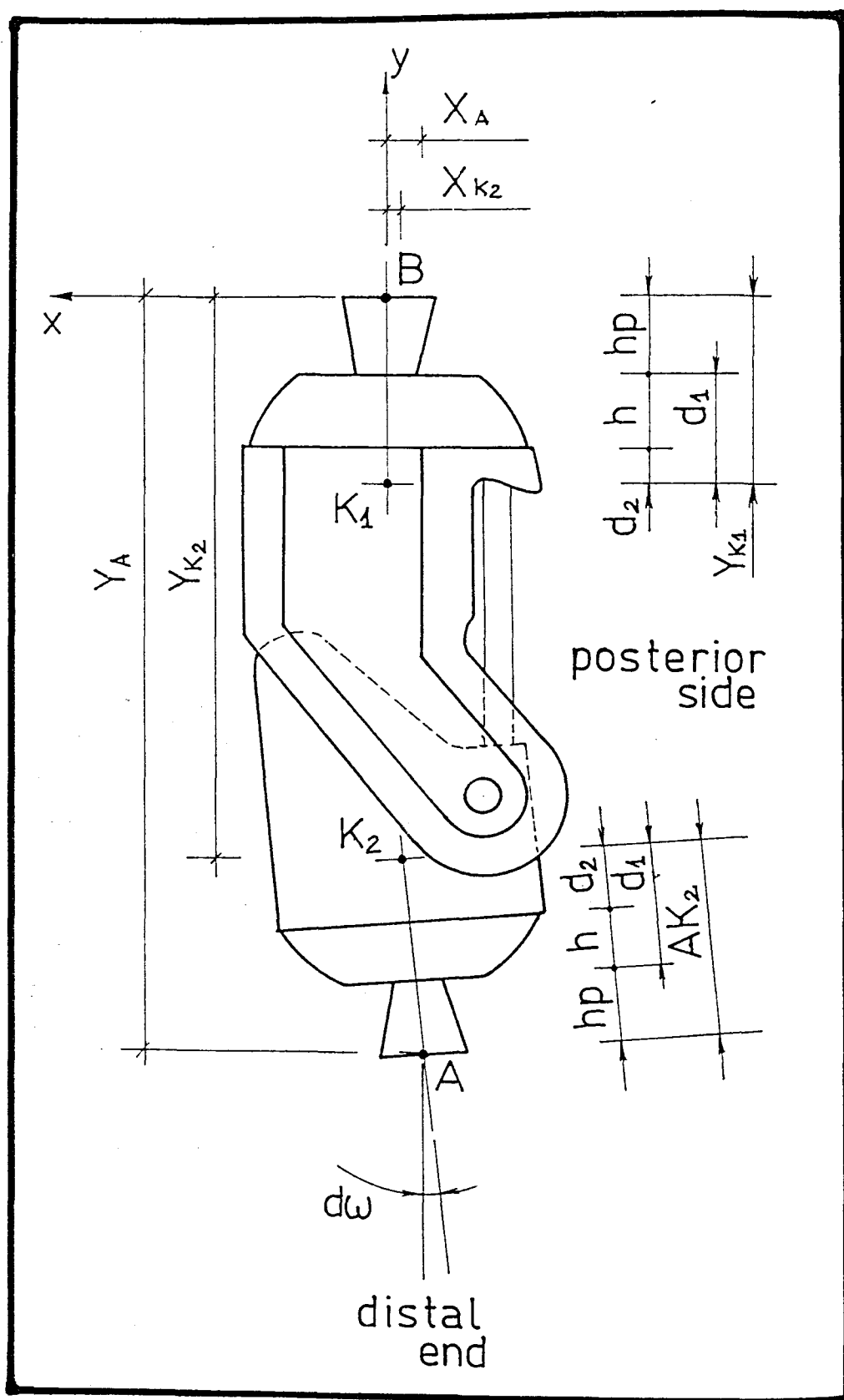


Fig 8.3a The geometry of an Otto Bock knee unit for modular prostheses (single axis).

Measurement of the Knee Unit

The knee unit is shown in figure 8.3a . The measurements carried out for these components were of the same kind as the previous ones :

for the proximal knee adaptor

$$\begin{array}{l|l} l_1 = 24.104 \text{ mm} & \\ l_2 = 39.099 \text{ mm} & \Rightarrow d_2 = 13.659 \text{ mm} \\ h = 6.920 \text{ mm} & \\ h_p = 10.880 \text{ mm} & \end{array}$$

for the distal knee adaptor

$$\begin{array}{l|l} l_1 = 24.505 \text{ mm} & \\ l_2 = 40.299 \text{ mm} & \Rightarrow d_2 = 13.818 \text{ mm} \\ h = 7.320 \text{ mm} & \\ h_p = 10.890 \text{ mm} & \end{array}$$

However, during the measurements on the prosthesis, the knee unit is positioned at the Initial Reference Position (IRP). As discussed in the next section, at this particular position it was convenient to locate points B and K_2 on the Y-axis of the rig frame. Therefore the knee unit had first to be measured using a frame directly related to the knee unit itself and then the results of these measurements had to be converted in terms of rig frame coordinates ; the reason being the existence of in-built flexion in the unit. This procedure was performed as follows :

The x-y frame shown in figure 8.3a has an origin at point B . With respect to this frame the coordinates of the various points are :

$$X_A = - 3.750 \text{ mm} \quad \text{and} \quad Y_A = -108.361 \text{ mm}$$

(angle ω of in-built flexion calculated to be -3.49°)

The distance AK_2 was calculated by :

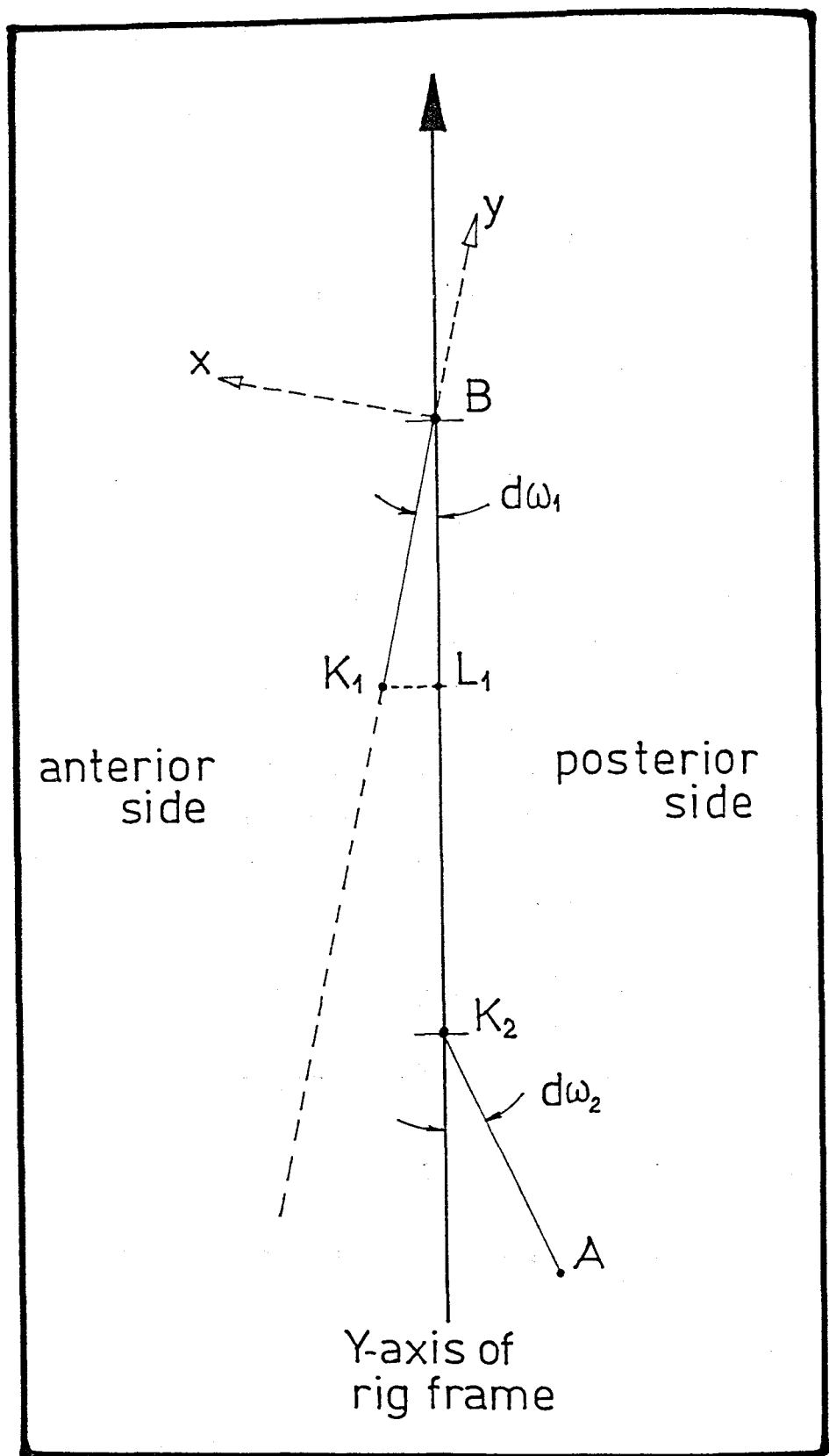


Fig 8.3b Frame configurations for the conversion of the coordinates on the knee unit .

$$AK_2 = d_2 + h + h_p = 13.818 + 7.320 + 10.890 = 32.028 \text{ mm}$$

Using X_A , Y_A , $d\omega$ and AK_2 , the coordinates X_{K2} and Y_{K2} were derived :

$$X_{K2} = X_A + [AK_2 \sin(d\omega)] = -1.800 \text{ mm}$$

$$Y_{K2} = Y_A + [AK_2 \sin(d\omega)] = -76.391 \text{ mm}$$

The coordinates for point K_1 were :

$$X_{K1} = 0.0 \text{ mm}$$

$$Y_{K1} = -(d_2 + h + h_p) = -(13.659 + 6.920 + 10.880) = -31.459 \text{ mm}$$

Having derived the coordinates in the x-y frame shown, next step was to convert them into the corresponding values for the rig frame. This frame is shown in figure 8.3b and the Y-axis of this frame is defined by points B and K_2 . It is also important at this stage to calculate the two components $d\omega_1$ and $d\omega_2$ of the in-built flexion angle $d\omega$. The calculations were performed as follows :

$$d\omega_1 = \tan^{-1}\left(\frac{X_{K2}}{Y_{K2}}\right) = 1.35^\circ \text{ and } d\omega_2 = d\omega - d\omega_1 = -2.14^\circ$$

$$(BK_2) = (X_{K2}^2 + Y_{K2}^2)^{1/2} = 76.412 \text{ mm} \quad (8.1)$$

$$(BK_1) = |Y_{K1}| = 31.459 \text{ mm}$$

$$(BL_1) = (BK_1) \cos(d\omega_1) = 31.450 \text{ mm} \quad (8.2)$$

$$(L_1K_1) = (BK_1) \sin(d\omega_1) = 0.741 \text{ mm}$$

The description of the measurements regarding the adaptors calibration and geometry of the prosthesis is presented in the next section.

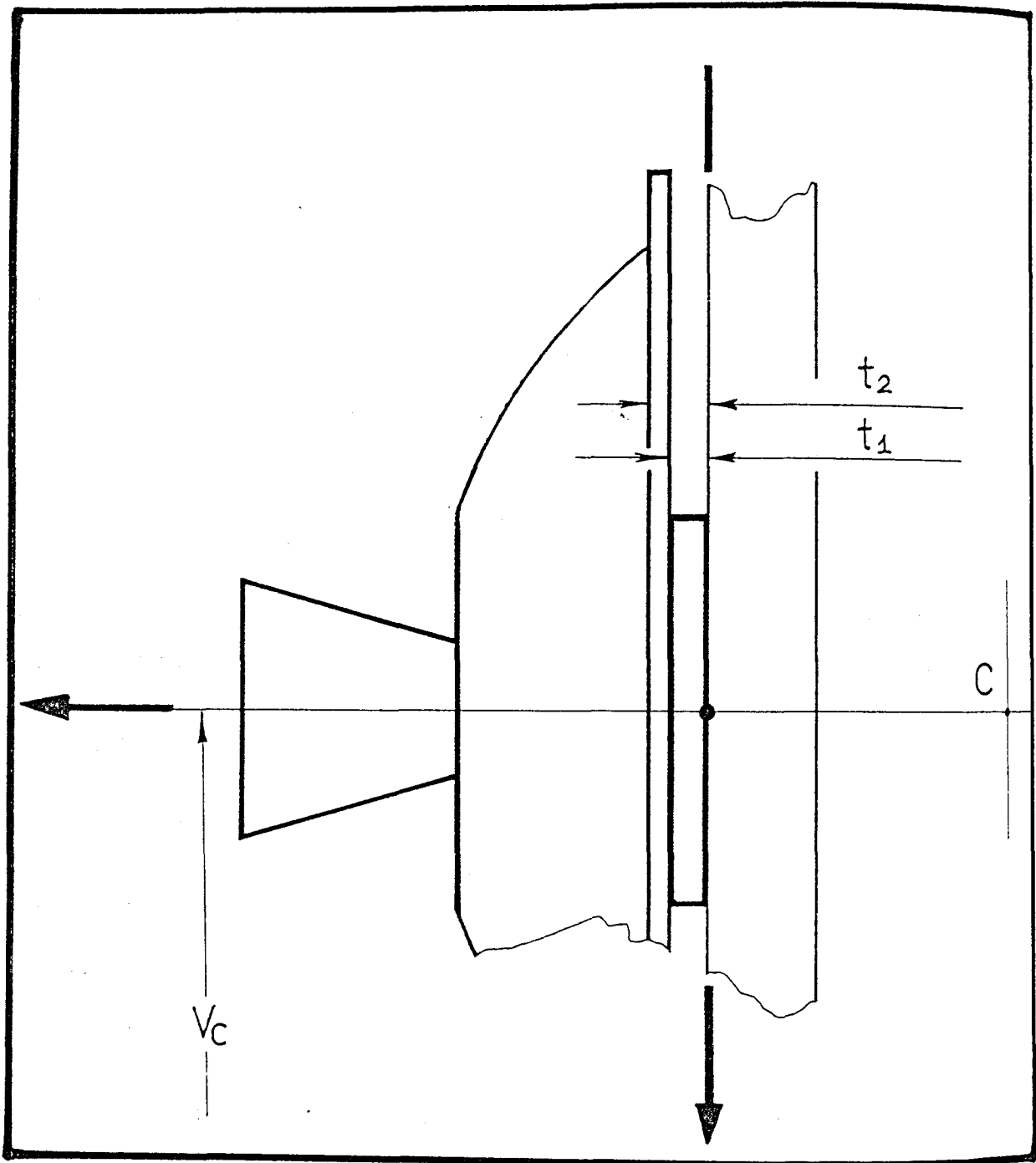


Fig 8.4 Detail of the ankle adaptor mounted on the alignment rig.

8.4 Measurement of the Prosthesis

8.4.1 Preparation of the Prosthesis

Before starting the measurements on the prosthesis itself, the measurements of the adaptors should have been completed as described above and the socket should have been marked using the Socket Axis Locator (SAL) as described in chapter 2 . The points needed to be marked were the proximal anterior, the proximal medial and lateral and the distal medial and lateral.

8.4.2 Procedure Followed

All measurements from this stage onwards were carried out on the alignment rig. A detailed presentation of the procedure followed is given below.

Step 1 : Secure the base to the rig, well aligned against the rig frame of reference.

Step 2 : Fix the ankle adaptor against the base of the rig with posterior side upwards and well aligned with the rig frame, using a foot bolt.

Step 3 : Measure the height V_c of the bolt axis in the rig frame and record it. Measure the distances t_1 and t_2 and record them (see fig 8.4).

Step 4 : Mark on the shank tube all the anterior, posterior, medial, lateral points to be used with a felt tip pen. These are the points close to the adaptor-screw holes on both distal and proximal rims (shown on the rim wall in fig 7.3). Mark also by " P " the posterior side of the tube and by " L " the lateral side of the tube.

Step 5 : Zero any rotation at the shank rotatable adaptor and fix the shank onto the ankle adaptor with posterior side upwards, using the screws provided.

Step 6 : Level the shank by bringing it to height V_c , checking that the height of the two proximal marks is equal to V_c . If this is not possible it means that the rotatable adaptor has not been zeroed.

Step 7 : Ensure that the shank is not deviating in the ML plane. If it is, then ML adjustment is required.

Step 8 : Take calibration measurements for the ankle adaptor in the AP plane, following the procedure analysed in section 7.4, recording the coordinates of the appropriate mark on the proximal rim and measuring the posterior screw.

Step 9 : Level the shank again and measure the protrusion length l_{post}^A of the posterior ankle screw for this position and record it.

Step 10 : Rotate the system by 90° with its lateral side upwards, making sure that the shank's orientation and height is not affected.

Step 11 : Take calibration measurements for the ankle adaptor in the ML plane by measuring the lateral screw.

Step 12 : Level the shank again and measure the protrusion length l_{lat}^A of the lateral ankle screw for this position and record it.

Step 13 : Rotate the system by 90° with its posterior side upwards again, making sure that the shank's orientation and height is not affected.

Step 14 : Fix the knee unit on the shank, using the screws provided with its posterior side upwards and mark the centre B (fig 8.3) of the proximal pyramid base.

Step 15 : Level the knee unit (ie proximal part level) checking that the height of point B is equal to V_c .

Step 16 : Make sure that the knee unit is not deviating in the ML plane. If it is, then ML adjustment is required.

Step 17 : Take calibration measurements for the distal knee adaptor in the AP plane, recording the coordinates of point B and measuring the posterior screw.

Step 18 : Level the knee unit again and measure the protrusion length $l_{\text{post}}^{\text{DK}}$ of the posterior distal knee screw and record it.

Step 19 : Rotate the system by 90° with its lateral side upwards, making sure, again, that height V_c and orientation are not affected.

Step 20 : Take calibration measurements for the distal

knee adaptor in the ML plane, recording the coordinates of point B and by measuring the lateral screw.

Step 21 : Level the knee unit again and measure the protrusion length l_{lat}^{DK} of the lateral distal knee screw and record it.

Step 22 : Rotate the system by 90° with its posterior side upwards again, making sure that height V_C and orientation are not affected.

Step 23 : Measure the coordinates of point B and of the knee centre, for the latter using two properly machined pins, belonging to the rig's associated equipment.

Step 24 : Zero any rotation at the socket rotatable adaptor and fix it onto the knee unit, using the screws provided, with its posterior side upwards.

Step 25 : Bring the socket to such a position that the proximal lateral mark is at height V_C , and the medial and lateral screws of the knee adaptor protrude by equal (by eye judgement) lengths.

Step 26 : Take calibration measurements for the proximal knee adaptor of the AP plane by recording the coordinates of the proximal lateral mark and measuring the posterior screw.

Step 27 : Bring the socket to its initial position described in step 25.

Step 28 : Rotate the system by 90° with its lateral side upwards, making sure that the height and orientation of the system distal to the socket, are not affected.

Step 29 : Bring the socket to such a position that the proximal posterior mark is at height V_C and the posterior and anterior screws of the proximal knee adaptor protrude by equal (by eye judgement) lengths.

Step 30 : Take calibration measurements for the proximal knee adaptor at the ML plane, by recording the coordinates of the proximal posterior mark and by measuring the lateral screw.

At this stage the calibration measurements of the

adaptors in both planes are completed and also the coordinates of all major landmarks, distal to the socket, recorded with respect to the rig frame. As mentioned in section 7.7 in the Initial Reference Position (IRP), the socket frame does not have a specific orientation and therefore its orientation can be chosen arbitrarily, defined by the user of the method. For the socket frame it was thus decided that this initial orientation could be that one corresponding to about equal protrusion lengths (by eye judgement) of the screws of the proximal knee adaptor.

Thus, the last steps of the procedure described, are:

Step 31 : Adjust the medial and lateral screws of the proximal knee adaptor so that they have about the same protrusion length and record the protrusion length l_{lat}^{PK} of the lateral one for this position.

Step 32 : Rotate the system by 90° with its posterior side upwards making sure that the height and orientation of the system distal to the socket are not affected.

Step 33 : Adjust the posterior and anterior screws of the proximal knee adaptor so that they have about the same protrusion length and record the protrusion length l_{post}^{PK} of the posterior one for this position.

Step 34 : Measure and record the coordinates of all the marks in the socket, namely Proximal Medial (PM) and Lateral (PL), Distal Medial (DM) and Lateral (DL) and Proximal Anterior (PA).

Step 35 : Measure and record the horizontal coordinate of the transverse section passing through the socket rotatable adaptor at the level of rotation (represented as point RS).

l (mm)	V (mm)	H (mm)
14.808	202.60	358.42
14.406	207.30	358.42
14.022	212.00	358.42
13.652	216.50	358.42
13.352	219.68	358.34
13.096	223.54	358.05
12.872	226.38	358.00
12.446	231.88	357.31
12.090	236.10	357.23
11.853	239.58	356.67

Table 8.3

The data for ankle adaptor in the AP plane .

l (mm)	V (mm)	H (mm)
16.080	201.04	465.20
15.540	202.38	465.20
15.094	203.52	465.20
14.536	204.58	465.20
14.177	205.82	465.20
13.797	207.20	465.10
13.316	207.78	465.00
13.020	208.76	464.90
12.607	209.88	464.90
12.360	210.68	464.64

Table 8.5

The data of distal knee adaptor in the AP plane .

l (mm)	V (mm)	H (mm)
15.558	199.62	733.40
15.175	204.54	733.40
14.776	208.22	733.40
14.364	212.46	733.40
13.961	217.28	733.40
13.458	222.96	733.20
13.005	228.48	732.81
12.400	234.62	731.65
11.759	241.30	731.03

Table 8.7

The data for proximal knee adaptor in the AP plane .

l (mm)	V (mm)	H (mm)
14.688	204.42	358.63
14.462	207.50	358.63
14.182	210.74	358.63
13.893	214.48	358.63
13.418	218.88	358.30
13.078	224.34	358.30
12.674	229.76	357.56
12.239	234.56	357.36
12.009	237.44	357.05
11.673	241.80	356.79

Table 8.4

The data for ankle adaptor in the ML plane .

l (mm)	V (mm)	H (mm)
13.880	201.24	465.25
13.183	203.14	465.25
12.835	204.08	465.25
12.380	205.18	465.25
12.046	206.04	465.25
11.718	207.04	465.25

Table 8.6

The data for distal knee adaptor in the ML plane .

l (mm)	V (mm)	H (mm)
17.134	199.62	741.88
16.851	202.94	741.88
16.474	205.70	741.88
16.109	208.92	741.88
15.716	213.04	741.00
15.262	216.86	741.00
14.845	220.94	741.00
14.384	226.20	740.66
14.032	230.40	740.30
13.595	235.12	740.00

Table 8.8

The data for proximal knee adaptor in the ML plane .

At this stage the entire procedure is finished. The actual data acquired following the sequence of the above steps are shown below.

8.4.3 Data Acquired from the Measurements

Step 3 : $V_C = 199.62 \text{ mm}$, $t_2 = 3.60 \text{ mm}$, $t_1 = 1.20 \text{ mm}$

Step 8 : Measurements shown in table 8.3

Step 9 : $l_{\text{post}}^A = 15.992 \text{ mm}$

Step 11 : Measurements shown in table 8.4

Step 12 : $l_{\text{lat}}^A = 15.034 \text{ mm}$

Step 17 : Measurements shown in table 8.5

Step 18 : $l_{\text{post}}^{\text{DK}} = 16.561 \text{ mm}$

Step 20 : Measurements shown in table 8.6

Note : the amount of data acquired at this step is less, as compared to the previous ones, because as shown in figure 8.3a, there is an already built-in flexion angle of absolute value 3.49° .

Step 21 : $l_{\text{lat}}^{\text{DK}} = 14.443 \text{ mm}$

Step 23 : $V_B = 199.62 \text{ mm} (=V_C)$ and $H_B = 465.87 \text{ mm}$
(the Transverse Coordinate = $T_B = 0.0 \text{ mm}$)

and $V_{\text{Knee}} = V_K = 206.90 \text{ mm}$ and $H_{\text{Knee}} = H_K = 427.37 \text{ mm}$
(the Transverse Coordinate = $T_K = 0.0 \text{ mm}$)

Step 26 : Measurements shown in table 8.7

Step 30 : Measurements shown in table 8.8

Step 31 : $l_{\text{lat}}^{\text{PK}} = 16.082 \text{ mm}$

Step 33 : $l_{\text{post}}^{\text{PK}} = 15.911 \text{ mm}$

Step 34 : $V_{\text{PM}} = 183.50 \text{ mm}$, $H_{\text{PM}} = 723.00 \text{ mm}$, $T_{\text{PM}} = -76.69 \text{ mm}$
 $V_{\text{PL}} = 195.74 \text{ mm}$, $H_{\text{PL}} = 735.00 \text{ mm}$, $T_{\text{PL}} = 79.16 \text{ mm}$
 $V_{\text{DM}} = 159.72 \text{ mm}$, $H_{\text{DM}} = 516.30 \text{ mm}$, $T_{\text{DM}} = -33.58 \text{ mm}$
 $V_{\text{DL}} = 161.16 \text{ mm}$, $H_{\text{DL}} = 521.39 \text{ mm}$, $T_{\text{DL}} = 46.50 \text{ mm}$
 $V_{\text{PA}} = 121.20 \text{ mm}$, $H_{\text{PA}} = 741.32 \text{ mm}$, $T_{\text{PA}} = 9.00 \text{ mm}$

Step 35 : $(V_{RS} = 199.62 \text{ mm})$
 $H_{RS} = 466.92 \text{ mm}$
 $(T_{RS} = 0.0 \text{ mm})$

8.4.4 Final Results from the Measurements

The results of the measurements with respect to the rig frame (dark axes in fig 8.4) were derived as follows :

i) the universal reference centre C :

$$H_C = t_2 - d_2 = 3.60 - 14.69 = -11.09 \text{ mm}$$

(because $d_2 = 14.689 = 14.69 \text{ mm}$)

$$V_C (\text{net}) = V_{Cn} = 199.62 - 199.62 = 0.0 \text{ mm}$$

$$T_C = 0.0 \text{ mm}$$

ii) the centre K_2 of the distal knee adaptor :

$$H_{K2} = H_B - BK_2 = 465.870 - 76.412 = 389.458 \text{ mm}$$

(with BK_2 taken from equation 8.1).

$$V_{K2} (\text{net}) = V_C - V_{K2} = 199.62 - 199.62 = 0.0 \text{ mm}$$

(because K_2 lies on the Y-axis of the rig frame)

$$T_{K2} = 0.0 \text{ mm},$$

iii) the centre K_1 of the proximal knee adaptor :

$$H_{K1} = H_B - BL_1 = 465.87 - 31.45 = 434.42 \text{ mm}$$

$$V_{K1} (\text{net}) = (V_C - V_B) + L_1K_1 = 0.741 \text{ mm}$$

$$T_{K1} = 0.0 \text{ mm}$$

(with BL_1 and L_1K_1 taken from 8.2).

iv) The knee centre K :

$$H_K = 427.37 \text{ mm}$$

$$V_K (\text{net}) = V_{Kn} = V_C - V_K = 199.62 - 206.90 = -7.28 \text{ mm}$$

$$T_K = 0.0 \text{ mm}$$

v) for the socket points only the vertical net values had to be calculated, the rest of the coordinates remaining the same. These values were calculated to be as follows :

l (mm)	ω (degrees)
14.808	0.46207
14.406	1.19068
14.022	1.91891
13.652	2.61557
13.352	3.10810
13.096	3.70754
12.872	4.14684
12.446	5.00450
12.090	5.65637
11.853	6.20131

Table 8.9
Results for ankle adaptor
in the AP plane .

l (mm)	ω (degrees)
16.080	-0.28754
15.540	0.72638
15.094	1.58962
14.536	2.38972
14.177	3.32566
13.797	4.37089
13.316	4.81387
13.020	5.55861
12.607	6.40023
12.360	7.02366

Table 8.11
Results for distal knee
adaptor in the AP plane .

l (mm)	ω (degrees)
15.558	0.00000
15.175	0.94274
14.776	1.64757
14.364	2.45903
13.961	3.38028
13.458	4.46660
13.005	5.52423
12.400	6.71565
11.759	7.99863

Table 8.13
Results for proximal knee
adaptor in the AP plane .

l (mm)	ω (degrees)
14.688	0.74382
14.462	1.22099
14.182	1.72276
13.893	2.30163
13.418	2.98470
13.078	3.82859
12.674	4.67398
12.239	5.41714
12.009	5.86557
11.673	6.54080

Table 8.10
Results for ankle adaptor
in the ML plane .

l (mm)	ω (degrees)
13.880	-0.13611
13.183	1.30041
12.835	2.01062
12.380	2.84090
12.046	3.48923
11.718	4.24196

Table 8.12
Results for distal knee
adaptor in the ML plane .

l (mm)	ω (degrees)
17.134	0.00000
16.851	0.61865
16.474	1.13284
16.109	1.73249
15.716	2.50634
15.262	3.21844
14.845	3.97790
14.384	4.96038
14.032	5.74601
13.595	6.62628

Table 8.14
Results for proximal knee
adaptor in the ML plane .

$$\begin{aligned}
V_{PM}(\text{net}) &= V_{PMn} = V_C - V_{PM} = 199.62 - 183.50 = 16.12 \text{ mm} \\
V_{PL}(\text{net}) &= V_{PLn} = V_C - V_{PL} = 199.62 - 195.74 = 3.88 \text{ mm} \\
V_{DM}(\text{net}) &= V_{DMn} = V_C - V_{DM} = 199.62 - 159.72 = 39.90 \text{ mm} \\
V_{DL}(\text{net}) &= V_{DLn} = V_C - V_{DL} = 199.62 - 161.16 = 38.46 \text{ mm} \\
V_{PA}(\text{net}) &= V_{PAn} = V_C - V_{PA} = 199.62 - 121.20 = 78.46 \text{ mm}
\end{aligned}$$

vi) the point RS of the socket rotatable adaptor :

$$H_{RS} = 466.92 \text{ mm}$$

$$V_{RS}(\text{net}) = V_{RSn} = V_C - V_{RS} = 199.62 - 199.62 = 0.0 \text{ mm}$$

$$T_{RS} = 0.0 \text{ mm}$$

The final results concerning the modelling of the adaptors were obtained as described in section 7.4. They exhibited a very high linearity and the models derived explained statistically more than 99% of the variation of the angular displacement ω with the screw length l . All the coefficients exhibited very low p-values, thus proving their significance. The final linear equations describing the behaviour of adaptors were derived as follows :

Ankle Adaptor : (data in tables 8.9 and 8.10)

$$(AP) \quad \omega = 29.1356 - 1.94080 l, \text{ r-square} = 99.9 \% ,$$

$$(ML) \quad \omega = 28.8669 - 1.91488 l, \text{ r-square} = 99.9 \% ,$$

$$\text{p-values to three decimal places} = 0.000$$

Distal Knee Adaptor : (data in tables 8.11 and 8.12)

$$(AP) \quad \omega = 30.9643 - 1.94790 l, \text{ r-square} = 99.6 \% ,$$

$$(ML) \quad \omega = 27.5873 - 1.99596 l, \text{ r-square} = 99.9 \% ,$$

$$\text{p-values to three decimal places} = 0.000$$

Proximal Knee Adaptor : (data in tables 8.13 and 8.14)

$$(AP) \quad \omega = 32.8778 - 2.11131 l, \text{ r-square} = 99.9 \% ,$$

$$(ML) \quad \omega = 31.5288 - 1.84433 l, \text{ r-square} = 99.7 \% ,$$

$$\text{p-values to three decimal places} = 0.000$$

Thus, the whole set of final results has been presented. In order to facilitate and organise the

manipulation of this set of values, a particular format had to be determined for their presentation, but more importantly , for their feeding to any subsequent programs. Therefore the set of values resulted from the measurements was given the following form :

11.09	Absolute value of H _c		
1.20	Distance t ₁		
X	Y	Z	Coordinates of landmarks
0.00	389.46	0.00	K ₂
-7.28	427.37	0.00	K
0.74	434.42	0.00	K ₁
0.00	466.92	0.00	RS
3.88	735.00	79.16	PL
16.12	732.11	-76.69	PM
38.46	521.39	46.50	DL
39.90	516.30	-33.58	DM
78.42	741.32	9.00	PA
1.35	-2.14	Built-in flexion angles dω ₁ and dω ₂	
Intercept	& Slope	of	Adaptor modelling equations
29.1356	1.94080		Ankle AP
28.8669	1.91488		Ankle ML
30.9643	1.94790		Distal Knee ML
27.5873	1.99596		Distal Knee AP
32.8778	2.11131		Proximal Knee AP
31.5288	1.84433		Proximal Knee ML
1.0	Side of amputation		

(8.3)

The last parameter refers to the fact that the presented prosthesis is a right side one and its

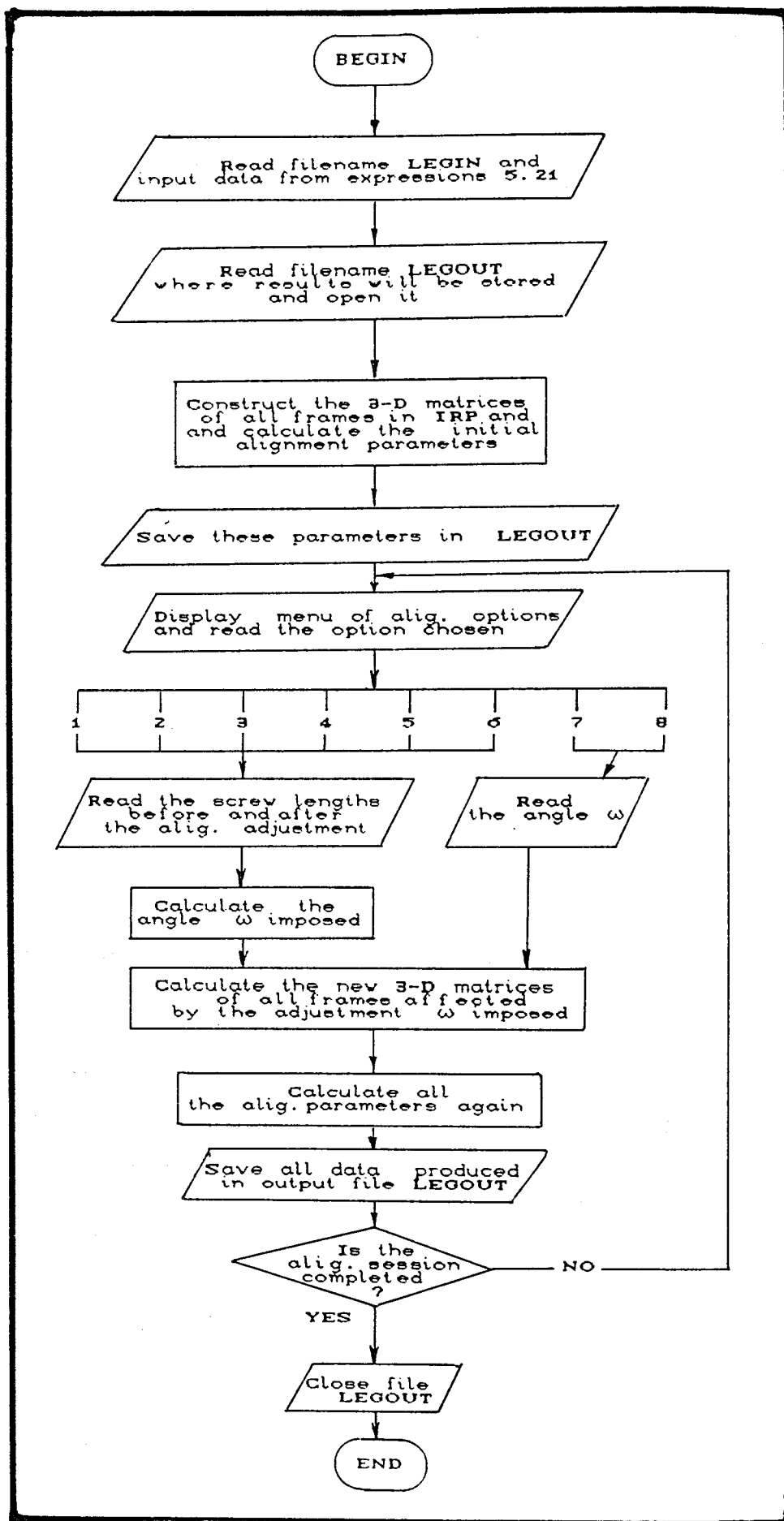


Fig 8.5 The flowchart for the program developed.

meaning is explained in the next section. It is in fact the same quantity with the factor (+1) in equations (7.19).

This set of values was stored in a file which can be found in appendix VI .

8.5 Simulation of the Alignment Procedure

8.5.1 The Program

With all the quantities required , measured or calculated and stored in a file corresponding to the particular prosthesis, the simulation of the alignment procedure could then be achieved.

The program developed for this purpose had to follow the flowchart shown in figure 8.5 .

The menu of alignment options was :

- (1) AP adjustment at the ankle adaptor
- (2) ML adjustment at the ankle adaptor
- (3) AP adjustment at the distal knee adaptor
- (4) ML adjustment at the distal knee adaptor
- (5) AP adjustment at the proximal knee adaptor
- (6) ML adjustment at the proximal knee adaptor
- (7) Toe-in-out angle at the shank rotatable adaptor
- (8) Socket rotation at the socket rotatable adaptor

The program can be found in appendix XIII.

It is important to note that the operations performed by the program are all following the same frame configuration as the one mentioned in the previous chapter for the modelling of the prosthesis (right side prosthesis). Therefore, in order to obtain results which are in agreement with the alignment conventions (see chapter 2), the alignment parameters must be calculated differently for right and left side prostheses. Referring to equations (7.19) the meaning of the factor (+1) is now obvious. This factor should be given (-1) if the prosthesis under study is a left

side prosthesis. Thus the alignment equations (7.19) can now be written in the following general form adopted in the program :

If the knee frame {KNEE} is described with respect to the universal reference by a (4x4) matrix called [K], its alignment parameters are :

$$\begin{aligned} \text{Knee AP Shift} &= \text{KAPS} = K(1,4) \\ \text{Knee ML Shift} &= \text{KMLS} = K(3,4) \\ \text{Knee Height} &= \text{KH} = K(2,4) - (H_C + t_1) \\ \text{Knee ML Tilt} &= \text{KMLT} = (\pm 1) \cdot \arctan \left(\frac{-K(2,3)}{K(3,3)} \right) \\ \text{Knee Rotation} &= \text{KR} = (\pm 1) \cdot \arctan \left(\frac{K(1,3)}{K(3,3)} \right) \end{aligned}$$

Similarly the socket frame {SOCKET} called [S] provides the following formulae :

$$\begin{aligned} \text{Socket AP Shift} &= \text{SAPS} = S(1,4) \\ \text{Socket ML Shift} &= \text{SMLS} = S(3,4) \\ \text{Socket Height} &= \text{SH} = S(2,4) - (H_C + t_1) \\ \text{Socket AP Tilt} &= \text{SAPT} = \arctan \left(\frac{-S(1,2)}{S(2,2)} \right) \\ \text{Socket ML Tilt} &= \text{SMLT} = (\pm 1) \cdot \arctan \left(\frac{-S(3,2)}{S(2,2)} \right) \\ \text{Socket Rotation} &= \text{SR} = \\ &= (\pm 1) \cdot \left[\arctan \left(\frac{-S(1,3)}{S(3,3)} \right) - \arctan \left(\frac{-K(1,3)}{K(3,3)} \right) \right] \end{aligned} \tag{8.4}$$

8.5.2 The Prosthetic Procedure

It has already been mentioned that the program developed was designed to be run at the same time as the actual alignment session. The prosthetic procedure, therefore, is carried out next to the terminal of the computer.

Before any bench, static or dynamic alignment, the prosthesis must be adjusted to the IRP, so that there is a rational reference for the program to start from.

The user of the program (who may well be the prosthetist) has then to run the program and give the filename of the file where the prosthesis' IRP data are

stored (as in expressions 8.3 for the prosthesis studied in this chapter).

The prosthetist can then observe the alignment parameters on the screen as they correspond to the IRP and decide whether any bench alignment is needed.

Then the amputee has to don the prosthesis. The prosthetist by means of subjective judgement and by the amputee's remarks, has to decide whether any static alignment is needed and proceed then to the dynamic alignment.

At this last stage, the functional performance of the leg is observed and the amputee's comfort considered in order to perform any alignment changes needed to achieve a more satisfactory result.

No matter at which stage of this procedure an alignment adjustment is meant to be performed the work needed for the program to run and produce intermediate results is as follows :

- 1) The prosthetist decides which adjustment is needed.
- 2) Keys in the corresponding menu option.
- 3) a) If the adjustment is one concerning a transverse rotation, the prosthetist performs it recording the value of the angle as occurring from the graduation on the rotatable adaptor (for the socket), or from the traversed arc length (for the shank).
b) If the adjustment is concerning an AP or an ML tilting, the prosthetist measures and records the length of the appropriate screw , performs the change and records the same length again, using for the measurement the special device provided.
- 4) The recorded data must be keyed in depending on the option chosen. Then, the new alignment parameters can be observed on the screen as resulting from the adjustment just performed.

These intermediate results may work as a further feed back criterion for the prosthetist to decide on the next step of his/her work.

At the end of the whole procedure, a print-out could be asked which describes the step-by-step development of the final alignment configuration obtained.

8.6 Simulated Alignment Sessions for Evaluation of the New Method

8.6.1 Introduction

The prosthesis mentioned in section 8.1, was subjected to several alignment changes, grouped in four sessions, in association with the program developed; the task being to evaluate the new method.

The final alignment of the prosthesis, as described by the program, was to be compared with the alignment (the values of alignment parameters) obtained by the usual way of rig measurements.

The measurements on the alignment rig were carried out on the prosthesis after the alignment sessions and all important values were recorded. Then these values were fed to another program developed for this purpose. The program calculated the alignment parameters of the artificial leg. These parameters were then compared to the ones predicted by the alignment program, already described.

The program needed for the calculation of the alignment parameters by the rig measurements is exhibited in appendix XIII .

The four alignment sessions mentioned were carried out on the prosthesis with no patient present. The changes were chosen arbitrarily and performed onto the artificial leg changing the alignment of it from IRP into new configurations.

In the four sessions presented next the alignment changes are presented with the corresponding software options. At the end of each section a table of the results obtained is provided for comparison with the results obtained by the rig measurements (figures

rounded off to one decimal digit). The full print-outs of the alignment sessions with all intermediate and final alignment results, are exhibited in appendix VI .

8.6.2 Simulated Alignment Session No 1

Option 5 :

Socket Extension in Proximal Knee Adaptor :

$l_{\text{before}} = 15.903 \text{ mm}$, $l_{\text{after}} = 17.013 \text{ mm}$

Option 6 :

Socket Adduction in Proximal Knee Adaptor :

$l_{\text{before}} = 16.101 \text{ mm}$, $l_{\text{after}} = 14.408 \text{ mm}$

Option 7 :

Toe-out in Shank Rotatable Adaptor :

$\omega = 12.91^\circ$

	Results using New Method	Results using Alignment Rig
KAPS =	-7.1 mm	-7.5 mm
KMLS =	1.6 mm	2.2 mm
KH =	426.2 mm	426.1 mm
KMLT =	0.0°	0.0°
KR =	12.9°	12.7°
SAPS =	25.6 mm	24.3 mm
SMLS =	12.1 mm	12.8 mm
SH =	732.2 mm	731.2 mm
SAPT =	4.9°	5.3°
SMLT =	2.9°	2.8°
SR =	-4.5°	-4.6°

8.6.3 Simulated Alignment Session No 2

Option 1 :

Dorsi Flexion in Ankle Adaptor :

$l_{\text{before}} = 15.157 \text{ mm}$, $l_{\text{after}} = 15.943 \text{ mm}$

Option 6 :

Socket Adduction in Proximal Knee Adaptor :

$l_{\text{before}} = 15.907 \text{ mm}$, $l_{\text{after}} = 14.948 \text{ mm}$

Option 7 :

Toe-out at Shank Rotatable Adaptor : $\omega = 17.95^\circ$

Results using
New Method

KAPS = 4.8 mm
KMLS = 2.2 mm
KH = 426.2 mm
KMLT = 0.5°
KR = 17.9°
SAPS = 32.6 mm
SMLS = 6.9 mm
SH = 731.6 mm
SAPT = 5.7°
SMLT = 2.8°
SR = -4.5°

Results using
Alignment Rig

6.2 mm
3.1 mm
426.3 mm
0.9°
17.8°
35.5 mm
11.4 mm
731.6 mm
6.4°
3.4°
-2.8°

8.6.4 Simulated Alignment Session No 3

Option 1 :

Plantar Flexion in Ankle Adaptor :

$l_{\text{before}} = 15.160 \text{ mm}$, $l_{\text{after}} = 14.313 \text{ mm}$

Option 5 :

Socket Extension in Proximal Knee Adaptor :

$l_{\text{before}} = 15.044 \text{ mm}$, $l_{\text{after}} = 15.963 \text{ mm}$

Option 6 :

Socket Adduction in Proximal Knee Adaptor :

$l_{\text{before}} = 15.941 \text{ mm}$, $l_{\text{after}} = 16.964 \text{ mm}$

Results using
New Method

KAPS = -19.9 mm
KMLS = 0.0 mm
KH = 425.8 mm
KMLT = 0.0°
KR = 0.0°
SAPS = -1.2 mm
SMLS = -8.6 mm
SH = 732.0 mm
SAPT = 7.5°
SMLT = -3.3°
SR = -4.6°

Results using
Alignment Rig

-17.6 mm
0.6 mm
426.4 mm
0.0°
0.0°
-3.4 mm
-7.1 mm
732.7 mm
8.5°
-2.5°
-3.1°

8.6.5 Simulated Alignment Session No 4

Option 5 :

Socket Flexion in Proximal Knee Adaptor :

$l_{\text{before}} = 15.903 \text{ mm}$, $l_{\text{after}} = 14.399 \text{ mm}$

Option 6 :

Socket Abduction in Proximal Knee Adaptor :

$l_{\text{before}} = 16.101$, $l_{\text{after}} = 18.195 \text{ mm}$

Option 5 :

Socket Flexion in Proximal Knee Adaptor :

$l_{\text{before}} = 14.474 \text{ mm}$, $l_{\text{after}} = 13.502 \text{ mm}$

Results using New Method

KAPS =	-7.3 mm
KMLS =	0.0 mm
KH =	462.2 mm
KMLT =	0.0°
KR =	0.0°
SAPS =	-17.3 mm
SMLS =	-18.9 mm
SH =	731.4 mm
SAPT =	13.0°
SMLT =	-5.3°
SR =	-4.8°

Results using Alignment Rig

-7.7 mm
1.0 mm
462.4 mm
0.0°
0.0°
-14.0 mm
-19.9 mm
731.2 mm
12.3°
-5.8°
-5.5°

8.7 Discussion

As a continuation of the work presented in the previous chapter, the method developed and presented in this one completes the initial task of the simulation of the alignment procedure for Otto Bock modular prostheses.

Despite the laborious process initially needed for the modelling of any prosthesis, the resulting program provides a flexible and user-friendly tool for the immediate measurement of the alignment of an artificial leg. However, the new method was only validated with tests performed on an AK prosthesis itself, without

patient nor prosthetist. These tests were only meant to prove whether the mathematical model worked well or not. Having given a positive answer to this question actual amputee tests should be carried out, which would assess the qualities of the new method from all prosthetic aspects.

Running the program during an actual alignment session will allow the prosthetist to assess the method and express comments about its usefulness, drawbacks and possible improvements.

The prosthetic advantage of the new method is considered to be the fact that , combining the program-provided information with objective judgement , the prosthetist can proceed into the next stage having based any decisions on an established quantitative feedback.

The results obtained from the new method were found satisfactory in comparison to the results obtained by means of the alignment rig. The small discrepancies are thought to be due to variations of the tightening effort on the adaptor screws (see discussion of chapter 7). In fact one could claim that the more adjustments are made the higher the discrepancies would be. This is true but , as mentioned in the previous chapter, ideally the adaptor screws must be set at a specific torque in order that the effort is kept as uniform as possible , in which case the errors would be kept to a minimum.

Two more points must be made here, regarding the measurements for the determination of the geometry and the modelling of the adaptors :

a) These measurements are very laborious. The accurate measurement of the adaptors, in particular, also demands the availability of a coordinate measuring machine (CMM). Therefore, taking into account what was stated above for the errors due to non-uniform tightening effort, one could question the necessity for these accurate measurements.

b) Furthermore, on the same ground , the necessity for different models among adaptors and adaptor planes could be questioned.

Particularly, if the errors due to the variation in the tightening effort are proved to be more significant than the ones possibly caused by poorer measurement techniques and adoption of one single adaptor model, then there may be no need for CMM-based measurements and different adaptor models.

An answer to the above comment can only be given with more experimental work and further statistical analysis of future results.

The work presented in this chapter has provided a new method for the immediate measurement of the prosthetic alignment at the very time it is established by the prosthetist. If the method is proved to be a useful prosthetic tool, then, further development could lead to an improved version of the procedures and software.

The amputee tests presented in the next chapter are the basis for the assessment of the new method.

8.8 Conclusions

From the work presented in this chapter the following conclusions can be drawn :

- 1) A new method for the immediate measurement of prosthetic alignment was developed, concerning Otto Bock modular prostheses.
- 2) The new method is based on the work presented in chapter 7 and a program developed during this project, which is meant to run at the same time with the actual prosthetic procedure and provide feedback to the prosthetist.
- 3) The comparative results between the new method and the alignment rig showed that the mathematical model

for the prosthesis as well as the adaptor models, developed in chapter 7 , are correctly performing their tasks.

4) The fact that the alignment procedure has been simulated is on its own a very positive step because, besides providing the prosthetist with a good tool, it also allows for future developments which could lead to a "clever" alignment software package.

The next chapter presents the experimental work carried out during patient walking tests, in which both the pylon transducer and the new method for assessment of prosthetic alignment are used.

CHAPTER 9

PROSTHETIC LOADING DURING LEVEL WALKING

- 9.1 Introduction
- 9.2 Equipment used
- 9.3 Preparation of the Prosthesis
- 9.4 Description of the Tests
- 9.5 Manipulation of the Files
- 9.6 Results
- 9.7 Discussion and Conclusions

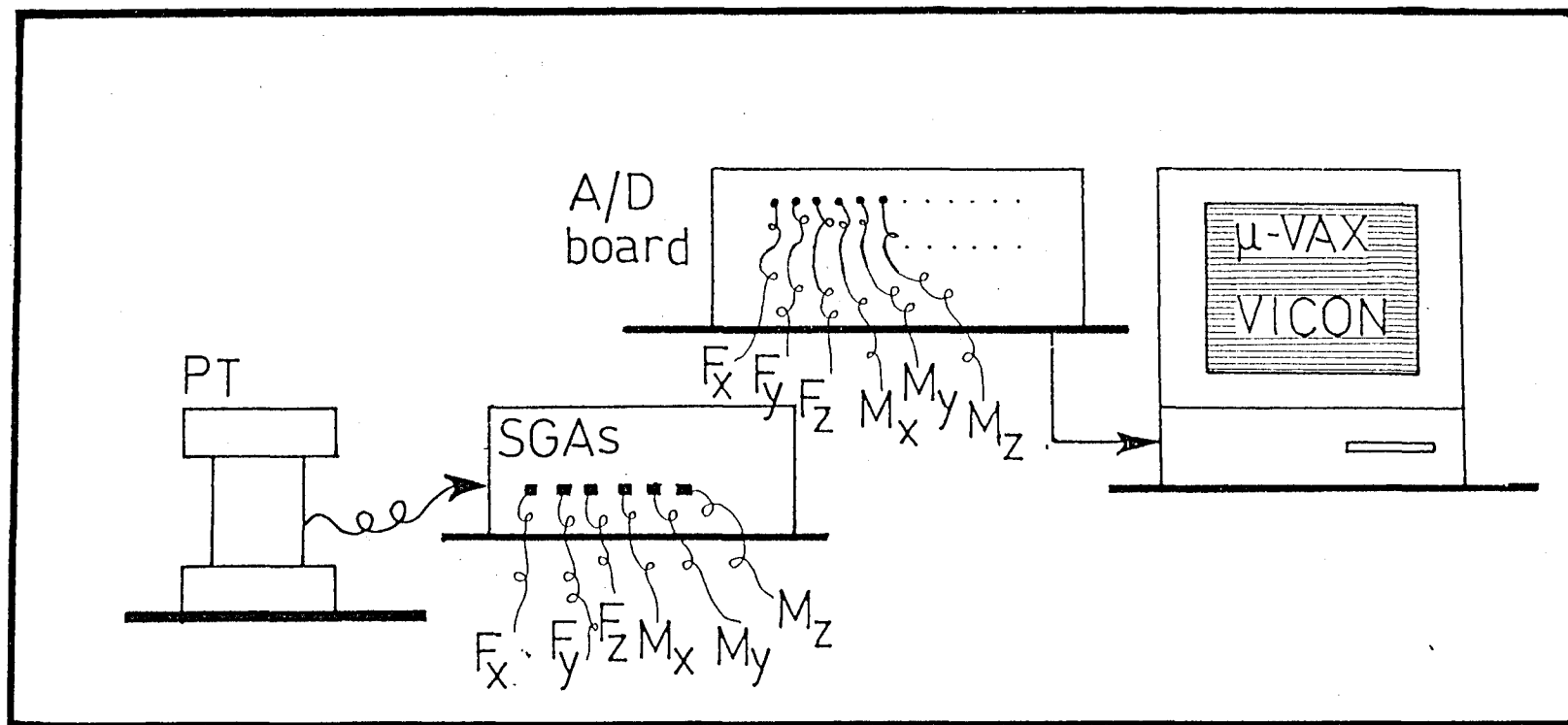


Fig 9.1 The equipment used for the walking tests

9.1 Introduction

The main reason for measuring prosthetic loading during amputee locomotion and other activities is the need for acquisition of data which would assist the formulation of testing standards for the lower limb prostheses.

This chapter presents the work carried out on amputee level walking. The next chapter presents the work carried out on amputee kneeling.

The experimental work presented in this chapter had two major tasks : a) to collect prosthetic loading data and compare them with the current international standard values (see section 2.5 in chapter 2) and b) to use the new method for alignment assessment, in order to draw conclusions based on the actual practice, which would help in the determination of future improvements and developments of this method.

These amputee level walking tests were carried out in the Gait Lab of the Bioengineering Unit. For the tests the services of an AK amputee were enrolled. This amputee was a heavily built male who was tested during two sessions, involving ten different tests.

The equipment used for the tests is described in section 9.2 , the prosthesis is described in section 9.3 and the actual tests are described in section 9.5 .

9.2 Equipment Used

The equipment involved in this study is shown in figure 9.1 and consisted of the following :

1. The Pylon Transducer with its Strain Gauge Amplifiers (shown as SGAs) and,
2. The microVAX computer of the Unit, to which all six channels of the amplifiers were connected through its AD Converter.
3. A terminal of the main frame VAX (not shown) which would be used to run the alignment assessment program presented in chapter 8.

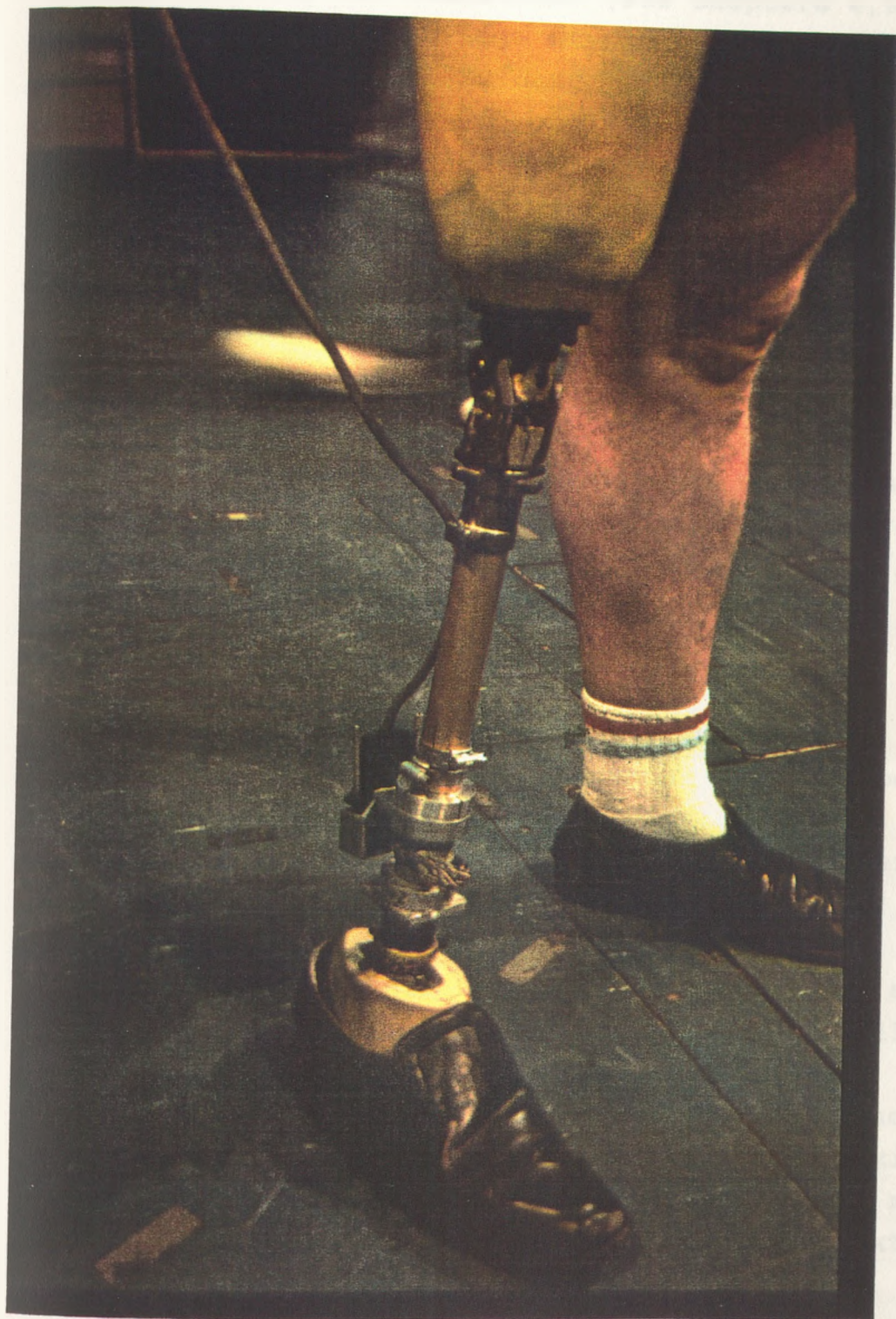


Fig 9.2 The pylon transducer
fitted in the prosthesis

No cameras were used, but one was assumed (dummy camera), in order to make the program run. The pylon transducer set-up was the same as that used for all tests involving the transducer (see chapters 4,5 and 6) ; gain settings and bridge supply voltages being also the same. A detailed description of the wiring connections is given in appendix IX .

The data acquisition procedure was governed by the VICON program installed in microVAX. The specifications of the above program were set as follows (presented with the format that VICON uses) :

- Highest Analog Channel = 6 (ie. the six channels of the pylon transducer),
- TV Channels used = 1 (ie. only one dummy camera was considered, since there were no cameras involved),
- Analog Data frame rate = 2 (ie. two digital samples from the analog data for each camera frame),
- Frame Intervals between samples =1
- Minimum TVD file size = 100 blocks
- TV frame rate = 50 Hz (the sampling frequency)
- Maximum capture time = 90 seconds (longest possible trial),
- AD gain = 8 (specification of the AD Converter),

9.3 Preparation of the Prosthesis

The AK prosthesis used for the tests was an Otto Bock modular prosthesis, fitted with a quadrilateral socket.

As shown in figure 9.2 , the pylon transducer was mounted in the shank of the prosthesis and proximal to an Otto Bock ankle adaptor. The knee unit was a modular Otto Bock single axis joint, with internal extension assist and adjustable constant friction.

Before the tests were carried out, the prosthesis was set to its Initial Reference Position (IRP) described in chapter 8. Thus, all joint frames as well

as the socket frame were set to their initial configuration, which was already stored in an appropriate data file and could be retrieved from the alignment assessment program ALIGNMENT.FOR exhibited in appendix XIII. This data file has already been presented in appendix VI and was called PATIENT3.DAT .

9.4 Description of the Tests

When the patient was fitted with his prosthesis, good knee and socket height were achieved by the prosthetist by cutting the shank tube appropriately.

Then the alignment assessment program was called on the VAX terminal and the data file for the patient was retrieved.

Each step of the procedure for the static and dynamic alignment of the prosthesis was performed by the prosthetist while the alignment program following the steps described in section 8.5.2 of chapter 8 was run. After each change that the prosthetist made on the alignment of the prosthesis, the new values of the alignment parameters were immediately displayed on the terminal and the prosthetist could proceed to the next step.

After having obtained a satisfactory alignment configuration the overall values of the alignment parameters were also shown on the screen. These values are exhibited in appendix VII.

The walking tests were carried out next. These tests were performed in two sessions :

a) One series of 4 tests involving walking on the "figure-8" path of the laboratory. The first 3 tests were on subject's own walking pace and the last test was on a faster pace. The subject's body mass including the prosthesis was 105.3 kg.

b) The second series of tests was carried out two

days later and consisted of 6 tests on the same walking path, but on subject's own pace only. The subject's body mass including the prosthesis was then 104.1 kg.

To distinguish between the nine tests carried out with a lower pace and the test carried out with a faster pace the tests were numbered from 1 to 9 for the former tests ; number 10 being given to the latter test.

Having carried out all tests further measurements on the patient were made in order to define quantities that might be useful in the processing :

greater trochanter to knee centre = 455 mm
ischial seat to bottom of heel = 870 mm
knee joint to bottom of heel = 500 mm
height of transducer center with
respect to top surface of foot = 97.5 mm

9.5 Manipulation of the Files

The data capture was done automatically by the microVAX computer and separate files for all tests were created. These files were given the extension .C3D by the VICON program itself and were not ASCII files.

To be converted to ASCII files they were all processed by the program ASCONV which is available in the microVAX. The results of this procedure were the ASCII files with extension .A3D, which unfortunately were not given a convenient form.

Thus a program called HAMECO.PAS written in the Pascal language was used in the main frame VAX, and provided easily readable versions of all files. This files were given the extension .DAT .

Thus the final versions of all the files were ready to be processed.

For the processing of pylon transducer loading data a computer program has been developed by Karagiannopoulos, 1991. This program is called GAIT.PAS

and is written in the Pascal language. The program is able to read the .DAT files acquired during amputee walking tests and to derive the six load components at any landmark of the prosthesis making use of the pylon transducer calibration matrix and of the alignment parameters of the prosthesis. Furthermore this program provides useful statistical information on the temporal parameters of the gait and the developed loads and thus it is possible to define the heaviest of the developed loads during the tests for the ankle, knee and hip joints.

It can be appreciated that the calculation of hip joint loads requires the use of a knee goniometer. However, since the current tests were only meant to monitor loads within the shank range of the prosthesis (ie from ankle to knee joints) no such goniometer was used and no hip-joint loads were calculated.

The program performed the processing of the acquired data in the following order :

First it converted all digital signals from computer units to mVolts. This was done by division of the signals by 1.625 *. Then the signals were converted to pylon transducer load components using the pylon transducer calibration matrix [C] (shown in table 4.4 in chapter 4). Finally, these loads were converted to ankle and knee joint loads using matrix calculations.

The print-outs provided by the program consist of a large number of results. In appendix VII only that part of the print-outs , which is useful for the present study, is shown. The next section presents the results obtained from the analysis of the data.

9.6 Results

As mentioned above the tests were carried out on the subject's own walking pace ; the only exception

* By the appropriate tests it was noticed that when 1 Volt input was applied to all channels of the ADC , the micro VAX recorded 1625 computer units in all channels.

test	cadence <u>steps</u> min	average duration of stance phase (sec)	average duration of gait cycle (sec)	<u>aver. stance phase</u> <u>aver. gait cycle</u> (sec/sec) %
1	83.99	0.871	1.429	60.95
2	82.24	0.885	1.459	60.66
3	84.87	0.863	1.414	61.03
4	82.66	0.858	1.452	59.09
5	83.81	0.887	1.432	61.94
6	83.99	0.841	1.429	58.85
7	84.41	0.844	1.422	59.35
8	85.86	0.832	1.398	59.51
9	82.78	0.870	1.450	60.00
10	91.37	0.761	1.313	57.96

Table 9.1 Average temporal data of the level walking tests
(in bold characters the values obtained with a higher walking pace)

being one test which was carried out in a faster pace. The results clearly confirmed the above. As shown in table 9.1 the cadence of the patient proved to be increased for that particular test (test 10).

Other temporal data are also shown in table 9.1. The percentage of gait cycle corresponding to the stance phase was very close to the expected value of 60% (see figure 2.1 in chapter 2). The only discrepancy in the above values was noted for test No 10 where the above percentage had a particularly low value in comparison to the rest of the tests (57.96 %) . This discrepancy was related to a decrease of the constant friction of the knee mechanism, which resulted in a longer swing phase.

Loading data for all tests are shown in table 9.2. These values correspond to the highest values of the load components occurring during each test at each level and at various moments of the gait cycles involved. Therefore, it can be appreciated that the maximum values shown are not simultaneous, but they can only provide an estimate of the magnitude of the developed loads.

The above values compare very well between the first nine different tests ; a fact that confirmed the repeatability of the measuring and recording equipment.

As far as test No 10 is concerned, there, the values of some components are clearly higher, as a result of the increased walking pace.

Despite the usefulness of the above values, it was not possible to compare the developed loads to the corresponding values of the standards for prostheses' testing, unless values occurring simultaneously during the tests were considered.

Therefore, using the cursor facility of program GAIT.PAS the simultaneous values of each set of five quantities were identified, for each one of the maximum values shown in table 9.2 . For example , for the maximum value 1268 N of F_y shown in table 9.2 for the

test	pylon transducer		ankle		knee		cross-over moment Mx (Nm)
	Fy (N)	My (Nm)	Mx (Nm)	Mz (Nm)	Mx (Nm)	Mz (Nm)	
1	1268	27	-24	121	49	87	73
2	1257	28	-22	119	49	86	71
3	1318	28	-25	120	53	85	78
4	1210	26	-20	119	45	88	65
5	1227	27	-18	120	49	83	67
6	1239	27	-17	120	43	85	60
7	1372	31	-19	120	41	89	60
8	1217	27	-13	122	41	89	54
9	1220	27	-15	121	37	87	52
10	1637	28	-28	121	59	95	87

Table 9.2 The loading data acquired from the level walking tests
(in bold characters the values obtained with a faster walking pace)

first test, the values of the other five load components were identified and for the maximum value 27 Nm of M_y shown in the same table, the values of the other five components were identified and so on. It can be appreciated that the above process resulted in six different configurations for each test ; each of which consisted of the maximum value of one load component and the five simultaneous values of the other components (60 configurations in total).

In order to facilitate inferences as well as the comparisons with the current values of international standards the following method was used to derive the "heaviest" of the possible configurations based on the obtained results :

For the nine tests carried out with normal walking pace, the nine configurations involving the maxima of F_y and the simultaneous values of the other five loads were considered. Then the maximum values of each one of these six load components were chosen to form a new configuration. This configuration although fictitious could very well be considered as the "heaviest" possible, since the load values were drawn from actual simultaneously occurring load components.

The same applied to all configurations and a set six different configurations was obtained for the normal-walking-pace tests. Each of these configurations was the "heaviest" possible involving one component only at its overall (through out all nine tests) maximum value. For test No 10, the above method was not used since it was the only one carried out at a faster walking pace. Tables 9.3 and 9.4 show the above loading configurations in comparison to the current values suggested by the current international standards (see figure 2.13 of chapter 2). It must be noted that the negative sign of bending moment Knee M_x in the values of the standards, is simply related a difference in the conventions.

Pylon Fy(N)	Pylon My (Nm)	Ankle Mx (Nm)	Ankle Mz (Nm)	Knee Mx(Nm)	Knee Mz(Nm)	Cross - over Mx (Nm)
1372	10	-9	-26	49	48	58
993	31	-23	114	16	69	39
989	30	-25	85	12	62	37
1006	23	-4	122	19	83	23
1248	5	7	-18	53	49	60
1023	23	8	118	25	89	33
1111	14	30	125	-44	86	74

Table 9.3 The maximum values of the six load components with the simultaneous values of the other five components compared with the Ottawa, 1991 international standards (for tests 1 to 9 with normal walking pace)

Pylon Fy(N)	Pylon My (Nm)	Ankle Mx (Nm)	Ankle Mz (Nm)	Knee Mx(Nm)	Knee Mz(Nm)	Cross - over Mx (Nm)
1637	0	2	-27	50	67	52
905	28	-25	64	-3	55	28
878	22	-28	92	1	57	29
900	23	-8	121	14	76	22
1500	1	3	-20	59	68	62
967	10	3	118	32	95	35
1111	14	30	125	-44	86	74

Table 9.4 The maximum values of the six load components with the simultaneous values of the other five components compared with the Ottawa, 1991 international standards (for test 10 with faster walking pace)

9.7 Discussion and Conclusions

When the first standards were formulated (see table 2.1 in chapter 2 or ISPO, 1978) , the suggested loading values were chosen to be all the maximum occurring values of the six load components under study and they were not simultaneous. This concept was later revised mainly because the "heavy" standard values led prostheses to failure when tested, while no such failures were reported in practice. The new concept was the formulation of standards which would consist of a compromise between the different load values . The standards presented in figure 2.13, are the most recently updated values. It was stated in chapter 2 that these values were produced at the Ottawa meeting of the ISO in 1991 (Paul,1991) and are here referred to as the "Ottawa standards".

Although the evaluation and update of the standards for the structural testing of prostheses should be the subject of extensive patient tests, the results obtained during the presented work could offer a first indication. In tables 9.3 and 9.4 the heaviest of the obtained configurations are compared with the Ottawa standards.

The load values recommended by the standards attempt to achieve a compromise between the maximum bending moments M_z (see values of Ankle and Knee M_z in table 9.3), the maximum values of bending moments M_x occurring at different moments of the gait cycle and finally the axial torque M_y and axial compression F_y .

However, the load values of the standards and the ones obtained during testing seem to be very close to ensure a reasonable safety factor. Although the values for the bending moments could be considered the result of a mechanical compromise, the recommended value for torque M_y is much lower than most of its experimentally derived counterparts and the recommended value for the axial compression F_y seems to be too low to anticipate its heavier counterpart occurring under a faster walking

pace (see table 9.4) .

The conclusions of this chapter, regarding the prosthetic loading and the measuring of prosthetic alignment , can be presented as follows :

- 1) Ten level walking amputee tests were carried out using the short pylon transducer and associated software and hardware. The results obtained for prosthetic loading compared to the recently updated Ottawa international standards showed a certain lack of safety factors of the latter, particularly for the bending moments in the antero-posterior plane and the axial torque. The same was also noticed for the axial compression in the case of a faster walking pace.
- 2) The evaluation and update of the standards can only be the subject of extensive tests, involving various walking surfaces and paces. This will be achieved with outdoor tests carried out with the new portable system.
- 3) The measuring of the length of the set screws of the adaptors was found time consuming and out of step with the computerized part of the method.
- 4) The presentation of the values of the alignment parameters on the screen as soon as they are achieved was considered impressive. However, in order to provide a simultaneous view of three successive alignment configurations, some programming alterations are needed.
- 5) The values of the parameters could be followed by a graphical display of the prosthesis in the form of a stick diagram in both AP and ML planes. That, if successful could even substitute the display of the values of the alignment parameters.
- 6) When the above requirements are met, the new method could consist a very good alignment assessment tool,

able to be used in association with the pylon transducer in combined prosthetic alignment and loading studies.

In the next chapter the patient tests on measurement of prosthetic loading are continued for a different application : the kneeling position .

CHAPTER 10

PROSTHETIC LOADING DURING KNEELING

10.1 Introduction

10.2 Equipment Used

10.3 Preparation of the Prosthesis

10.4 Method for the Analysis

10.4.1 Introduction

10.4.2 Stick-Diagram of the Prosthesis

10.4.3 Mathematical Considerations

10.4.4 Free Body Diagram Study

10.4.5 A Flowchart for the Method

10.5 Planning and Execution of the Test Procedure

10.6 The Manipulation of the Files

10.7 Results

10.8 Discussion and Conclusions

10.1 Introduction

The International Standards Organisation (ISO) are presently developing design criteria for artificial legs, related to the loads applied onto the prostheses, during various amputee activities. From experience in the field it has been reported that several AK prostheses have exhibited heavy wear on the knee mechanism, related to high loads occurring during kneeling of the amputees. It has also been reported that high static loads under these conditions led several knee units to failure.

Having realised the significance of such events, both in terms of amputee safety and in terms of the mechanical behaviour of the prosthesis, a series of tests were conducted, in order to evaluate the loads developed on artificial legs during kneeling. The first pilot tests are described in detail in this chapter.

Since the reason of failure was understood to be the development of high static loads, the tests were meant to monitor the maximum loads developed under a static loading configuration, with a heavy amputee.

It was thought that various types of feet and various toe-out angles may result in different kneeling loads, for the same prosthesis. Therefore the tests had to be conducted in a way that would incorporate a study of these parameters as well.

For the tests carried out the routine developed is discussed in this chapter, along with the results obtained. The required analysis is presented in a step-by-step detailed description and refers to a Blatchford modular AK prosthesis (Endolite leg), which was the one used for the pilot tests.

10.2 Equipment Used

The equipment involved in this study consisted of the following (see figure 10.1) :

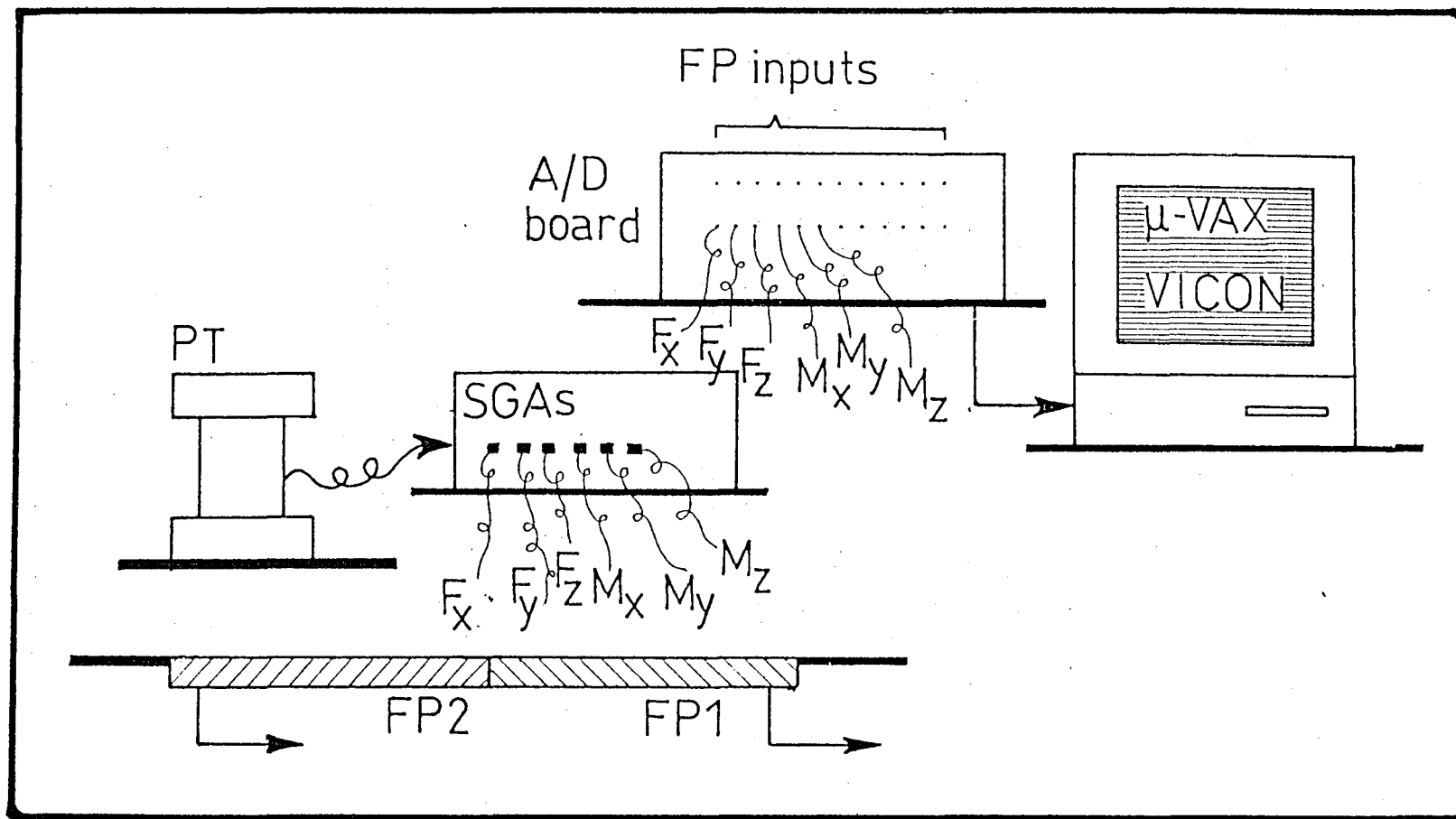


Fig 10.1 The equipment used in the kneeling tests.

1. Two Kistler force platforms (shown as FPs).
2. The Pylon Transducer with its Strain Gauge Amplifiers (shown as SGAs) and,
3. The microVAX computer to which all previously mentioned devices were connected through its AD Converter.

The set-up shown in figure 10.1 is the same with the set-up used for the walking tests described in chapter 9 (figure 9.1); the only difference being that this set up also involves the two force platforms.

No cameras were again used, but one had to be assumed (dummy camera), in order to make the VICON program run. Comparing figures 10.1 and 9.1 it can be seen that the connection of the channels to the A/D board, for the kneeling tests, the pylon transducer output signals are connected to the lower series of board inputs. This difference simply has to do with the internal connections of the board to the two force platforms. The specifications set in the VICON program for data acquisition and sampling were :

- Highest Analog Channel = 18
- TV Channels used = 1
- Analog Data frame rate = 1
- Frame Intervals between samples = 1
- Minimum TVD file size = 100 blocks
- TV frame rate = 50 Hz (sampling frequency)
- Maximum capture time = 30 seconds
- AD gain = 8

The FPs were directly connected through their own installation (ie charge and buffer amplifiers) to the first 12 channels of the AD Converter of the microVAX. The SGAs were connected with BNC-BNC cables to the next six channels of the AD Converter through the board shown (eighteen analog channels in total).

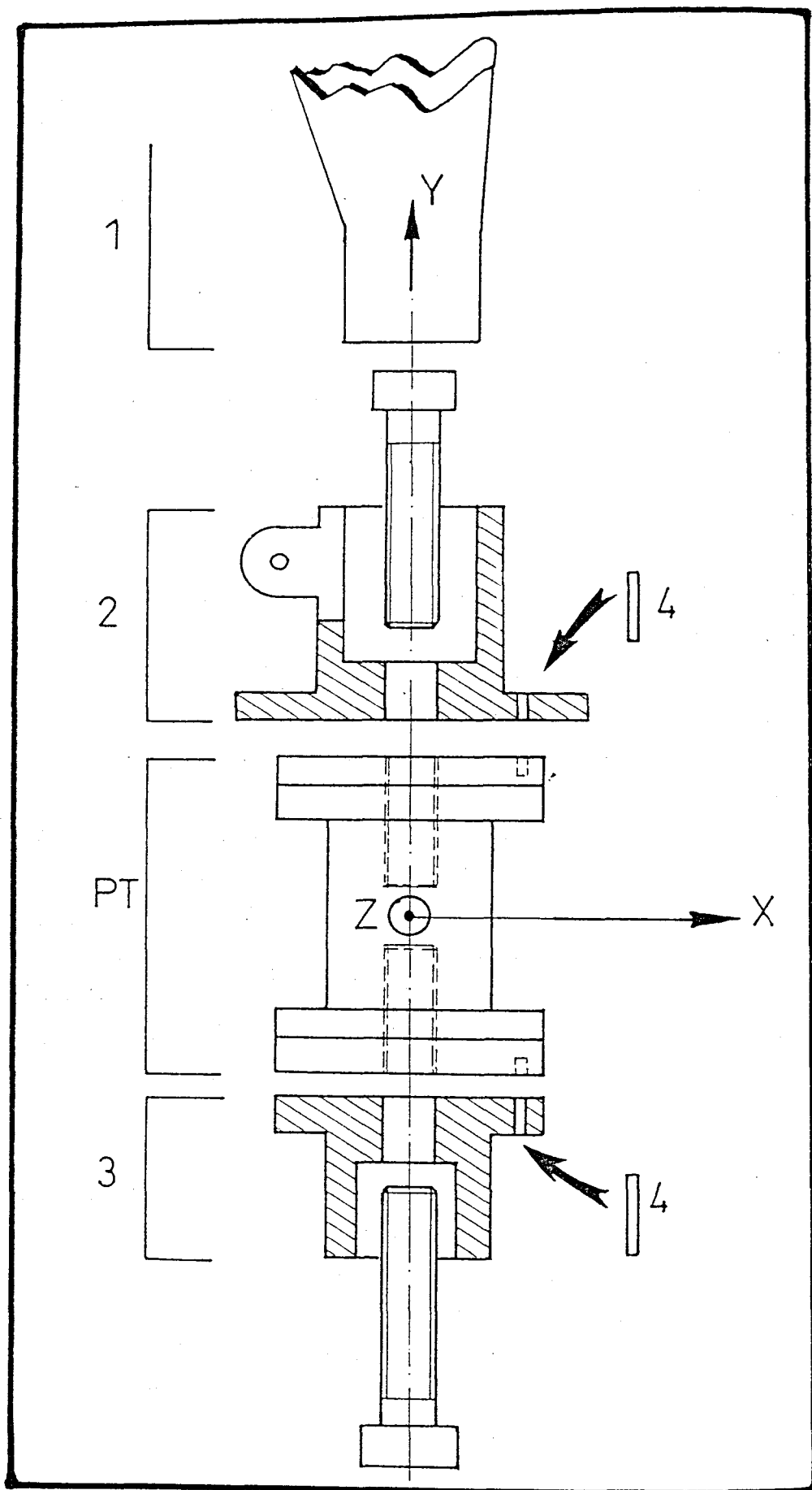


Fig10.2 The pylon transducer mounted within the Endolite shank.

10.3 Preparation of the Prosthesis

For the pilot tests , a Blatchford Endolite AK prosthesis was used. The space available in the prosthesis, for fitting the pylon transducer, was very restricted, because the swing phase control unit extended far down the shin tube. It was therefore decided to enlist the services of a tall amputee so that the pylon transducer could be fitted without problems regarding the length of the artificial side of the subject. The subject chosen was also heavily built (mass=100 kg) and would create high kneeling loads as required. However, it was recognised that the lack of space for the incorporation of the pylon transducer would result to more problems when testing shorter subjects , in the future.

A quadrilateral socket was prepared for the subject and mounted onto the proximal adaptor of the prosthesis and the alignment device was set to its neutral position.

The pylon transducer (shown as PT) was fitted on the shank of the prosthesis as shown in figure 10.2. At the proximal side an adaptor for SACH feet (2) provided by Blatchford was fixed and tightened against the shin (1). At the distal side of the pylon transducer a specially machined adaptor (3) was fixed. Two pins (4) were used to secure the system against rotation due to torque transmission.

The adaptor (3) would either be used to attach a SACH foot with its adaptor, or to attach a multiflex foot with its adaptor, depending on the test.

The pylon transducer frame was, as shown, with its X-axis facing anteriorly, Y-axis upwards and Z-axis laterally (since the subject was a right side amputee, this latter axis was directed from left to right).

10.4 Method for the Analysis

10.4.1 Introduction

The data acquired during these tests were :

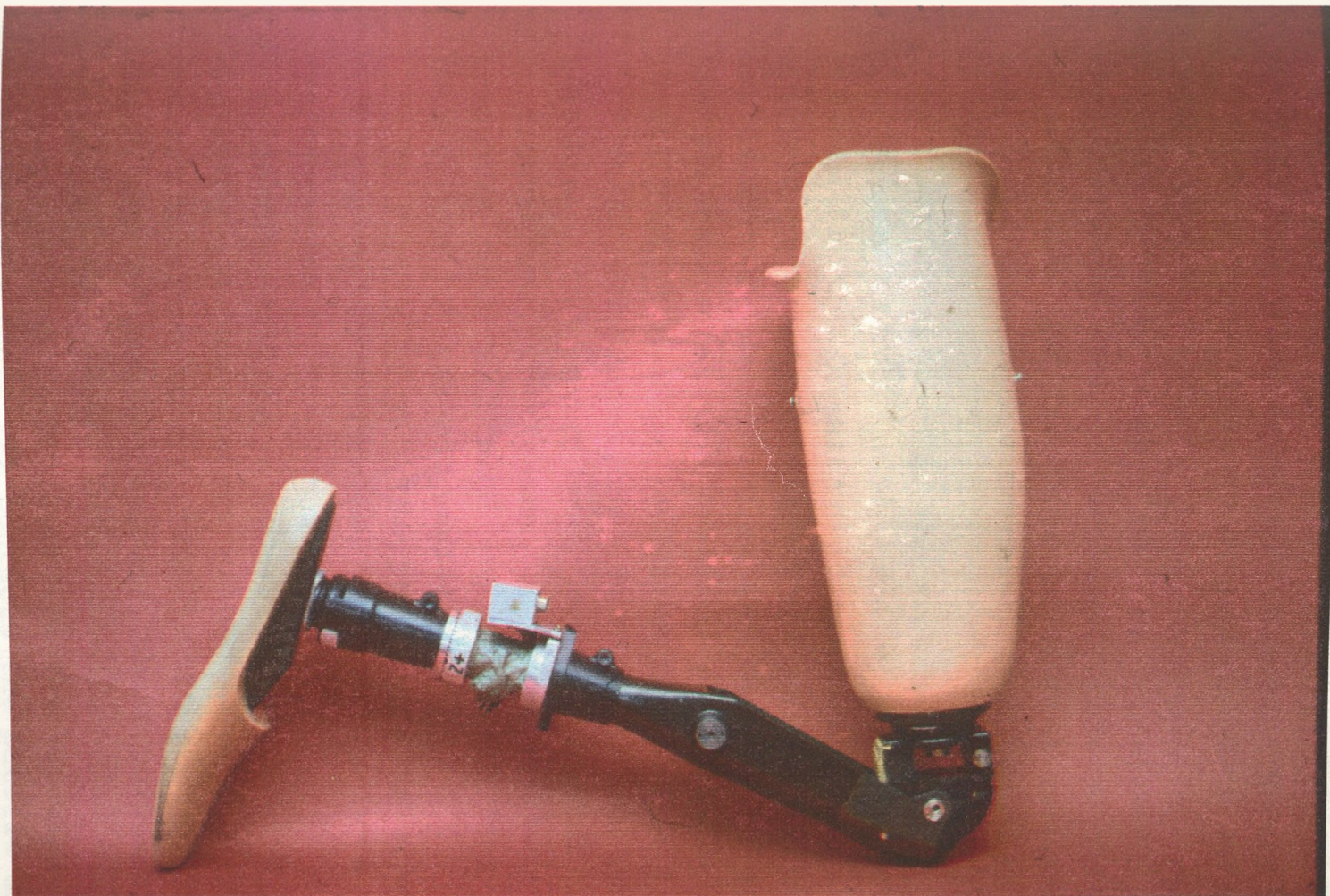


Fig 10.3a The kneeling position

- i) the six loads applied on FP1,
- ii) the six loads applied on FP2 and
- iii) the six loads applied on the pylon transducer,
all expressed in three different frames.

The results had to be expressed, within a frame matching the prosthesis, and therefore having the same orientation with the pylon transducer's frame (see figure 10.2).

For this task to be achieved, several considerations had to be made, from a mathematical point of view and furthermore, several assumptions had also to be made from a practical point of view.

10.4.2 Stick-Diagram of the Prosthesis.

For a better understanding of the free body diagram in the kneeling position and the mechanics involved, a stick-diagram of the Blatchford prosthesis was developed. This diagram was derived by inspecting the prosthesis at the kneeling position in order to identify all the major landmarks involved in the study.

These considerations, had to be as general as possible, in order to cover several kneeling configurations. The reason was that the tests would be conducted with both SACH and Multiflex feet and with both 0° and 90° toe-out angles.

In figure 10.3a the prosthesis is shown fitted with the pylon transducer and being in a kneeling configuration.

In figure 10.3b a general configuration is shown, depicting all the contact points along the prosthesis between toes and knee (which is the area of interest) for 0° and 90° toe-out angles . These points are :

for 0° toe-out angle

- point F1, where FP1 contacts the toe area,
- point F2, where FP2 contacts the patella area,
- point S, where the knee chassis contacts the shin,
- point K, which corresponds to the knee centre.

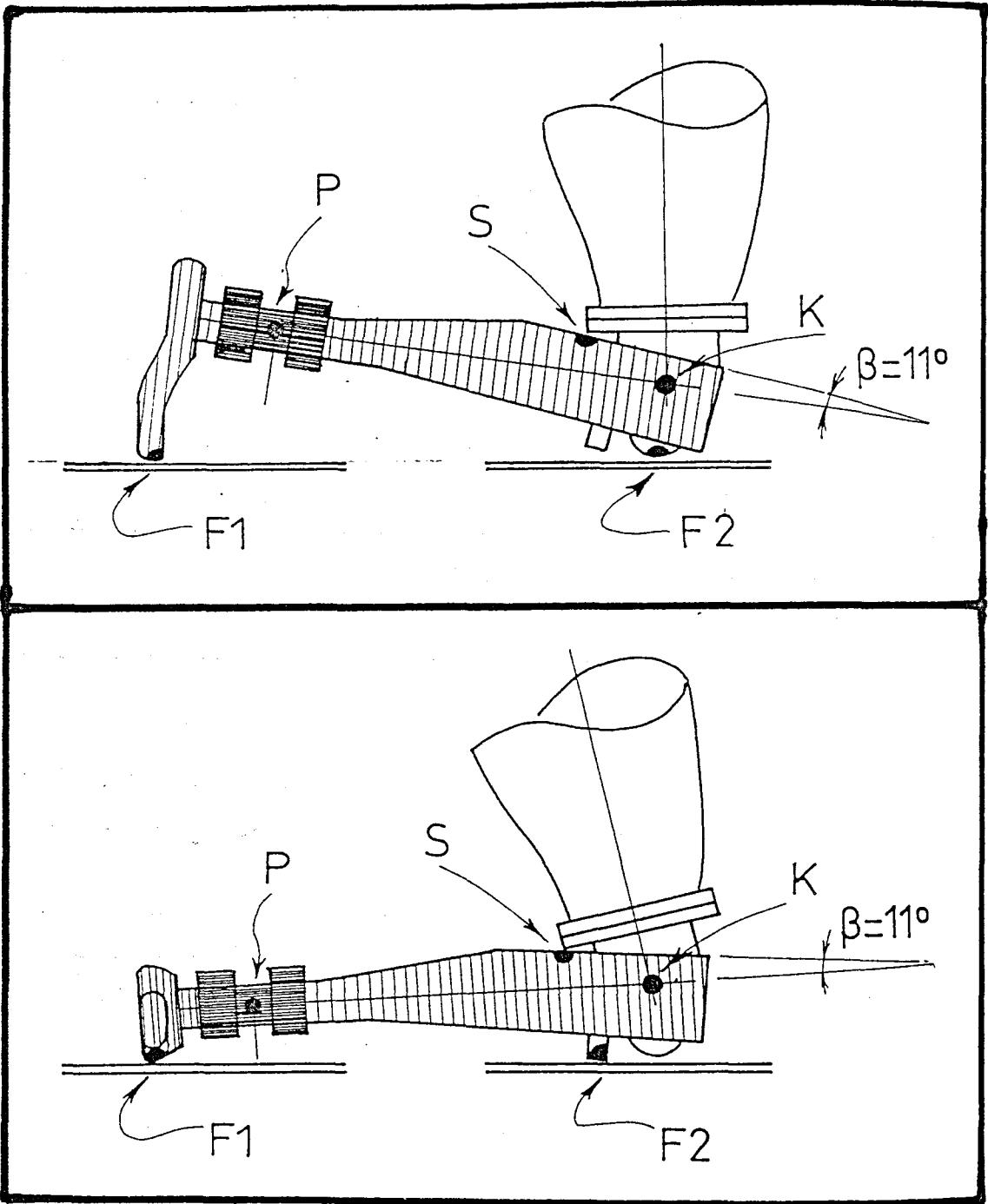


Fig10.3b The prosthesis at the kneeling position.

for 90° toe-out angle

- point F1, where FP1 contacts the medial side of the rotated foot,
- point F2, where FP2 contacts a small protrusion glued distally to the patellar component,
- point S, where the knee chassis contacts the shin,
- point K, which corresponds to the knee centre,

Point P, representing the centre of the pylon transducer and is also shown in both cases.

If therefore a free body diagram of the prosthesis was to be drawn and studied, these major landmarks had to be considered. Since the pylon transducer is also involved, two separate free body diagrams could be studied. These two different diagrams involve :

- a) The whole of the prosthesis distal to the knee axis (points F1, F2, S and K).
- b) The portion of the prosthesis between the centre of the pylon transducer and knee axis (points P, F2, S and K).

Having identified the major landmarks involved, the stick diagram of the prosthesis could be drawn for a general configuration.

As shown in figure 10.3b, the axis of the tubular distal position of the shin passes through the knee centre K. Therefore this line is considered the main axis of the diagram, on which both P and K are located.

Since, the structure is symmetrical about the sagittal plane passing through this axis, points S and F2 can be considered located on this plane (at the posterior and anterior sides respectively, when the subject is standing and at the superior and inferior sides respectively, when the subject is kneeling).

For the stick diagram to be completed, point F1 had to be identified against the main axis. To simplify

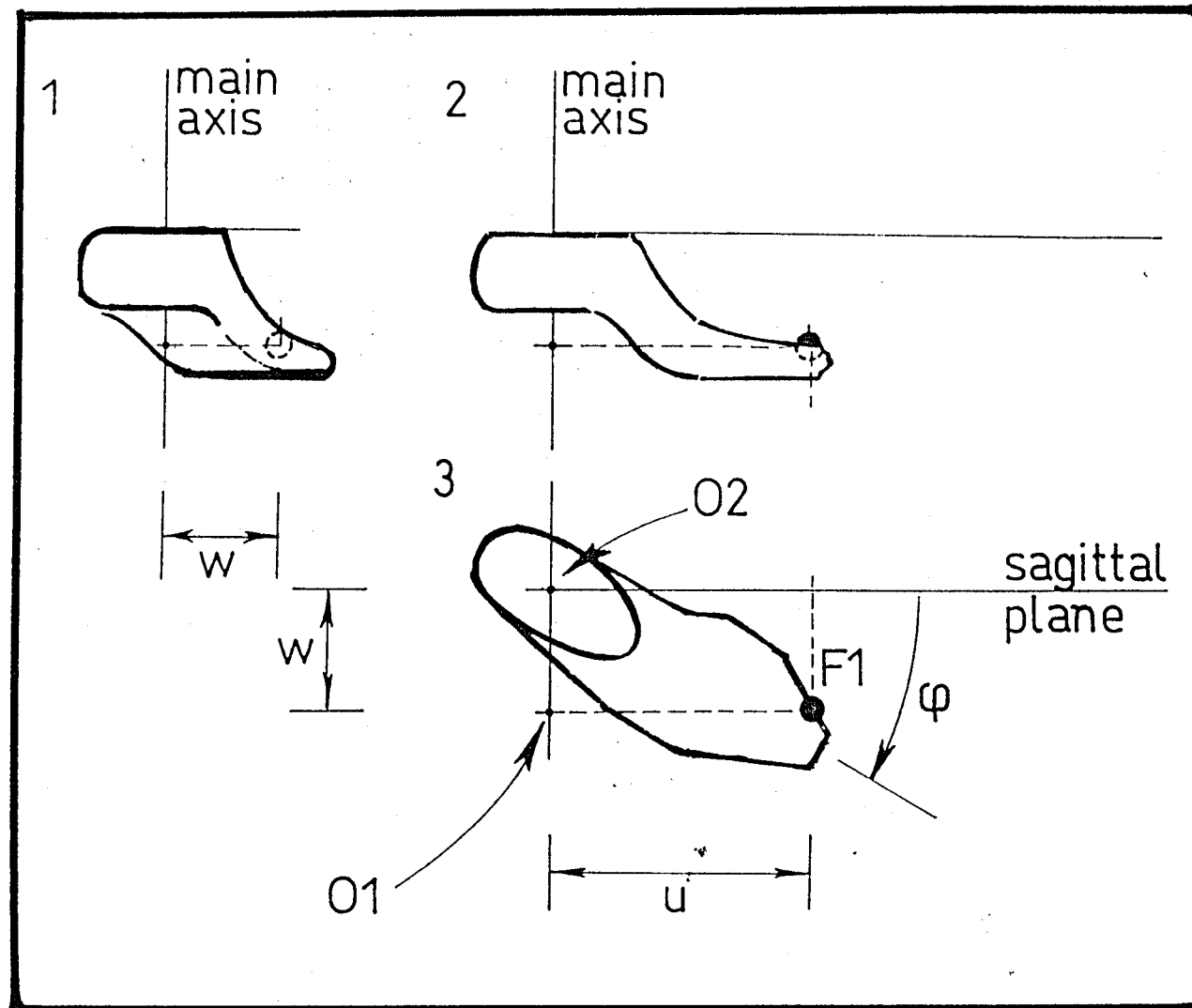


Fig 10.4 The foot at a general toe-out angle ϕ .

this task the following considerations were made :

In figure 10.4, a foot, in a general toe-out angle ϕ , is shown (no floor reference considered yet). The main axis of the shin is also shown in views 1 and 2, as well as the trace of the sagittal plane of symmetry of the shin in view 3.

When the subject is kneeling the contact point F1 occurs (floor reference introduced), depending on ϕ , somewhere between the big toe and heel on the medial side of the foot. Since, this figure represents a general case, let us consider point F1 to be where shown in view 3.

It is then obvious that F1 could be identified within the stick diagram by the two parameters u and w shown and could be connected to the main axis by means of the "sticks" $\overline{F1\ O1}$ and $\overline{O1\ O2}$. Thus the stick diagram was completed.

In figure 10.5, the stick diagram produced, is shown. Parameters P_1 , P_2 , P_3 , P_4 , P_5 , P_6 , P_7 and P_8 could be determined by measurements and thus known for any configuration chosen. It may be noted that parameter P_1 equals u (fig 10.4) and parameter P_3 equals w (fig 10.4) .

The prosthesis could then be fully described within frame { F1 } which was chosen as a reference. With respect to this frame, the x , y and z coordinates of all major landmarks shown, were as follows :

	x	y	z	
F1	0	0	0	: origin
F2	$(P_2 - P_1)$	P_4	$-P_3$	
K	$-P_1$	P_8	$-P_3$	
S	$-(P_1 + P_5)$	P_7	$-P_3$	
P	$-P_1$	P_6	$-P_3$	
O2	$-P_1$	0	$-P_3$	
O1	$-P_1$	0	0	

Thus, the prosthesis can be replaced by this stick diagram, and its free body diagram can be studied much easier.

However, whereas the pylon transducer loads are provided in axes parallel to the frame { F1 } axes, the loads of the FPs are expressed initially, in terms of the FPs frames. Therefore, a few more mathematical considerations were needed to convert these loads to the frame { F1 } and allow the study of the mechanics of the free body diagram.

10.4.3 Mathematical Considerations

The mathematical analysis required was based upon the following (fig. 10.5) :

(i) Points F1 and F2 lie in the floor plane (the patient is kneeling) and therefore vector $\overrightarrow{F1F2}$ also lies in the floor plane. In the stick diagram frame {F1} this vector could be described as :

$$(\overrightarrow{P_2} - \overrightarrow{P_1}) \mathbf{i} + \overrightarrow{P_4} \mathbf{j} + (-\overrightarrow{P_3}) \mathbf{k} \quad (10.1)$$

where \mathbf{i} , \mathbf{j} , \mathbf{k} the unit vectors of frame { F1 }.

(ii) Assuming that the sagittal plane of the shin was vertical to the floor (ie. the knee axis was horizontal), then the Z-axis of {F1} also lies on the floor plane .

Thus, it was clear that the Z-axis and vector $\overrightarrow{F1F2}$ could define the floor plane, with respect to the frame {F1} shown in figure 6.5. Vector $\overrightarrow{F1F2}$ was called, for obvious reasons \overrightarrow{FOR} (ward) . One more axis could then be defined : axis \overrightarrow{VER} (tical) which was normal to the floor plane and could be derived by :

$$\overrightarrow{VER} = \overrightarrow{k} \times \overrightarrow{FOR} = \det \begin{vmatrix} \overrightarrow{i} & \overrightarrow{j} & \overrightarrow{k} \\ 0 & 0 & 1 \\ (p_2-p_1) & p_4 & -p_3 \end{vmatrix} \Rightarrow$$

$$\overrightarrow{VER} = -p_4 \overrightarrow{i} + (p_2 - p_1) \overrightarrow{j} \quad (10.2)$$

A third vector could then also be defined, with respect to frame {F1}, being perpendicular to \overrightarrow{FOR} and \overrightarrow{VER} and facing laterally; forming a right hand system with the other two. This vector \overrightarrow{LAT} (eral) could be again derived by :

$$\overrightarrow{LAT} = \overrightarrow{FOR} \times \overrightarrow{VER} = \det \begin{vmatrix} \overrightarrow{i} & \overrightarrow{j} & \overrightarrow{k} \\ (p_2 - p_4) & p_4 & -p_3 \\ -p_4 & (p_2 - p_1) & 0 \end{vmatrix} \Rightarrow$$

$$\overrightarrow{LAT} = p_3(p_2 - p_1) \overrightarrow{i} + p_3 p_4 \overrightarrow{j} + [p_4^2 + (p_2 - p_1)^2] \overrightarrow{k} \quad (10.3)$$

The magnitude of these three vectors were calculated :

$$(10.1) \Rightarrow FOR = [(p_2 - p_1)^2 + p_4^2 + p_3^2]^{1/2}$$

$$(10.2) \Rightarrow VER = [p_4^2 + (p_2 - p_1)^2]^{1/2} \quad \text{and}$$

$$(10.3) \Rightarrow$$

$$LAT = [p_3^2 (p_2 - p_1)^2 + p_3^2 p_4^2 + [p_4^2 + (p_2 - p_1)^2]^2]^{1/2} \quad (10.4)$$

The frame of these three axes was thus a frame with two axes (\overrightarrow{FOR} and \overrightarrow{LAT}) belonging to the floor plane and therefore it was the most convenient way to relate the force platform frames to frame {F₁}. This frame was called {FVL}, after the initials of its three axes.

To totally describe frame {FVL} of these three vectors with respect to the frame {F1}, the direction cosines l, m, n of its three axes with respect to frame {F1} were needed. These cosines were derived as follows :

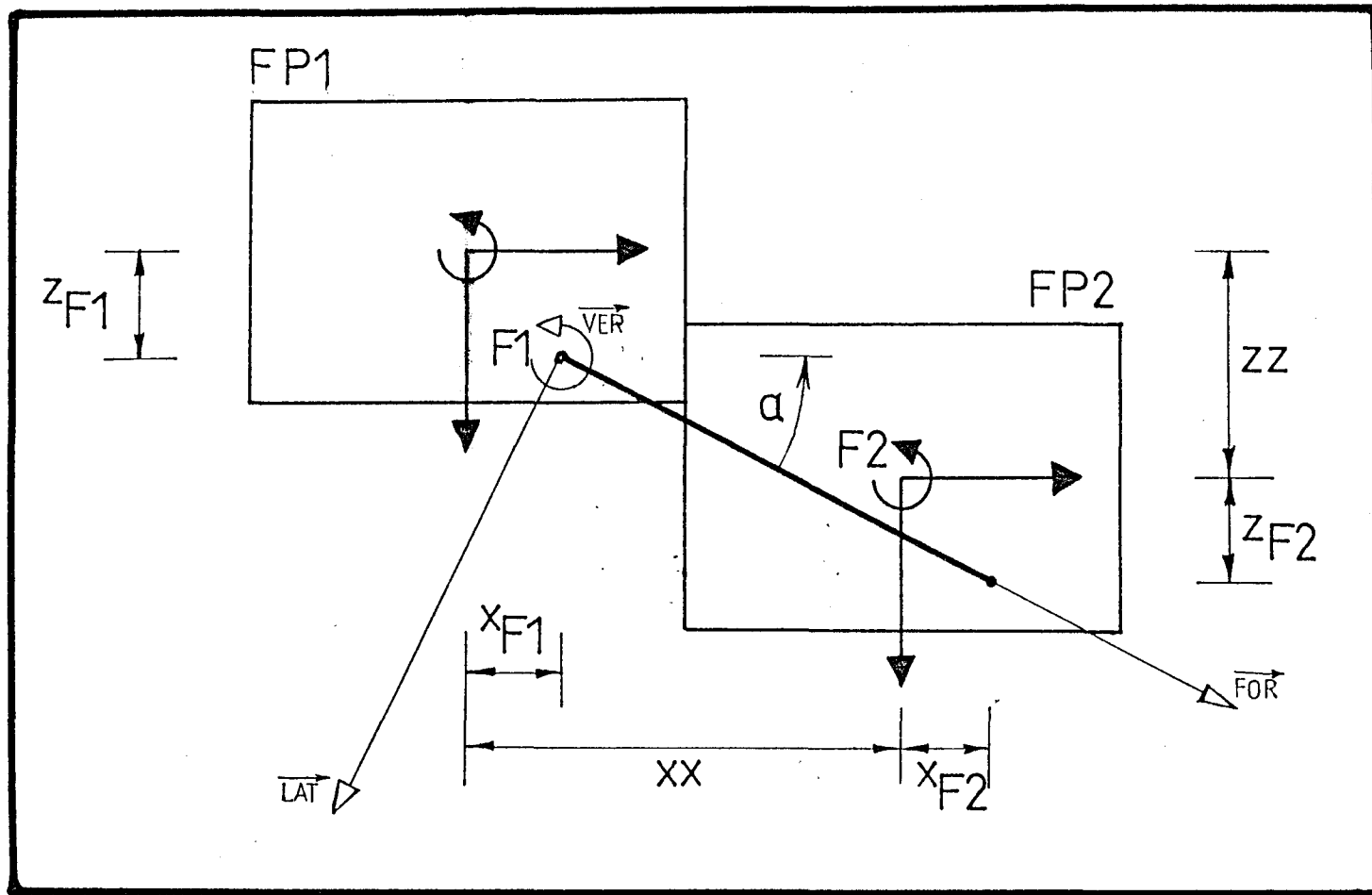


Fig10.6 The frames of the force platforms and the frame {FVL}.

$$\begin{aligned}
l_{FOR} &= \frac{p_2 - p_1}{FOR} & m_{FOR} &= \frac{p_4}{FOR} & n_{FOR} &= \frac{-p_3}{FOR} \\
l_{VER} &= \frac{-p_4}{VER} & m_{VER} &= \frac{p_2 - p_1}{VER} & n_{VER} &= 0 \\
l_{LAT} &= \frac{p_3 (p_2 - p_1)}{LAT} & m_{LAT} &= \frac{p_3 p_4}{LAT} & & \text{and} \\
n_{LAT} &= \frac{[p_4^2 + (p_2 - p_1)^2]}{LAT} & & & & (10.5)
\end{aligned}$$

Referring to Appendix V it is concluded that the orientation matrix R of frame $\{FVL\}$ with respect to frame $\{F_1\}$ was derived to be :

$${}^{F1}_{FVL} R = \begin{bmatrix} l_{FOR} & l_{VER} & l_{LAT} \\ m_{FOR} & m_{VER} & m_{LAT} \\ n_{FOR} & n_{VER} & n_{LAT} \end{bmatrix} \quad (10.6)$$

implying that : $\xrightarrow{\quad}$ FOR corresponds to X direction,
 $\xrightarrow{\quad}$ VER corresponds to Y direction,
 $\xrightarrow{\quad}$ LAT corresponds to Z direction.

To describe the two force platform frames with respect to frame $\{F1\}$: the orientation matrix of force platform frames with respect to frame $\{FVL\}$ had to be calculated.

Figure 10.6 shows the two force platforms FP1, FP2 with their frames and the corresponding contact points F1 and F2, already mentioned. The frame $\{FVL\}$ is also shown as imposed by the kneeling position. The angle α is defined as follows :

$$\tan \alpha = \frac{ZZ + Z_{F2} - Z_{F1}}{XX + X_{F2} - X_{F1}} \quad (10.7)$$

where: XX and ZZ are geometrical constants and $X_{F1}, Z_{F1}, X_{F2}, Z_{F2}$ are the coordinates of the contact points F1, F2 in the force platform frames (known as coordinates of the centres of pressure in the force platform literature), derived by the force platform data, as follows (see also fig 2.4 in chapter 2) :

$$\begin{aligned} X_{F1} &= (M_{Z1} + F_{X1} \cdot 0.040) / F_{Y1} & (m) \\ Z_{F1} &= (-M_{X1} + F_{Z1} \cdot 0.040) / F_{Y1} & (m) \\ X_{F2} &= (M_{Z2} + F_{X2} \cdot 0.040) / F_{Y1} & (m) \\ Z_{F2} &= (-M_{X2} + F_{Z2} \cdot 0.040) / F_{Y1} & (m) \end{aligned} \quad (10.8)$$

where the loads of the force plates $F_{X1}, F_{Y1}, F_{Z1}, M_{X1}, M_{Z1}$ and $F_{X2}, F_{Y2}, F_{Z2}, M_{X2}, M_{Z2}$ are expressed in N and Nm. The orientation matrix R of {FP1}, with respect to {FVL} can be readily derived as :

$$\begin{matrix} \text{FVL} \\ \text{FP1} \end{matrix} R = \begin{bmatrix} \cos \alpha & 0 & \sin \alpha \\ 0 & 1 & 0 \\ -\sin \alpha & 0 & \cos \alpha \end{bmatrix} \quad (10.9)$$

Finally to describe frame {FP1} with respect to the initial frame {F1} shown in figure 10.5, the following operation is needed :

$$\begin{matrix} \text{F1} \\ \text{FP1} \end{matrix} R = \begin{matrix} \text{F1} \\ \text{FVL} \end{matrix} R \circ \begin{matrix} \text{FVL} \\ \text{FP1} \end{matrix} R = \begin{bmatrix} r_{11} & r_{12} & r_{13} \\ r_{21} & r_{22} & r_{23} \\ r_{31} & r_{32} & r_{33} \end{bmatrix} \quad (10.10)$$

$$\begin{aligned}
\text{where : } r_{11} &= l_{\text{FOR}} \cos \alpha - l_{\text{LAT}} \sin \alpha \\
r_{12} &= l_{\text{VER}} \\
r_{13} &= l_{\text{FOR}} \sin \alpha + l_{\text{LAT}} \cos \alpha \\
r_{21} &= m_{\text{FOR}} \cos \alpha - m_{\text{LAT}} \sin \alpha \\
r_{22} &= m_{\text{VER}} \\
r_{23} &= m_{\text{FOR}} \sin \alpha + m_{\text{LAT}} \cos \alpha \\
r_{31} &= n_{\text{FOR}} \cos \alpha - n_{\text{LAT}} \sin \alpha \\
r_{32} &= n_{\text{VER}} \\
r_{33} &= n_{\text{FOR}} \sin \alpha + n_{\text{LAT}} \cos \alpha
\end{aligned} \tag{10.11}$$

Equation (10.10) described the orientation of frame {FP1}, with respect to frame {F1}. Referring to figure 10.5, another frame {F2} could also be considered in the same way as {F1} but with origin at point F2. It was obvious that equation (10.10) also described the orientation of frame {FP2}, with respect to frame {F2}.

Having completed the presentation of the necessary mathematical equations, the problem is solved :

If force platform FP1 detects at point F1 three forces F_{X1} , F_{Y1} , F_{Z1} and force platform FP2 detects at point F2 three forces F_{X2} , F_{Y2} , F_{Z2} then using equation (6.10) these forces can be converted to the convenient frames {F1}, {F2} as follows :

$$\begin{bmatrix} R1 \\ R2 \\ R3 \end{bmatrix} = \begin{bmatrix} r_{11} & r_{12} & r_{13} \\ r_{21} & r_{22} & r_{23} \\ r_{31} & r_{32} & r_{33} \end{bmatrix} \circ \begin{bmatrix} F_{X1} \\ F_{Y1} \\ F_{Z1} \end{bmatrix} \quad \text{and}$$

$$\begin{bmatrix} R4 \\ R5 \\ R6 \end{bmatrix} = \begin{bmatrix} r_{11} & r_{12} & r_{13} \\ r_{21} & r_{22} & r_{23} \\ r_{31} & r_{32} & r_{33} \end{bmatrix} \circ \begin{bmatrix} F_{X2} \\ F_{Y2} \\ F_{Z2} \end{bmatrix} \Rightarrow$$

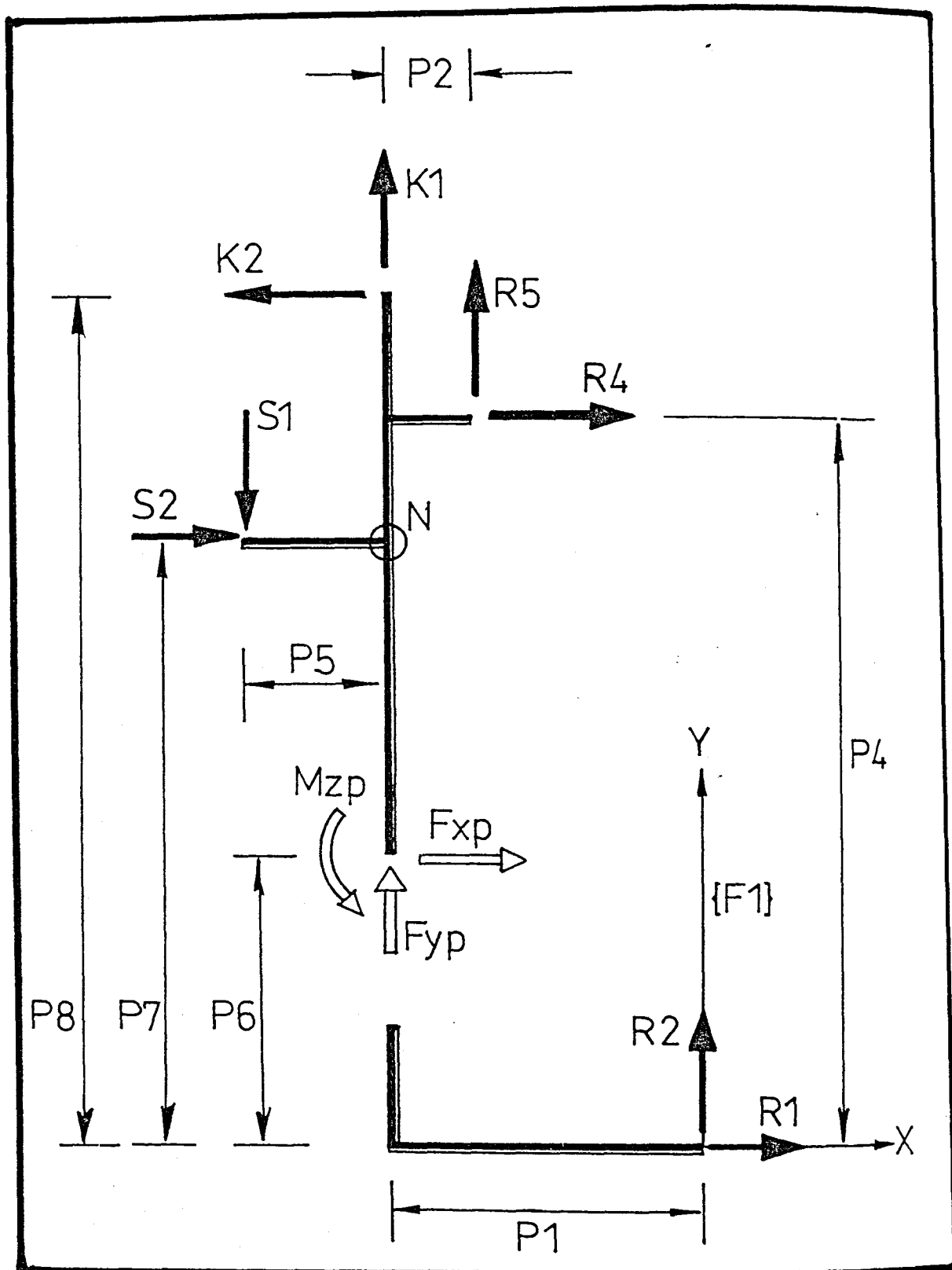


Fig 10.7 The free-body diagram of the prosthesis.

$$\begin{aligned}
R1 &= r_{11}^F X1 + r_{12}^F Y1 + r_{13}^F Z1 \\
R2 &= r_{21}^F X1 + r_{22}^F Y1 + r_{23}^F Z1 \\
R3 &= r_{31}^F X1 + r_{32}^F Y1 + r_{33}^F Z1 \\
R4 &= r_{11}^F X2 + r_{12}^F Y2 + r_{13}^F Z2 \\
R5 &= r_{21}^F X2 + r_{22}^F Y2 + r_{23}^F Z2 \\
R6 &= r_{31}^F X2 + r_{32}^F Y2 + r_{33}^F Z2
\end{aligned} \tag{10.12}$$

10.4.4 Free Body Diagram Study

The study of the free body diagram on the stick diagram of figure 10.5, is now possible with unique reference to the convenient frame {F1}, shown in the same figure.

In figure 10.7 the loads applied by the force platforms, as well as those applied through the pylon transducer, are considered in their positive sense. The loads K1, K2 applied on the knee axis, as well as the loads S1, S2 applied on the shin are considered in the sense anticipated for the kneeling position.

As shown in figure 10.3, the load on the shin by the knee chassis is applied at an angle β . Therefore :

$$S1 / S2 = \tan \beta \tag{10.13}$$

Writing the equations for the whole diagram, loads K1, K2, S1, S2 can be derived :

$$\sum F_x = 0 \Rightarrow R1 + S2 + R4 - K2 = 0$$

$$\sum F_y = 0 \Rightarrow R2 - S1 + R5 + K1 = 0 \quad \text{and}$$

$$\begin{aligned}
\sum M \text{ (at point F1)} &= 0 \Rightarrow \\
-R4 p_4 - R5(p_1 - p_2) - K1 p_1 + K2 p_8 + S1(p_1 + p_5) - S2 p_7 &= 0
\end{aligned} \tag{10.14}$$

Solving the system of equations (10.13) and (10.14) the solution is:

$$\begin{aligned}
S2 &= - \frac{R1 p_8 + R2 p_1 + R4 (p_8 - p_4) + R5 p_2}{(p_8 - p_7 + p_5 \tan \beta)} \\
S1 &= S2 \tan \beta \\
K1 &= S1 - R2 - R5 \\
K2 &= S2 + R1 + R4
\end{aligned} \tag{10.15}$$

the "nutcracker" moment which is of major interest in the tests, is the moment at the point N :

$$M_N = R1 p_7 + R2 p_1 \tag{10.16}$$

Writing the equations of the free body diagram again, but this time considering only the portion above the centre of the pylon transducer, loads K1 , K2 , S1 and S2 can be derived :

$$\begin{aligned}
\sum F_x &= 0 \Rightarrow F_{Xp} + R4 - K2 + S2 = 0 \\
\sum F_y &= 0 \Rightarrow F_{Yp} - S1 + R5 + K1 = 0 \\
\sum M \text{ (at point P)} &= 0 \Rightarrow \\
&-R4(p_4 - p_6) + R5 p_2 + K2(p_8 - p_6) + S1 p_5 - S2 (p_7 - p_6) + M_{Zp} = 0
\end{aligned} \tag{10.17}$$

Solving the system of equations (10.13) and (10.17) the solution is :

$$S2 = - \frac{R4 (p_8 - p_4) + R5 p_2 + F_{Xp} (p_8 - p_6) + M_{Zp}}{(p_8 - p_7 + p_5 \tan \beta)}$$

and,

$$\begin{aligned}
S1 &= S2 \tan \beta \\
K1 &= S1 - F_{Yp} - R5 \\
K2 &= S2 + F_{Xp} + R4
\end{aligned} \tag{10.18}$$

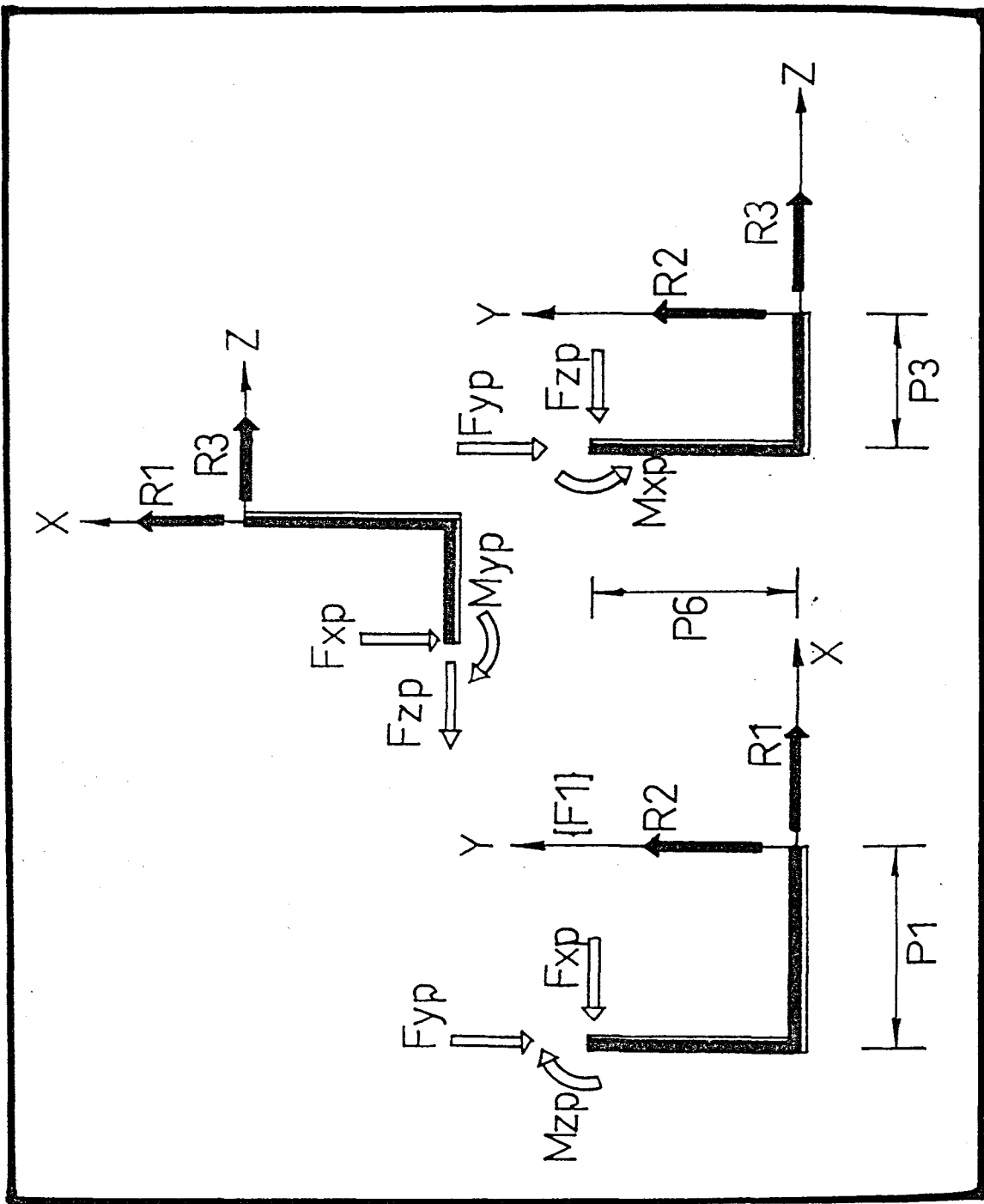


Fig 10.8 The free-body diagram of the prosthesis for the part distal to the pylon transducer.

and the "nutcracker" moment for this case is,

$$M_N = F_{Xp} (p_7 - p_6) + M_{Zp} \quad (10.19)$$

Having solved the system both ways, a cross check can be obtained, by comparing the results from equations (10.15), (10.16) and (10.18), (10.19).

Furthermore the pylon transducer can be checked against force platform FP1 and vice versa. This can be achieved by solving the free body diagram of the part of the prosthesis below the pylon level (see fig 10.8). The following can be derived from the three views available :

Note : The pylon transducer loads are now shown from proximal to distal (opposite than in fig 10.7) .

$$\begin{aligned} F_{Xp} - R1 &= 0 \\ F_{Yp} - R2 &= 0 \\ F_{Zp} - R3 &= 0 \quad \text{and} \\ M_{Xp} + R2 p_3 + R3 p_6 &= 0 \\ M_{Yp} - R1 p_3 + R3 p_1 &= 0 \\ M_{Zp} - R1 p_6 - R2 p_1 &= 0 \end{aligned} \quad (10.20)$$

From equations (10.20) the following three equations can be derived involving pylon transducer loads only :

$$\begin{aligned} F_{Xp} p_6 + F_{Yp} p_1 - M_{Zp} &= 0 \\ F_{Yp} p_3 + F_{Zp} p_6 + M_{Xp} &= 0 \\ F_{Xp} p_3 - F_{Zp} p_1 - M_{Yp} &= 0 \end{aligned} \quad (10.21)$$

Equations (10.20) and (10.21) were incorporated in the program developed for the solution of the problem and described in the next section. Nine quantities equal to the value of the above expressions (ideally zero) can be found in the listing of the program under the notation DIFF1 to DIFF6 (for equations 10.20) , and the notation EVAL1 to EVAL3 (for equations 10.21) .

10.4.5 A Flowchart for the Method

Since there are a lot of intermediate steps in the method, an overall flowchart is presented in this section for an easier following of the successive steps :

- 1) Determine parameters p_1 to p_8 for the configuration under study.
- 2) Determine the particular instant the data will be drawn from as well as the corresponding signals (see later in this section).
- 3) Determine coordinates X_{F1} , Z_{F1} , X_{F2} , Z_{F2} (eq 10.8).
- 4) Determine angle α (eq 10.7).
- 5) Determine FOR, VER, LAT (eq 10.4).
- 6) Determine direction cosines l , m , n of the axes of frame {FVL} with respect to frame {F1} (eq 10.5).
- 7) Determine elements r_{ij} (eq 10.11).
- 8) Determine $R1$ to $R6$ (eq 10.12).
- 9) Determine $S1$, $S2$, $K1$, $K2$ and M_N for FPs data (eq 10.15 and 10.16).
- 10) Repeat step 9 for transducer data (eq 10.18 and 10.19).
- 11) Use equations 10.20 and 10.21 to draw any further conclusions, regarding the results obtained using force platforms and pylon transducer.

A program was written following this flowchart to analyse the data acquired and is exhibited in appendix XIII. The whole method is based on the set of the first eight parameters (p_1 to p_8) and the $(3 \times 6)=18$ signals representing the loads of the FPs and PT.

Therefore the following point is of major importance. Attention must be drawn to the fact that the data acquisition routine of the microVAX provides a large amount of data. Referring to section 2 of this chapter the values given result to an analog data rate of $(1 \times 50) = 50$ samples/sec for each channel. This leads to an overall maximum of $(50 \times 30) = 1500$

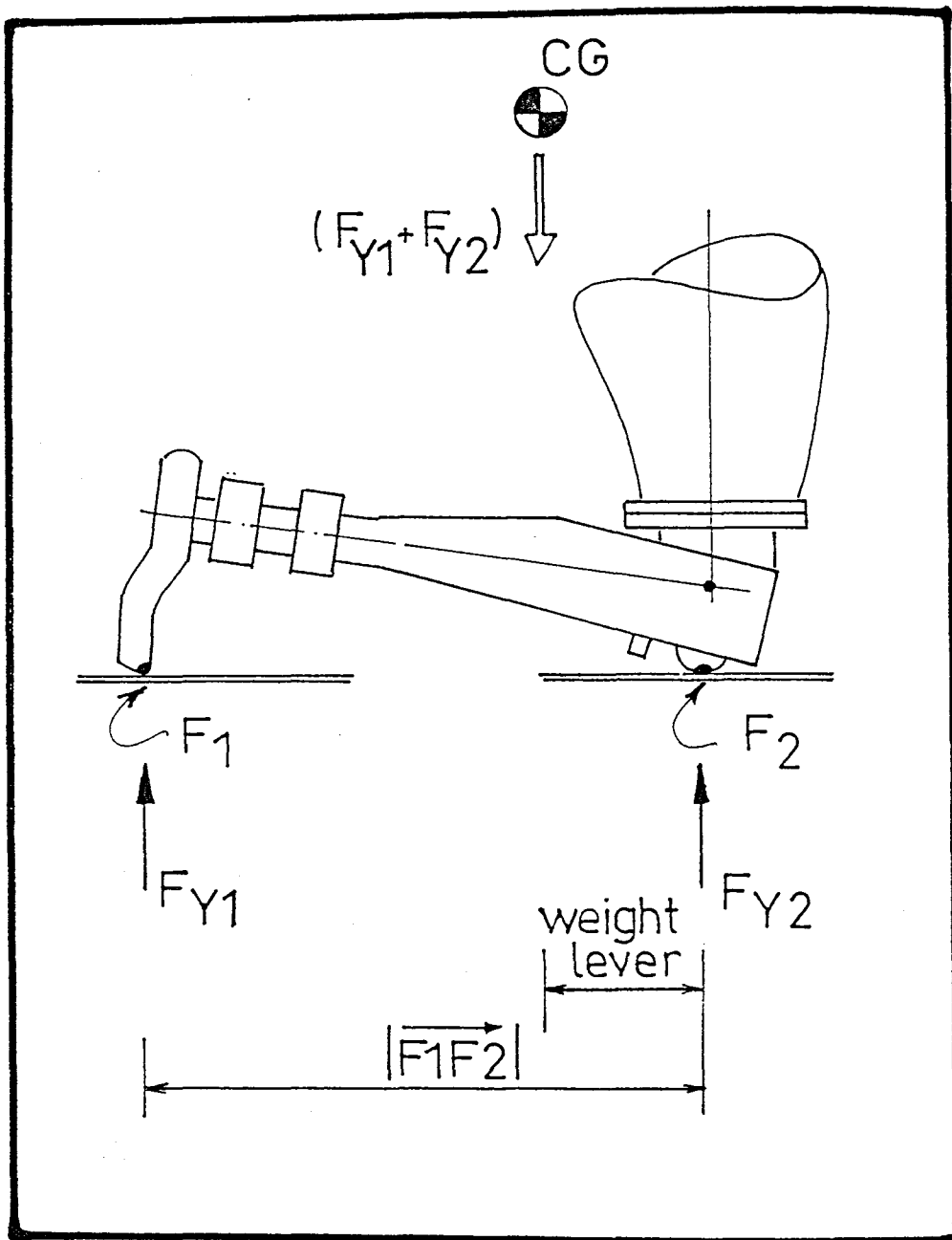


Fig 10.9 The system of forces and levers at the kneeling position.

samples per channel . This amount of data is received by the program developed and the issue arises about which is the set of signals to be considered for the test. In other words , since the kneeling position is to be studied statically, it must be determined which time moment's the data will be the ones to be processed and analysed.

Since the problem is being statically studied and the objective is to monitor the highest loads occurring, the data to be considered should be the data exhibiting the highest value of F_{Y1} ie. the vertical load of FP1 should be at its highest value. The more the amputee leans further back the higher the kneeling loads and of course the higher the reaction from FP1 which is posterior to the subject.

This criterion is incorporated into the program and provides the method with a set of data to work with.

At this stage another parameter was introduced to the study of the kneeling position, namely the position of the subject's centre of gravity (CG). It was recognised that during kneeling the amputee would be able to change the position of his CG over the prosthesis, because of his control over the hip flexors and therefore the monitoring of this position was considered important if more objective conclusions were to be drawn.

The position of the CG could be derived by studying the leverarms of the two vertical force plate reactions F_{Y1} and F_{Y2} . In figure 10.9 the system of leverarms is shown, and the following equation can be derived :

$$\text{Weight lever} = (F_{Y1} \cdot F1F2) / (F_{Y1} + F_{Y2}) \quad (10.22)$$

where the length $F1F2$ can be determined either by equations (6.4) or directly from the coordinates of the centres of pressure as :

$$(F1F2)^2 = (ZZ + Z_{F2} - Z_{F1})^2 + (XX + X_{F2} - X_{F1})^2 \quad (10.23)$$

A relative quantity could then be defined as the percentage of the distance $F1F2$ covered by the weight leverarm :

$$\text{Weight lever (\%)} = (\text{Weight lever}) \cdot 100 / (F1F2) \quad (10.24)$$

In addition to the above another quantity was also defined : the percentage of body weight supported by the artificial side.

$$\text{Percentage of weight} = (F_{Y1} + F_{Y2}) \cdot 100 / W \quad (10.25)$$

where : W is the amputee's weight in N .

Equations (10.24) and (10.25) were also incorporated in the program KNEE.FOR developed for the analysis of the data, and were meant to give a strong indication of the amputee's feeling of stability and confidence.

10.5 Planning and Execution of the Test Procedure

Initially the knee chassis alignment device adjustments of the prosthesis was set in neutral position. However, it was anticipated that any AP changes would alter the loading configuration and therefore the effect of two parameters had to be studied : the effect of Socket AP shift and of Socket flexion. As a result of this the following combinations had to be tried :

- i) socket AP shift set to maximum backward position (SAPS -) and Socket flexion set to its maximum and
- ii) socket AP shift set to maximum forward position (SAPS +) and Socket flexion set to its maximum.

The study had to include results for 0° and 90° toe-out angle, the reason being the evaluation of the effect of the foot's orientation on the resulting kneeling loads . Thus, another two parameters were introduced :

- iii) toe-out angle 0° and
- iv) toe-out angle 90° .

The Blatchford Endolite modular prosthesis may be provided with a rubber stance flex mechanism, whose major contribution is the absorption of shocks by a rectangular rubber block fitted in the mechanism. The effect of this mechanism during kneeling was to be studied and therefore an identical rectangular block machined from steel was to be used to allow for comparative studies. Thus , another two parameters were introduced :

- iv) rectangular rubber block (stance flex active) and
- v) rectangular steel block (stance flex locked).

Finally, the performance of SACH and Multiflex feet had also to be evaluated, introducing two more parameters :

- vi) Multiflex foot and
- vii) SACH flex foot.

All the above requirements resulted in the following planning of the experimental procedure :

<u>Test N^o</u>	<u>Description of parameters involved</u>			
1	Neutral alignment - Multiflex -	0° -	Rubber	
2	"	"	0°	Steel
3	"	"	90°	Rubber

4	Neutral alignment	SACH	0°	Rubber
5	"	"	90°	"
6	Socket max.flexion and SAPS (-)	"	0°	"
7	"	"	90°	"
8	Socket max.flexion and SAPS (+)	"	0°	"
9	"	"	90°	"

Each of the above tests was repeated three times. Before and after the whole of the test procedure zero readings were taken with all eighteen channels under no load; as far as the pylon transducer is concerned, for these readings to be taken the subject had to sit at a certain height and suspend his artificial shank without contacting the floor and in a balanced condition .

10.6 Manipulation of the Files

The data capture was done automatically by the microVAX computer and separate files for all sessions were created. These files were given the extension .C3D by the VICON program itself and were not ASCII files.

For the conversion of these files to ASCII files with the extension .DAT, the same method , as described in chapter 9, was used.

Before any actual processing the datum for each acquired signal had to be determined. Software based on the Minitab program available in the main frame VAX, averaged the data of the files corresponding to zero-readings and provided with values for the base-lines of all eighteen channels. The net values of all signals could thus be calculated.

The program was responsible for the conversion of the force plates signals into forces and moments. This was done by multiplying the net force platforms signals by the appropriate factors already determined by calibration of the force plates. These factors are

Socket Tilt	Socket AP Shift	Foot	Foot Rotation	"Nutcracker" Moment (Nm) (absolute values)				Shear force S developed against the shin (kN)				Shear force K developed at the knee axis (kN)			
neutral	neutral	Multiflex	0°	rubber stop		steel stop		rubber stop		steel stop		rubber stop		steel stop	
				force plates	pylon tran.	force plates	pylon tran.	force plates	pylon tran.	force plates	pylon tran.	force plates	pylon tran.	force plates	pylon tran.
				59.7	56.1	85.0	85.0	2.8	2.6	3.7	3.7	2.3	2.2	3.3	3.3
			62.1	57.7	68.8	64.6	2.9	2.7	3.1	2.9	2.5	2.3	2.9	2.5	
			61.9	59.2	107.0	104.4	2.9	2.8	4.7	4.6	2.5	2.4	4.3	4.2	
			90°	145.0	136.8			6.5	6.2			5.9	5.6		
		118.4	110.9	5.4	5.0			4.8	4.5						
		109.2	103.0	5.0	4.2			4.4	4.2						
		SACH	0°	59.9	55.9			2.8	2.6			2.4	2.2		
				54.7	48.7			2.5	2.3			2.1	1.9		
68.3	63.1		3.2	2.9	2.7			2.5							
90°	88.1		84.7	4.1	4.0			3.6	3.5						
	88.7	85.7	4.2	4.1	3.6			3.5							
*	*	*	*	*	*										
flexed at the limit	backward limit (-)	SACH	0°	79.8	74.6			3.5	3.3			3.1	2.9		
				79.1	73.5			3.6	3.3			3.1	2.9		
				94.7	88.2			4.2	3.9			3.7	3.5		
			90°	76.9	74.6			3.6	3.3			3.1	2.8		
				82.2	73.5			3.6	3.3			3.2	2.9		
				95.8	88.2			4.3	4.1			3.8	3.6		
	forward limit (+)		0°	91.8	86.3			4.1	3.9			3.6	3.4		
				80.9	75.4	3.6	3.4	3.1	2.9						
				92.2	86.1	4.1	3.8	3.6	3.3						
			90°	115.4	113.6	5.1	5.0	4.6	4.6						
				133.2	126.6	5.8	5.5	5.3	5.0						
				109.3	99.7	4.9	4.5	4.4	4.0						

* Unsuccessful data acquisition

Table 10.1 The results for the "nutcracker" moment M_N and shear forces S and K.

always stored in the parameters file of the VICON package, in the microVAX computer.

The program was also responsible for the conversion of the pylon transducer signals into loads. This was done by first converting the net microVAX signals to mVolts (division by 1.625 as mentioned in chapter 9) and then by using the pylon transducer calibration matrix.

10.7 Results

The values of the parameters p_1 to p_8 for every configuration tested, as well as an analytical presentation of the results from the pilot tests are exhibited in appendix IV.

There was practically no difference between the first and last zero readings and therefore those recorded in the beginning of the tests were taken as the general base lines.

The maximum developed loads, as derived from force platform data and from pylon transducer data are shown in table (10.1). These loads are the "nutcracker" moment M_N , the shear force S developed at the contact between knee chassis and the shin and the shear force K developed at the knee axis.

Table 10.2 exhibits the values of weight leverarm for each configuration and figures 10.10 and 10.11 show the change in the "nutcracker" moment M_N and the forces S and K with the weight leverarm, for the results obtained using the force platforms .

After having carried out the pilot tests, another set of tests was conducted. It consisted of 15 tests and it only involved one configuration. The patient was the same patient as before, but his new weight was increased to 104.1 kg .

The main objective in this series of tests was to acquire further data using only one configuration on the artificial leg. This configuration was chosen to be

Socket Tilt	Socket AP Shift	Foot	Foot Rotation	Weight Leverarm (%)	
neutral	neutral	Multiflex	0°	rubber stop	steel stop
				24.9	35.4
				25.9	28.6
		25.9	44.7		
		SACH	90°	64.7	
				52.7	
				48.9	
		SACH	0°	24.9	
22.6					
28.4					
SACH	90°	40.7			
		40.9			
		*			
flexed at the limit	backward limit (-)	SACH	0°	33.2	
				32.9	
			39.4		
			90°	35.7	
	38.4				
	44.4				
	forward limit (+)	SACH	0°	38.2	
				33.7	
38.4					
90°			53.7		
	62.0				
50.2					

* Unsuccessfull data acquisition

Table 10.2 The results for the weight leverarm .

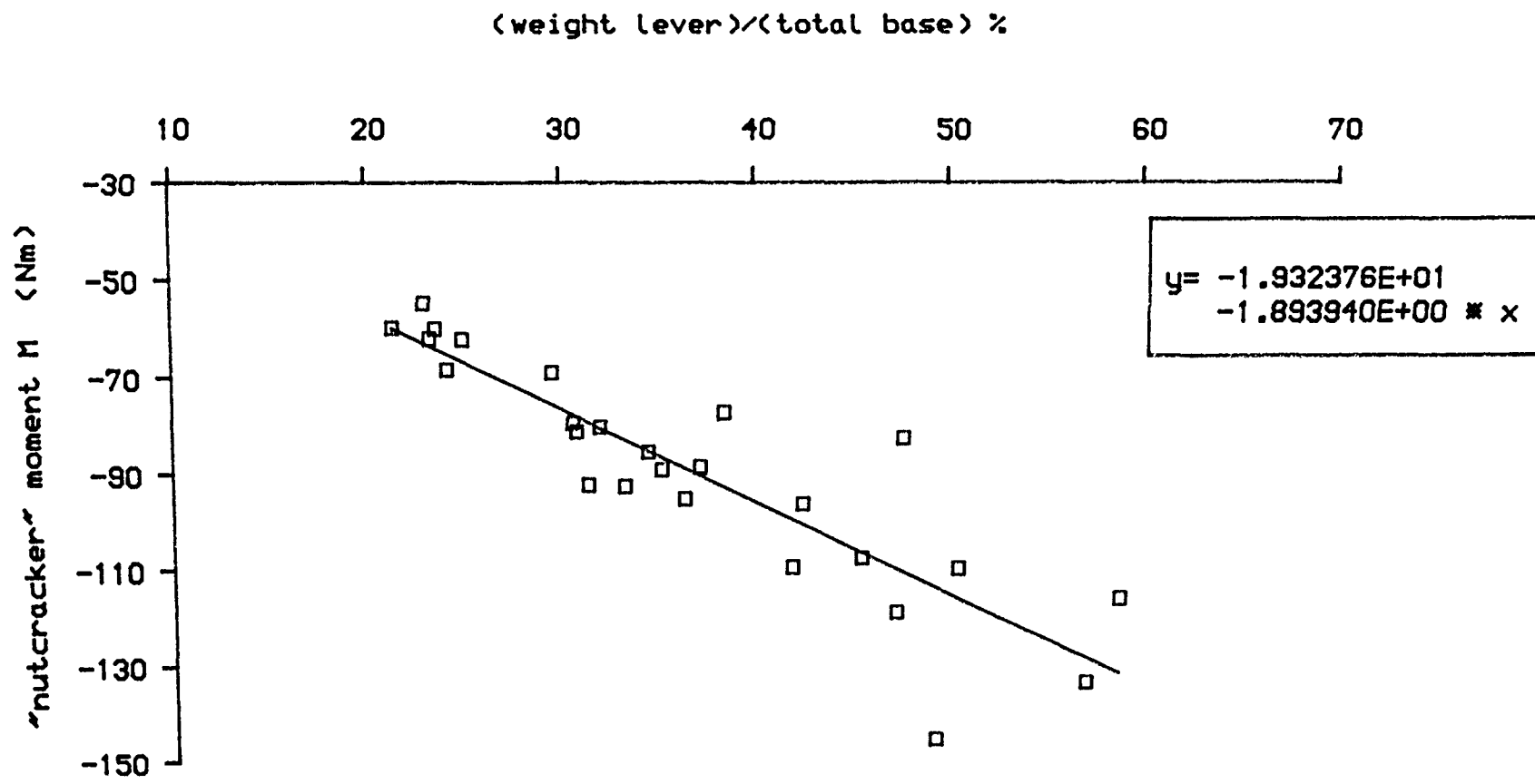


Fig 10.10 The change in “nutcracker” moment with the weight lever

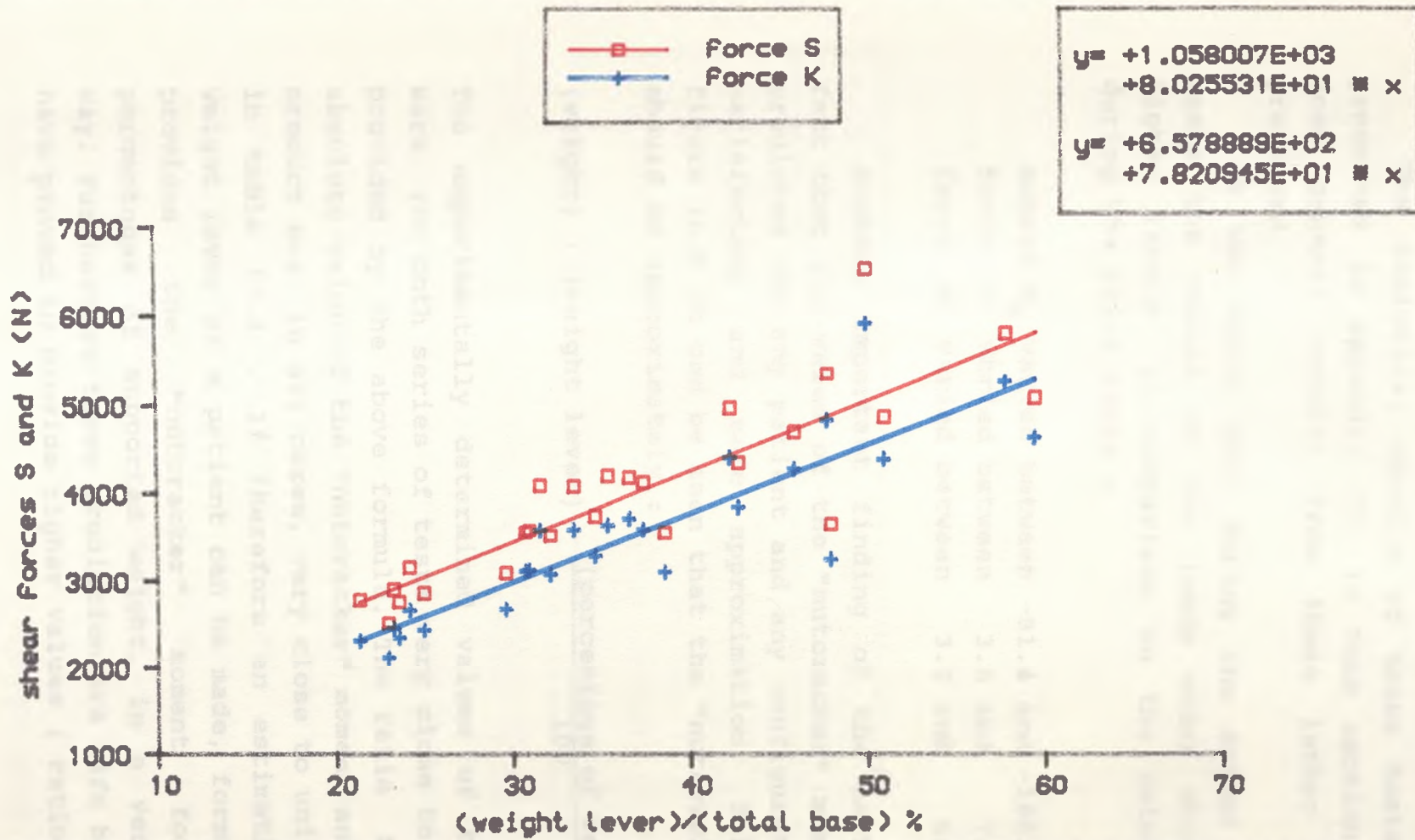


Fig 10.1 The change in shear Forces S and K with the weight lever

the configuration the patient felt more comfortably with. No toe-out rotation was used and the foot mounted on the prosthesis was of SACH type.

The analytical results of these tests are also presented in appendix IV. In this section, however, some general results from these latter tests are presented.

It was noted that during the second series of tests the values of the loads under study reached higher levels, in comparison to the values reached during the pilot tests :

moment M_N	varied between	-81.4 and -165.6	Nm
force S	varied between	3.6 and 7.1	kN
force K	varied between	3.2 and 6.6	kN

Another important finding of the tests was the fact that the value of the "nutcracker" moment can be predicted for any patient and any configuration with a satisfactory and safe approximation. Referring to figure 10.9 it can be seen that the "nutcracker" moment should be approximately :

$$(\text{weight}) \cdot (\text{weight lever}) \cdot \frac{(\text{percentage of weight})}{100} \quad (10.26)$$

The experimentally determined values of this moment were, for both series of tests very close to the values provided by the above formula. The ratio between the absolute value of the "nutcracker" moment and the above product was, in all cases, very close to unity as shown in table 10.3 . If therefore an estimation of the weight lever of a patient can be made, formula (10.26) provides the "nutcracker" moment for various percentages of supported weight, in a very accurate way. Furthermore these prediction are safe because they have proved to provide higher values (ratios < 1).

	minimum value	maximum value	mean value	standard deviation
pilot tests	0.9266	0.9727	0.9554	0.0152
second series of tests	0.9344	0.9554	0.9514	0.0052

Table 10.3 The statistical data of the ratio between the "nutcracker" moment and the product of formula 10.26

10.8 Discussion and Conclusions

The main objective of the tests was the establishment of values for the high static loads developed at the kneeling position. The loads of interest were found to be the "nutcracker" moment M_N and the two forces S and K acting on the shin wall and the knee axis respectively.

Another objective of the tests was the study of the influence that various parameters have on the resulting loads. Since the beginning of the tests, the anticipated result was that the loads would be increased for any configuration favouring the translation of the amputee's centre of gravity (CG) towards the posterior side; in other words, for any configuration which would allow the subject to lean farther back. From figures 10.3 and 10.9 it can be appreciated that such a configuration would involve socket set-back, socket full flexion, toe-out rotation and maybe use of the rubber stop in the stance flex mechanism (flexible component). It was also anticipated that the configuration involving all the above simultaneously would result in the heaviest loads.

However the results obtained from the tests did not support all the assumptions stated above : although the loads did increase as a result of the increase in the weight lever (see figures 10.10 and 10.11) , this latter increase was not always obtained by the anticipated configurations.

This observation was thought to be due to the subject's own positioning and control over it. The amputee's hip musculature was able to compensate for any configuration, which was not felt safe enough. Therefore each time the subject felt that the particular setting would impose a leaning too far back, used the hip flexors to translate the CG forward. Although this was possible for socket set-back and full flexion, in the case of 90° toe-out rotation, where the displacement of the ischial seat was very large

(see figure 10.3), the patient had little control and as a result of this situation the loads were increased.

It is interesting to note that whereas the 90° toe rotation has beneficial effects on the artificial legs of BK amputees as Al-Turaiki (1990) has reported , the work presented in this chapter proved that such a rotation is dangerous for the AK artificial legs because it results in very high static loads.

The tests were also to answer whether the type of foot makes any difference. From the results presented in tables 10.1 to 10.4 such conclusion cannot be drawn. In fact the use of multiflex or SACH feet did not result in different values. There is however a difference which was observed during the actual tests : due to the flexibility of the multiflex ankle and the shape of this foot, the centre of pressure was displaced towards the axis of the shank, thus decreasing the ML lever (parameter P3 in figure 10.5) of the ground reaction. This change did not affect the results because the study concerns the AP plane in which there was no change. Even if parameter P3 was not measured from the beginning, but was derived by the program as the ratio of the pylon loads (MYp/FXp), the results would not be different either, for the same reason.

Finally, the results obtained by the force plates and pylon transducer were considered in most of the cases comparable and therefore satisfactory. Discrepancies were thought to be due to the assumptions regarding the geometry of the tests.

The major conclusions drawn from this work may be presented as follows :

- 1) During kneeling the AK amputee applies very heavy static loads on the prosthesis. The 41 tests carried out showed that the "nutcracker" moment can reach values as high as 165 Nm for a heavily built subject with corresponding shear forces at the shin wall and

knee axis of about 7 kN. As a general conclusion it can be stated that the loads developed during kneeling can reach very high values and could well lead to wear of the knee mechanism and fracture of the shin wall, particularly when of dynamic nature.

2) The "nutcracker" moment can be predicted by formula (10.26) for any configuration. Using this value and the prosthesis' geometry the shear forces can also be estimated. The fact that this prediction method takes into account the two percentage values shown gives to the method a general validity, because during the tests it was noted that the patient may generally have a considerable control on the position of the body centre of gravity as well as on the amount of body weight applied on the artificial side.

3) The only alignment change that has a drastic effect on the developed loads is the toe-out angle. When a 90° toe-out angle is established the developed loads should be expected to reach relatively higher values.

This chapter was the concluding part of the presentation of the work carried out during this project. The next chapter presents a global discussion and the general conclusions of the work as well as a series of recommendations for future work.

CHAPTER 11
DISCUSSION , CONCLUSIONS
AND FUTURE RECOMMENDATIONS

11.1 Discussion

The multi-component pylon transducer designed and reported by Berme et al. (1976) has been used, in prosthetic loading measurements for the assessment of many tasks during various amputee activities. The project work conducted and reported in this thesis consists of a series of theoretical studies and experimental work which were carried out in order to establish the behaviour of the transducer and develop further equipment, methods and techniques for its use in various prosthetic research applications.

The theoretical analysis of the pylon transducer, presented in chapter 3, resulted in the quantitative evaluation of its main effects. The main effects, as explained in chapter 2, are the sensitivities of the six channels of the transducer to the corresponding load components. The fact that the sensitivity coefficients obtained theoretically, were found to compare very closely to the values derived during calibration using dead-weights, conducted by former researchers, was a verification that the design and the main behaviour of the six channels is acceptable.

As discussed in detail in the thesis, strain-gauge transducers generally exhibit cross-effects, which must be quantified by calibration together with the main effects. The dead-weights method used by former researchers proved to be the most accurate approach for this purpose. The use of the Instron materials testing machine, despite the highly controllable mode of load application it provides, generally introduces unwanted friction-effects.

The above comment is a conclusion drawn from the presented work and is in agreement with the force measurement literature (eg Bray et al. 1990, chapter 7). The use of the Instron machine, particularly when it involves complex devices, is likely to result in peculiar propagation of the stress field and therefore is not recommended for tests like the calibration or

the evaluation of force transducers. The set - ups developed and presented in chapters 4 and 5 of this thesis led to various problems and uncertainties. Some of these set-ups proved not suitable at all (see bending moment and torque tests) and some others remain under question until more tests are carried out to justify their reliability (see axial load and validation tests). The shear load set-up, however, was not considered affected by any of the problems mentioned above.

It is always desirable to conduct tests of a similar nature using the same equipment , for reasons related to metrological and statistical considerations. Therefore , the author of this thesis suggests that a specially designed rig should be developed in the future for all the above tests, which using dead-weights and the useful principles already established by former researchers, would provide the possibility of single and multiple loading configurations of any order . Particularly the multi - load component configurations are of major importance because they supply information about the behaviour of the transducer under combined loading.

The second-order calibration model presented in the introductory investigation of chapter 6 and the subsequent comparisons to the linear model proved that, despite the ambiguity of some of the results, the contribution of higher order terms is not, practically, sizeable.

The pylon transducer can also be used in order to evaluate the effect of alignment on the walking pattern of amputees. The assessment of prosthetic alignment for such a purpose should be a fast process allowing the determination of the alignment parameters among different trials without any need of removing the prosthesis from the subject and measuring it separately. The new alignment assessment method presented in chapter 7 and 8 provides such an important

possibility. The method was used during amputee tests; it was evaluated and further improvements became clear.

This method based on a 3-D modelling of the Otto Bock modular system and the adjustability of its adaptors was simulated with a computer program and can provide the prosthetist with an immediate quantitative feed-back. By calculating the position and orientation of all frames of reference of the prosthesis this method also provides the mathematical background for the pylon transducer detected loads to be transferred to all prosthetic or anatomical joints.

The amputee tests presented in chapters 9 and 10 supplied useful information on the loads occurring on the prosthetic side of an amputee during level walking and kneeling. The walking tests showed that some of the loading values currently recommended by the standards might be rather low to meet the loads applied by a "heavily built" active amputee. Loads encountered during kneeling are well above the corresponding values during walking. This was the reason that the international committee actually asked for such tests to be conducted.

The study of kneeling presented in chapter 10 is the first ever conducted study on this in particular activity. Its significance relates to the fact that many amputees, due to cultural or religious reasons, very often kneel and therefore the loads measured during the presented tests are some time of repetitive nature. Such loads could lead to unexpected failure and subsequent injuries.

11.2 Conclusions

1) The theoretical analysis of the pylon transducer and the comparison of the results to experimentally derived values proved that the main effects of the transducer in practice behave very similarly to the theoretical predictions (refer to table 4.5) .

2) The use of the Instron machine was not successful for all loading configurations during calibration tests because of friction and possibly other unquantified effects (refer to figures 4.7 to 4.9). The tests which were not affected by the above effects did, however, provide results comparing closely to the theoretically predicted values (refer to table 4.5).

3) The validation of the calibration matrix , by applying a known combined load, is a major determinant for the reliability of the pylon transducer and must always be carried out after a calibration. The results of the tests carried out for this purpose are questionable, mainly because further investigations are needed for the justification of the device used. However, the prediction errors calculated were generally not very high and can be used as a reference for future work (refer to table 5.1 and figures 5.7 and 5.8).

4) The introductory investigations of the second-order calibration model showed that for most combinations of load components the adoption of this model, instead of the simple linear model, is not recommended. Further investigations are, however, recommended for a full justification of the above comment (for results refer to tables 6.3 and 6.4).

5) The mathematical modelling of Otto Bock modular prostheses and the simulation of prosthetic alignment changes has provided a useful tool for the assessment of alignment ; and if further developed could successfully be used in association with the pylon transducer for combined prosthetic loading and alignment studies (for results refer to section 8.6).

6) Amputee kneeling proved to apply very high loads, which in some cases are of dynamic nature. The bending

moment applied through the shin of the Endolite prosthesis reached the value of 165 Nm, corresponding to shear forces of 7 kN at the knee axis and the posterior edges of the cradle (for highly loaded areas refer to figure 10.3 b).

11.3 Future Recommendations

The work presented highlighted some topics where further developments and more research work is needed :

1) A specially designed rig should be developed which, making use of dead-weights will provide the possibility of collecting data for derivation and validation of the calibration models (refer to the discussions in chapters 4 and 5).

2) The new method for the assessment of prosthetic alignment should be further developed and improved in order to obtain greater accuracy , decrease of the time needed for the measurements and a more versatile display of the alignment results (refer to the discussions in chapters 7, 8 and 9).

3) Further investigations are required for the solution of the inverse alignment problem, which is presented in detail in appendix X and the factorial experimentation described in appendix XII.

The use of pylon transducers in prosthetics has contributed greatly in the development of the field and the quality of amputee management. However, there are more tasks to be met and requirements to be fulfilled and undoubtedly there is always a good motive : the relief and the satisfactory service provided to the amputee.

BIBLIOGRAPHY

Ainscough, D.N. (1991)
MSc thesis under preparation.

Al-Turaiki, M.H.S. (1990),
A foot rotary mechanism for the modular below - knee
prosthesis, *Orthotics and Prosthetics* 2, pp 119-125.

Anderson, M.H. and Sollars, R.E. (eds) (1957),
Manual of above knee prosthetics, UCLA,
School of Medicine.

Andres, R.O. and Stimmel, S.K. (1990),
Prosthetic alignment effects on the gait symmetry :
a case study, *Clinical Biomechanics* 5, pp 88-96.

Arcan, M. Brull, M.A. and Steinbach, T. (1982),
A computerized FGP approach to mechanical alignment
prostheses, at " Uses of computers in aiding the
disabled", IFIP-IMIA, Haifa, pp 99-107.

Banerjee, S.N. (ed) (1982),
Rehabilitation management of the amputees, Williams and
Wilkins, Baltimore.

Bannister, B.R. and Whitehead, D.G. (1986)
Transducers and Interfacing/ Principles and Techniques,
Van Norstrand Reinhold (UK) Ltd.

Berme, N. Lawes, P. Solomonidis, S.E. and Paul, J.P. (1976)
A shorter Pylon Transducer for measurement of
prosthetic forces and moments during amputee gait,
Engineering in Medicine 4(4).

Berme, N. Purdey, and Solomonidis, S.E. (1978),
Measurement of prosthetic alignment, *Prosthetics and
Orthotics International* 2(2), pp 73.

Blatchford CAB (1983),
Standard alignment recommended for Endolite,
Chas A. Blatchford & Sons Ltd, Basinstoke, Hampshire.

Boenick, U. Steffens, H.P. Zenke, R. and Engelke, E. (1978)
Amputee performance measurement outside the laboratory,
Proceedings of Bioengineering Symposium, University of
Strathclyde, Glasgow.

Box, G.E.P. Hunter, W.G. and Hunter J.S. (1978),
Statistics for experimenters, John Wiley & Sons, Inc.

Bray,A. (1981)

The role of stress analysis in the design of force standard transducers / The William Murray lecture, Experimental Mechanics, Jan(1981), pp 1-20.

Bray,A. Barbato,G and Levi,R. (1990)

Theory and Practice of Force Measurement, Academic Press Ltd, 1990.

Bray,A. Ferrero,C. Levi,R and Marinari,C. (1978)

An investigation on parasitic effects on force standards machines, VDI Berichte No 312, 1978, pp 113-123.

Breaky,J.W. (1973),

Wedge adaptors for the alignments of lower limb prostheses, Orthotics and Prosthetics 27(4), pp 38-43.

British Standard Institute (1990)

British Standard 7313, Prosthetics and Orthotics part 1: terminology.

Casolo,F. and Legnani,G. (1990),

Choice and measurement of Angular variables for Biomechanics - 3D analysis and simulation / Discussion of results collected by a commercial system, First World Congress of Biomechanics , San Diego, published by Instituto delli azionamenti meccanici, Polytecnico di Milano.

Chatfield,C. (1983),

Statistics for technology, third edition, Chapman & Hall, New York.

Cobbold,R.S.C. (1974),

Transducers for biomedical measurements, John Wiley and Sons.

Cochran,W.G and Cox,G.M. (1968),

Experimental Design, John Wiley & Sons, Inc.

Committee on Prosthetic Research and Development and

Committee on Prosthetic-Orthotic Education (1970), Artificial Limbs-Selected articles (Jan.54-Spring 66), Robert E.Krieger Publishing Co.,Huntington, New York.

Committee on Prosthetic Research and Development (1971)

'Cosmesis and the modular prostheses', a report from a Conference held in San Francisco, USA, 1971.

Craig,J.J. (1986)

Introduction in Robotics, Addison-Wesley Publishing Company, Inc.

Cunningham,D.M. and Brown,G.W. (1952),
Two devices for measuring the forces acting on the
human body during walking,
Society of Experimental Stress Analysis IX(2), pp 75.

Den Hartog,J.P. (1949)
Strength of Materials
Mc Graw-Hill, Inc, USA.

Deutschman,A.D. Michels,W.J. and Wilson,C.E. (1975),
Machine Design, Macmillan Publishing Co, New York.

Dewar,M.E. (1977),
'Prosthetic load patterns in the normal environment',
BRADU report, Roehampton.

DHSS (Department of Health and Social Security) (1972),
Lower Limb Modular Prostheses, Report from a conference
held in Ascot, England (29/10 - 4/11/1972).

DHSS (Department of Health and
Social Security) and ISPO (1974),
Physical testing of prostheses,
Report from an International Conference convened by
the DHSS and ISPO at Heathrow 25-29/3/1974.

Doran,M. Spence,W.D.
Zahedi,M.S. and Solomonidis,S.E. (1985),
Survey of prosthetic knee joint design criteria,
Journal of Rehabilitation Research and Development
Progress Reports 22(4).

Dubois,M. (1972),
" Experimental Study of Strain Gauge High Precision
Dynamometers at the ONERA Modane Test Centre ",
IMECO meeting, the Hague, Sept.1971,
VDI Berichte No 176, 1972, pp 61-72.

Dubois,M. (1974)
Design and manufacture of high-precision strain gauge
dynamometers and balances at the ONERA Modane Centre,
Strain, October 1974, pp 188-194.

Dubois,M. (1976)
"Calibration of six-component dynamometric balances",
Office National d'Etudes et Recherche Aerospatiales
ONERA TP No 1976-79.

Dubois,M. (1978)
Progress in the precision of the 250 kN ONERA force
standard machine, VDI Berichte No 312, 1978,
pp 85-93.

- Dubois, M. (1982),
Six component strain-gauge balances for large wind
tunnels, *Experimental mechanics* Nov.81, pp 401-407.
- Dudley, S. et al. (1989),
Functional biomechanical characterisation and
functional design specification : lower extremity
prosthetics, *Journal of Rehabilitation Research and
Development* 26, p 31.
- Elftman, H. (1938),
The measurement of the external force in walking,
Science 88, pp 152.
- Ferrero, C. Marinari, C. and Martino, E. (1986)
Main metrological characteristics of IMGC
six-component dynamometer, *RAM* 2(2), pp 21-28.
- Flowers, W.C. (1985),
Microcomputer controlled individualized multimode
prostheses for lower extremity amputees,
*Journal of Rehabilitation Research and Development
Progress Reports* 22(4).
- Foort, J. and Hobson, D.A. (1964),
'A pylon prosthesis system for shank BK amputees',
Prosthetics and Orthotics Research Unit of Manitoba
Rehabilitation Hospital, Report No 3, Winnipeg, Canada.
- Foort, J. and Hobson, D.A. (1965),
'The wedge disc alignment unit',
Prosthetics and Orthotics Research Unit of Manitoba
Rehabilitation Hospital, Report No 6, Winnipeg, Canada.
- Foort, J. (1979),
Alignment of the above knee prosthesis,
Prosthetics and Orthotics International 3, pp 137-139.
- Foort, J. (1984),
Power management of prosthetic alignment,
University of Strathclyde, Glasgow, Paper No.5.
- Freund, J.E. and Walpole, R.E. (1980),
Mathematical Statistics, third edition,
Prentice Hall Inc.
- Gardner, H.F. (1971),
Endoskeletal structure for lower extremity prostheses,
Bulletin of Prosthetic Research 10-13, pp 113-119.
- Goldner, J.L. (1962),
Rotational and angular deformities of the lower
extremities and their effect on prosthetic fitting and
gait, *ICIB* 1(6), pp 1-5.

- Grant-Thompson, J.C. (1977),
Amputee gait analysis techniques using pylon data,
MSc thesis, University of Strathclyde, Glasgow.
- Grieve, D.W. and Gear, R.J. (1966),
The relationship between length of stride,
step frequency, time of swing and speed of walking for
children and adults, *Ergonomics* 9(5), pp.379-399.
- Grieve, D.W. (1969),
A device called the Polgon for the measurement of the
orientation of parts of the body relative to a fixed
external axis, *Journal of Physiology* 201, p 70P.
- Haddan, C.C. (1968)
The principles of Fitting, in " Human Limbs and their
substitutes", P.E.Klopsteg and P.D.Wilson,
Hafner Publishing Co, New York.
- Hannah, R.E Morrison, J.B Chapman, A.E. (1984)
Prostheses alignment : Effect on gait of persons
with below-knee amputations, *Archives of Physical
Medicine and Rehabilitation* Vol 65, 1984.
- Higdon, A. (1976)
Strength of Materials, John Wiley and Sons, Inc, USA.
- Hobson, D.A. (1972),
A powered aid for aligning the lower limb prosthesis,
Bulletin of Prosthetic Research, Fall 1972, pp 159-163.
- Holman J.P. (1978)
Experimental methods for engineers, third edition,
Mc Graw-Hill, Inc, USA.
- Hughes, J. (ed) (1976),
International study week on prosthetics and orthotics
education, HMSO, Edinburgh.
- Huney, D.O. (1975),
The Zoroc technique for early or check fitting and
alignment of lower limb prostheses : a technical note,
Orthotics and Prosthetics 29(2), pp 69-70.
- Institution of Mechanical Engineers (1976),
Human Locomotion Engineering.
- Ishai, G.A. (1975),
Whole body gait kinetics,
PhD thesis, University of Strathclyde, Glasgow.
- Ishai, G.A. Bar, A. and Susak, Z. (1983),
Effect of alignment variables on the thigh axial torque
during swing phase in AK amputee gait,
Prosthetics and Orthotics 7, pp 41-47.

ISPO and DHSS (1973),
Design criteria in lower limb prostheses - Amputee
performance measurement, Report of a meeting in Dundee,
Scotland, 18-20/ 6 / 1973.

ISPO (1978),
Standards for lower limb prostheses,
Report of a Conference in Philadelphia, USA, June 1977.

Jarrett, M.O. Moore, P.R. and Swanson, A.J. (1980),
Assessment of gait using components of the ground
reaction force vector, Medical and Biological
Engineering and Computing 18, pp 685-688.

Jones, D. (1976),
Data handling in amputee analysis of Gait,
PhD thesis, University of Strathclyde, Glasgow.

Jones, D. and Paul, J.P. (1978),
Analysis of variability in pylon transducer signals,
Prosthetics and Orthotics International 2(3) pp 161-166.

Judge, G.W. Murray, D. (1973),
'Laboratory studies of amputee loading patterns',
BRADU Report, Roehampton.

Kadaba, M.P. (1985),
Quantitative Gait Analysis (human),
Journal of Rehabilitation Research and Development
Progress Report 22(4).

Kapandji, I.A. (1987),
The Physiology of the joints / Volume II (Lower Limb),
Churchill Livingstone, New York.

Karagiannopoulos, L. (1991)
MSc thesis under preparation.

Kay, H.W. and Newman, J.D. (1973),
Report of workshop on below and above knee prostheses,
Orthotics and Prosthetics 27(4), pp 9-25.

Kerr, G. Saleh, M. and Jarrett, M.O. (1983),
An angular alignment protractor for use in the dynamic
alignment of BK amputees,
at "IV World Congress of ISPO", London.

Klopsteg, P.E. and Wilson, P.D. (1968),
Human Limbs and their substitutes, second edition,
Hafner Publishing Co, New York.

Kreyszig, E. (1988),
Advanced engineering mathematics,
John Wiley & Sons Ltd, New York.

Krieger,W. (1991)
Personal communication.

Lawes,P. Jones,D. Loughran,A. and Berme,N. (1975),
Measurement of Prosthetic Alignment and determination
of anatomical frames of reference in gait analysis and
lower limb amputees, in " Proceedings of the Biological
Engineering Society 15th Anniversary International
Conference ", Edinburgh, Scotland.

Lawes,P. (1982),
Alignment kinetics in patient - prosthesis matching,
PhD thesis, University of Strathclyde, Glasgow.

Levi,R. (1972)
Multicomponent calibration of machine-tool dynamometers
Transactions of ASME / Journal of Engineering
in Industry, Nov 1972, pp 1067-1072.

Lord,M. and Smith,D.M (1984),
Foot loading in amputee stance,
Prosthetics and Orthotics International 8, pp 159-164.

Lovely,D.F. (1981),
Portable tape recorder system for prosthetic load data
acquisition, PhD thesis, University of Strathclyde,
Glasgow.

Lowe,P.J. (1969),
Knee mechanisms performance during amputee activity,
PhD thesis, University of Strathclyde, Glasgow.

McCourt,P.M. (1977),
Laboratory studies of amputees loading performance,
BRADU/DHSS, pp 155-156.

McCubbin,K.J. (1976),
Design and development of transducers for
bioengineering uses, MSc thesis, University of
Strathclyde, Glasgow.

Meriam,J.L. (1980),
Engineering mechanics / Vol I & II,
John Wiley & Sons, Inc, USA.

Measurement Group UK Ltd
"Optimizing Strain Gage Excitation Levels",
Technical Note TN-502.

Meyer,S.L (1975),
Data analysis for scientists and engineers,
John Wiley and Sons Ltd.

Mital, M.A. and Pierce, D.S. (1971),
Amputees and their Prostheses, Little Brown and
Company, Boston.

Mizrahi, J. Susak, Z. and Seliktar, R. (1985),
Comprehensive alignment procedure of below knee
artificial leg, Journal of Rehabilitation Research
and Development 22(4).

Morimoto, S. and Tsuchiya, K. (1984),
Evaluation of amputee prosthesis system of lower limb
using pylon study method,
Bulletin JSPE 18(2), pp 57-58.

Morimoto, S. Yamashita, T. and Tsuchiya, K. (1985),
Measurement of six quantity forces acting on the
artificial legs of light weight amputees,
from a research report submitted to EIREC,
Rehabilitation Engineering Centre for Employment
Injuries, Japan, pp 91-119.

Murdoch, G. (ed) (1970),
Prosthetic and Orthotic Practice,
E. Arnold, London.

Murdoch, G. (mod) (1969),
'Lower extremity prosthetics',
in "Research in lower prosthetics and orthotics",
a report from an International Conference sponsored by:
Committee on Prosthetics Research and Development of
the division of Engineering / National Research
Council and the International Committee on Prosthetics
and Orthotics of the International Society for
Rehabilitation of the disabled, Conference at Cacapon,
Berkeley Springs, West Virginia 28/4-2/5 /1969.

Murdoch, G. and Donovan, R.G. (eds) (1988),
Amputation surgery and lower limb prosthetics,
Blackwell Scientific Publications.

Murphy, E.F. (1968),
The fitting of BK prostheses,
in "Human limbs and their substitutes", P.E. Klopsteg
and P.D. Wilson, Hafner Publishing Co, New York.

Nader, M. (1987),
Otto Bock Prosthetic Compendium : Lower Extremity
Prostheses, Schiele & Schon, Berlin.

Nettelhorts, H. Boenick, U. and Steffens, H.P. (1978),
An electronic storage system with histographical
representation for axial load measurement in modular
prostheses, Biomedizinische Technik 23, p 311.

- Nishihara,K. Kawamura,J. and Kanda,A. (1989),
A much shorter pylon load cell and its wide range of
applications in prosthetics, at " VI World Congress
of ISPO ", Kobe, Japan.
- Olsen,G.A. (1974)
Elements of Mechanics of Materials, third edition
Prentice-Hall, Inc, USA.
- Otto Bock Company (1990),
Lower Extremity Prosthetic Catalog, Otto Bock, Germany.
- Pandy,M.G. and Berme,N. (1989),
Quantitative assessment of gait determinants during
single stance via a 3-D model Part 1: normal gait,
Journal of Biomechanics 22.
- Pandy,M.G. and Berme,N. (1989),
Quantitative assessment of gait determinants during
single stance via a 3-D model Part 2: pathological
gait, Journal of Biomechanics 22.
- Pashalides,S. (1989)
Design of a portable recording system
for the measurement of prosthetic loading
PhD thesis, University of Strathclyde, Glasgow.
- Pathokinesiology Service and Physical
Therapy Department of Los Amigos Hospital (1981)
Normal and Pathological Gait Syllabus,
Downey, California.
- Paul,J.P. (1991)
Personal communication.
- Pierron,G. Ralfray,M. and Berthet,M. (1985),
The PAD : A new alignment device for prosthetic systems
(The case of an AK endoskeletal prosthesis),
Orthotics and Prosthetics 38(4), pp 58-62.
- Poulson,J. (1973),
Biomechanics of the leg,
PhD thesis, University of Strathclyde, Glasgow.
- Quinn,T.P. and Mote,C.D. (1990)
Optimal design of an uncoupled six-degree of freedom
dynamometer, Experimental Mechanics 30(1), pp 40-48.
- Radcliffe,C.W. (1951),
'Use of the adjustable knee and alignment jig for the
alignment of the AK prosthesis',
A Report from the Prosthetic Devices Research Project
in UCB to the Advisory Committee on Artificial Limbs,
NRC.

- Radcliffe,C.W. (1954),
Mechanical aids for alignment of lower extremity
prostheses, Artificial Limbs 1,pp 20-28.
- Radcliffe,C.W. (1955),
Functional considerations in the fitting of AK
prostheses, Artificial Limbs 2(1), pp 35-60.
- Radcliffe,C.W. (1955),
The biomechanics of BK prostheses in walking,
Artificial Limbs 6(2), pp 16-24.
- Radcliffe,C.W. and Foort,J. (1961),
The patellar tendon bearing below knee prosthesis,
Biomechanics Laboratory of the Department of
Engineering / UC Berkeley and School
of Medicine / UC San Francisco.
- Radcliffe,C.W. and Lamoreux,L. (1968),
Functional considerations in the fitting above-knee
prostheses, Artificial Limbs 2(1), pp 35-60.
- Radcliffe,C.W. (1955),
Functional considerations in the fitting of AK
prostheses,in "Human Limbs and their substitutes",
P.E.Klopsteg and P.D.Wilson, Hafner Publishing Co,
New York.
- Radcliffe,C.W. (1977),
The Knud Jansen Lecture: Above knee prosthetics,
Prosthetics and Orthotics International 1, pp 146-160.
- Roark,R.J. (1954)
Formulas for stress and strain, third edition,
Mc Graw-Hill Book Company,Inc, New York.
- Ryan,B.F. Joiner,B.L. and Ryan,J.A.Jr. (1985),
Minitab Handbook,
PWS - Kent Publishing Company, Boston.
- Saleh,M. Bostock,S. (1988)
An aid to alignment in the below-knee amputee,
The Journal of Bone and Joint Surgery, Vol 70-B (3).
- Saunders,C.G. Foort,J. Davies,R.M et al (1985),
CAD/CAM, Prosthetics and Orthotics
International 9(1).
- Saunders,J.B. et al (1953),
The major determinants in normal and pathological gait,
Journal of Bone and Joint Surgery 35A, pp 543-558.

- Schuch,C.M. (1988),
Report from an International workshop
on above-knee fitting and alignment techniques,
Clinical Prosthetics and Orthotics 12, pp 81-98.
- Schuch,C.M. (1988),
Modern above-knee fitting practice (a report on the
Ispo workshop on above-knee fitting and alignment
techniques, May 15-19 in Miami,USA),
Prosthetics and Orthotics International 12,pp 77-90.
- Seliktar,R.; Mizrahi,J. and Susak,Z. (1982)
Computer-aided dynamic alignment of Below Knee
Prostheses, in "Uses of Computers in Aiding the
Disabled", J.Raviv, North Holland Publ. Inc.
- Shorter,J.J. (1985),
Endolite - The high technology prosthesis,
Journal of Rehabilitation Research and Development
Progress Reports 22(4).
- Skinner,H.B. (1985),
SACH foot study, Journal of Rehabilitation
Research and Development Progress Reports 22(4).
- Slemon,D. (1989)
Design and fabrication of a three component balance
for measuring the forces exerted on an orthopaedic
prosthesis, B.Eng. thesis, University of Limerick,
Ireland.
- Smith,J.D. (1976)
Misuse of regression techniques in Calibration,
Strain, July 1976, pp 120-121.
- Smith,J.D. (1977)
Practical problems in calibration of torque tubes,
Strain, October 1977, pp 148-151.
- Solomonidis,S.E. (ed) (1975),
'Modular Artificial Limbs / First report on a programme
of clinical and laboratory evaluation / BK systems',
HMSO.
- Solomonidis,S.E. (ed) (1980),
'Modular Artificial Limbs/ Second report on a programme
of clinical and laboratory evaluation / AK systems',
SHHD.
- Solomonidis, S.E. (1989)
Personal communication.

Solomonidis, S.E. and Lawes, P. (1975),
Evaluation of above-knee modular prostheses,
in " Proceedings of the Biological Engineering Society
15th Anniversary International Conference ", Edinburgh,
Scotland.

Solomonidis, S.E. Lawes, P. Loughran, A.J. (1974),
Amputee performance measurement at University of
Strathclyde, Bioengineering Unit, Glasgow,
at "Physical testing of prostheses", DHSS/ISPO,
Heathrow, England.

Solomonidis, S.E. Lowe, P.J.
Taylor, J. and Hughes, J. (1974),
Evaluation of modular below-knee prosthetic systems,
at " I World Conference of ISPO ", Montreux,
Switzerland.

Solomonidis, S.E. and Paul, J.P. (1986),
Study of alignment in lower limb prostheses,
Journal of Rehabilitation Research and Development
Progress Report 24(1).

Solomonidis, S.E. Yacoob, P.E.Y. and Paul, J.P. (1986),
Survey of design criteria for prosthetic knee and ankle
joints, Journal of Rehabilitation Research and
Development , Progress Report 24(1).

Solomonidis, S.E. Zahedi, M.S. Spence, W.D.
Lovely, D. Kardoulas, D. and Tilford, C. (1985),
Prosthetic loading data for the development of
standards for lower limb prostheses,
Journal of Rehabilitation Research and Development
Progress Report 22(4).

Spiegel, M.R. (1975)
Probability & Statistics,
Schaums Series, McGraw Hill, New York.

Staros, A. (1963),
Dynamic alignment of artificial legs with the
adjustable coupling, Artificial Limbs 7(1), pp 31-43.

Szulc, J. (1984),
Telescopic limbs for above-knee amputees,
PhD thesis, University of Strathclyde, Glasgow.

Taylor, J.S. (1979),
Modular assembly above-knee prostheses,
Prosthetics and Orthotics International 3, pp 144-146.

Taylor, J.S. (1979),
Above-knee prosthetic alignment,
Prosthetics and Orthotics International 3, pp 82-84.

- Thomas,A. (1944),
Anatomical and physiological considerations in the
alignment and fitting of prostheses,
Journal of Bone and Joint Surgery 26, pp 645-659.
- Thomson,R.G. (1977),
Report: Panel on lower limb prosthetics,
Orthotics and Prosthetics 31(4), pp 54-60.
- Tilford,C. (1985)
Collection and analysis of prosthetic load
data during outdoor activities, MSc Thesis,
University of Strathclyde, Glasgow.
- University of California Berkeley (1947),
Fundamental studies of human locomotion and other
information relating to design of artificial limbs,
Submitted by : H.D.Eberhart.
- Vanderby,R. and Van Vorhis,R.L. (1985),
Computer aided alignment of lower limb prostheses and
expert systems, Journal of Rehabilitation Research and
Development Progress Reports 22(4).
- Van Vorhis,R.L. and Leibowitz,L. (1986),
Computer aided alignment of lower limb prostheses and
expert systems, Journal of Rehabilitation Research
and Development Progress Reports 24(1).
- Verrini,A and Levi,R. (1968)
Improved program for multiple regression analysis,
Calcolo 6(1), p 51.
- Verstraete,M.C. and Soutas-Little,R.W. (1989),
A method for computing the 3-D forces and moments in
the lower limb during gait (abstract),
Journal of Biomechanics 22, p 1094.
- Wilson,A.B. (1970),
Limb Prosthetics-1970, Artificial Limbs 14(1), pp 1-56.
- Wilson,A.B. (1975),
Lower Limb Modular Prostheses: A Status Report,
Orthotics and Prosthetics 29(1),pp 23-32.
- Woolvet,G.A. (1977),
Transducers in Digital Systems,
Institution of Electrical Engineering.
- Zahedi,M.S. Spence,W.D.
Solomonidis,S.E. and Paul,J.P.(1983),
'Study of Alignment in lower limb prostheses',
University of Strathclyde, Glasgow.

Zahedi, M.S. (1985)
PhD thesis under preparation

Zahedi, M.S. Spence, W.D.
Solomonidis, S.E. and Paul, J.P. (1986),
Alignment of lower limb prostheses,
Journal of Rehabilitation Research and Development
23(2), pp 2-19.

Zompi, A. Levi, R. (1978)
Practical Experimental designs for multicomponent
dynamometer calibration, VDI Berichte No 312, 1978,
pp 95-102.